NASA Contractor Report 3531

Development of Quality Assurance Methods for Epoxy Graphite Prepreg

J. S. Chen and A. B. Hunter

NASA

NASA Contractor Report 3531

Development of Quality Assurance Methods for Epoxy Graphite Prepreg

J. S. Chen and A. B. Hunter
Boeing Commercial Airplane Company
Seattle, Washington

NASA

National Aeronautics
and Space Administration

**Scientific and Technical
Information Branch**

1982

CONTENTS

TABLES

FIGURES

1.0 SUMMARY

This report documents work performed by The Boeing Company for the National Aeronautics and Space Administration-Langley Research Center under Contract NAS1-15222. The objective of the program was to develop quality assurance methods for epoxy graphite prepreg and to correlate the methods developed to processing parameters and mechanical properties of graphite laminates.

The work was performed in six tasks over 3 years. Liquid chromatography was investigated in Task A, differential scanning calorimetry in Task B, and gel permeation chromatography in Task C. In Task D, the analytical methods developed were applied to a second prepreg system. Dynamic mechanical analysis of resin casts and graphite laminates was conducted in Task E, and fracture toughness of graphite laminates was investigated in Task F. The material studied in Tasks A, B, and C was Narmco 5208. In Tasks D and F, the material evaluated was Hercules 3501-5A. Both Narmco 5208 and Hercules 3501-5A were investigated in Task E.

Quality assurance methods were optimized in Tasks A, B, and C. Data indicate that the reverse-phase liquid chromatography method developed in Task A is the most sensitive to formulation variations. In Task D, the optimized methods developed in Tasks A, B, and C were successfully applied to the second prepreg system. Tasks E and F were completed and the dynamic mechanical analysis and fracture toughness results obtained are reported. No correlation could be established between chemistry variations and current mechanical tests.

2.0 INTRODUCTION

Escalation of jet-fuel prices is causing a reassessment of the technology concepts and trades used in designing and building aircraft. There is significant potential for weight and fuel savings through the use of advanced composites in primary structure. To ensure that epoxy graphite composites will meet the demands of primary structure, more stringent material controls are required than those currently used for nonstructural composites. Improved quality assurance methods for epoxy graphite prepreg are essential to obtain consistent, high-quality structure. No allowables program, component test program, or in-service evaluation can achieve its full potential without the assurance that the initial material is of high quality, uniformity, and continuing consistency. This program was designed to ensure that these material concerns were met and provides the impetus required to achieve a new level of confidence in advanced composite primary structure.

The program was conducted in six tasks:

- Task A—Liquid Chromatography
- Task B—Differential Scanning Calorimetry
- Task C—Gel Permeation Chromatography
- Task D—Second Resin Evaluation
- Task E—Dynamic Mechanical Analysis
- Task F—Fracture Toughness

A detailed discussion of the procedures used and results obtained in each task is contained in Section 4. Section 5 presents conclusions resulting from the work.

Use of trade names or names of manufacturers in this report does not constitute an official endorsement of such products or manufacturers, either expressed or implied, by the National Aeronautics and Space Administration.

3.0 SYMBOLS AND ABBREVIATIONS

a	crack length, cm
A	area, cm^2
Å	angstrom
ASTM	American Society for Testing and Materials
AUF	absorbance units full scale
b	specimen width, cm
c	specimen compliance, Pa^{-1}
^oC	degree Celsius
cal/g	calorie per gram
$^oC/cm$	degree Celsius per centimeter
$^oC/min$	degree Celsius per minute
cm	centimeter
cm^2	square centimeter
cm^{-1}	1 per centimeter
cm/min	centimeter per minute
DDS	diaminodiphenylsulfone
deg	degree (angular)
DEP	diethyl pimelate
DMA	dynamic mechanical analysis
DMF	dimethyl formamide
DMP	dimethyl pimelate
DSC	differential scanning calorimetry
E	instrument calibration coefficient
^oF	degree Fahrenheit
$^oF/in.$	degree Fahrenheit per inch

°F/min	degree Fahrenheit per minute
FTIR	Fourier transform infrared spectroscopy
g	gram
G'	elastic (storage) modulus, Pa
G"	viscous (loss) modulus, Pa
G_{IC}	energy release rate of crack propagation, mode I loading
GPa	gigapascal
GPC	gel permeation chromatography
HMW	high molecular weight
HP	Hewlett Packard
HPLC	high-pressure liquid chromatography
hr	hour
Hz	hertz
ID	inside diameter
IGDA	Interactive Graphic Display Analysis
in.	inch
in.^{2}	square inch
in.-lb/in.^{2}	inch pound per square inch
in./min	inch per mintue
IR	infrared spectroscopy
IR&D	independent research and development
J/kg	joule per kilogram
J/m^2	joule per square meter
K	column capacity
kg	kilogram
kHz	kilohertz

lb	pound
lbf/in.^{2}	pound force per square inch
LC	liquid chromatography
LMW	low molecular weight
mcal	millicalorie
mcal/in.	millicalorie per inch
mcal/s/in.	millicalorie per second per inch
MeV	million electron volts
mg	milligram
mg/liter	milligram per liter
mg/ml	milligram per milliliter
min	minute
min/cm	minute per centimeter
min/in.	minute per inch
ml	milliliter
ml/min	milliliter per minute
mm	millimeter
mm^2	square millimeter
mm/min	millimeter per minute
MPa	megapascal
MW	molecular weight
MΩ	megohm
N	column plate count (column efficiency)
NBS	National Bureau of Standards
N$_{DEP}$	column plate count using diethyl pimelate
N$_{DMP}$	column plate count using dimethyl pimelate

nm	nanometer
P	load, kg
Pa	pascal
Pa·s	pascal second
PRT	platinum resistance thermocouple
r	correlation factor
rad/s	radian per second
rel. σ	relative standard deviation, %
RMS	Rheometrics mechanical spectrometer
rpm	revolution per minute
R_S	column resolution
RT	room temperature
s	second
SAMPE	Society for the Advancement of Materials and Process Engineers
SEM	scanning electron microscope
SP	Spectra Physics
T	temperature, $^\circ$C
tan δ	viscous modulus/elastic modulus (G"/G') ratio
T_e	reaction temperature endpoint, $^\circ$C
T_g	glass transition temperature, $^\circ$C
TGMDA	tetraglycidylmethylenedianiline
THF	tetrahydrofuran
TLC	thin-layer chromatography
T_o	reaction temperature onset, $^\circ$C
T_p	reaction temperature peak, $^\circ$C
TSIR	thermal scanning infrared spectroscopy

UV	ultraviolet
V	retention volume, ml
V_W	baseline peak width
W	watt
W/cm	watt per centimeter
wt %	weight percent
$\bar{x}$	mean
%	percent
α	column selectivity
α-transition	glass transition, chain movement of network structure
β-transition	crankshaft rotation of sidechain structure
ΔH_f	heat of fusion, J/kg
ΔH_p	heat of polymerization, J/kg
μl	microliter
μm	micrometer
$\mu m/m$	micrometer per meter
$\mu V \cdot s$	microvolt second
η	complex viscosity, Pa·s
σ	standard deviation
ω	angular frequency, rad/s

4.0 PROCEDURES, RESULTS, AND DISCUSSION

This section presents the procedures used to accomplish each of the six program tasks:

- Task A—Liquid Chromatography
- Task B—Differential Scanning Calorimetry
- Task C—Gel Permeation Chromatography
- Task D—Second Resin Evaluation
- Task E—Dynamic Mechanical Analysis
- Task F—Fracture Toughness

Results obtained during each task are presented, along with a discussion of the results.

4.1 TASK A—LIQUID CHROMATOGRAPHY (LC)

The purpose of this task was to develop and optimize liquid chromatography (LC) techniques to provide a reliable quality assurance method for epoxy graphite prepreg. The Task A work flow is shown in Figure 1.

Six batches of epoxy graphite prepreg were ordered from Narmco Materials. The batch formulations are listed in Table 1. These batches were identical to those analyzed by Rockwell International under Contract F33615-77-C-5243 (ref 1) and were selected at the suggestion of the NASA technical monitor, with Boeing's concurrence.

4.1.1 Prepreg Physical and Mechanical Properties

Receiving inspection of the six batches of Narmco 5208 epoxy prepreg included physical and mechanical property tests. The physical and mechanical test matrix is shown in Table 2.

Prepreg physical property tests consisted of resin content, volatile content, resin flow, and gel time. Test results are reported in Table 3. Resin content was determined by measuring weight change after a 30-min exposure at 177°C (350°F). Resin flow was determined using the standard flow test method contained in Boeing material specification BMS 8-212 (ref 2). This specification contains test methods and requirements for receiving inspection of 177°C (350°F) curing epoxy graphite prepreg. Gel time was determined using a Fisher-Johns melting-point apparatus at 170 ±2°C (338 ±3.6°F). Gel time test results correlated well with the resin formulation alterations, from 29 min for the overcatalyzed system to 34 min for the undercatalyzed system.

Mechanical testing was conducted on unidirectional laminates fabricated using the cure cycle shown in Figure 2. Laminate tests included fiber volume, 0-deg tension strength and modulus, and 0-deg short-beam-shear strength. All mechanical tests were conducted in accordance with BMS 8-212 (ref 2).

Fiber volume tests were conducted on the laminates using nitric acid to digest the epoxy resin from the graphite fiber, and fiber volume was calculated from laminate and fiber density and weight. Tension strength and modulus were determined in the 0-deg direction to define fiber-dominant properties. The tension test specimen is shown in Figure 3. Short-beam-shear strength was determined in the 0-deg direction to define resin-graphite composite shear properties. Figure 4 illustrates the short-beam-shear test specimen. Mechanical test results are contained in Table 4.

The chemical variations of the Narmco altered resin batches, shown in Table 1, were not revealed by either the short-beam-shear or the 0-deg tension test results (table 4). Additional mechanical tests, including 0-deg compression, 90-deg tension, and short-beam shear, were performed on the standard prepreg (batch 1072), least catalyzed (batch 1074), and most catalyzed (batch 1077) materials. Results of these tests are shown in Tables 5, 6, and 7. Examination of the results indicates that the chemical variations in the formulations were not revealed by any of the mechanical tests performed.

4.1.2 Extraction Method

Boeing independent research and development (IR&D) funds were used to conduct the initial LC analysis of the components in Narmco 5208. Tetrahydrofuran (THF), an excellent organic solvent, was added to the epoxy graphite prepreg, and the solution was agitated using an ultrasonic bath to dissolve the resin.

During this contract, a scanning electron microscope (SEM) photograph of the fibers (fig. 5) was obtained and showed that the organic resin was completely removed by the THF. A control extraction on T300 fiber was conducted similarly, using THF. The SEM photograph of this extraction is shown in Figure 6. Examination of the photomicrographs revealed that the organic residue on T300 fibers was extracted by THF, and examination of the T300 fiber from the prepreg also revealed that the resin was completely removed from the fiber.

A chromatogram of the T300 fiber finish removed by THF is shown in Figure 7. The following instrument parameters were used to obtain the chromatogram:

- Column: Waters μ-Bondapak/C_{18}
- Solvent: 30/70% acetonitrile/water (CH_3CN/H_2O) in 15 min, linear
- Flow rate: 1.8 ml/min
- Detector: ultraviolet (UV), 280 nm

A sample size 60 times larger than the normal size for prepreg analysis was used to exaggerate the effect of fiber sizing. Absorption peaks with retention times of 16.7 and 23.5 min were observed.

Using the same parameters as described above, except for a smaller sample size (1/60), a typical chromatogram of the Narmco resin matrix was obtained (fig. 8). The results indicated that in the LC analysis of Narmco graphite prepregs, the peak contribution from the graphite fiber sizing was insignificant.

Through further evaluation and optimization of the LC parameters, an isocratic solvent (63/37% CH_3CN/H_2O) was selected as the mobile phase and UV 220 nm as the detector for resin analysis. To avoid the complication of using THF as the extracting solvent and to improve the lifetime of the LC column (i.e., avoid sedimentation of resin in the column head), the isocratic mobile phase (63/37% CH_3CN/H_2O) was chosen as the prepreg extracting solvent.

4.1.3 Mode Selection

Thin-layer chromatography (TLC) is an excellent tool for systematically evaluating nonaqueous solvent systems for LC. Aqueous systems are best evaluated with LC

itself, because the binder used on the TLC plates is soluble in water. One cannot use more than 40% water before the TLC plates are affected.

A pre-evaluation of both adsorption and partition chromatography by circular TLC was performed, followed by high-pressure liquid chromatography (HPLC) analyses. The parameters evaluated included:

- Mobile phase
- Flow rate
- Detector

A Waters μ-Porasil adsorption-phase column and a Waters μ-Bondapak/C_{18} reverse-phase column were used for the initial LC mode evaluation.

The following TLC plates representing both adsorption and partition chromatography were used:

- Silica gel silanized RP-2 from Merck
- Silica gel KC_{18} from Whatman
- Silica gel GF from Anoltech, Inc., prepared by Merck

The specific developing technique was the Schleicher and Schuell Selectasol solvent selector circular developing system. The dyes were bromocresol green that was allowed to dry, followed by Erhlick's solution.

Optimum solvent strength was determined and the proper solvent mix defined. The following solvent systems gave the best separation by TLC:

- RP-2—solvent strength of 0.50 using 6.2%(volume) CH_3CN in toluene (C_7H_8); an alternate mixture is 0.2% (volume) methanol (CH_3OH) in chloroform ($CHCl_3$)

- KC_{18}—solvent strength of 0.45 using propanol (C_3H_8O) in $CHCl_3$

- GF—solvent strength of 0.80 using 8.15% (volume) CH_3OH in C_7H_8

Some adjustments were required in the solvent ratio when transferring the TLC data to the LC. The UV absorbance of C_7H_8 also presented problems with wavelength selection for the UV detector used with LC.

Figures 9 through 11 show typical TLC separations obtained to determine solvent polarity. Examination of Figure 9 reveals that the diaminodiphenylsulfone (DDS) curing agent was readily detected by the chosen dye system. Figures 9(b) and 9(c) show the best separations. Figure 9(c) shows the sharpest separation, with four definite components. Figure 9(b) shows many components, but with poorer resolution.

Examination of Figure 10 also reveals that the DDS curing agent was easily detected by the selected dye system. Although both solvent mixes gave many components with fairly good resolution, the mix used for Figure 10(b) showed the best resolution.

A single enlarged separation using the same solvent mix as used in Figure 10(b) is shown in Figure 11. Many bands are visible in the separation. DDS is the inner, light-colored ring. The other bands are epoxy resin components.

The results of the TLC investigation indicated that the best LC modes to pursue would be reverse-phase partition chromatography and adsorption chromatography. Because of the excellent separation obtained with the reverse-phase method, it was decided that there would be no advantage in pursuing normal-phase partition chromatography.

The data from the TLC investigation were used to further develop LC solvent selection methodology. The test matrix for this investigation is presented in Table 8. Table 8 identifies the columns used with the various mobile phases and their respective flow rates. The best chromatogram (fig. 12) resulted from a mobile phase of 0.2% CH_3OH in $CHCl_3$ (isocratic) and a 0.5-ml/min flow rate. The two components, MY 720 and DDS, were resolved, but detailed peaks from resin staging and minor components in the organic matrix of Narmco batch 286 were masked.

4.1.3.1 Adsorption Chromatography

A μ-Porasil column from Waters Associates was used to evaluate adsorption chromatography. The following parameters were evaluated:

- Flow rate: 0.5, 1.0, and 2.0 ml/min
- Detector: UV, 254 and 280 nm
- Mobile phase: THF/$CHCl_3$, isocratic

Flow Rate and Detector Evaluation—The test matrix for the flow rate (0.5 to 2.0 ml/min) and detector wavelength (254 and 280 nm) evaluation is shown in Table 9. Table 9 identifies the samples evaluated at the various flow rates and detector wavelengths. The chromatogram for each combination also is listed. Comparison of the chromatograms (figs. 13 through 17) leads to the following conclusions:

- It was possible to assign peaks by comparing chromatograms of the resin matrix with those of the individual ingredients.

- A detector wavelength of 280 nm was preferred over one of 254 nm because of the higher absorptivity of the reaction product of MY 720 and DDS at 280 nm.

- Better resolution was obtained with a slower flow rate (0.5 versus 1.0 ml/min). A flow rate of 2.0 ml/min did not provide a chromatogram with sufficient resolution for analysis.

Mobile-Phase Evaluation (Gradients)—A THF and $CHCl_3$ solvent pair was selected for evaluation with six separate gradients ranging from 60/30 to 10/50% THF/$CHCl_3$. Comparison of the chromatograms obtained indicates that the following conditions were the best among the six tested:

- Solvent: 10/50% THF/$CHCl_3$ in 15 min, curve 7 (Waters solvent program)
- Flow rate: 1 ml/min
- Detector: UV, 280 nm

Using the instrument conditions described above, chromatograms of DDS (fig. 18), MY 720 (fig. 19), and Narmco batch 286 (fig. 20) were obtained. Comparison of the Figure 18 and 19 chromatograms made possible the peak assignment shown in Figure 20.

Although adsorption chromatography gave good separations, it did not give the detail yielded by reverse-phase partition chromatography. In addition, the greater the nonpolarity of the reverse-phase packing, the more detailed the chromatogram became. This was determined by comparing data obtained using the C_{18} packing with data obtained using the C_2 packing. Therefore, the C_{18} packing was used for the remainder of the program.

4.1.3.2 Mobile-Phase Variations

In the analyses for LC mode selection, Waters μ-Bondapak/C_{18} was arbitrarily chosen as the reverse-phase column. A detailed comparison of reverse-phase columns made by different manufacturers is contained in Section 4.1.4.1.

As part of the mode evaluation, the mobile phase was varied as shown in Table 10. The chromatograms resulting from each mobile-phase variation are shown in Figures 21 through 23. Changes in peak resolution were observed as the mobile phase was varied and, under all conditions, the curing agent (DDS), major epoxy (MY 720), and reaction product peaks were well resolved and could be used for quantification.

4.1.4 Parameter Optimization

4.1.4.1 Column and Mobile-Phase Optimization

Five reverse-phase columns were evaluated:

- Waters Associates μ-Bondapak/C_{18} (10 μm)
- Whatman Partisil 10, ODS-2 (10 μm)
- Merck Lichrosorb RP-8 (5 μm)
- Merck Lichrosorb RP-2 (10 μm)
- Merck Lichrosorb RP-8 (10 μm)

Column efficiency and reproducibility were determined by a plate-count measurement that provided a numerical check of the column quality. Parameters for plate-count measurement were as follows:

- Sample: acenaphthene
- Solvent: 60/40% CH_3CN/H_2O, isocratic
- Flow rate: 2.5 ml/min
- Detector: UV, 280 nm, 2.0 absorbance units full scale (AUF)
- Chart speed: 5.0 cm/min (2.0 in./min)
- Sample concentration: 1.0%
- Injection volume: 5 μl

Plate-count measurements on the five reverse-phase columns are shown in Table 11.

The five columns were directly compared by analyzing standard Narmco resin batch 286 using the following parameters:

- Solvent: 30/70% CH_3CN/H_2O in 15 min
- Flow rate: 1.8 ml/min
- Detector: UV, 280 nm

Results of the comparison are shown in Table 12, and the chromatograms obtained are shown in Figures 24 through 28.

The μ-Bondapak/C_{18}, Lichrosorb RP-8 (5 μm), and Partisil 10, ODS-2 columns were compared further using two more mobile phases:

- Mobile phase 1

    - Solvent: 24/82% CH_3CN/H_2O in 20 min, linear
    - Flow rate: 2.0 ml/min

- Mobile phase 2

    - Solvent: 40/80% CH_3CN/H_2O, concave
    - Flow rate: 2.0 ml/min

The chromatograms obtained are shown in Figures 29 through 31. Results of the column comparison using mobile phase 1 are summarized in Table 13. Mobile phase 2 reduced the time required to complete a chromatogram by 50%; however, peak resolution also decreased significantly.

To minimize the differences between the chromatograms and improve technique reproducibility between laboratories and instruments, considerable effort was devoted to development of an isocratic mobile phase for LC characterization of Narmco 5208. Preliminary results showed that CH_3CN/H_2O mobile phase revealed the most chromatographic detail in an analysis of Narmco 5208. To facilitate quick solvent changes, two high-pressure pumps and a solvent programmer were used initially to evaluate the composition of various isocratic mobile phases.

The following solvent ratios and flow rates were evaluated to obtain an optimized chromatogram:

- Solvent ratios:

CH_3CN, %	H_2O, %
50	50
60	40
40	60
70	30
65	35
68	32

- Flow rates: 1.5, 1.8, and 2.0 ml/min

The best results were obtained with a flow rate of 1.5 ml/min and CH_3CN/H_2O ratios of 65/35 and 68/32.

The flow rate of the mobile phase is important in obtaining good chromatogram resolution. A slower flow rate sometimes can improve chromatogram resolution, but longer instrument running time is required for the analysis. A compromise was developed that optimized chromatogram resolution and instrument running time.

The effect of flow rate on chromatogram peak-area calculations was evaluated using the following LC parameters:

- Sample: Narmco prepreg batch 1072
- Column: Waters μ-Bondapak/C_{18}
- Solvent: 30/70% CH_3CN/H_2O in 15 min, linear
- Detector: UV, 280 nm, 0.05 AUF
- Chart speed: 1.0 cm/min (0.4 in./min)
- Integrator: Varian CDS-111

The effects of flow-rate variation on peak area and retention time are summarized in Table 14. The data are averages of two experiments. Examination of Table 14 produces the following observations:

- The retention times for DDS, MY 720, and reaction product increased with a decrease in flow rate.

- The peak-area percentages for DDS and MY 720 appear to be independent of the flow rate. For the reaction product, the larger peak-area percentage at slower flow rates (1.0 to 1.5 ml/min) may indicate a problem with resolution rather than an actual quantitative increase of reaction product.

- The direct integration output demonstrates that for DDS, MY 720, and the reaction product peaks, the slower the flow rate, the larger the integrated area observed.

The change of integrated area with flow-rate variation may be due to the "response delay" setting of the detector. In other words, the detector detects more sample at slower flow rates than at faster flow rates. The integration method also may contribute to the variation. A smaller area is integrated for a sharp peak (from a faster flow rate) than for a broad peak (from a slower flow rate).

A final solvent ratio combination was studied by mixing the mobile phase manually and using one calibrated pump. The chromatogram obtained is shown in Figure 32. The optimized isocratic LC parameters are as follows:

- Column: Waters μ-Bondapak/C_{18}
- Solvent: 63/37% CH_3CN/H_2O, isocratic
- Flow rate: 1.5 ml/min
- Detector: UV, 220 nm, 0.2 AUF
- Sample concentration: 0.5%
- Injection volume: 5 μl

The solvent ratio difference, 63/37% CH_3CN/H_2O (premixed solvent) versus 65/35% CH_3CN/H_2O (solvent mixed using two LC solvent pumps), may be due to the lack of LC pump calibration.

A Whatman Partisil 10, ODS-2 column also was evaluated using the optimized LC isocratic condition. The chromatogram resulting from an analysis of Narmco batch 286 is shown in Figure 33. Examination of Figures 32 and 33 reveals greater peak retention time using the Whatman column (retention time for last peak, 26 min); however, resolution of the peaks did not improve.

Examination of the chromatogram in Figure 32 shows that the curing agent (DDS), major epoxy (MY 720), second epoxy, and reaction product of resin staging were well resolved. This provides an LC method for quality assurance of Narmco epoxy graphite prepreg. The isocratic solvent method was selected for the LC round-robin evaluation.

The efficiency of the isocratic method was evaluated by TLC. Runs were made on Narmco 5208, major resin, second resin, and DDS. TLC/C_{18} reverse-phase plates were used with a mobile phase identical to that used in the proposed LC method. Results showed that the DDS had a single band with no residue. Both the second resin and major resin showed many bands with slight residue. The Narmco 5208 showed good separation of the DDS from the resin. The resin had many bands, but a very small residue remained. The TLC data correlated quite well with the LC data. In the LC analysis, good separation was obtained, but after each run, upon increasing the gradient to 100% CH_3CN, there were minor peaks that eluted. These minor peaks were apparently residue from the two resin systems, as indicated by TLC.

4.1.4.2 Detector Optimization and Integrator Comparison

Once the isocratic method was established, the optimum wavelength for detection with the new mobile-phase ratio was pursued. With a variable-wavelength UV detector, chromatograms of Narmco batch 286 were obtained at 220 nm (fig. 34), 230 nm (fig. 35), and 240 nm (fig. 36). For comparison, an analysis at 280 nm is shown in each figure. The following observations were made:

- The second resin in Narmco resin matrices was barely detected at 280 nm; detection was only slightly better at 240 nm. The second resin could be detected very readily at 220 and 230 nm.

- The DDS peak (retention time 5.0 min), staged resin peak (retention time 14.8 min), and MY 720 peak showed higher absorptivity at 220 nm than at 230 nm. The absorptivity of the second resin (retention time 16.9 min) was only slightly less (11%) at 220 nm than at 230 nm.

- With a relatively high sample concentration (0.5%) and a low detector sensitivity setting (0.2 AUF), the previously observed baseline drift at 220 nm was minimized significantly.

UV at 220 nm was finally selected as the detector for the LC round-robin procedure.

Instrument linearity at different attenuations was evaluated. Three UV detectors were evaluated: a Spectra 2 made by DuPont, and Models 835 and 837, both sold by DuPont but manufactured by Schoeffel. The Spectra 2 and Model 837 are variable-wavelength detectors, and the Model 835 is a fixed-wavelength detector. The evaluation was made at 254 nm, and the area integration was done in each case by a Spectra Physics (SP) 4000. The integration at each attenuation for the three detectors was performed on the same sample injection. The tabulated data are presented in Table 15.

Peak heights also were measured to determine any differences caused by changes in attenuation. The data indicate that one cannot expect straight-line linearity when changing attenuation. However, the data do fit a geometric curve of $Y = aX^b$ with a correlation of 1.00 and the attenuation and area represented by Y and X, respectively.

The terms a and b are constants defining curvature and curve placement. This non-linearity demonstrates the need to use an internal standard and measure other peaks relative to the standard. The attenuation cannot be changed during the run.

4.1.5 Internal Standard Selection

Benzaldehyde is commonly accepted in the aerospace industry as an internal standard for the gradient LC analysis of the organic matrices of 177°C (350°F) curing epoxy graphite composite. Because benzaldehyde is chemically unstable, it was essential to select a new internal standard for quantitative LC analysis. The criteria for the internal standard were as follows:

- Chemically stable in solution
- Sensitive to detection (high absorptivity for UV detection)
- No standard peak interference with the other chromatogram peaks

The following chemicals were evaluated as candidates for an LC internal standard in the gradient mobile-phase evaluation:

- Quinone
- Hydroquinone
- Acetophenone
- Diphenyl ether
- Biphenyl
- Phenyl salicylate
- Anthrone
- Dioctyl phthalate
- 9-fluorenone

The LC parameters used for this evaluation were as follows:

- Column: Waters μ-Bondapak/C$_{18}$
- Solvent: 30/70% CH$_3$CN/H$_2$O, in 15 min, linear
- Flow rate: 1.8 ml/min
- Detector: UV, 280 nm, 0.05 AUF; UV, 230 nm, 0.04 AUF

Examination of the chromatograms obtained for each compound resulted in the following conclusions:

- Quinone, hydroquinone, acetophone, diphenyl ether, biphenyl, phenyl salicylate, and anthrone were eliminated as LC internal standards because of chromatogram peak interference.

- Dioctyl phthalate was eliminated because of its low UV absorptivity.

- 9-fluorenone was considered to be the best internal standard because of its high UV absorptivity, chemical stability, and minimum interference with the other chromatogram peaks.

Using the μ-Bondapak/C$_{18}$ LC column and isocratic mobile-phase condition, the following compounds were investigated as an internal standard under the isocratic condition:

16

- Acenaphthene
- Benzaldehyde
- Fluorene
- Perylene
- Triphenylphosphate
- Tri-p-tolyl phosphate

Tri-p-tolyl phosphate appeared to be the best candidate, with an absorption peak (fig. 37) at a retention time of 14 min and no peak interference. It was used as the internal standard in the LC round-robin procedure. At a fixed concentration, tri-p-tolyl phosphate was used to standardize the sensitivity setting of the LC detector. Once this was done, chromatograms of similar peak size could be obtained from the round-robin evaluation.

Two integrators, an SP 4000 and a Hewlett Packard (HP) 3380, were compared by identical, simultaneous runs. The results of three separate runs on Narmco batch 294 at different attenuations are shown in Table 16. Correlation was done by calculating the least-squares fit, with r being the correlation factor. There was excellent correlation between the two integrators, with the correlation factor approaching 1.00. However, the comparison pointed out a potential problem, especially in the smaller peaks: a large variation in peak-area data was noted between the two integrators. The problem could be caused by either the method of calculating area or the baseline determination.

4.1.6 Quantification of Altered Resin Batches

During LC parameter optimization, the six Narmco alterations were quantified using both peak-area ratios (Varian CDS-11 integrator) and peak-height (absorbance) ratios. Quantifications were performed on both the neat resins and the graphite prepregs to check the resolution and sensitivity of the LC procedure. The instrument parameters were as follows:

- Column: Waters μ-Bondapak/C_{18}
- Solvent: 30/70% CH_3CN/H_2O in 15 min, linear
- Flow rate: 1.8 ml/min
- Detector: UV, 280 nm, 0.05 AUF
- Sample concentration: 0.1%
- Injection volume: 5 μl

Results of the analysis are summarized in Table 17 for the neat resin alterations and in Table 18 for the corresponding graphite prepregs. The DDS/MY 720 peak-height and peak-area ratios increased in the order expected from the formulation variations shown in Table 1. Reasonably good agreement between resin and prepreg analyses indicates that there was no selective extraction of the resin components by the THF extracting solvent.

The six graphite prepregs were analyzed using the LC round-robin procedure. The peak-area-ratio results are summarized in Table 19. Area integration was done using a Varian CDS-111 integrator. The DDS/MY 720 ratio increased as expected from the formulation changes. The ratio of reaction product to MY 720 is an indication of the extent of resin advancement—the larger the ratio, the greater the resin advancement.

The reproducibility of retention time and peak-area percentage of chromatograms of Narmco batch 1072 was examined in 10 separate chromatograms using a reverse-phase solvent gradient system with UV detector at 280 nm. A summary of the results of the reproducibility check is shown in Table 20.

Quantitative determination of the unreacted second resin in the Narmco resin mix (batch 286) and prepreg (batch 1072) was performed using the following conditions:

- Column: Waters μ-Bondapak/C_{18}
- Solvent: 30/70% CH_3CN/H_2O in 15 min, linear
- Flow rate: 1.8 ml/min
- Detector: UV, 230 nm, 0.04 AUF

A calibration curve (fig. 38) was established by injecting different known amounts of second resin, followed by peak-height measurements. Duplicate measurements were performed for resin batch 286, and triplicate measurements were performed for prepreg batch 1072. Results are shown in Table 21.

Concentrations of the curing agent (DDS) in the altered Narmco resin batches were determined by infrared spectroscopy (IR). The sulfone absorption at 1107 cm^{-1} was quantitatively determined by Fourier transform infrared spectroscopy (FTIR). A curve of absorbance versus wavenumber for DDS is shown in Figure 39. Scale expansion was used for both ordinate and abscissa.

DDS concentrations in the altered Narmco resin batches also were determined using ion chromatography. The ion chromatograph contains an anion exchange column with a thermal conductivity detector. The sample is ignited in an oxidizing atmosphere and then injected into the column. The DDS is measured as sulfate ion.

DDS concentrations in the six altered Narmco resin batches, as determined by IR and ion chromatography, are reported in Table 22. There was good agreement between the data obtained using each method.

4.1.7 Column Calibration

A detailed calibration procedure was developed to give better column definition. The procedure enabled column resolution (R_S) to be tracked by monitoring column selectivity (α), column capacity (K), and column efficiency (N). Details of the procedure are given in Appendix A.

4.1.8 Round-Robin Evaluation

After the instrument parameters were optimized, the detailed LC procedure was sent to 10 round-robin participants in July 1979. Also sent were samples of standard Narmco graphite prepreg batch 1072 and four additional chemicals for instrument calibration. The detailed round-robin procedure is contained in Appendix A. The participants listed below submitted round-robin results. The letters in parentheses refer to the quality assurance methods conducted by each participant during the entire program: LC, liquid chromatography; DSC, differential scanning calorimetry; GPC, gel permeation chromatography.

- Army Materials and Mechanics Research Center (LC, DSC, GPC)

- Boeing Aerospace Company, Quality Control (LC, DSC)

- Boeing Commercial Airplane Company, Materials Technology (LC, DSC, GPC)

- Boeing Commercial Airplane Company, Quality Control Research and Development (LC, DSC, GPC)

- Ciba-Geigy Corporation (LC, DSC, GPC)

- Hercules, Inc. (LC, DSC, GPC)

- Lockheed Missiles and Space Company, Inc. (LC, DSC, GPC)

- Narmco Materials (LC, DSC)

- NASA-Langley Research Center (LC, DSC, GPC)

- Rockwell Science Center (DSC)

The instruments used by the round-robin participants for the LC analysis are listed in Table 23. One representative chromatogram from each participant is presented in Figures 40 through 48. The participants are coded from A through J, and the same code for each participant will be used throughout this report, although the identity of each participant is not given.

A comparison of the retention times obtained by the round-robin participants for the following three peaks is shown in Table 24:

- Eporal major component (DDS) peak
- Resin advancement peak
- MY 720 monomer peak

Reasonably good agreement in retention-time data was obtained among the participants, with relative standard deviations of less than 10%. Better results can be obtained, as shown by the numbers in parentheses in Table 24 for mean ($\bar{x}$), standard deviation (σ), and relative standard deviation (rel. σ), by disregarding the data from participant C. This level of agreement provides the possibility of using retention time as the comparator for individual peaks between laboratories.

Visual examination of chromatograms is an important aspect of LC. A fair visual comparison can be made only by examining chromatograms of similar peak size. Because of the large variation in the sensitivity of individual detectors, a known quantity of tri-p-tolyl phosphate was used to standardize the detector sensitivity setting. This provided chromatograms of similar peak size from different instruments. Tri-p-tolyl phosphate was selected as a standard because of its chemical stability and because its chromatogram peak does not interfere with the resin component peaks under the round-robin conditions.

Peak-area percentages for the peaks of interest were recalculated from the original data by disregarding the tri-p-tolyl-phosphate peak; they are summarized in Table 25.

High relative standard deviations were observed for the three components. The resin advancement peak (smallest and partially resolved) showed the largest relative standard deviation (20.15%). As shown by the numbers in parentheses in Table 25, the statistical data can be improved by disregarding the data from participant C.

Peak-area ratios of the pertinent peaks were calculated and are summarized in Table 26. Peak-area-ratio data also showed large scatter.

Examination of the chromatograms from the round-robin participants reveals a tremendous variation in peak resolution, even though the same LC procedure was followed. Chromatogram resolution relies heavily on solvent strength, solvent flow rate, and column efficiency. The previously recommended procedure—using an isocratic premixed solvent rather than using dual pumps to obtain solvent composition—ensures consistent solvent strength in the LC analysis.

A summary of the column-efficiency results from the round-robin evaluation is shown in Table 27. With the exception of participant A, whose chromatogram showed excellent peak resolution with poor column efficiency (N_{DEP} 1495, R_S 2.58), it seems generally true that a column with high efficiency will generate a chromatogram with good resolution; e.g., participants D, F, and I.

Examination of the original data from each participant shows excellent reproducibility within each participant's data both in retention time and in peak-area percentage calculations. The scatter in peak-area percentage data among laboratories may be attributed to the following factors:

● Detector wavelength needs to be calibrated. Since the molar extinction coefficients are different for the three components and also are different at each wavelength, significant data scatter among laboratories may result. This source of data scatter can be avoided by detector wavelength calibration.

● Integrator parameters need to be specified. As shown in Table 23, several different integrators were used in the analysis. Unless integrator parameters such as peak threshold, minimum peak area, and partially resolved peak calculations are specified, a large scatter in peak-area percentage may result.

● It has been demonstrated that chromatograms with good resolution are essential for interlaboratory agreement. The data scatter may be reduced dramatically if well-resolved chromatograms can be obtained from all participants.

Use of a standard solution method is an alternative approach to improving interlaboratory data agreement. Rather than standardizing the instruments (liquid chromatograph, detector, and integrator) among laboratories, a standard solution is used to calibrate the individual instruments. A standard solution can be prepared at each laboratory, provided that agreement is reached on composition of the standard components. Better results can be obtained if the concentrations of the individual components are specified. The selected concentration, however, could be different from the actual resin formulation. This procedure allows a response factor (peak area per milligram of sample or peak height per milligram of sample) for the components to be obtained through analysis of a standard solution. From the response factor for each ingredient, the weight percentages of the components in the unknown sample can be calculated.

The possible disadvantages of this method are as follows:

● Weight percentage can be obtained only on the components in the initial formulation. The weight percentage of the reaction product formed during the resin mixing cannot be obtained readily.

● The chemical stability of the standard solution needs to be established.

● To prepare the standard solution, proprietary formulation information may be required from the supplier.

Another approach to improving interlaboratory data agreement is to establish calibration procedures for the instruments themselves. Requirements should be established for the following parameters:

● The column—Although a column calibration method is described in the round-robin procedure (Appendix A) for Narmco 5208 material, column requirements have not been established. Table 27 contains the column-efficiency data obtained by the round-robin participants. As can be seen in this table, the variability in column data from the round-robin participants is quite wide. The variation in mobile phase from the calibration procedure to the actual run may have caused confusion and could be a source of variability in the data. If limits for column capacity (K) and column selectivity (α) are set within one standard deviation and minimum requirements are set for column plate count (N) and resolution (R_S), the parameters would be as follows:

  ● K_1 = 0.48 to 0.70
  ● K_2 = 1.01 to 1.53
  ● α = 1.91 to 2.09
  ● N_{DMP} = 2000 minimum
  ● N_{DEP} = 2000 minimum
  ● R_S = 3.0 minimum

  Four participants would meet these requirements. Tables 28 and 29 show the reduction in variability of retention-time and peak-area data obtained by using controls on column parameters. Table 30 summarizes the data from Tables 24, 25, 28, and 29. Allowing data from the "specified" columns only in Table 30, only partial improvement in the data variability is obtained. If plate count alone were used to calibrate the columns, only three columns out of the nine participants would meet a minimum plate count of 3000. Setting the minimum plate count at 2500 would qualify six columns. Tables 31 and 32 show the reduction in variability of retention-time and peak-area data obtained by using a minimum plate count of 2500. In Table 33, the data from Tables 24 and 25 are compared with the data from Tables 31 and 32. These results indicate that column calibration should consist of all factors in the resolution formula.

● Detector wavelength—The absorbance variability observed when the participant data for the three component peaks are compared indicates a need to establish wavelength calibration. The difference in the UV extinction coefficients for the three components makes it necessary to establish an acceptable wavelength tolerance.

- Detector response—Calibration of detector response may be performed with ratio techniques. This program has shown that the ratio of detector attenuation to detector response is not linear.

- Flow rate—The instrument flow rate must be calibrated periodically.

- Gradient—It is not certain that the mobile phase was premixed by all participants. Therefore, the instrument gradient capability should be calibrated.

To write an instrument calibration procedure general enough to cover the various instruments used would be very difficult. However, once completed, it would be useful for all materials, not just Narmco 5208, while the standard solution technique discussed above is useful only for Narmco 5208 material.

4.2 TASK B—DIFFERENTIAL SCANNING CALORIMETRY (DSC)

The objective of Task B was to differentiate, by thermal analysis, the variations in resin chemical formulation that were introduced into the six batches of Narmco prepreg (table 1). The primary emphasis was placed on differential scanning calorimetry (DSC) using a DuPont 990 thermal analyzer. The Task B work flow is shown in Figure 49.

Preliminary work was done on the neat resin only. The technique then was transferred to the prepreg. This approach was used because of our previous experience of obtaining accurate and reproducible data on prepreg using normal DSC methods.

4.2.1 Interpretation of DSC Scan

Methods used to interpret the DSC thermal analysis scan included thermal gravimetric analysis (TGA), thermal scanning infrared spectroscopy (TSIR), and dielectrometry.

A DSC scan of the Narmco standard neat resin (batch 300) is presented in Figure 50. For TGA, a DuPont 990 thermal analyzer was used under the following conditions:

- Heating rate: $10^\circ C/min$ ($18^\circ F/min$)
- Sample weight: 10.63 mg
- Reference: empty pan
- Atmosphere: ambient air
- Scale x-axis: $7.9^\circ C/cm$ ($36^\circ F/in.$)
- Scale y-axis: 0.0017 W/cm (1 mcal/s/in.), 0.0034 W/cm (2 mcal/s/in.)

The double curve shown in Figure 50 represents a dual range sensitivity plotted simultaneously. For this run, the heat of polymerization (ΔH_p) was 656 072 J/kg (157.6 cal/g) and the reaction temperature onset (T_o) was $203^\circ C$ ($397^\circ F$). Reaction temperature onset was determined by the intersection of an extended baseline with an extended tangent drawn at the point of greatest slope. Figure 51 represents a duplicate run with one curve being a normal DSC scan and the other the first derivative.

TSIR analysis was performed using a Digilab FTS-15 Fourier transform spectrometer with a Boeing-developed heated cell. The scans were made on Narmco neat resin batch 300 using a heating rate of $10^\circ C/min$ ($18^\circ F/min$). Infrared scans were recorded

at increasing temperatures without interrupting the heating rate. The sample remained in place as a film on a sodium chloride block throughout the run.

The TSIR spectra are shown in Figures 52 through 54. As can be seen in Figure 53, drastic changes began to occur at 200°C (392°F). This was evidenced by the depletion of epoxy band at 910 cm^{-1} and changes occurring in bands present from DDS at 1620, 3390, and 3490 cm^{-1}. The change was drastic between 200 and 250°C (392 and 482°F) and correlated well with the DSC reaction temperature onset of 203°C (397°F) and the derivative change in slope at 212°C (414°F).

The depletion of the two bands at 3400 cm^{-1} by 250°C (482°F), followed by the drastic changes occurring at 1200 to 1400 cm^{-1} by 300°C (572°F), correlates well with the fast completion of the DSC exotherm before 300°C (572°F). The two bands at 3400 cm^{-1} are typical of the amine functional group of DDS. With the exception of the band at 1300 cm^{-1}, which is related to DDS, the bands from 1200 to 1400 cm^{-1} are related to tetraglycidylmethylenedianiline (TGMDA), probably to the aryl-N- and -CH$_2$- functional groups. The TSIR analysis followed the reaction quite well through the DSC scan.

Dielectric analysis of the altered Narmco resins was performed using a DuPont 990 thermal analyzer interfaced with a General Radio capacitance bridge and a Boeing-designed capacitance cell. Results of the dielectric analysis are shown in Figures 55 through 60. Each of the altered resins peaked at 160°C (320°F), which correlates well with the DSC results that indicate baseline deviation occurring at approximately 160°C (320°F). Also, the overcatalyzed systems did tend toward greater dissipation factors. The dissipation factor is a measure of the molecular dipole movement in the resin. The greater the ability of the molecular dipoles to orient themselves to the changing field, the greater the dissipation factor. Several of the dielectric analysis scans had a shoulder at 100°C (212°F). This event was not reproducible and appeared to be related to solvent entrapment in the sample.

Results from the three methods—TGA, TSIR, and dielectrometry—correlate well and give valuable information in understanding the DSC scan. Based on the data, several observations can be made:

- Drastic changes in gelation occur at about 160°C (320°F), where the dissipation factor peaks and the DSC scan deviates from baseline.

- Crosslinking begins rapidly, shortly after 200°C (392°F), as revealed by the DSC reaction temperature onset of 203°C (397°F) and the TSIR indication of epoxy functional group depletion between 200 and 250°C (392 and 482°F).

- The reaction goes to completion very rapidly, shortly after 250°C (482°F), as revealed by the DSC peak at 260°C (500°F), followed by a sharp return to baseline and by the changes in resin structure revealed by TSIR.

4.2.2 Effects of Variables on DSC Scan

Reproducibility between laboratories is a problem with DSC methods. Because of this difficulty, we attempted to determine which variables affect DSC data. The following variables were evaluated:

- Sample weight
- Heating rate
- Atmosphere
- Sample container
- Balance accuracy
- Resin homogeneity
- Area determination
- Instrument error

The effects of these variables were assessed by measuring reaction temperature onset (T_o), reaction temperature peak (T_p), reaction temperature endpoint (T_e), and heat of polymerization (ΔH_p).

A statistical evaluation of DSC analysis results obtained using normal, nonoptimized conditions was performed; results are tabulated in Table 34. The analysis conditions were as follows:

- Instrument: DuPont 990
- Sample: Narmco batch 300
- Sample size: 8 mg
- Heating rate: 10^oC/min (18^oF/min)
- Atmosphere: air
- x-axis: 7.9^oC/cm (36^oF/in.)
- y-axis: 0.0017 W/cm (1 mcal/s/in.)
- y' axis: 0.5

The samples were run as sets. Samples 1 through 5 were run on one day and samples 6 through 10 several days later to determine any variability caused by shutting down the instrument and restarting it at a later date. The experiment also evaluated repeatability in making one run right after another.

The temperature events had excellent repeatability, with the largest standard deviation being 0.89^oC (1.79^oF) with a mean of 203.4^oC (398^oF), giving a variability of 0.45%. The heat of polymerization showed greater variability, with the first five samples having a standard deviation of 20 480 J/kg (4.89 cal/g) with a mean of 621 404 J/kg (148.4 cal/g), giving a variability of 3.30%. It is believed that some of this variability was caused by impurities present in the material. The results of Table 34 indicate good repeatability from day to day. However, the variation in heat of polymerization from sample to sample indicated the need to investigate the cause of the variability.

Table 35 presents data resulting from the analysis of Narmco batch 300 under various conditions. The instrument conditions were the same as those listed in Table 34 except as noted in Table 35. For example, the condition identified as "sealed" in Table 35 is the DSC sample cup hermetically sealed, whereas the condition of Table 34 is open cup. The other conditions varied were atmosphere, sample weight, and heating rate. Comparing the data of Table 35 with that of Table 34 to determine the effect of varying the identified conditions, and using the grand average with plus or minus one standard deviation as the normal, each of the ΔH_p values of Table 35 falls outside the normal. Also, most of the temperature indicators fall outside the normal. Inconsistencies in the data indicated that something was causing variability that had not been detected. For example, the average heat of polymerization at a heating rate of

10°C/min (18°F/min) was 632 542 J/kg (151.08 cal/g), at 5°C/min (9°F/min) was 530 886 J/kg (126.8 cal/g), and at 2°C/min (3.6°F/min) was 602 899 J/kg (144.0 cal/g). Also, the variability of data from samples 1 through 5 in Table 34 indicated reproducibility problems.

Table 36 shows the effect of certain variables on the heat of polymerization. All samples were run at 10°C/min (18°F/min) in time-base mode. The use of time-base mode on the DuPont instrument puts the x-axis in time rather than temperature, allowing for increased sensitivity by spreading out the curve. As shown in Table 36, two standards were run to determine reproducibility of the instrument itself. Three runs each were made with indium and tin. The heat of fusion (ΔH_f) of indium was 29 015 J/kg (6.93 cal/g), with a standard deviation of 208.9 J/kg (0.05 cal/g) and a variation of 0.72%. The tin standard had a heat of fusion of 54 973 J/kg (13.13 cal/g), with a standard deviation of 1677 J/kg (0.40 cal/g) and a variation of 3.05%. The tin standard had some variability within the tin itself, as well as larger particles with a greater particle size distribution, which probably affected the distribution of heat of fusion data. However, the indium standard gave very reproducible data, indicating the instrument's repeatability. Samples also were run in different atmospheres on Narmco batch 300 to determine the effect of atmosphere on heat of polymerization. The data variability in the different atmospheres was still greater than desired.

A prime suspect for the source of variability then became weighing and/or area measurement errors. For example, a weighing error of ±0.01 mg on a 4-mg sample could result in a standard deviation of 0.5. Errors of similar magnitude would be expected for area determinations. Area measurements were made with a planimeter, with the average of three recordings used. The three area readings typically showed very little variability, indicating that the problem was not with area measurements. Samples then were evaluated using a microbalance with an accuracy of better than ±0.01 mg at 4 mg. Even with the increased weighing accuracy, the variability in the heat of polymerization data did not show significant improvement.

In search of a solution to the problem, microscopic examination of the DSC samples was performed after analysis and revealed the presence of foreign particles. Later, several batches of neat resin were examined for contamination, and all were found to contain foreign particles ranging from wear metal to bits of cotton. An acetone extract of the resin was centrifuged and particles were observed at the bottom of the centrifuge tube. The acetone solution was poured into a petri dish and allowed to evaporate overnight under partial vacuum. Samples of the resin residue were evaluated by DSC, and an average heat of polymerization of 547 215 J/kg (130.7 cal/g) was obtained with a standard deviation of 3557 J/kg (0.85 cal/g) and a relative standard deviation of 0.65%, as shown in Table 36.

The contamination present in Narmco neat resin batch 300 was identified and photographed. Photographs and identifications are shown in Figures 61 through 68. For comparison, other neat resins were evaluated for contamination—two epoxy resins and one polyimide. These resins had neither the amount nor the different kinds of contamination present in the Narmco neat resins.

The key variables that affect DSC results of Narmco resin are as follows:

● Atmosphere
● Heating rate

- Instrument calibration
- Weight error
  - Contamination of sample
  - Balance error
- Area measurement error

4.2.3 Method Optimization

An optimized method was developed using the information from the variables study (sec. 4.2.2.). The method showed good reproducibility; however, as work progressed, it became obvious that the DSC method was not as sensitive as the LC method to formulation variations or resin staging. The DSC method was very suitable, however, for characterizing the polymerization reaction. The optimized method developed is shown schematically in Figure 69 and described below.

A 0.5g resin sample is dissolved in 10 ml of acetone. The sample is centrifuged for 15 min, and the supernatant liquid is poured into a 10-cm (4-in.) diameter petri dish and allowed to evaporate under vacuum. Once the acetone has completely evaporated, as determined by TGA, approximately 4 mg of material is placed in the DSC cup. A cover is placed onto the cup and sealed. A small hole is punctured in the cover to allow gases to escape. Without this hole, the cup tends to bulge and cause improper contact with the calorimeter. The sample pan is placed in the calorimeter, and an empty sealed pan is placed on the reference side. The run is made in an air atmosphere at 10°C/min (18°F/min). The chart speed is 1 cm/min (0.4 in./min).

Table 37 is a summary of data collected on Narmco batch 300 showing the data variability under the conditions identified. The analysis was performed under the following instrument conditions unless otherwise noted in Table 37:

- Instrument: DuPont 990
- Sample size: 8 mg
- Heating rate: 10°C/min (18°F/min)
- Atmosphere: air
- x-axis: 8°C/min (14.4°F/min)
- y-axis: 0.0017 W/cm (1 mcal/s/in.)
- y'-axis: 0.5

The variability in heat of polymerization data obtained using the optimized method (table 36) was considerably less than that obtained using nonoptomized conditions (table 37). The variability calculated in Table 36 was 0.65%, while that in Table 37 ranged from a low of 1.98% to a high of 11.11%.

The optimized method has several advantages. It eliminates any nonsoluble contaminants and allows the resin to be completely removed from the graphite fiber, resulting in a known weight of resin used for the determination. The question of interest is whether the resin advances during the acetone evaporation at 60 to 65°C (140 to 149°F).

Resin advancement was evaluated by dielectric analysis, TSIR, and LC. Dielectric analysis was performed on a modified DuPont 990 thermal analyzer that controls a Boeing-designed capacitance cell. The cell operates at a frequency of 1000 Hz, and

the temperature is controlled by the thermal analyzer. The resin sample is impregnated onto glass cloth and placed in the capacitance cell. The output is recorded as time, temperature, and dissipation factor. The dissipation factor is a measure of the molecular dipole movement in the resin. The greater the ability of the molecular dipoles to orient themselves to the changing field, the greater the dissipation factor.

Table 38 gives the dielectric analysis results of Narmco batch 300 as received. The data show the dissipation factor peaking at 160.1°C (320.2°F) with a reading of 7.8. Table 39 presents the data obtained by holding the sample at 60 to 65°C (140 to 149°F) for 6.5 hr and then increasing the temperature up to cure. Here, the dissipation factor peaks out with a reading of 8.3 at 162.8°C (325°F). The 8.3 reading shows no loss in reactivity from the 7.8 reading, indicating that no resin advancement was detected by dielectric analysis. It is believed that the initial peak in Table 39 of 4.9 at 0.08 hr is primarily due to volatilization. Table 40 shows dielectric analysis results at two other temperatures, 110 and 150°C (230 and 302°F). At both of these temperatures, the resin advanced considerably, as indicated by the dissipation factors of 8.8 and 11.3 at 0.08 hr for 110 and 150°C (230 and 302°F), respectively. Although the dielectric analysis readily detected staging at 110°C (230°F), it was not sensitive enough to detect advancement at 65°C (149°F).

Advancement also was evaluated by TSIR. A film of Narmco batch 300 resin was placed on a salt block. The block then was placed into the TSIR oven chamber and heated immediately to 65°C (149°F). Infrared scans were taken periodically through a 5-hr hold period at 65°C (149°F). No resin advancement was detected by TSIR.

Resin advancement also was evaluated by LC using the following parameters:

- Column: Waters μ-Bondapak/C_{18}
- Solvent: 63/37% CH_3CN/H_2O
- Flow rate: 1.5 ml/min
- Detector: UV, 280 nm

Samples were made of Narmco prepreg batch 1072 using both LC and DSC extraction methods. The DDS-to-MY 720 and reaction product-to-MY 720 absorbance ratios were determined for both extraction methods (table 41). Comparison of absorbance ratios indicates that advancement occurred in the DSC method of solvent evaporation. The LC technique is apparently much more sensitive to staging than the TSIR or dielectric analysis methods, which did not show any resin advancement.

Even though some advancement did occur in the optimized DSC method, as determined by LC, the test still is useful as a characterization tool to compare different batches of resin. With proper controls on time and temperature of solvent removal, the advancement will remain the same for each batch. The test, therefore, will give a relative heat of polymerization for comparing batches.

4.2.4 Curve Symmetry

In making repetitive runs on the DSC, the symmetry of the curve sometimes changes. This lack of symmetry may be caused by a shift in the pan or sample during the run and indicates poor contact between the sample and the DSC cell base. The poor contact can easily affect the data. Lack of symmetry can be detected by drawing a line from the apex of the peak perpendicular to the baseline, as shown in Figures 70

and 71. If there is proper symmetry, these lines should be superimposable on each other. In a series of runs, the problem runs can be detected and their data disregarded.

4.2.5 Round-Robin Evaluation

The DSC test method described in Appendix A, samples of Narmco prepreg batch 1072, and a National Bureau of Standards (NBS) sample of $KClO_4$ were submitted to the round-robin participants listed in Section 4.1.8. The $KClO_4$ was used as an internal instrument standard. The test data obtained by the round-robin participants are tabulated in Table 42, and DSC curves from each participant are contained in Figures 72 through 81. The same code, A through J, is used for the DSC round-robin participants as was used for the LC participants.

For the most part, each participant obtained good correlation within its own data. However, for the raw data, the correlation among participants was very poor. Even the heat of fusion data for the NBS $KClO_4$ standard had poor correlation. By normalizing the data to a heat of fusion for $KClO_4$ of 100 483 J/kg (24.0 cal/g), the data correlation improved significantly.

The lack of correlation of the raw data can be attributed to the following factors:

● Difficulty in determining a baseline
● Nonlinearity of the various instruments
● Improper instrument calibration

The fact that good correlation could be obtained by normalizing indicates that the method is effective.

4.3 TASK C—GEL PERMEATION CHROMATOGRAPHY (GPC)

Concurrently with Tasks A and B, gel permeation chromatography (GPC) was developed and optimized as an acceptable and reliable method in itself and to complement LC and DSC for quality assurance of Narmco 5208/T300.

A diagram of the GPC technique is shown in Figure 82. Gels with controlled pore sizes are used to exclude large molecules from all pores so that they then "wash" around the outside of the gel and move quickly down the column. Medium-sized molecules diffuse into some of the pores and, therefore, are retained longer. The smallest molecules fit into all pores and also are retained longer.

The work plan for Task C is shown in Figure 83.

4.3.1 Parameter Optimization

A Waters ALC/GPC-244 system was used for the primary GPC evaluation, with a DuPont Model 850 for backup and confirmation. The GPC technique was optimized using parameters similar to those described in Section 4.1.4, including mobile phase, column, flow rate, and detector.

THF, $CHCl_3$, and other solvents were evaluated as the GPC mobile phase. In the chemical characterization of Narmco 5208/T300, Boeing data indicated that a much

better resolution of DDS and MY 720 was obtained using $CHCl_3$ instead of THF as the mobile phase. Chromatograms were obtained of Narmco resin batch 300 using the following instrument parameters:

- Column: Waters μ-Styragel, 2 x 100Å, 2 x 500Å, 1 x 1000Å
- Solvent: THF and $CHCl_3$
- Flow rate: 2 ml/min
- Detector: UV, 280 nm

Chromatograms obtained using THF and $CHCl_3$ are shown in Figures 84 and 85. The elution order for DDS and MY 720 is reversed in Figure 85, where MY 720 elutes first and DDS elutes second, compared with Figure 84, where DDS elutes first and MY 720 elutes second. This behavior reveals a different degree of solvation for DDS and MY 720 in the THF solution.

Columns from different manufacturers were evaluated for separation capability. For example, a μ-Styragel column from Waters Associates was compared with a Shodex column from Showa Denko of Japan. Combinations of columns with different pore sizes also were examined.

A bank of three μ-Styragel columns (500Å, 2 x 100Å) was evaluated using $CHCl_3$ as the mobile phase. As expected, the time required to complete a chromatogram was reduced significantly, from 21 to 14 min, and so was the resolution between MY 720 monomer and the reaction product, as shown in the Figure 86 chromatogram.

Shodex columns, manufactured by Showa Denko and distributed by Perkin-Elmer in the United States, have shown good peak separation. The procedure requires only one column, compared to the five Waters μ-Styragel columns required. A Shodex GPC column (A-802S) was examined; the chromatogram shown in Figure 87 was obtained using the following conditions:

- Column: Shodex GPC A-802S
- Solvent: THF
- Flow rate: 0.5 ml/min
- Detector: UV, 254 nm

Another Shodex column (A-801S) with larger pores also was tested using Narmco resin; a comparison of the chromatograms obtained using the A-802S and A-801S columns showed the superiority of column A-802S over column A-801S in analyzing Narmco resin.

The effects of flow rate on GPC separation were examined. Because of the physical properties of the column packing material, a maximum flow rate of 3 ml/min is specified by the manufacturers of μ-Styragel and Shodex columns to prevent shrinkage of the packing. Flow rates from 0.5 to 3.0 ml/min were evaluated.

The effects of solvent flow rate on chromatogram resolution are shown in Figure 88. For this run, the flow rate was increased from 0.5 to 1.0 ml/min. A comparison of the chromatograms shown in Figures 87 and 88 reveals that a faster flow rate (1.0 versus 0.5 ml/min) did not affect the peak resolution significantly, but did reduce the time required to complete a chromatogram from 15 to 8 min.

To detect the second resin in Narmco 5208 and be consistent with LC procedures, a detector wavelength of 220 nm was used. A chromatogram of Narmco neat resin batch 300 (fig. 89) was obtained under the following conditions:

- Column: Shodex GPC A-802S
- Solvent: THF
- Flow rate: 1 ml/min
- Detector: UV, 220 and 254 nm
- Sample concentration: 0.15%
- Injection volume: 5 µl

The components of the resin matrix were resolved and identified, as shown in the chromatogram.

4.3.2 Quantification of Altered Resin Batches

To evaluate the sensitivity of the GPC technique, quantification of the Narmco altered resin batches was performed periodically. Peak-area and peak-height ratios for a few selected peaks were measured with variations in mobile phase, detector wavelength, column, and flow rate. Shodex column plate counts also were followed closely to check column deterioration.

With µ-Styragel columns, quantification of the Narmco neat resin (batch 300) was performed using both THF and CHCl$_3$ mobile phases. Instrument parameters were as follows:

- Column: Waters µ-Styragel, 500Å, 4 x 100Å
- Solvent: THF and CHCl$_3$
- Flow rate: 2 ml/min
- Detector: UV, 280 nm

The chromatograms obtained using THF and CHCl$_3$ solvents are shown in Figures 90 and 91. Results of analyses for the THF and CHCl$_3$ solvents are summarized in Tables 43 and 44.

The peak-height ratio of DDS to MY 720 is an indication of the amount of curing agent (DDS) present relative to the amount of major epoxy monomer (MY 720) in absorbance measurement. The ratio of reaction product peak height to MY 720 peak height indicates the relative amount of high-molecular-weight (HMW) material (resin advancement product and oligomer of MY 720) to MY 720 monomer. Using either THF or CHCl$_3$, the ratio of DDS to MY 720 increased in the order expected from the formulation variations described in Table 1.

Quantifications using Shodex A-802S columns also were performed on both neat resins and graphite prepregs using THF (0.5 ml/min) as the mobile phase and UV detector at 254 nm. Peak-height-ratio and peak-area-ratio results are summarized in Table 45. Excellent agreements in peak area and peak height were obtained between neat resin and prepreg resin. The measured DDS concentrations agreed with the original formulation variations described in Table 1.

Using the round-robin parameters described below, analyses of the six prepreg resins were accomplished; the results are summarized in Table 46.

- Column: Shodex GPC A-802S
- Solvent: THF
- Flow rate: 1 ml/min
- Detector: UV, 220 nm
- Sample concentration: 0.15%
- Injection volume: 5 µl

Examination of Table 46 shows that both peak-area-ratio and peak-height-ratio results correlated with the formulation variations described in Table 1.

4.3.3 Round-Robin Evaluation

The GPC round-robin procedure described in Appendix A and samples of Narmco prepreg batch 1072 were sent to the round-robin participants listed in Section 4.1.8. Comments from the participants are summarized as follows:

- One participant commented that the procedure was well written and easily understood.

- Because of the particular combination of instruments used, the attenuation limitations for one participant's recorder were such that an injection volume of 15 µl rather than 5 µl was required to obtain a 60 to 80% full-scale projection of the largest peak; otherwise, the operating parameters were as specified.

- One participant reported that the power to the freezer where the prepreg was stored was off over a weekend and some advancement may have occurred. This event did not affect GPC results.

- In the GPC calibration conducted by one participant, impurities in the o-dichlorobenzene prevented use of the computer plate-count calculation.

- One participant reported that solvent impurities interfered with o-dichlorobenzene separation.

The instruments used by the round-robin participants for the GPC analysis are shown in Table 23. Due to the unavailability of the Shodex GPC A-802S column, only seven participants submitted GPC round-robin results. One chromatogram from each participant is presented in Figures 92 through 98. The same code, A through J, is used for the GPC round-robin participants as was used for the LC participants.

The column-efficiency results and the retention times for the following component peaks are summarized in Table 47:

- Eporal DDS peak
- Resin advancement and reaction product peak
- MY 720 monomer peak

Mean ($\bar{x}$), standard deviation (σ), and relative standard deviation (rel. σ) also are shown in Table 47. Relative standard deviations for all three identified peaks were less than 4%, indicating that chromatogram peaks from different laboratories can be identified using retention time.

Peak-area percentages of the three peaks listed above are summarized in Table 48. The statistical results were obtained by excluding results from participant E. Relatively large scatters (rel. σ = 12.48 and 15.60%) in peak-area percentages were obtained for the DDS peak and the resin advancement peak. Relatively good agreement was obtained for the MY 720 monomer peak (rel. σ = 8.59%).

The peak heights of the three peaks listed above were measured from the chromatogram. Peak-height ratios are summarized in Table 49. The interlaboratory agreement was improved slightly by measuring peak heights from the original chromatograms and calculating peak-height ratios.

Examination of the chromatograms obtained by the round-robin participants reveals a large variation in total appearance of the chromatograms and in peak resolution. Extra peaks were observed on the chromatograms shown in Figures 93 and 94. These extra components are likely to be contaminants.

The interlaboratory scatter in peak-area percentage data may be improved by:

●   Detector wavelength calibration—Since the molar extinction coefficients are different for the three components and also are different at each wavelength, significant data scatter among laboratories may result. The degree of scatter can be decreased by detector wavelength calibration.

●   Integrator specification—The integrator parameters, such as peak threshold, minimum peak area, and method of calculating unresolved peaks, need to be specified to obtain interlaboratory agreement.

An alternative approach to improving interlaboratory data agreement is to use a standard solution method. (Details of the procedure were described in Section 4.1.8.) Instruments are calibrated using a standard solution, and the response factor (peak area per milligram or peak height per milligram) of each ingredient is obtained. From the response factor for each ingredient, the weight percentages of the components in the unknown sample can be calculated.

4.4   TASK D—SECOND RESIN EVALUATION

The purpose of Task D was to verify the methods developed in the previous tasks using another resin system. The material chosen for this task was Hercules 3501-5A. This material was the same as that used by Grumman Aerospace Corporation under Contract F33615-77-C-5196 (ref 3). Eleven batches of Hercules 3501-5A graphite prepreg and eight batches of corresponding neat resin were sent to Boeing by Grumman. These systems are identified in Table 50.

Because of the differences in formulation between Narmco 5208 and Hercules 3501-5A, it was necessary to modify the methods developed for Narmco material. The following methods were investigated:

●   Liquid chromatography
●   Differential scanning calorimetry
●   Gel permeation chromatography
●   Ion chromatography
●   Physical and mechanical property testing

4.4.1 Liquid Chromatography

Selected batches of Hercules prepreg and neat resin were analyzed using the optimized reverse-phase LC method developed under Task A. The following parameters were used:

- Column: Waters μ-Bondapak/C_{18}
- Solvent: 63/37% CH_3CN/H_2O
- Flow rate: 1.5 ml/min
- Detector: UV, 220 nm

A typical chromatogram of the Hercules 3501-5A resin matrix is given in Figure 99. Peak-area ratios of the prepreg and neat resin batches evaluated are tabulated in Table 51.

The ratios of reaction product to MY 720 were consistently higher in the prepreg than in the neat resin, indicating that advancement occurred during the impregnation process. The correlation factor of neat resin to prepreg staging is 0.99, showing good consistency.

Efforts were made to modify the LC procedure to detect the boron trifluoride (BF_3) complex present in Hercules material. Pure standards of BF_3 monoethylamine were made in the standard mobile phase of 63/37% CH_3CN/H_2O. Injections were made on the reverse-phase C_{18} column. Both refractive index and UV detectors were evaluated. The UV detector at 190 nm had the greatest sensitivity. The BF_3 complex showed a single peak early in the chromatogram.

The effect of mobile-phase strength on the chromatogram was evaluated. Increasing the CH_3CN concentration caused the BF_3 to begin dropping out of solution. The standard mobile phase gave the best data with good peak resolution.

Problems were encountered in transferring the technique to the neat resin mix. Since BF_3-amine elutes at the very front of the chromatogram and is of such low concentration that detectability is marginal, the only way that its presence could be confirmed was to collect fractions and analyze for the presence of fluoride ion by ion chromatography. The presence of BF_3-amine in the initial portion of the chromatogram was confirmed by ion chromatography. Because of the marginal detection limits of BF_3 in the resin matrix, it was determined that the BF_3 concentration can best be monitored by ion chromatography of the resin itself.

4.4.2 Differential Scanning Calorimetry

The same method as developed under Task B was used. For comparison, a TSIR analysis of Hercules resin was performed with acetone extraction of the resin film on a salt block. All spectra were made at a heating rate of 10°C/min (18°F/min). Scans were made every 25°C (45°F) and are presented in Figures 100 through 104.

The TSIR spectra indicate the reaction beginning at approximately 100°C (212°F). This correlates quite well with the DSC scan (fig. 105), which shows initial baseline deviation at 101°C (213.8°F) and reaction onset at 115°C (239°F). As noted in the TGA scan (fig. 106), the reaction proceeds in several steps. The smaller exotherm occurring before the main reaction peak is probably due to the BF_3-amine complex.

The TSIR scans indicate the DDS beginning to react at approximately 150°C (302°F) and peaking between 225 and 250°C (437 and 482°F). This information also correlates with the DSC curve (fig. 105). where the main exotherm begins at 165°C (329°F) and peaks at 220°C (428°F). Finally, the TSIR analysis indicates some oxidation beginning after 250°C (428°F). This also can be seen on both the DSC curve (fig. 105), where a gradual exotherm begins at 264°C (507.2°F), and the TGA scan (fig. 106), where thermal degradation begins at 250°C (482°F).

Using the method developed for Narmco 5208, comparative DSC scans were made of Hercules resin batches 727-1A, 727-3A, and 727-7A. The scans are shown in Figures 107 through 109.

The DSC thermal scan readily detected differences between Narmco 5208 (fig. 50) and Hercules 3501-5A (fig. 105). However, formulation variations made within each resin system as defined by this contract were not detected. The optimized LC procedure is much more sensitive than the DSC method to small variations within the resin system.

4.4.3 Gel Permeation Chromatography

Selected batches of Hercules prepreg and neat resin were analyzed using the optimized GPC procedure developed in Task C. Parameters were as follows:

- Column: Shodex GPC A-802S
- Solvent: THF
- Flow rate: 1 ml/min
- Detector: UV, 220 nm

A typical chromatogram of Hercules resin batch 707-1A is shown in Figure 110. A summary of the peak-area-ratio results is contained in Table 52. Relative hardener concentration is indicated by the chromatogram peak-area ratio, DDS/MY 720, which correlates well with the supplier's information on resin variation. The greater ratio of the reaction product to MY 720 in the prepreg resin indicates that resin advancement occurred during the impregnation process.

4.4.4 Ion Chromatography

Ion exchange chromatography using electrical conductimetric detection was developed to quantitatively measure sulfur and fluorine in the resin matrix. Procedures are contained in Appendixes B and C. These procedures produce accurate results, assuming that no other source of sulfur or fluorine is present.

Selected batches were analyzed; data are presented in Table 53. There was considerable difference between reported and measured variation, especially in the BF_3-amine content.

To determine the accuracy of the data, the method was repeated using various standards of known concentration, as follows:

- Fluoride determination:

Peak height	Concentration
85 mm	0.8 mg/liter
27 mm	0.25 mg/liter
55 mm	0.5 mg/liter
80 mm	0.75 mg/liter

Determining linear regression:

$$Y = 1.34 + 105.06X$$
$$r = 1.00$$

where:

Y = peak height
X = concentration
r = correlation factor

Standards used:

- NBS 2143 p-fluorobenzoic acid
- Boron trifluoride monoethylamine
- Inorganic standards

- Sulfate determination:

Peak height	Concentration
14.5 mm	5 mg/liter
29.0 mm	10 mg/liter
60 mm	20 mg/liter

Determining linear regression:

$$Y = -1.00 + 3.04X$$
$$r = 1.00$$

where:

Y = peak height
X = concentration
r = correlation factor

Standards used:

- Thioacetamide
- 4,4-diaminodiphenylsulfone
- Inorganic standards

The correlation factor for both determinations was 1.00.

Other methods of determining sulfur and fluorine concentration were used for comparison. The method used with the LECO sulfur analyzer was ASTM D1552 (ref 4). In this method, the sample is burned in a stream of oxygen at a sufficiently high temperature to convert about 97% of the sulfur to sulfur dioxide. A standardization factor is used to obtain accurate results. The combustion products are passed into an absorber containing an acid solution of potassium iodide and starch indicator. A light blue color is developed in the absorber solution by the addition of standard potassium iodate solution. As combustion proceeds, bleaching the blue color, more iodate is added. The amount of standard iodate consumed during combustion is a measure of the sulfur content of the sample. The repeatability of this test, as given by ASTM D1552, should be within 0.05%. Our repeatability of 0.02% is well within these limits.

Table 54 presents a comparison of the data obtained by ion chromatography and using the LECO sulfur analyzer. Each data point represents an individual sample taken from the same roll of prepreg. The variability within the nine individual ion chromatograph readings is quite high, with a standard deviation of 0.16 and a relative standard deviation of 5.39%. Variations reported previously have been as high as 9.51%. The data from the LECO analyzer confirm the ion chromatography data with a variability between them of 2.5%.

The reproducibility of ion chromatography data on the same sample is very good, as shown by Table 55. This table contains results of analyses for sulfur and fluorine content conducted four times on the same sample.

The test data indicate considerable variability from area to area on a prepreg roll and within a batch. The variability is much greater for fluorine content than it is for sulfur content. The fluorine variability would be expected because of solubility problems in making the resin mix.

The sulfur content also was determined using LC. The LC data correlated quite well with the ion chromatography data, as shown in Table 56.

The fluorine contents of the standard Hercules batch and its formulation variations also were determined by neutron activation analysis. Neutron activation analysis was performed on a Texas Nuclear Model 150-1H neutron activation analyzer with fast (14-MeV) neutron flux. Results of the analyses are shown in Table 57. Good agreements were obtained between the reported and measured fluorine contents by both neutron activation analysis and ion chromatography.

To summarize the variability problem, the data indicate that there is considerable variation of the hardener and accelerator content within a roll. The fluorine variation is much greater than the sulfur variation, but this would be expected because of the solubility problems with BF_3-amine. Ion chromatography does give sulfur and fluorine concentrations accurately and, therefore, is a useful tool for testing and controlling the resin ingredients.

4.4.5 Physical and Mechanical Property Testing

Mechanical and physical property tests were performed on laminates of Hercules batches 707-1A, 727-3A, 727-7A, and 727-9A. The test matrix is shown in Table 58. Laminates were prepared using grade 145 graphite tape and the cure cycle shown in Figure 2. The physical property results are presented in Table 59. Short-beam-shear

strength, 0-deg compression modulus, and 90-deg tension stress, strain, and modulus results are shown in Tables 60, 61, and 62. Graphic representations of the mechanical test results at room temperature are shown in Figures 111 through 113.

Due to the large standard deviation of the mechanical test data, no obvious correlation could be established between chemistry variations and current mechanical tests.

4.5 TASK E—DYNAMIC MECHANICAL ANALYSIS (DMA)

As an alternative method of evaluating mechanical properties, dynamic mechanical analysis (DMA) of both Narmco and Hercules composites was performed.

The viscoelastic nature of polymers is unique in the field of material properties. Viscoelastic properties describe the time-temperature dependence of a polymer that could behave either as an elastic solid or as a viscous fluid. Understanding the viscoelastic behavior of polymers and its relation to molecular structure is essential to understanding both processing and end-use properties.

Measurement of viscoelastic properties is based on the difference in response of viscous and elastic elements to a sinusoidally varying strain. A material acting like a linear spring (elastic element) would give a resulting stress in phase with the applied strain. However, a material acting like a purely viscous element would produce a resulting stress 90 deg out of phase with the applied strain. A viscoelastic response, then, could be represented as shown in Figure 114. Also shown in Figure 114 is the resulting stress, which is resolved into the in-phase elastic (storage) modulus (G') and the out-of-phase viscous (loss) modulus (G"). The ratio G"/G' is designated as tan δ. The quantities G', G", and tan δ, when studied at controlled rates, temperatures, and time, have a significant relationship to the molecular structure.

Master curves of G' and tan δ of a typical polymer, as a function of temperature (T) and frequency (ω), are shown in Figure 115. Such curves may be separated into characteristic regions that are descriptive of the physical properties. At low temperatures or high frequencies, the material responds as if it were a glass. As the temperature is increased (or the frequency decreased), the polymer assumes a more flexible or "leathery" response, and tan δ goes through its principal maximum, which is frequently taken as glass transition temperature (T_g). This is followed by a relatively flat response in both tan δ and G', called the rubbery plateau. If the polymer is a true crosslinked rubber, the elastic modulus will actually increase slightly with temperature in this region, and the final two regions indicated in Figure 115 will be absent. If the polymer is a highly crosslinked material (e.g., epoxy thermoset), the rubbery plateau is frequently very small and is followed by a rapid decrease in G' and increase in tan δ.

The DMA tests were performed on a Rheometrics mechanical spectrometer (RMS). A schematic of RMS system flow and interconnection is illustrated in Figure 116. Testing is accomplished by controlling the amplitude and frequency of the sinusoidal deformation applied to the test sample and measuring the resultant deformation force. A direct-current torque motor used in an analog-position servomechanism applies the shear strain to the test sample. The strain program is selected by the operator and controlled by the central processor. To eliminate errors caused by servo dynamics, actual strain rather than commanded strain is used in the computation.

Deformation force is measured by a precise, very low-compliance transducer. Both the strain and the deformation forces are amplified and input to the central processor where they are used together with sample geometry to compute the dynamic viscosity or shear modulus.

The computer contains a sampling sine-wave correlator that is used in dynamic mode to reject both harmonics and noise and to separate the viscous and elastic components of the deformation force. Output data and graphs are provided by an online data terminal and X-Y plotter. The data terminal also is used by the operator to program the test profile and data output parameters.

Sample temperature can be programmed over a range of -150 to 400°C (-238 to 752°F). Both stepped and linear sweeps are provided. A platinum resistance thermocouple (PRT) located in the oven is used as the feedback element in an integral-plus-proportional temperature-control loop to provide temperature stability to within ±0.5°C (±0.9°F). An independent measurement of sample temperature is provided by a thermocouple imbedded in the upper test fixture and adjacent to the PRT element.

Test geometries for fluids and melts include the cone and plate, parallel plate, and couette. Solids in the form of fibers, films, rods, or bars can be accommodated by different test fixtures.

4.5.1 Resin Casts

Resin casts were made from Narmco standard and altered (+25% and -25% DDS concentration) resins. The dynamic mechanical properties of the resin casts were obtained using a torsional/rectangular mode with a test frequency of 1 Hz and a temperature range of -100 to 300°C (-148 to 572°F).

Elastic modulus (G') data obtained from the samples are shown in Figure 117. The sample with -25% DDS concentration showed a decrease in elastic modulus at a lower temperature than was observed for the samples with baseline or +25% DDS concentration. This result is what one would expect for a sample with a lower DDS concentration and, presumably, a lower crosslink density. At higher temperatures—approximately 220 to 240°C (428 to 464°F)—a sharp peak was observed in the samples with -25% and baseline DDS concentration, but not in the sample with +25% DDS concentration. Because these temperatures are high enough for secondary crosslinking to occur, the sample with high DDS concentration did not have sufficient amounts of uncrosslinked material in sufficiently close proximity to show the secondary crosslinking peak.

Figure 118 shows the viscous modulus (G") values for the tested matrix formulations. A large peak was observed for the samples with baseline and +25% DDS concentrations at approximately -60°C (-76°F); this has been labeled as a β transition. The sample with -25% DDS concentration showed two large peaks at approximately 166 and 220°C (331 and 428°F). The sample with baseline DDS concentration showed two peaks, the first at 220°C (428°F) and the second at 250°C (482°F). The sample with +25% DDS concentration showed only one peak at 240°C (464°F). Because G" values are proportional to the amount of energy dissipated in each cycle, these peaks represent increases in the energy dissipation at the test frequency of 1 Hz and at the indicated temperatures. The first high-temperature peak for the samples with -25% and baseline DDS concentration is suggested to be the normal glass transition peak for the

matrix material. The second high-temperature peak for these two samples is hypothesized to be due to the same secondary crosslinking reaction as described for the G' data above.

Using the above logic, the first high-temperature peak would be the α-transition peak of the native material, while the second peak would be the new α' peak for the more crosslinked material formed during the test cycle. Using the first high-temperature peak as an indicator of the glass transition of the original cured state of the material, the peak maximum temperature may be defined as a glass transition temperature (T_g). This yields T_g (low DDS) less than T_g (medium DDS) less than T_g (high DDS), which appears to be a sensible interpretation.

4.5.2 Epoxy Graphite Laminates

In previous testing of Narmco and Hercules solid laminates, difficulties were encountered in obtaining reproducible mechanical spectra. Sample slippage caused by temperature variation during testing was considered to be the major cause of the random data generation. Efforts were made to improve the sample gripping fixture, as shown in Figure 119.

Graphite laminates of the prepreg batches were fabricated using an eight-ply quasi-isotropic layup (0/±45/90/90/∓45/0) and cured according to Boeing material specification BMS 8-212D (ref 2). The laminates were machined to 3.25 x 1.15 x 0.10 cm (1.3 x 0.46 x 0.04 in.) and tested using the same torsional/rectangular mode as used for the resin casts. A temperature sweep from -100 to 300°C (-148 to 572°F) was performed with a 5°C (9°F) increment rise after a 1-min soak period. At least two runs were made on each laminate batch, and reasonably reproducible data were generated. The data generated were plotted by Interactive Graphic Display Analysis (IGDA) on a PDP 11/70 computer. The test matrix is shown in Table 63.

4.5.2.1 Unexposed Laminates

The G' and tan δ (G"/G') data for Narmco and Hercules laminates are graphically presented in Figures 120 through 125. A comparison of G' data obtained on Narmco and Hercules resin variations (figs. 120 and 122) did not reveal any chemistry alteration. However, the Narmco resin variations were revealed by tan δ comparisons (fig. 121). The differences appeared between 270 and 340°C (518 and 644°F) in Figure 121. Batch 1074, with the lowest hardener concentration, showed a delay signal indicating further cure compared to batches 1073 and 1076. The chemical variations in the Hercules prepreg batches were not revealed by either G' or tan δ comparisons (figs. 122 and 123). This could be due to the sensitivity of the DMA test to the chemistry of the graphite laminates. A comparison of G' data (fig. 124) obtained on standard Narmco and Hercules laminates indicates that Hercules standard laminates showed a sharp decrease in elastic modulus starting at about 180°C (356°F), leveling off between 225 and 275°C (437 and 527°F), and followed by another sharp decrease in modulus after 275°C (527°F). Narmco 5208 laminates showed one obvious sharp decline of modulus starting at about 225°C (437°F).

Comparison of the tan δ data (fig. 125) obtained on Narmco and Hercules laminates shows that the α-transition temperatures were 265 and 220°C (509 and 428°F), respectively. The upward trends after α transition for both Hercules and Narmco laminates indicate the possibility of either resin postcure or resin degradation during

the experiment. A rerun of the same laminate specimen with a decrease of the α-transition maximum is an indication of resin degradation rather than resin postcure, which should result in an increase in T_g.

4.5.2.2 Humidity-Exposed Laminates

The matrix of DMA testing on the moisture-exposed specimens of Narmco and Hercules laminates is shown in Table 63. Comparison of the test results shows that the chemistry variations present in Narmco and Hercules prepreg batches were not revealed by the elastic modulus (G') of the moisture-exposed specimens. The Narmco resin alterations, however, were shown partially by the tan δ comparison (fig. 126). As expected, batch 1076, with the highest DDS concentration, showed a higher α-transition maximum—250°C (482°F)—than did batches 1073 and 1074 with lower DDS concentration—235°C (455°F). The chemistry alterations in Hercules prepregs were not revealed by G' or tan δ (fig. 127).

The effect of loosely bonded water on the mechanical spectra was investigated by heating the moisture-exposed specimens in a 49°C (120°F) oven for 30 min. No difference was observed in either G' or tan δ for Hercules laminates. However, there was a 15°C (27°F) increase in T_g and a higher elastic modulus (G') at a fixed temperature for the oven-dried Narmco samples than for the moisture-exposed Narmco laminates.

Mechanical spectra of the humidity-exposed standard Narmco and Hercules composites are shown in Figures 128 and 129. As was observed in the unexposed laminates (fig. 124), there were two obvious transitions for Hercules and one for Narmco in the G' spectra (fig. 128). The tan δ comparison is shown in Figure 129. The Narmco material had a slightly higher T_g—235°C (455°F)—than did the Hercules material—220°C (428°F)—which also showed a second transition at 180°C (356°F) that was absent in the unexposed sample. The lower transition at 180°C (356°F) did not disappear in the oven-dried specimens. The significance of this transition was not investigated, although it appeared to be moisture related.

4.5.3 Laminate Thickness and Ply Orientation Effects

The effect of laminate thickness on mechanical properties was evaluated by fabricating laminates with 6, 8, and 10 plies of Hercules batch 707-1A graphite prepreg. Mechanical spectra are shown in Figure 130. Laminate thickness did not seem to affect the viscous modulus (G"). The lower G" obtained for a 10-ply laminate between 100 and 150°C (212 and 302°F) could be due to improper sample gripping during the test.

The effects of prepreg ply orientation in the laminates also were examined using unidirectional and quasi-isotropic specimens. A difference was observed between the two spectra shown in Figure 131. The significance of the difference needs to be evaluated further.

4.5.4 Neat Resin Complex Viscosity

Complex viscosity is derived as follows:

$$\eta = \frac{\left(G' + G''\right)^{1/2}}{\omega}$$

where:

η = complex viscosity, Pa·s
G' = elastic modulus, Pa
G'' = viscous modulus, Pa
ω = angular frequency, rad/s

Complex viscosity-versus-temperature (time) profiles of the Narmco altered neat resins were obtained using an RMS. Tests were performed with parallel plates using the following instrument parameters:

- Gap between plates: 0.5 mm (0.02 in.)
- Starting temperature: 50 ±2°C (122 ±3.6°F)
- Heating rate: 2°C/min (3.6°F/min)
- Mode of test: cure
- Frequency: 10 rad/s
- Strain: 75%

The mechanical spectrum of batch 293 (fig. 132) is included as an example. A summary of the preliminary analysis results is shown in Table 64.

For Narmco batches 289, 300, and 294, good correlation was established between DDS concentration and time span in the viscosity spectrum (fig. 132). (Time span is defined as the width, in minutes, of the viscosity profile at a fixed viscosity.) Narmco resin batches 290A and 293 did not always follow the trend (the higher the DDS concentration, the smaller the time span). It appears from the data in Table 64 that the viscosity-versus-temperature profiles are independent of the percentage strain.

More thorough investigation needs to be done to establish the usefulness of DMA as an analytical method for quality assurance of epoxy graphite composites.

4.5.5 Summary

The initial impression of this preliminary survey of DMA as a tool for quality assurance is not very encouraging. Resin matrices with known, substantially different amine concentrations showed almost identical variation in elastic and viscous modulus as a function of temperature (figs. 122 and 123). The only significant differences measured in the Narmco resin formulations (figs. 120 and 121) occurred when the composite specimens were heated to their decomposition temperature, where it was observed that the formulation with excess amine decomposed slightly faster and the one with deficient amine decomposed slower than the standard formulation. This is hardly a surprising result and offers little hope of providing a means for detecting accidental fluctuations in chemical composition.

DMA did clearly distinguish between the standard Narmco and Hercules resin matrices (figs. 124 and 125), but this also is not surprising since these resins have significantly different glass transition temperatures, which can be measured in a number of ways.

Exposure of samples to 100% relative humidity slightly lowered the glass transition temperature and induced a second transition or dispersion at 160 to 180°C (320 to 356°F). This secondary dispersion was much more pronounced in the Hercules than in the Narmco resins (fig. 129). Again, there was no distinctive difference in the behavior of the Hercules formulations (fig. 127), and the differences observed in the Narmco formulations (fig. 126) were consistent with the assumption that the added amine would produce a more highly crosslinked material that would be more resistant to the effects of moisture.

It would appear from the data generated in this program that DMA of composite materials offers little possibility for use as a means of quality assurance or control, since relatively large variations in the composition of the matrix produced only moderate or undetectable differences in the measured properties. We suggest that this might be a rather shortsighted conclusion, even though it is clearly supported by all the evidence presented.

Despite the experimental evidence to the contrary, we believe that it would be premature to conclude that DMA can make no contribution to quality assurance and control of epoxy composites. In the first place, all of the tests performed during this program were adapted directly from procedures designed for measuring the moduli of homogeneous materials. The composites used in this study were laid up in a quasi-isotropic form, where it is known that the fiber will dominate the measured moduli. Secondly, the RMS instrument was operated only in the rectangular/torsion mode, where the strain and strain rate vary nonuniformly throughout the specimen. Finally, and most importantly, the software furnished with the RMS was presumably designed to operate solely within the region of linear viscoelasticity. This software is not easy to change or even check, so it must be accepted largely on faith. In the low-amplitude or linear region of viscoelasticity, it is not too surprising to find that even substantial changes in the quantitative composition of the matrix polymer molecule do not have measurable effects. By varying the ply layup to one more favorable to the performance of the matrix; by using a tension-compression rather than a torsional mode; and, most of all, by extending measurements into the nonlinear viscoelastic region, it should be possible to devise new techniques that would be much more sensitive to fluctuations in the chemical and physical properties that determine the quality and performance of the epoxy matrix.

4.6 TASK F—FRACTURE TOUGHNESS

Positive correlation of mechanical properties with chemical composition has not been successfully accomplished for a variety of experimental parameters for Narmco 5208 (ref 5) and Hercules 3501-5A (ref 6). In Task F, a fracture mechanics approach was used to correlate mechanical properties with chemical composition. Mechanical property characteristics were monitored using the energy release rate of crack propagation, G_{IC}.

G is the "energy required to extend a pre-existing crack an infinitesimal unit of area" (ref 7). Following Ripling et al. (ref 5):

$$G = \frac{P^2}{2b} \left(\frac{\partial c}{\partial a}\right)_P$$

where:

P = load, kg
b = specimen width, cm
c = specimen compliance, Pa^{-1}
a = crack length, cm

Specimens were tested in mode I (opening mode) only, with G determined at the critical load for crack extension. Thus, G values for these conditions are labeled G_{IC} values.

Unlike most other traditional mechanical tests, G_{IC} measurements are not controlled by flaw sensitivity on the macroscopic scale. Conceptually, this removes one source of data scatter and should result in a more precise measurement. Boeing's experience has been that G_{IC} tests are among the most sensitive.

A width-tapered beam was used to test Hercules tapes. The samples were oriented such that the crack front extended perpendicular to the fiber orientation. This is the 0-deg case. Samples were laid up and cured at 177°C (350°F) in accordance with Boeing process specification BAC 5562 (ref 8). BAC 5562 covers processing of advanced composite structural parts at 177°C (350°F) cure. All samples were cured on the same caul plate in the same autoclave cycle to remove the possible effects of slight variations in cure cycles.

Table 65 shows the systems evaluated and the corresponding G_{IC} data. The G_{IC} values are low, indicating that the specimens were all quite brittle. These values are in the range expected from previous studies of similar systems. While it is tempting to speculate on differences between groups, the data scatter is too large to permit any conclusions.

Within the observed data scatter, the chemical alterations studied did not cause significant changes in the G_{IC} values. These specimens were all cured in the same autoclave cycle to remove any effects of altered cure cycles. Substantial undercure or overcure may cause observable changes between groups, although this is speculative.

Factors not varied in this study that could influence the toughness of these materials include resin content, fiber weave, and cure cycle.

Higher resin contents may be expected to increase the average interfiber and interlaminar spacing. Because these variables appear to affect the toughness of advanced composite systems, a higher resin content should increase the G_{IC} values. The intrinsic resin G_{IC} value will place an upper bound on the toughness achievable by such a method.

Fiber weaves affect the interlaminar G_{IC} values of advanced composites by altering the microscopic crack path length. As the crack front traverses the specimen, the fibers force the crack path to deviate and require more energy for propagation. This

increases the G_{IC} values. Fabrics, therefore, have higher G_{IC} values than do unidirectional tapes such as used here.

Cure cycles affect the final network structure of the matrix. Extreme undercuring should produce a tougher material at the expense of other mechanical properties and environmental durability. Overcuring should produce a more crosslinked network that would be expected to have lower G_{IC} values. However, because these materials already have a very low toughness, this effect may not be readily apparent as long as the overcure did not significantly degrade the material.

In summary, the chemical alterations of the Hercules materials did not correspond to the G_{IC} values of composites made with these materials. This is consistent with other mechanical property studies of related systems. These systems, in general, are fortunately insensitive to slight chemistry changes when the processing conditions are held at the nominal cure of Boeing process specification BAC 5562 (ref 8).

5.0 CONCLUSIONS

The analytical methods developed during this contract are very sensitive to formulation differences. The reverse-phase liquid chromatography method is extremely sensitive to quantitative changes, as well as to resin advancement. The ion exchange chromatography method quantitatively detects total fluorine and sulfur. The differential scanning calorimetry method readily differentiates between Narmco 5208 and Hercules 3501-5A; however, it is not as sensitive to quantitative changes in the resin as the two previously mentioned methods. Gel permeation chromatography gives a good fingerprint of the resin systems, but does not show the detail of the reverse-phase liquid chromatography method.

Mechanical tests and dynamic mechanical analysis had inherent problems in consistently detecting formulation differences during this program. These tests are very flaw sensitive in causing premature failure. For example, the contamination found in various resins can easily become a stress focal point for early failure. These inherent problems prevented us from obtaining the desired correlation with mechanical properties and analytical methods as developed. These mechanical tests do establish minimum test values, but are not sensitive to formulation changes. The formulation changes may have a drastic effect on long-term use properties that cannot be satisfactorily monitored by mechanical tests.

It is apparent from the results of this contract that some type of mechanical testing is necessary. However, to control formulation, the reverse-phase liquid chromatography and ion exchange chromatography techniques also are required. As a result of this contract, Boeing is presently using both chromatography techniques, as well as mechanical tests, to control various incoming resin systems.

In summary, the resin formulation variations were detected by analytical tests, but not by mechanical tests. Within the scope of this contract, the resin has been removed as a major source of variability. The recommended analytical tests for quality control of the resin are:

- Reverse-phase liquid chromatography
- Ion chromatography, if BF_3 is used

Boeing Commercial Airplane Company
   P.O. Box 3707
      Seattle, Washington 98124
        November 13, 1981

APPENDIX A

ROUND-ROBIN PROCEDURES FOR LIQUID CHROMATOGRAPHY, DIFFERENTIAL SCANNING CALORIMETRY, AND GEL PERMEATION CHROMATOGRAPHY

LIQUID CHROMATOGRAPHY (LC)

A. Column Calibration

1. Calibrate a Waters C_{18} column using the following parameters:

Column:	μ-Bondapak/C_{18}; 3.9-mm ID x 30 cm (0.156-in. ID x 12 in.); Waters #2724
Sample:	Dimethyl formamide (DMF), 3% Dimethyl pimelate (DMP), 5% Diethyl pimelate (DEP), 6% % = percent by volume in CH_3CN
Solvent:	60/40% CH_3CN/H_2O (water from J.T. Baker or Milli-Q-System was used) (use graduated cylinder for individual volume measurement; thorough mixing is essential for reproducibility)
Flow rate:	1 ml/min
Detector:	UV
Attenuation:	x 32
Injection volume:	5 μl
Chart speed:	5 cm/min (2 in./min)

2. Procedure:

    Prepare a sample of 3% DMF, 5% DMP, and 6% DEP in CH_3CN. Prepare, filter, and deaerate solvent (60/40% CH_3CN/H_2O). Using the above flow rate, detector, and chart settings, inject a 5-μl aliquot of sample and obtain a chromatogram as illustrated in Figure A-1. After converting retention times to retention volumes (V), calculate the following calibration parameters:

    - K_1 = capacity factor = $\dfrac{V_1 - V_0}{V_0}$

    where:

    V_1 = retention volume of DMP
    V_0 = retention volume of DMF
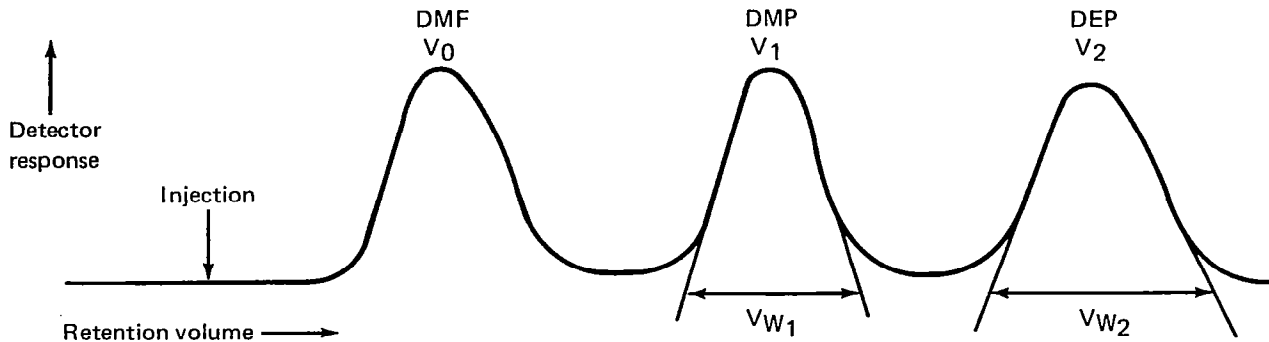
Figure A-1. Example LC Chromatogram for Column Calibration

- K_2 = capacity factor = $\dfrac{V_2 - V_0}{V_0}$

where:

V_2 = retention volume of DEP
V_0 = retention volume of DMF

- α = selectivity = K_2/K_1

- N_{DMP} = column plate count = $16\left(\dfrac{V_1}{V_{W_1}}\right)$

where:

V_1 = retention volume of DMP
V_{W_1} = baseline peak width of DMP

- N_{DEP} = column plate count = $16\left(\dfrac{V_2}{V_{W_2}}\right)$

where:

V_2 = retention volume of DEP
V_{W_2} = baseline peak width of DEP

- $R_S = \dfrac{1}{4}\left(\dfrac{\alpha - 1}{\alpha}\right)\sqrt{N_{DEP}}\left(\dfrac{K_2}{K_2 + 1}\right)$

3. Report:

K_1, K_2

α

N_{DMP}, N_{DEP}

R_S

B. Prepreg Analysis

1. Sample Preparation:

Dissolve 90 mg prepreg and 6 mg tri-p-tolyl phosphate (internal standard) in 15 ml solvent (63/37% CH_3CN/H_2O). Ensure dissolution by mechanical shaking for 10 min. Filter the solution through a 0.5-μm millipore FH filter.

2. Instrument Parameters:

Column:	Waters μ-Bondapak/C_{18}
Solvent:	Premixed 63/37% CH_3CN/H_2O (water from J.T. Baker Chemical Co. or Milli-Q-System was used)
Flow rate:	1.5 ml/min
Sample size:	5 μl
Detector:	UV, 220 nm (adjust attenuation so that the internal standard peak, retention time 13 to 14 min, is 55 to 75% of full scale)
Chart speed:	1 cm/min (0.4 in./min)

3. Procedure:

After preparing the sample and the solvent and setting the above instrument parameters, inject a 5-μl aliquot of sample and obtain a chromatogram. Using an integrating printer, obtain for each of the peaks the retention time and the peak-area percentage.

4. Report:

a. Chromatogram

b. Retention time and peak-area percentage from digital output

c. Manufacturer and model number of liquid chromatograph, detector, and integrator

d. Actual instrument parameters

DIFFERENTIAL SCANNING CALORIMETRY (DSC)

A. Machine Calibration

    1.   Standard reference materials: $KClO_4$ and indium

    2.   Instrument parameters:

        a.   DuPont 990

Heating rate:	20°C/min (36°F/min)
x-axis:	0.4 min/cm (1 min/in.) time base
y-axis:	temperature at 20°C/cm (90°F/in.)
y'-axis:	0.0017 W/cm (1.0 mcal/s/in.)

        b.   Perkin-Elmer DSC-1B/DSC-2

Heating rate:	20°C/min (36°F/min)
Range:	to keep on chart
Chart speed:	160 mm/min (6.3 in./min)

    3.   Record:

Indium weight, heating rate, range, and chart speed or x-axis, y-axis, and y'-axis.

B. Prepreg Analysis

    1.   Sample Preparation:

Dissolve 0.5g neat resin (or an amount of prepreg that contains an equivalent amount of resin) in 10 ml reagent-grade acetone. Centrifuge the sample for 20 min at 15 000 rpm. Decant the solution into an 8.9-cm (3.5-in.) diameter petri dish. Place under a vacuum of 71 cm (28 in.) Hg at 60 to 65°C (140 to 149°F) for 4 hr.

    2.   Instrument Parameters:

        a.   Dupont 990

Heating rate:	20°C/min (36°F/in.)
x-axis:	0.4 min/cm (1 min/in.) time base
y-axis:	temperature at 20°C/cm (90°F/in.)
y'-axis:	0.0017 W/cm (1.0 mcal/s/in.)

        b.   Perkin-Elmer DSC-1B/DSC-2

Heating rate:	20°C/min (36°F/min)
Range:	0.0068 to 0.034 W/cm (4 to 20 mcal/s/in.)
Chart speed:	20 mm/min (0.8 in./min)

3. Procedure:

Place approximately 4 mg dried resin into a DSC sample pan. Hermetically seal the sample pan and puncture a small hole in the lid to allow for outgassing.

Weigh the sample to the nearest 0.01 mg. Place 2.5 to 3.0 mg $KClO_4$ in the reference pan. Make the first run up to 350°C (662°F) with the sample and $KClO_4$. Make subsequent runs without the $KClO_4$.

Establish baseline on all runs except the initial calibration run. Allow the run to proceed until reaction is complete and baseline has stabilized. Cool the cell to at least 50°C (90°F) below reaction onset, then heat up again under the same conditions. Baseline will be as recorded by the second heatup.

4. Calculations:

Determine heat of polymerization, reaction temperature onset, reaction temperature peak, and reaction temperature endpoint. Determine the reaction temperature onset by the point of intersection of the baseline with a tangent drawn at its maximum slope of the front side of the curve. The reaction temperature peak is the point of intersection of two tangents drawn at maximum slope of the front and back sides of the curve. The reaction temperature endpoint is the intersection of the tangent on the back side of the curve to the baseline.

Overlay the baseline and sample curve and trace the baseline onto the sample curve. Measure the peak area with a planimeter or equivalent. Calculate the heat of polymerization from the recorded peak areas as follows:

a. DuPont 990:

$$\Delta H_p = \frac{(E)(A)(R)(S)(60)}{Wr}$$

where:

ΔH_p = heat of polymerization, J/kg (cal/g)
E = calibration coefficient of instrument
A = area under curve, cm^2 ($in.^2$)
R = range, x-axis, min/cm (min/in.)
S = sensitivity, y-axis, W/cm (mcal/s/in.)
W = sample weight, mg
r = heating rate, °C/min (°F/min)

b.   Perkin-Elmer DSC-1B/DSC-2

$$\Delta H_p = \Delta H_{in} \frac{\left(W_{in}\right) \left(A_{sam}\right) \left(R_{sam}\right) \left(S_{in}\right)}{\left(W_{sam}\right) \left(A_{in}\right) \left(R_{in}\right) \left(S_{sam}\right)}$$

where:

ΔH_p =   heat of polymerization, J/kg (cal/g)
W   =   weight, g
A   =   area, mm^2 ($in.^2$)
R   =   range, W (mcal/s)
S   =   chart speed, mm/min (in./min)

subscripts:

in   =   indium
sam   =   sample

5.   Reporting:

Record material identity, heat of polymerization, reaction temperature onset, reaction temperature peak, and reaction temperature endpoint. The data must be the average of three runs. Include all of the data charts for:

a.   Sample thermograms with machine parameters

b.   Baseline with machine parameters

c.   Indium curve with machine parameters

Sample curves are shown in Figures A-2 and A-3.
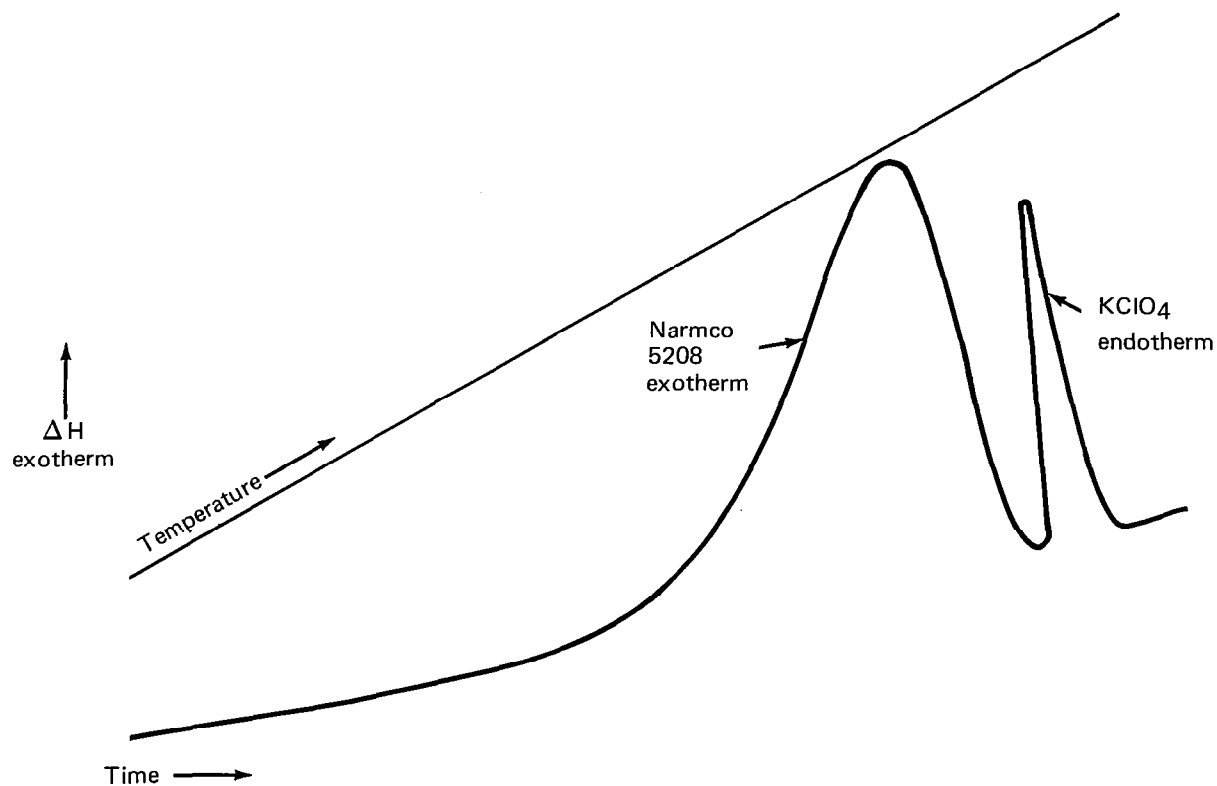
Figure A-2. Example DSC Curve—Resin and KClO₄ Standard
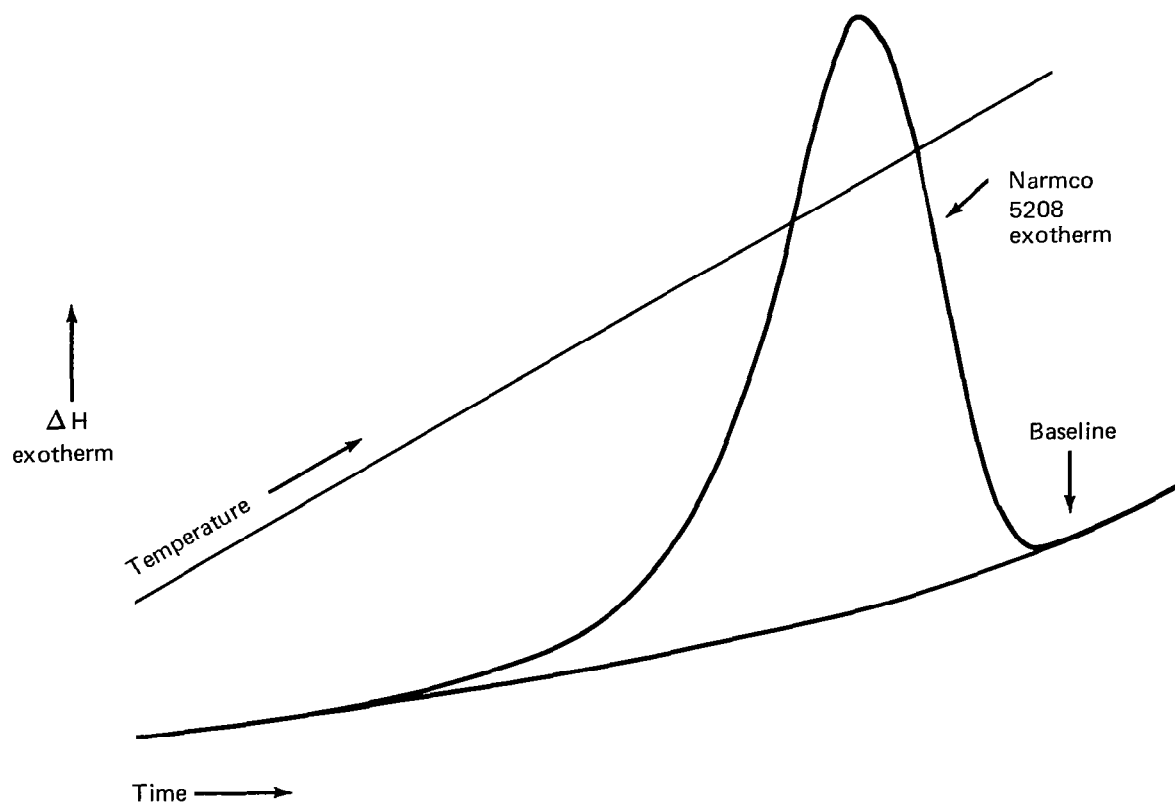
Figure A-3. Example DSC Curve—Resin and Baseline

52

GEL PERMEATION CHROMATOGRAPHY (GPC)

A. Column Calibration

1. Calibrate a Perkin-Elmer Shodex column using the following parameters:

Column:	Shodex GPC A-802/S (Perkin-Elmer #258-8286)
Sample:	o-dichlorobenzene (2 mg/ml THF)
Flow rate:	1 ml/min, THF
Detector:	UV, 254 nm (adjust attenuation so that largest peak is 60 to 80% of full scale)
Chart speed:	5 cm/min (2 in./min)
Injection volume:	5 µl

2. Procedure:

Prepare a sample by dissolving 2 mg o-dichlorobenzene in 1 ml THF. After setting the above instrument parameters, inject 5 µl of sample and obtain a chromatogram as shown in Figure A-4. After converting retention times to retention volumes (V), calculate the number of theoretical plates (N) as shown in Figure A-4.

$$N = 16\left(\frac{V}{V_W}\right)^2$$
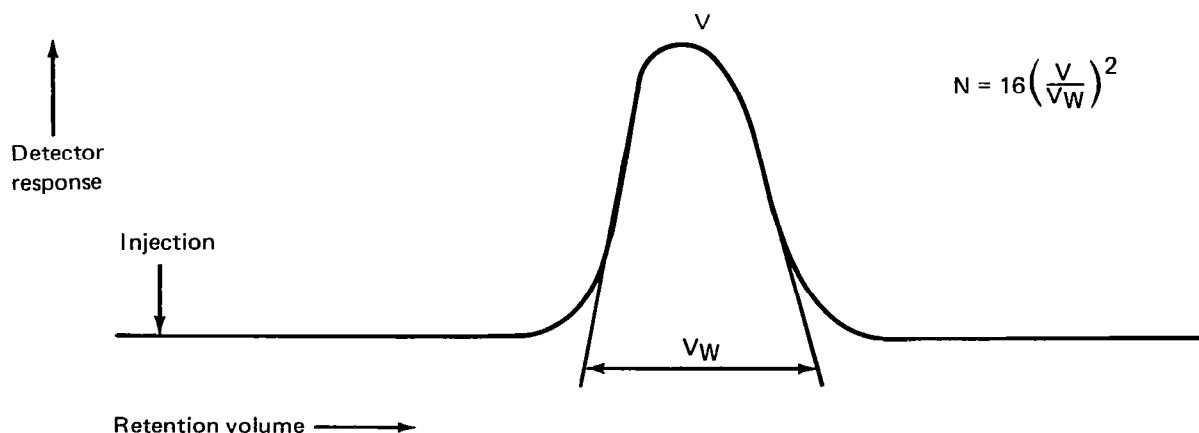
Figure A-4. Example GPC Chromatogram for Column Calibration

3. Report:

N (in duplicate)

B. Prepreg Analysis

1. Sample Preparation:

Dissolve 85 mg prepreg in 25 ml THF (0.15% by weight in resin). Ensure dissolution by mechanical shaking for 10 min. Filter the solution through a 0.5-μm millipore FH filter.

2. Instrument Parameters:

Column:	Shodex GPC A-802/S (Perkin-Elmer #258-8286)
Sample:	0.15% solution
Solvent:	THF
Flow rate:	1 ml/min
Injection volume:	5 μl
Detector:	UV, 220 nm (adjust attenuation so that the largest peak is 60 to 80% of full scale)
Chart Speed:	1 cm/min (0.4 in./min)

3. Procedure:

After preparing the sample and setting the above instrument parameters, inject 5 μl of sample and obtain a chromatogram. Using an integrating printer, obtain for each peak its retention time and its peak-area percentage.

4. Report:

a. Chromatogram

b. Retention time and peak-area percentage from digital output

c. Manufacturer and model number of liquid chromatograph, detector, and integrator

d. Actual instrument parameters

APPENDIX B

METHOD FOR DETERMINATION OF DIAMINODIPHENYLSULFONE (DDS) IN EPOXY RESINS BY ION CHROMATOGRAPHY

1.0 SCOPE

This method describes a procedure for the determination of diaminodiphenylsulfone $[(H_2NC_6H_4)_2(SO_2)]$ (DDS) in epoxy resin matrix by ion chromatography.

2.0 FACILITIES

    a.   Ion Chromatograph Model 10

        (1)   3 x 500-mm (0.12 x 20-in.) anion separator column

        (2)   3 x 150-mm (0.12 x 6-in.) anion precolumn

        (3)   6 x 250-mm (0.24 x 10-in.) anion suppressor column

    b.   Reagents

        (1)   Dapsone—99% minimum—Aldrich Chemical Co.

        (2)   Potassium sulfate (K_2SO_4)—Bakers analyzed only

        (3)   Hydrogen peroxide—30%—Bakers analyzed only

        (4)   Tetrahydrofuran (THF)—spectrophotometric grade

    c.   Combustion Apparatus

        (1)   Thomas Ogg oxygen flask infrared igniter

        (2)   Schoniger flask apparatus

        (3)   Sample wrappers—black filter paper flags

        (4)   Oxygen gas

3.0 REQUIREMENTS

3.1 Conditions

Perform the test on a suitable instrument while controlling the following variables:

    a.   Sample size (see Section 3.5.a)

    b.   Eluent (carrier solution): Dissolve 1.01g $NaHCO_3$ and 1.02g Na_2CO_3 in 4 liters of totally deionized (18MΩ) water. Mix thoroughly.

c. Pump stroke: 30%

d. Recorder speed: 1.27 cm/min (0.5 in./min)

e. Recorder: two pen; attenuation: x 100, x 50

f. Instrument attenuation: x 30

g. Sample loop: 100 µl

3.2 Procedure

a. Standards

Dapsone, 99% molecular weight (MW) 248.3 [$(H_2NC_6H_4)_2(SO_2)$], 12.89% sulfur, 11.28 nitrogen. Dissolve 0.7866g Dapsone in approximately 60 ml THF. Dilute to volume and mix thoroughly.

b. Sulfate: 1.00 mg SO_4/1.00 ml. Transfer 1.8142g potassium sulfate to a 1-liter volumetric flask containing 500 ml deionized water. Dilute to volume with deionized water and mix thoroughly.

3.3 Standard Curve

a. Using a 10.00-ml burette, transfer 2.5, 5.0, 10.0, and 15.0 ml standard sulfate solution (1.00 mg SO_4/1.00 ml) to 100-ml volumetric flasks containing approximately 60 ml standard eluent solution. Dilute to volume and mix thoroughly. The standards represent 2.5, 5.0, 10.0, and 15.0 mg sulfate per liter.

b. Inject each standard. Measure the peak height (in millimeters) from the baseline to the top of the peak. The baseline is drawn across the bottom of the peak tangent to the two shoulders. Plot the peak height in millimeters as the y-axis and milligrams per liter of sulfate as the x-axis.

3.4 Oxidizing Solution

Transfer 10 ml hydrogen peroxide solution to a 100-ml volumetric flask. Dilute to volume with eluent solution and mix thoroughly. Make fresh daily.

3.5 Preparation of Sample

a. Weigh and transfer the sample to a 100-ml Teflon beaker. As a guide to sample size, a 2% sulfur content should have a sample size of 1.0g. Add 25 ml THF and stir gently to speed dissolution. Transfer the solution quantitatively to a clean, dry, 50-ml volumetric flask. Dilute to volume and mix thoroughly.

b. Transfer three 100-µl samples to the appropriate black flags and allow the solvent to evaporate. Place the flags in the metal holders on the Schoniger flasks by folding the flags three times. Carry a blank through from here on with a sample flag.

56

c. Add 15 ml eluent-scrubber solution to four Schoniger flasks; avoid wetting the sides of the flasks.

d. Run a stream of oxygen gas (vigorously) into the Schoniger flasks for at least 15 s to displace the air. Avoid blowing the eluent solution up the sides of the flask. Quickly close the flask with the top assembly, then attach and tighten the screw clamp. Fix the clamp so that it is on the opposite side of the black flag.

e. Place the flask in the Thomas-Ogg infrared igniter facility. Adjust the flask so that the top of the black flag will be ignited first. This is done by setting the Variac to 50; then, while raising or lowering the lamp, push the on-off switch intermittently until the red light is focused at the top of the sample flag. Close the safety door. Set the Variac to 100. Switch the igniter on just enough to ignite the sample, then switch off. After ignition, remove the Schoniger flask and invert several times to wet the sides. Heat on a hot plate with the <u>lowest</u> setting for 30 min. Invert the flasks several times during the oxidation period to rinse the sides. Remove the flasks from the hot plate and cool. Remove the clamp and the ball joint closure. Rinse the closure with eluent into the flask. Place the flask on the steam bath and drive off the excess hydrogen peroxide as evidenced by no outgassing.

Carry all the flasks through in the above manner. Remove the flasks from the steam bath and allow to cool. Transfer the contents quantitatively to a clean, 50-ml volumetric flask. Dilute to the mark and mix thoroughly.

f. Inject the blank and samples using the operating conditions outlined in Section 3.1.

g. Calculations

    (1) Determine the peak height of the blank and samples as outlined in Section 3.3.b.

    (2) Subtract the blank from each sample.

    (3) From the standard curve of Section 3.3, determine the sulfate concentration of each sample.

    (4) Calculate percent sulfur as follows:

    $$S, \% = \frac{0.8345a}{W}$$

    where:

    a = milligrams of sulfate per liter of sample as derived from standard curve

    W = sample weight, mg

APPENDIX C

METHOD FOR DETERMINATION OF FLUORIDE IN ORGANIC COMPOUNDS BY ION CHROMATOGRAPHY

1.0 SCOPE

This method describes a procedure for the determination of fluoride in organic compounds by ion chromatography.

2.0 FACILITIES

a. Combustion flask, 500-ml, 100-ml Thomas-Ogg type with ball-joint stopper; A. H. Thomas Co., Philadelphia, PA

b. Combustion flask accessories and replacements, A. H. Thomas Co., Philadelphia, PA

c. Oxygen flask infrared igniter, Thomas-Ogg, A. H. Thomas Co., Philadelphia, PA

d. Combustion flask, Thomas Lisk type, 1000-ml complete with accessories, A. H. Thomas Co., Philadelphia, PA

3.0 REQUIREMENTS

3.1 Reagents

a. Hydrogen peroxide 30%—J. T. Baker only

b. Sodium carbonate reagent—J. T. Baker only

c. Sodium bicarbonate reagent—J. T. Baker only

d. Water—reagent grade Millipore Corp. (Milli-Q grade) or equivalent

e. Acetone reagent—J. T. Baker or equivalent

3.2 Miscellaneous

a. Steam table

b. Hot plate—Corning PC-35 or equivalent

c. Electrobalance, microbalance, Cahn Model 25

d. Analytical balance, ±0.1 mg Mettler or equivalent

e. Micropipettes, sizes as required

f.   Sample wrappers, black paper, unsized; 32 x 30-mm (1.26 x 1.18-in.) ignition area and 8 x 35-mm (0.31 x 1.38-in.) fuse length; A. H. Thomas Co., Philadelphia, PA

g.   Pinch clamp, size 12, screw type

h.   Volumetric flasks—sizes as required

i.   Wash bottles, polyethylene, squeeze-type, 500 ml

3.3   Preparation of Reagents

Eluent #1: To 4 liters reagent-grade water, add 1.0080g sodium bicarbonate and 1.0176g sodium carbonate. Mix thoroughly.

3.4   Method

a.   Direct ignition:

(1)   Using scissors or a scalpel, cut a sample of the material approximately 25 x 1 mm (1 x 0.04 in.). Fold the sample in the ignition flag (three folds) and place in the platinum basket-ground glass stopper assembly. NOTE: Avoid touching the flag and sample with the fingers. The assembly may be conveniently placed next to the oxygen gas source in a clean, dry, 100-ml graduate.

(2)   Carry the analysis through as outlined in Section 3.4.c.

b.   Indirect ignition:

(1)   Weigh and transfer an appropriate sample to a 50-ml Teflon beaker.

(2)   Add a suitable solvent that will dissolve the sample completely.

(3)   Transfer the sample quantitatively to a 50-ml volumetric flask, dilute to volume with the solvent, and mix thoroughly.

(4)   Using the microliter pipette, transfer 100 ml to an ignition flag.

(5)   Allow the solvent to evaporate and place in the metal holders on the Schoniger flasks by folding the flag three times. This should be done in triplicate.

(6)   Carry a blank through the procedure from this point on.

c.   Transfer 25 ml eluent and 3 ml 30% hydrogen peroxide solution to a Schoniger flask, being careful to avoid wetting the sides of the flask that may contact the ignition flag.

d.   Flush the Schoniger flask with oxygen gas vigorously for 1 min. Quickly seal the flask with the sample-glass stopper assembly using pinch clamps with a locking device.

e.   Ignite the flag with the infrared ignition device. Observe the ignition carefully. Any black smoke or soot formation indicates too large a sample size for the available oxygen. NOTE: Fire retardants in the material being tested will produce the same effect. In either case, the sample size must be reduced or the flask size increased.

f.   Following ignition, shake the flask vigorously to dislodge the platinum basket. The platinum aids the decomposition of the excess peroxide that must be removed prior to analysis.

g.   Warm the flask gently on the hot plate with intermittent shaking for 30 min.

h.   Remove the clamp assembly and place the flasks on a steam bath (preferably) or hot plate. Allow the hydrogen peroxide to decompose until there is no evidence of gassing while at elevated temperature. If the flasks are allowed to go dry, repeat the analysis. Rinse the sides of the flask with reagent-grade water.

i.   Transfer the solution quantitatively to a 50-ml volumetric flask. Dilute to volume with eluent and mix thoroughly.

3.5 Ion Chromatography

a.   Fluoride standards: Prepare a series of three fluoride standards required to bracket the concentration in the sample. Usually, 0.25 to 0.75 mg/liter fluoride will suffice.

b.   Normal operating procedures:

(1)   Attenuation: x 30

(2)   Flow rate: 30% pump stroke (approximately 2.3 ml/min)

(3)   Sample loop size: 100 µl

(4)   Recorder speed: 1.27 cm/min (0.5 in./min)

c.   Adjust the specific conduction meter to zero with the offset knob. Start the recorder.

d.   Load the sample into the chromatograph and inject when convenient. Push the "Pip" button to note the point of injection.

e.   Continue to inject the sample and standards. NOTE: There is no significant fluoride blank from the black flags; however, the hydrogen peroxide, if present, will indicate a "blank."

3.6 Calculations

a. Using a millimeter rule, measure the peak height of the standards and samples. The peak height is measured from the apex of the peak to the baseline and perpendicular to it. The baseline is a line drawn tangent to the two shoulders at the bottom of the peak.

b. Plot a fluoride curve from the prepared standards. Plot the peak height in millimeters as the y-axis and milligrams per liter of fluoride as the x-axis.

c. If a blank was run, subtract from the sample peak height.

d. Determine milligrams of fluoride per liter in samples from the standard plot.

e. Calculate percent fluorine as follows:

$$F, \% = \frac{2.5a}{W}$$

where:

a = milligrams of fluorine per liter in sample as derived from standard curve

W = sample weight, g

REFERENCES

1. McGann, T. W.: Chemical Composition and Processing Specifications for Air Force Advanced Composite Matrix Materials. AFML-TR-4180, February 1980.

2. Pryor, J. M.: Epoxy Preimpregnated Graphite Tapes and Woven Fabrics - 350°F (177°C) Cure. Boeing material specification BMS 8-212, September 30, 1977; cf., Boeing Commercial Aircraft Company: Advanced Composite Elevator for Boeing 727 Aircraft. NASA CR-159258, Vol. II - Final Report, November 1980.

3. Bortsell, H.: Chemical Composition and Processing Specifications for Air Force Advanced Composite Matrix Materials. AFML-TR-4166, November 1979.

4. Sulfur in Petroleum Products (High Temperature Method), Test Method for. ASTM D1522-79.

5. Ripling, S.; Mostovoy, E.; and Corten, H.: Fracture Mechanics: A Tool for Evaluating Structural Adhesives. J. Adhesion, Vol. 3, 1971, pp. 107-123.

6. Miller, A. G.; and Barbee, J. H.: The Correlation of Chemical Composition and Mechanical Properties of Epoxy Resins Used in Carbon/Epoxy Composites. SAMPE Proc., Vol. 24, Book 2, 1979, pp. 1223-1235.

7. Miller, A. G.; Hertzberg, P. E.; and Rantala, V. W.: Toughness Testing of Composites. SAMPE Quarterly, Vol. 12, January 1981, pp. 279-293.

8. Bannerman, W.; and Christensen, S.: Advanced Composite Structural Parts - 350°F (177°C) Cure. Boeing process specification BAC 5562, September 30, 1977; cf., Boeing Commercial Aircraft Company: Advanced Composite Elevator for Boeing 727 Aircraft. NASA CR-159258, Vol. II - Final Report, November 1980.

Table 1. Identification of Narmco Prepreg Batches

Resin batch number	Prepreg batch number	Resin formulation alterations
286	1072	No alteration, baseline standard 341-kg (750-lb) production batch
300	1073	No alteration, except smaller 136-kg (300-lb) production batch to represent the mass size of altered batches
290A	1074	The undercatalyzed nature of the resin batch is due to a low-amine-content hardener consolidated with major and minor epoxy constituents with a low epoxy equivalent weight mixed to nominal concentration levels
289	1075	The undercatalyzed nature of the resin batch due to a low-amine-content hardener consolidated with major and minor epoxy constituents with a low epoxy equivalent weight is amplified by varying the concentration level of the amine to specification minimum and the epoxies to specification maximum
293	1076	The overcatalyzed nature of the resin batch is due to a high-amine-content hardener consolidated with major and minor epoxy constituents with a high epoxy equivalent weight mixed to nominal concentration levels
294	1077	The overcatalyzed nature of the resin batch due to a high-amine-content hardener consolidated with major and minor epoxy constituents with a high epoxy equivalent weight is amplified by varying the concentration level of the amine to specification maximum and the epoxies to specification minimum

Table 2. Physical and Mechanical Test Matrix for Narmco Materials

Test	Number of specimens					
	Test temperature, dry			Test temperature, water saturated[a]		Total
	$-54°C$ $(-65°F)$	RT	$82°C$ $(180°F)$	RT	$82°C$ $(180°F)$	
Weight change	—	—	—	27	27	54
Thermal mechanical analysis	—	9	—	9	—	18
Fiber volume	—	9	—	—	—	9
Void content	—	9	—	—	—	9
Density	—	9	—	—	—	9
90-degree tension stress, modulus and strain	9	9	9	9	9	45
0-degree short-beam-shear strength	9	9	9	9	9	45
0-degree compression modulus	9	9	9	9	9	45

[a] Exposed to $49°C$ $(120°F)$ and 95% relative humidity until moisture equilibrium obtained (500 hr maximum)

Table 3. Physical Properties of Narmco Prepreg

Resin batch number	Prepreg batch number	Roll number	Volatile content, wt %	Resin content, wt %	Gel time, min	Resin flow, wt %
286	1072	64	0.36	35.9	31	17.8
300	1073	11	0.38	37.4	30	18.8
290A	1075	5	0.34	38.6	32	19.6
289	1074	7A	0.43	38.9	34	21.3
293	1076	5	0.33	37.5	29	18.9
294	1077	5	0.38	39.7	29	19.6

Table 4. Mechanical Properties of Narmco Unidirectional Laminates

Batch number	0-deg tension at RT			Short-beam-shear ultimate stress, MPa (lbf/in.^{2} x 10^3)			Fiber volume, %
	Ultimate stress, MPa (lbf/in.^{2} x 10^3)	Modulus, GPa (lbf/in.^{2} x 10^6)	Strain, μm/m	At -54°C (-65°F)	At RT	At 132°C (270°F)	
1072	1575 (228.460)	145.567 (21.115)	9 290	101.6 (14.740)	84.3 (12.230)	55.8 (8.100)	67.2
Rel. σ, %	2.9	4.5	3.2	18.9	7.8	10.2	—
1073	1543 (223.890)	130.469 (18.925)	10 660	126.7 (18.380)	102.9 (14.930)	67.3 (9.760)	65.3
Rel. σ, %	3.1	3.5	4.8	11.9	12.2	1.9	—
1074	1623 (235.370)	136.191 (19.755)	10 920	128.4 (18.620)	102.8 (14.920)	65.1 (9.440)	63.7
Rel. σ, %	4.0	4.5	1.8	7.5	3.8	11.8	—
1075	1572 (227.980)	138.452 (20.083)	10 560	138.4 (20.070)	95.3 (13.830)	66.2 (9.600)	62.5
Rel. σ, %	5.8	11.9	13.7	2.1	8.5	4.9	—
1076	1627 (236.020)	133.454 (19.358)	11 080	121.8 (17.670)	102.1 (14.810)	67.0 (9.720)	65.0
Rel. σ, %	4.9	7.6	8.0	20.7	8.7	2.4	—
1077	1599 (231.870)	131.276 (19.042)	11 180	135.7 (19.680)	102.4 (14.860)	66.4 (9.630)	63.8
Rel. σ, %	5.1	10.6	9.0	7.3	5.6	3.0	—

Table 5. Short-Beam-Shear Strength, Narmco Laminates

Batch number	Short-beam-shear strength, MPa (lbf/in.^{2} x 10^3)				
	Test temperature, dry			Test temperature, water saturated[a]	
	−54°C (−65°F)	RT	82°C (180°F)	RT	82°C (180°F)
1072	106.355 (15.425)	87.222 (12.650)	73.197 (10.616)	78.603 (11.400)	66.744 (9.680)
Rel. σ, %	11.7	9.6	8.1	−	−
1074	125.289 (18.171)	100.377 (14.558)	84.905 (12.314)	97.075 (14.079)	71.281 (10.388)
Rel. σ, %	9.5	10.6	8.1	7.6	4.2
1077	129.061 (18.718)	107.341 (15.568)	84.085 (12.195)	97.385 (14.124)	72.935 (10.578)
Rel. σ, %	4.0	1.7	3.5	3.2	2.2

[a]Exposed to 49°C (120°F) and 95% humidity until moisture equilibrium obtained (500 hr maximum)

Table 6. 0-deg Compression Modulus, Narmco Laminates

Batch number	0-deg compression strength, GPa (lbf/in.^{2} x 10^6)				
	Test temperature, dry			Test temperature, water saturated[a]	
	−54°C (−65°F)	RT	82°C (180°F)	RT	82°C (180°F)
1072	120.959 (17.543)	117.229 (17.002)	112.844 (16.366)	120.904 (17.535)	114.436 (16.597)
Rel. σ, %	7.6	5.8	4.6	6.1	4.7
1074	176.995 (25.670)	125.951 (18.267)	123.710 (17.942)	114.347 (16.584)	119.263 (17.297)
Rel. σ, %	19.4	9.8	6.3	7.4	6.6
1077	164.556 (23.866)	125.730 (18.235)	141.416 (20.510)	103.060 (14.947)	105.756 (15.338)
Rel. σ, %	26.3	9.8	19.2	8.6	6.7

[a]Exposed to 49°C (120°F) and 95% relative humidity until moisture equilibrium obtained (500 hr maximum)

Table 7. 90-deg Tension Stress, Modulus, and Strain, Narmco Laminates

Batch number	Test	Test temperature, dry			Test temperature, water saturated[a]	
		−54°C (−65°F)	RT	82°C (180°F)	RT	82°C (180°F)
1072	Stress, MPa	27.346	31.069	21.974	25.705	24.801
	(lbf/in.^{2} x 10^3)	(3.966)	(4.506)	(3.187)	(3.728)	(3.597)
	Rel. σ, %	26.0	18.8	14.0	24.5	12.5
	Modulus, GPa	9.067	8.584	7.350	7.840	6.254
	(lbf/in.^{2} x 10^6)	(1.315)	(1.245)	(1.066)	(1.137)	(0.907)
	Rel. σ, %	4.9	8.0	2.4	4.7	6.9
1074	Stress, MPa	24.201	27.504	21.671	28.104	24.629
	(lbf/in.^{2} x 10^3)	(3.510)	(3.989)	(3.143)	(4.076)	(3.572)
	Rel. σ, %	47.5	21.8	7.5	12.3	21.6
	Modulus, GPa	11.335	9.763	7.109	7.750	6.109
	(lbf/in.^{2} x 10^6)	(1.644)	(1.416)	(1.031)	(1.124)	(0.886)
	Rel. σ, %	43.9	7.8	5.6	10.3	11.4
	Strain, μm/m	1893	2224	3080	−	−
	Rel. σ, %	17.6	26.2	10.2		
1077	Stress, MPa	22.960	19.030	23.367	28.794	27.256
	(lbf/in.^{2} x 10^3)	(3.330)	(2.760)	(3.389)	(4.176)	(3.953)
	Rel. σ, %	21.4	15.4	19.2	17.9	8.6
	Modulus, GPa	10.418	8.109	6.743	8.267	6.378
	(lbf/in.^{2} x 10^6)	(1.511)	(1.176)	(0.978)	(1.199)	(0.925)
	Rel. σ, %	8.3	4.3	8.6	18.6	22.6
	Strain, μm/m	1914	2340	3456	−	−
	Rel. σ, %	23.7	15.5	19.6		

[a]Exposed to 49°C (120°F) and 95% relative humidity until moisture equilibrium obtained (500 hr maximum)

Table 8. Test Matrix of Mobile-Phase Evaluation by TLC

Mobile phase	Flow rate, ml/min	Column		
		Merck RP-2	Merck RP-8	Waters μ-Bondapak/C_{18}
0.2% $CH_3OH/CHCl_3$	2	–	–	x
0.2% $CH_3OH/CHCl_3$	1	x	x	x
0.2% $CH_3OH/CHCl_3$	0.5	x	–	–
100% CH_3OH	1	x	–	–
100% $CHCl_3$	1	x	–	–
2% $CH_3OH/CHCl_3$	1	x	–	x

Table 9. Test Matrix of Flow-Rate and Detector Evaluation

Flow rate, ml/min	Sample		Detector wavelength		Figure number
	MY 720	Narmco batch 286	254 nm	280 nm	
0.5	–	x	–	x	16
1	x	–	–	x	13
1	–	x	–	x	14
1	–	x	x	–	17
2	–	x	–	x	15

Mobile phase: THF/$CHCl_3$, 50/50%, isocratic

Table 10. Mobile-Phase Variations

Mobile phase number	Solvent	Gradient profile	Flow rate, ml/min
1	24/82% CH_3CN/H_2O in 20 min	Linear	2.0
2	30/70% CH_3CN/H_2O in 15 min	Linear	1.8
3	40/80% CH_3CN/H_2O in 10 min	Concave	2.0

Table 11. Plate-Count Measurements on Reverse-Phase Columns

Column	Plate count
Waters μ-Bondapak/C$_{18}$ (10 μm)	4760
Whatman Partisil 10, ODS-2 (10μm)	5560
Merck Lichrosorb RP-8 (5μm)	8690
Merck Lichrosorb RP-2 (10 μm)	2355
Merck Lichrosorb RP-8 (10 μm)	3610

Table 12. Results of Comparison of Reverse-Phase Columns

Parameter	μ-Bondapak/ C$_{18}$	Lichrosorb RP-8 (5 μm)	Partisil 10-ODS-2	Lichrosorb RP-8 (10 μm)	Lichrosorb RP-2 (10 μm)
Figure number	24	25	26	27	28
Time, min[a]	20	19	24	19	18
Ability to resolve reaction product peak, rank (visual)	2	3	1	4	3
Internal standard interference (benzaldehyde)	No	No	Yes	No	No
Ability to resolve end group, rank (visual)[b]	2	1	3	3	4

[a] Time taken to complete a chromatogram

[b] Resolution of the four peaks shown near the end of the chromatogram

Table 13. Results of Comparison of Reverse-Phase Columns Using Mobile Phase 1

Parameter	Column		
	μ-Bondapak/ C_{18}	Lichrosorb RP-8	Partisil 10-ODS-2
Figure number	29	30	31
Time, min[a]	20	20	25
Ability to resolve reaction product peak, rank (visual)	2	3	1
Internal standard interference (benzaldehyde)	No	No	Yes
Ability to resolve end group, rank (visual)[b]	2	1	2

[a]Time taken to complete a chromatogram

[b]Resolution of the four peaks shown near the end of the chromatogram

Table 14. Effect of Flow-Rate Variation on Retention Time and Peak Area

Flow rate ml/min	Retention time, min			Peak area, %			CDS 111 integration, μV·s		
	DDS	MY 720	Reaction product	DDS	MY 720	Reaction product	DDS	MY 720	Reaction product
1.0	8.81	20.34	19.38	48.70	23.49	4.76	12 021 833	5 799 498	1 173 964
1.5	5.92	16.59	15.89	50.14	24.34	5.74	7 937 185	3 852 484	909 358
1.8	4.89	15.14	14.58	51.17	24.40	3.87	6 678 859	3 184 015	505 311
2.0	4.44	14.53	14.02	51.01	24.34	3.74	6 087 096	2 903 995	445 968
2.5	3.62	13.16	12.80	50.65	25.06	3.65	4 841 397	2 395 650	349 183

Table 15. Sample Area Integration

Attenuation	Integration, µV·s		
	Integrator model		
	835	837	Spectra 2
1	50 955	71 340	45 823
2	35 042	38 243	23 642
4	26 293	20 795	12 204
8	12 298	11 351	9 419
16	5 514	6 707	5 162
32	3 412	4 030	1 749
64	1 571	1 739	862
128	421	449	—
256	556	368	185

Table 17. Results of LC Analysis of Narmco Neat Resin Batches

Batch number	DDS/MY 720 absorbance ratio (a)	DDS/MY 720 peak-area ratio (a)
294	2.819	2.288
293	2.626	2.127
286	2.551	2.048
300	2.363	1.838
290A	2.035	1.700
289	1.985	1.560

a Numbers recorded are average of two runs

Table 18. Results of LC Analysis of Narmco Graphite Prepreg Batches

Batch number	DDS/MY 720 absorbance ratio (a)	DDS/MY 720 peak-area ratio (a)
1077	2.758	2.493
1076	2.503	2.256
1072	2.371	2.147
1073	2.180	1.922
1075	2.156	1.890
1074	1.840	1.603

a Numbers recorded are average of two runs

Table 16. Comparison of Attenuation of SP-4000 and HP-3380 Integrators

Run number	Integrator Model			
	SP-4000		HP-3380	
	Retention time, s	Peak area	Retention time, min	Peak area
1	238	36 119	3.99	36 292
	418	740	6.97	719
	461	576	7.72	598
	889	4 701	14.85	4 645
	922	8 529	15.39	9 450
	961	173	16.02	154

Retention time
$$Y = -1.37 + 60.01X$$
$$r = 999.99620 \times 10^{-3}$$

Peak area
$$Y = -117.99 + 0.99X$$
$$r = 999.65253 \times 10^{-3}$$

Run number	Retention time, s	Peak area	Retention time, min	Peak area
2	123	6	2.08	342
	313	47 675	5.24	44 154
	415	30	7.76	443
	503	789	8.39	762
	658	1 232	10.99	1 220
	865	1 197	14.46	1 275
	891	3 819	14.86	4 294
	926	9 091	15.44	10 115
	1096	301	18.69	300
	1151	824	19.31	184
	1176	783	19.62	177

Retention time
$$Y = -10.69 + 60.21X$$
$$r = 999.03320 \times 10^{-3}$$

Peak area
$$Y = -188.13 + 1.07X$$
$$r = 999.84764 \times 10^{-3}$$

Run number	Retention time, s	Peak area	Retention time, min	Peak area
3	243	46 712	4.09	45 233
	422	381	7.08	386
	469	636	7.86	665
	878	345	14.67	159
	903	4 985	15.09	4 831
	937	10 084	15.66	11 177
	975	216	16.29	190
	1143	1 241	19.69	204
	1201	2 635	20.01	205

Retention time
$$Y = 4.46 + 59.21X$$
$$r = 999.44069 \times 10^{-3}$$
Peak area
$$Y = 357.79 + 1.02X$$
$$r = 997.77617 \times 10^{-3}$$

X = correlation, HP-3380
Y = correlation, SP-4000
r = correlation factor

Table 19. Results of HPLC Analysis of Narmco Resin Batches

Batch number	Peak-area ratio	
	DDS/MY 720	Reaction product/ MY 720
1074	0.585	0.169
1075	0.688	0.134
1072	0.753	0.114
1073	0.698	0.139
1076	0.812	0.098
1077	0.969	0.120

Table 20. Results of LC Reproducibility Check

	MY 720	DDS	Reaction product
Retention time, min			
$\bar{x}$	15.23	5.01	14.67
σ	0.07	0.08	0.07
Rel. σ, %	0.5	1.5	0.5
Peak area, %			
$\bar{x}$	28.23	51.83	—
σ	0.74	0.73	—
Rel. σ, %	3	1.4	—

Table 21. Quantification of Second Resin in Narmco Matrix

	Resin batch 286	Prepreg batch 1072
Unreacted second resin in the matrix, wt %	6.71 7.06	6.35 6.67 7.07
Range, %	0.35	0.72

Table 22. Comparison of DDS Concentration by IR and Ion Chromatography

Batch number	DDS concentration, wt % (by IR)	DDS concentration, wt % (by ion chromatography)
289	20.35	20.48
300	21.15	21.49
286	22.40	21.96
290A	22.15	22.03
293	—	22.89
294	24.10	25.06

Table 23. LC Instrumentation Used by Round-Robin Participants

Participants	Liquid chromatograph	Detector	Integrator
Army Materials and Mechanics Research Center	Waters GPC/ALC 244	Perkin-Elmer LC 75, variable UV	Spectra Physics SP-4000 data system
Boeing Aerospace Company, Quality Control	DuPont Model 850	DuPont Spectra 2	Spectra Physics SP-4000
Boeing Commercial Airplane Company, Materials Technology	Waters ALC/GPC 244	Waters Model 450, variable wavelength	Varian CDS-111
Boeing Commercial Airplane Company, Quality Control Research & Development	Waters ALC/GPC 244	Waters Model 450, variable wavelength	PDP 11/34 minicomputer
Ciba-Geigy Corporation	Masters Model 6000A pump with UGK injector	Schoeffel SF 770 spectro-flow monitor	Spectra Physics minigrator
Hercules, Inc.	Waters Associates 6000A pump, 660 solvent programmer, Rheodyne 7120 variable injection valve	Varian-Aerograph VUV-10 Varichrome, variable wavelength	IBM System 7 Integrator
Narmco Materials	Spectra Physics SP-8000 Model #SP8000-BFGA	Kipp detector #SF 770 monitor + SFA 339 drive	Spectra Physics SP-4000 integrator system
NASA-Langley Research Center	Waters Associates ALC 202/R401 HPLC	Waters Model 450, variable wavelength	Spectra Physics Autolab System I
Lockheed Missiles and Space Company	Waters Model 244	Varian Varichrome, variable UV	Hewlett-Packard Model 3385A automation system
Rockwell Science Center	—	—	—

Table 24. Retention-Time Data Obtained by LC Round-Robin Participants

Participant	Retention time, min		
	DDS major component peak	Resin advancement peak	MY 720 monomer peak
A	2.25	3.57	4.50
B	2.70	4.17	5.17
C	2.74	4.55	5.74
D	2.33	3.77	4.72
E	2.16	3.73	4.21
F	2.40	4.08	5.21
G	—	—	—
H	2.35	3.95	4.92
I	2.25	3.69	4.56
J	2.33	3.90	4.91
$\bar{x}$	2.39 (2.35)[a]	3.93 (3.86)[a]	4.88 (4.77)[a]
σ	0.188 (0.151)[a]	0.282 (0.191)[a]	0.429 (0.322)[a]
Rel. σ, %	7.87 (6.4)[a]	7.18 (4.95)[a]	8.79 (6.75)[a]

[a] Values obtained by disregarding data from participant C

Table 25. Peak-Area Data Obtained by LC Round-Robin Participants

Participant (a)	Peak area, %		
	DDS major component peak	Resin advancement peak	MY 720 monomer peak
A (6)	29.06	5.79	42.60
B (4)	35.85	6.02	41.93
C (4)	33.93	3.10	53.45
D (3)	30.43	4.78	37.53
E (2)	32.70	4.15	42.29
F (6)	34.86	5.10	42.71
G	—	—	—
H (1)	24.75	4.25	44.75
I (2)	31.37	4.80	39.39
J (3)	24.90	6.51	49.01
$\bar{x}$	30.87 (30.48)[b]	4.94 (5.18)[b]	43.74 (42.53)[b]
σ	3.80 (3.86)[b]	0.995 (0.797)[b]	4.57 (3.21)[b]
Rel. σ, %	12.30 (12.66)[b]	20.15 (15.39)[b]	10.45 (7.55)[b]

[a] Numbers in parentheses refer to number of runs

[b] Values obtained by disregarding data from participant C

Table 26. Peak-Area-Ratio Data Obtained by LC Round-Robin Participants

Participant (a)	Peak-area ratio	
	DDS major component/ MY 720 monomer	Resin advancement/ MY 720 monomer
A (6)	0.684	0.136
B (4)	0.855	0.144
C (4)	0.635	0.058
D (3)	0.811	0.127
E (2)	0.773	0.108
F (6)	0.816	0.120
G	—	—
H (1)	0.553	0.095
I (2)	0.796	0.122
J (3)	0.508	0.133
$\bar{x}$	0.714 (0.724)[b]	0.116 (0.123)[b]
σ	0.118 (0.121)[b]	0.025 (0.014)[b]
Rel. σ, %	16.53 (16.71)[b]	21.56 (11.38)[b]

[a] Numbers in parentheses refer to number of runs

[b] Values obtained by disregarding data from participant C

Table 27. Column-Efficiency Data Obtained by LC Round-Robin Participants

Participant	K_1	K_2	α	N_{DMP}	N_{DEP}	R_S
A	0.56	1.13	2.01	2120	1495	2.58
B	0.58	1.21	2.09	2013	2149	3.30
C	0.56	1.19	2.11	2803	3434	4.19
D	0.62	1.20	1.96	5240	5780	5.08
E	0.45	0.91	2.05	1662	2151	2.83
F	0.99	1.82	1.83	3798	4276	4.68
G	—	—	—	—	—	—
H	0.80	1.55	1.94	3410	2605	3.76
I	0.60	1.18	1.98	5162	5025	4.75
J	0.59	1.21	2.05	2921	2984	3.83
$\bar{x}$	0.64	1.27	2.00	3236.56	3322.11	3.89
σ	0.16	0.26	0.09	1302.74	1439.53	0.87
Rel. σ, %	25.02	20.77	4.32	40.25	43.33	22.41

Table 28. Reduction in Variability of Retention-Time Data Obtained
with Controls on Column Capacity, Selectivity, Efficiency, and Resolution

Participant	Retention time, min		
	DDS component	Resin advancement	MY 720 monomer
B	2.70	4.17	5.17
D	2.33	·3.77	4.72
I	2.25	3.69	4.56
J	2.33	3.90	4.91
$\bar{x}$	2.40	3.88	4.84
σ	0.20	0.21	0.26
Rel. σ, %	8.41	5.42	5.42

Table 29. Reduction in Variability of Peak-Area Data Obtained with
Controls on Column Capacity, Selectivity, Efficiency, and Resolution

Participant	Peak area, %		
	DDS component	Resin advancement	MY 720 monomer
B	35.85	6.02	41.93
D	30.43	4.78	37.53
I	31.37	4.80	39.39
J	24.90	6.51	49.01
$\bar{x}$	30.64	5.53	41.97
σ	4.50	0.87	5.03
Rel. σ, %	14.86	15.82	11.99

Table 30. Summary of Variability in Retention-Time and
Peak-Area Data Obtained With and Without Column Controls

	Retention time, min		Peak area, %	
	All data	Specified columns	All data	Specified columns
DDS				
$\bar{x}$	2.39	2.40	30.87	30.64
σ	0.20	0.20	4.03	4.50
Rel. σ, %	8.36	8.41	13.07	14.68
Resin advancement				
$\bar{x}$	3.93	3.88	4.94	5.93
σ	0.30	0.21	1.06	0.87
Rel. σ, %	7.63	5.42	21.36	15.82
MY 720				
$\bar{x}$	4.88	4.84	43.74	41.97
σ	0.46	0.26	4.85	5.03
Rel. σ, %	9.32	5.42	11.09	11.99

Table 31. Reduction in Variability of Retention-Time Data
Obtained with Minimum Plate Count of 2500

Participant	Retention time, min		
	DDS component	Resin advancement	MY 720 monomer
C	2.74	4.55	5.74
D	2.33	3.77	4.72
F	2.40	4.08	5.21
H	2.35	3.95	4.92
I	2.25	3.69	4.56
J	2.33	3.90	4.91
$\bar{x}$	2.40	3.99	5.01
σ	0.17	0.31	0.42
Rel. σ, %	7.23	7.68	8.36

Table 32. Reduction in Variability of Peak-Area Data
Obtained with Minimum Plate Count of 2500

Participant	Peak area, %		
	DDS component	Resin advancement	MY 720 monomer
C	33.93	3.10	53.45
D	30.43	4.78	37.53
F	34.86	5.10	42.71
H	24.75	4.25	44.75
I	31.37	4.80	39.39
J	24.90	6.51	49.01
$\bar{x}$	30.04	4.76	44.47
σ	4.35	1.11	5.97
Rel. σ, %	14.49	23.39	13.43

Table 33. Summary of Variability in Retention-Time and
Peak-Area Data Obtained With and Without Plate-Count Controls

	Retention time, min		Peak area, %	
	All data	Minimum plate count of 2500	All data	Minimum plate count of 2500
DDS				
$\bar{x}$	2.39	2.40	30.87	30.04
σ	0.20	0.17	4.03	4.35
Rel. σ, %	8.36	7.23	13.07	14.49
Resin advancement				
$\bar{x}$	3.93	3.99	4.94	4.76
σ	0.30	0.31	1.06	1.11
Rel. σ, %	7.63	7.68	21.36	23.39
MY 720				
$\bar{x}$	4.88	5.01	43.74	44.47
σ	0.46	0.42	4.85	5.99
Rel. σ, %	9.32	8.36	11.09	13.43

Table 34. Statistical Evaluation of DSC Analysis Results

Sample number	Sample weight, mg	ΔH_p, J/kg (cal/g)		$T_{o'}$ °C (°F)		$T_{p'}$ °C (°F)		$T_{e'}$ °C (°F)	
1	8.44	613 366	(146.5)	203	(397)	263	(505)	272	(521)
2	7.80	613 366	(146.5)	204	(399)	264	(507)	274	(525)
3	7.58	630 950	(150.7)	204	(399)	265	(509)	274	(525)
4	8.02	651 466	(155.6)	205	(401)	264	(507)	273	(523)
5	8.32	597 875	(142.8)	205	(401)	264	(507)	274	(525)
Total		3 107 023	(742.10)	—	—	—	—	—	—
$\bar{x}$		621 404	(148.42)	204.2	(399.4)	264	(507)	273.4	(523.8)
σ		20 480	(4.89)	0.84	(1.67)	0.71	(1.41)	0.89	(1.79)
6	8.10	638 068	(152.4)	202	(396)	264	(507)	273	(523)
7	8.09	638 068	(152.4)	204	(399)	263	(505)	273	(523)
8	8.33	638 068	(152.4)	203	(397)	263	(505)	273	(523)
9	7.59	648 535	(154.9)	204	(399)	264	(507)	273	(523)
10	8.24	655 653	(156.6)	204	(399)	263	(505)	273	(523)
Total		3 218 392	(768.70)	—	—	—	—	—	—
$\bar{x}$		643 678	(153.74)	203.4	(398)	263.4	(505.8)	273	(523)
σ		8 084	(1.93)	0.89	(1.79)	0.55	(1.10)	0	(0)
Grand total		6 325 415	(1510.80)	—	—	—	—	—	—
Grand $\bar{x}$		632 542	(151.08)	203.8	(398.7)	263.7	(506.4)	273.2	(523.4)
Grand σ		18 795	(4.49)	0.92	(1.83)	0.67	(1.35)	0.63	(1.26)

Heating rate: 10°C/min (18°F/min)

Table 35. DSC Variables Study

Condition	Sample weight, mg	Heating rate, °C (°F)		ΔH_p, J/kg (cal/g)	$T_{o'}$ °C (°F)		$T_{p'}$ °C (°F)		$T_{e'}$ °C (°F)	
Sealed	7.69	10	(18)	705 476 (168.5)	203	(397)	265	(509)	273	(523)
N_2, 2068 kPa (300 lbf/in.^{2})	7.49	10	(18)	651 885 (155.7)	203	(397)	264	(507)	274	(525)
4 mg	4.09	10	(18)	666 539 (159.2)	203	(397)	264	(507)	274	(525)
5°C/min (9°F/min)	7.76	5	(9)	530 886 (126.8)	183	(361)	246	(475)	259	(498)
2°C/min (3.6°F/min)	8.29	2	(3.6)	602 899 (144.0)	161	(322)	221	(430)	242	(468)

Table 36. Effect of Variables on DSC Heat of Polymerization Data

| | Standard | | Atmosphere | | | Optimized DSC method, acetone extract centrifuged |
	Indium	Tin	Helium, 100 ml/min	Air,100 ml/min, covered pan, hole in lid, crimped	Nitrogen, 100 ml/min, crimped, with hole	
ΔH_f, J/kg (cal/g)						
$\bar{x}$	29 015 (6.93)	54 973 (13.13)	—	—	—	—
σ	208.9 (0.05)	1 677 (0.40)	—	—	—	—
Rel. σ, %	0.72	3.05	—	—	—	—
ΔH_p, J/kg (cal/g)						
$\bar{x}$	—	—	336 619 (80.40)	501 286 (119.73)	604 155 (144.3)	547 215 (130.7)
σ	—	—	10 677 (2.55)	10 978 (2.62)	15 590 (3.82)	3 557 (0.85)
Rel. σ, %	—	—	3.17	2.19	2.64	0.65

Table 37. DSC Operating Parameter Variations

	Sample size			Atmosphere		Heating rate		
	Normal, ~8 mg, 10°C/min (18°F/min)	~4 mg	Sealed container	N_2, 2068 kPa (300 lbf/in.^{2})	N_2, ambient pressure	2°C/min (3.6°F/min)	5°C/min (9°F/min)	20°C/min (36°F/min)
Number of specimens	3	4	4	4	1	4	4	3
ΔH_p, J/kg (cal/g)								
$\bar{x}$	552.239 (131.9)	560 110 (133.78)	621 949 (148.55)	549 559 (131.26)	551 402 (131.37)	547 592 (130.79)	548 010 (130.89)	589 962 (140.91)
σ	20 212 (4.83)	25 877 (6.18)	24 069 (2.94)	21 268 (5.08)	–	44 191 (10.55)	60 884 (14.54)	20 000 (4.77)
Rel. σ, %	3.66	4.62	1.98	3.87	–	8.07	11.11	3.39
T_o, °C (°F)								
$\bar{x}$	203.8 (398.8)	203.0 (397.4)	206.25 (403.25)	203.0 (397.4)	204 (399.2)	161.5 (322.7)	183.5 (362.3)	226.5 (439.7)
σ	0.83 (1.64)	0.82 (1.59)	2.50 (4.88)	0.82 (1.59)	–	0.58 (1.16)	0.58 (1.16)	1.73 (3.34)
Rel. σ, %	0.41	0.40	1.21	0.40	–	0.36	0.32	0.76
T_p, °C (°F)								
$\bar{x}$	263.9 (507.0)	263.8 (506.8)	264.75 (508.55)	264.0 (475.2)	264 (475.2)	222.0 (431.6)	247.3 (477.1)	281.0 (537.8)
σ	0.69 (1.32)	0.50 (0.96)	1.26 (2.44)	0	–	0.82 (1.60)	0.96 (1.86)	0
Rel. σ, %	0.26	0.19	0.48	0	–	0.37	0.39	0
T_e, °C (°F)								
$\bar{x}$	273.4 (524.1)	274.0 (525.2)	272.8 (523.0)	273.3 (523.9)	274 (525.2)	242.8 (469.0)	259.3 (498.7)	289.0 (552.2)
σ	0.65 (1.26)	0.82 (1.58)	0.96 (1.83)	0.50 (0.94)	–	0.96 (1.88)	0.50 (0.95)	0.82 (1.55)
Rel. σ, %	0.24	0.30	0.35	0.18	–	0.40	0.19	0.28

Table 38. Dielectric Analysis Determination of
Resin Advancement, As-Received Material

Time, hr	Temperature, °C (°F)	Dissipation factor
0	29.9 (85.8)	0.0
0.03	62.4 (144.3)	0.3
0.17	81.8 (179.2)	1.4
0.25	105.7 (222.3)	3.4
0.33	129.5 (265.1)	5.5
0.42	152.8 (307.0)	7.5
0.43	160.1 (320.2)	7.8
0.45	164.7 (328.5)	7.7
0.48	284.0 (543.2)	7.4

Table 39. Dielectric Analysis Determination of Resin
Advancement, Material Staged at 60 to 65°C (140 to 149°F)

Time, hr	Temperature, °C (°F)	Dissipation factor
0	21.7 (71.0)	0.5
0.03	51.0 (123.8)	2.4
0.08	65.5 (149.9)	4.9
0.17	65.5 (149.9)	4.0
0.33	63.4 (146.1)	3.0
0.5	63.4 (146.1)	2.7
0.67	63.4 (146.1)	2.5
0.83	63.4 (146.1)	2.4
1.00	63.4 (146.1)	2.2
1.5	63.4 (146.1)	1.9
2.0	63.4 (146.1)	1.6
2.5	62.8 (145.0)	1.4
3.0	62.7 (144.9)	1.2
3.5	62.7 (144.9)	1.1
4.0	63.4 (146.1)	1.0
4.5	63.4 (146.1)	0.9
5.0	63.4 (146.1)	0.8
5.5	63.4 (146.1)	0.7
6.0	63.4 (146.1)	0.7
6.33	63.4 (146.1)	0.6
6.5	95.5 (203.9)	2.5
6.67	143.9 (291.0)	7.1
6.73	162.8 (325.0)	8.3
6.83	198.6 (389.5)	0.8
7.0	242.5 (468.5)	0.6

Table 40. Dielectric Analysis Determination of Resin Advancement, Material Staged at 110 and 150°C (230 and 302°F)

Time, hr	Material staged at 110°C (230°F)		Material staged at 150°C (302°F)	
	Temperature, °C (°F)	Dissipation factor	Temperature, °C (°F)	Dissipation factor
0	22.5 (72.5)	0.4	21.6 (70.9)	0.7
0.03	68.2 (154.8)	5.5	55.4 (131.7)	4.2
0.08	110.2 (230.4)	8.8	149.4 (300.9)	11.3
0.17	110.5 (230.9)	4.3	150.0 (302.0)	5.5
0.33	110.5 (230.9)	2.7	149.9 (301.8)	4.0
0.50	110.5 (230.9)	2.3	149.9 (301.8)	2.5
0.67	110.4 (230.7)	2.0	149.9 (301.8)	1.0
0.83	110.5 (230.9)	1.8	149.9 (301.8)	0.7
1.00	110.5 (230.9)	1.7	149.9 (301.8)	0.5
1.5	110.2 (230.4)	1.3	149.4 (300.9)	0.1
2.0	109.8 (229.6)	1.1	149.2 (300.6)	0.1
2.5	111.2 (232.2)	0.9	149.2 (300.6)	0
3.0	110.5 (230.9)	0.7	149.2 (300.6)	0
3.5	110.5 (230.9)	0.5	149.2 (300.6)	0
4.0	110.5 (230.9)	0.4	149.1 (300.4)	0
4.5	110.5 (230.9)	0.3	148.5 (299.3)	0
5.0	110.5 (230.9)	0.2	149.9 (301.8)	0
5.5	162.2 (324.0)	1.0	149.9 (301.8)	0
6.0	227.3 (441.1)	0.5	149.9 (301.8)	0
6.3	—	—	149.9 (301.8)	0
6.5	—	—	149.9 (301.8)	0
6.7	—	—	149.9 (301.8)	0
6.7	—	—	149.9 (301.8)	0
6.8	—	—	148.7 (299.7)	0
7.0	—	—	214.2 (417.6)	0.1
7.1	—	—	249.2 (480.6)	0.3

Table 41. LC Evaluation of Resin Advancement for DSC Analysis

Sample	DDS/MY 720 absorbance ratio	Resin advancement/ MY 720 absorbance ratio
Prepreg batch 1072	4.38	0.186
	4.42	0.189
Average	4.40	0.188
Acetone- extracted resin from batch 1072	4.60	0.273
	4.60	0.272
Average	4.60	0.272

Table 42. Results of DSC Round-Robin Evaluation

	Participant A	Participant B	Participant C	Participant D	Participant E	Participant F	Participant G	Participant H	Participant I	Participant J	Grand average
ΔH_p, J/kg (cal/g)											
x̄	312 754 (74.70)	467 791 (111.73)	565 092 (134.97)	775 144 (185.14)	545 331 (130.25)	374 426 (89.43)	574 973 (137.33)	559 650 (133.67)	638 320 (152.46)	673 447 (160.85)	548 680 (131.05)
σ	5 630 (1.35)	2 526 (0.61)	5 990 (1.43)	17 208 (4.11)	—	29 055 (6.94)	27 886 (6.66)	11 305 (2.02)	18 128 (4.32)	4 108 (0.98)	136 841 (32.69)
Rel. σ, %	1.80	0.54	1.06	2.22	—	7.76	4.85	1.51	2.84	0.61	24.94
ΔH_f KClO$_4$, J/kg (cal/g)	43 543 (10.40)	78 000 (18.63)	89 346 (21.34)	105 717 (25.25)	86 039 (20.55)	48 358 (11.55)		99 227 (23.70)		103 749 (24.78)	81 768 (19.53)
Normalized[a] ΔH_p, J/kg (cal/g)											
x̄	723 479 (172.38)	623 582 (148.94)	636 729 (152.08)	736 584 (175.93)	636 896 (152.12)	778 033 (185.83)	—	566 725 (135.36)	638 320 (152.46)	652 262 (155.79)	663 315 (158.43)
σ	—	—	—	—	—	—	—	—	—	—	68 122 (16.27)
Rel. σ, %	—	—	—	—	—	—	—	—	—	—	10.27
Normalized[b] ΔH_p, J/kg (cal/g)											
x̄	—	—	—	—	—	—	—	—	—	—	641 041 (153.11)
σ	—	—	—	—	—	—	—	—	—	—	7 500 (1.79)
Rel. σ, %	—	—	—	—	—	—	—	—	—	—	1.17
T_o, °C (°F)											
x̄	219.00 (426.20)	215.10 (419.18)	218.83 (425.89)	213.40 (416.12)	219.00 (426.20)	151.77 (305.19)	213.33 (415.99)	216.93 (422.47)	215.20 (419.36)	160.85 (321.53)	204.34 (399.81)
σ	1.73 (3.37)	0.30 (0.59)	1.47 (2.85)	9.21 (17.98)	—	6.11 (12.30)	2.52 (4.91)	1.89 (3.68)	0.84 (1.64)	0.98 (1.96)	25.49 (49.90)
Rel. σ, %	0.79	0.14	0.67	4.32	—	4.03	1.18	0.87	0.39	0.61	12.48
T_p, °C (°F)											
x̄	281.00 (537.80)	280.00 (536.00)	282.17 (539.91)	277.00 (530.60)	282.50 (540.50)	277.20 (530.96)	272.33 (522.19)	279.70 (535.46)	278.40 (533.12)	212.33 (414.19)	272.23 (522.01)
σ	1.00 (1.94)	0.28 (0.54)	0.75 (1.45)	4.66 (8.91)	—	1.01 (1.96)	0.58 (1.10)	0.69 (1.34)	0.55 (1.07)	2.08 (4.06)	21.25 (40.77)
Rel. σ, %	0.36	0.10	0.27	1.68	—	0.37	0.21	0.25	0.20	0.98	7.81
T_e, °C (°F)											
x̄	291.00 (555.80)	288.28 (550.90)	291.00 (555.80)	289.00 (522.20)	292.00 (557.60)	314.13 (597.43)	281.00 (537.80)	288.20 (550.76)	287.80 (550.04)	286.67 (548.01)	290.91 (555.64)
σ	1.00 (1.89)	0.40 (0.77)	0.63 (1.22)	3.83 (7.34)	—	2.68 (5.08)	0	0.69 (1.32)	1.92 (3.69)	1.53 (2.90)	9.72 (16.67)
Rel. σ, %	0.34	0.14	0.22	1.33	—	0.85	0	0.24	0.67	0.53	3.00

[a]Normalized to a heat of fusion for KClO$_4$ of 24.0

[b]Normalized using selected data

Table 43. GPC Results Using THF as Mobile Phase

Resin batch number	DDS/MY 720 peak-height ratio	Average	Reaction product/ MY 720 peak-height ratio	Average
289	2.500 2.553	2.526	0.425 0.421	0.423
290A	2.707 2.641	2.674	0.463 0.461	0.462
300	2.930 2.934 2.902	2.922	0.372 0.391 0.366	0.376
286	3.162 3.065	3.113	0.351 0.348	0.349
293	3.175 3.286 3.167	3.209	0.341 0.371 0.381	0.364
294	3.568 3.435	3.501	0.351 0.370	0.360

Table 44. GPC Results Using $CHCl_3$ as Mobile Phase

Resin batch number	DDS/MY 720 peak-height ratio	Average
289	1.068 1.086	1.077
290A	1.185 1.192	1.188
300	1.281 1.280	1.280
286	1.407 1.412	1.410
293	1.474 1.482	1.478
294	1.667 1.667	1.667

Table 45. GPC Comparison of Narmco Neat Resin Versus Prepreg Resin

| Resin batch number | DDS/MY 720 | | Prepreg batch number | DDS/MY 720 | |
	Peak-height ratio	Peak-area ratio		Peak-height ratio	Peak-area ratio
289	0.527	0.507	1074	0.511	0.497
290A	0.522	0.547	1075	0.566	0.565
300	0.603	0.584	1073	0.572	0.565
286	0.616	0.610	1072	0.615	0.604
293	0.646	0.640	1076	0.628	0.610
294	0.712	0.691	1077	0.685	0.663

Table 46. GPC Comparison of Peak-Area and Peak-Height Ratios of Narmco Prepreg

Batch number	DDS/MY 720 peak-area ratio	DDS/MY 720 peak-height ratio
1074	0.814	0.858
1075	0.936	0.962
1072	0.984	1.030
1073	0.904	0.970
1076	1.010	1.070
1077	1.078	1.150

Table 47. Retention-Time Data Obtained by GPC Round-Robin Participants

| Participant | Column plate count | Retention time, min | | |
		DDS peak	Resin advancement and reaction product peak	MY 720 monomer peak
A	6100	7.00	6.38	7.42
C	7900	7.48	6.85	7.88
D	7880	6.88	6.28	7.32
E	4412	7.21	6.58	7.62
F	5471	7.63	7.04	8.00
H	7549	7.33	6.73	7.77
I	9344	6.98	6.45	7.39
$\bar{x}$	—	7.22	6.62	7.63
σ	—	0.259	0.252	0.244
Rel. σ, %	—	3.59	3.81	3.20

*Table 48. Peak-Area Data Obtained
by GPC Round-Robin Participants*

Participant (a)	Peak area, %		
	DDS	Resin advancement and reaction product	MY 720 monomer
A (5)	32.33	15.22	40.19
C (2)	36.00	17.22	37.00
D (1)	26.63	16.48	39.53
E (1)	16.62	4.44	19.68
F (5)	33.25	23.63	35.06
H (1)	25.26	16.02	32.37
I (2)	33.68	17.66	32.45
x̄	31.19	17.70	36.1
σ	3.89	2.76	3.10
Rel. σ, %	12.48	15.60	8.59

[a] Numbers in parentheses refer to number of runs

*Table 49. Peak-Height-Ratio Data Obtained
by GPC Round-Robin Participants*

Participant (a)	Peak-height ratio	
	DDS/MY 720 monomer	Reaction product/ MY 720
A (5)	0.930	0.289
C (2)	0.875	0.340
D (1)	0.762	0.289
E (1)	0.9797	0.343
F (5)	0.9442	0.432
H (1)	0.751	0.322
I (2)	1.053	0.310
x̄	0.8993	0.332
σ	0.1032	0.0455
Rel. σ, %	11.47	13.69

[a] Numbers in parentheses refer to number of runs

Table 50. Identification of Hercules Prepreg Batches

Prepreg batch number	Resin	Resin variations
707-1A	x	Standard production batch
727-1A	x	Low-viscosity base resin
727-2A	—	Ductile resin, +10% hardener, −20% accelerator
727-3A	x	Hardener concentration, +10%
727-4A	x	Accelerator concentration, +20%
727-5A	x	Increased accelerator moisture content
727-6A	—	Standard subscale batch
727-7A	x	Accelerator concentration, −20%
727-8A	x	High-viscosity base resin
727-9A	—	Brittle resin, −10% hardener, +20% accelerator
727-10A	x	Hardener concentration, −10%

Table 51. Results of LC Analysis of Hercules Prepreg and Neat Resin

Batch number	Peak-area ratio			
	Prepreg		Neat resin	
	DDS/MY 720	Reaction product/ MY 720	DDS/MY 720	Reaction product/ MY 720
707-1A	0.997	0.214	1.026	0.142
727-3A	1.134	0.190	1.227	0.094
727-4A	0.872	0.209	1.038	0.131
727-7A	1.020	0.187	1.054	0.098
727-9A	0.811	0.192	—	—

Table 52. Results of GPC Analysis of Hercules Prepreg and Neat Resin

Batch number	Peak-area ratio			
	Prepreg		Neat resin	
	DDS/MY 720	Reaction product/ MY 720	DDS/MY 720	Reaction product/ MY 720
707-1A	1.229	0.564	1.268	0.520
727-3A	1.398	0.559	1.460	0.470
727-4A	1.239	0.567	1.261	0.504
727-7A	1.254	0.547	1.261	0.466
727-9A	1.019	0.492	—	—

Table 53. Results of Ion Chromatography Analysis of Hercules Resin

Batch number	Sulfur content, %	Fluorine content, %	Resin content, %	BF$_3$ amine content, %	DDS content, %	Component	Variation from standard batch, %	
							Reported	Measured
727-7A	3.55	0.417	37.2	0.817	27.53	DDS BF$_3$	Std -20	0 -36
727-9A	3.68	0.88	40.4	1.74	28.54	DDS BF$_3$	-10 +20	-16 +37
707-1A	3.55	0.64	43.6	1.27	27.53	DDS BF$_3$	Std Std	0 0
727-3A	3.90	0.68	41.8	1.35	30.25	DDS BF$_3$	+10 Std	+10 +6

Table 54. Comparison of Data on Sulfur Content of Hercules Resin, Ion Chromatograph Versus LECO Sulfur Analyzer

Sulfur content, %	
Ion chromatograph	LECO Model 532
3.06	3.06
2.77	3.06
3.13	3.04
3.14	—
3.04	—
2.96	—
2.89	—
3.03	—
2.67	—
$\bar{x}$ = 2.97 σ = 0.16 Rel. σ, % = 5.39	$\bar{x}$ = 3.05 σ = 0.01 Rel. σ, % = 0.33

Table 55. Reproducibility of Data on Sulfur and Fluorine Content of Hercules Resin, Ion Chromatography

Sulfur content, %	Fluorine content, %
2.90	0.49
2.90	0.47
2.84	0.49
2.96	0.48
$\bar{x}$ = 2.90 σ = 0.05 Rel. σ, % = 1.72	$\bar{x}$ = 0.48 σ = 0.01 Rel. σ, % = 2.08

Table 56. Comparison of Data on Sulfur Content of Hercules Resin, Ion Chromatography Versus LC

Batch number	Sulfur content, %		
	Reported variation from standard	Ion chromatography data	LC data
727-7A	0	0	+2
727-9A	–10	–16	–23
727-1A	0	0	0
727-3A	+10	+10	+12

Table 57. Comparison of Data on Fluorine Content of Hercules Resin, Ion Chromatography Versus Neutron Activation Analysis

Batch number	Fluorine content, %		
	Reported variation from standard	Ion chromatography data	Neutron activation analysis data
707-1A	0	0.53	0.49
727-4A	+20	0.69 (+30)	0.62 (+26)
727-1A	–20	0.43 (–19)	0.41 (–16)

90

Table 58. Physical and Mechanical Test Matrix for Hercules Materials

| Test | Number of specimens | | | | | Total |
| | Test temperature, dry | | | Test temperature, water saturated[a] | | |
	-54°C (-65°F)	RT	82°C (180°F)	RT	82°C (180°F)	
Fiber volume	—	3	—	—	—	3
Void content	—	3	—	—	—	3
Density	—	3	—	—	—	3
90-deg tension stress, strain, and modulus	9	9	9	9	9	45
0-deg short-beam-shear strength	9	9	9	9	9	45
0-deg compression modulus	9	9	9	9	9	45

[a] Exposed to 49°C (120°F) and 95% relative humidity until moisture equilibrium obtained (500 hr maximum)

Table 59. Physical Properties of Hercules Prepreg

Batch number	Fiber volume, %	Void content, %	Density, kg/m^3
707-1A	61.89	0.24	1606
727-3A	64.10	0.47	1615
727-7A	63.60	0.10	1620
727-9A	64.48	0.37	1619

Table 60. 0-deg Short-Beam-Shear Strength, Hercules Laminates

Batch number	0-deg short-beam-shear strength, (lbf/in.^{2} x 10^3)				
	Test temperature, dry			Test temperature, water saturated[a]	
	-54°C (-65°F)	RT	82°C (180°F)	RT	82°C (180°F)
707-1A Rel. σ, %	132.399 (19.205) 9.8	105.892 (15.360) 7.1	80.508 (11.678) 2.0	84.817 (12.303) 3.9	57.206 (8.298) 4.0
727-3A Rel. σ, %	132.971 (19.288) 5.8	106.464 (15.443) 5.9	79.336 (11.508) 2.9	83.245 (12.075) 3.6	56.793 (8.238) 4.2
727-7A Rel. σ, %	123.547 (17.921) 10.7	102.583 (14.880) 6.7	84.893 (12.314) 6.6	80.094 (11.618) 7.8	58.447 (8.478) 3.3
727-9A Rel. σ, %	135.695 (19.683) 3.2	106.940 (15.512) 4.8	84.865 (12.310) 5.4	81.363 (11.802) 7.1	53.649 (7.782) 8.7

Four specimens tested per condition

[a]Exposed to 49°C (120°F) and 95% relative humidity until moisture equilibrium obtained (500 hr maximum)

Table 61. 0-deg Compression Modulus, Hercules Laminates

Batch number	0-deg compression modulus, GPa (lbf/in.^{2} x 10^6)				
	Test temperature, dry			Test temperature, water saturated[a]	
	-54°C (-65°F)	RT	82°C (180°F)	RT	82°C (180°F)
707-1A Rel. σ, %	122.775 (17.809) 4.6	121.300 (17.595) 4.8	111.442 (16.165) 3.6	129.580 (18.796) 7.4	157.100 (22.788) 13.2
727-3A Rel. σ, %	128.980 (18.709) 9.1	115.040 (16.687) 4.1	110.731 (16.062) 2.9	128.994 (18.711) 5.3	144.443 (20.952) 13.5
727-7A Rel. σ, %	126.719 (18.381) 15.4	117.191 (16.999) 6.6	116.447 (16.891) 5.3	126.422 (18.338) 3.7	142.444 (20.662) 19.8
727-9A Rel. σ, %	152.709 (22.151) 14.3	116.709 (16.929) 5.4	110.318 (16.002) 5.9	134.323 (19.484) 8.8	123.830 (17.962) 0.6

Three specimens tested per condition

[a]Exposed to 49°C (120°F) and 95% relative humidity until moisture equilibrium obtained (500 hr maximum)

Table 62. 90-deg Tension Stress, Modulus, and Strain, Hercules Laminates

Batch number	Test	Test temperature, dry			Test temp, water saturated[a]	
		−53°C (−65°F)	RT	82°C (180°F)	RT	82°C (120°F)
707-1A	Stress, MPa (lbf/in.^{2} x 10^3) Rel. σ, %	50.802 (7.369) 14.2	50.368 (7.306) 11.7	37.014 (5.396) 18.2	36.800 (5.338) 9.3	29.169 (4.231) 16.0
	Modulus, GPa (lbf/in.^{2} x 10^6) Rel. σ, %	10.431 (1.513) 3.2	9.686 (1.405) 2.5	8.314 (1.206) 6.3	8.969 (1.301) 2.1	7.956 (1.154) 2.9
	Strain, μm/m Rel. σ, %	4580 20.0	5047 13.4	4449 19.9	3922 13.3	3983 16.4
727-3A	Stress, MPa (lbf/in.^{2} x 10^3) Rel. σ, %	47.989 (6.961) 7.4	39.082 (5.669) 12.0	33.174 (4.812) 10.6	33.305 (4.831) 13.9	28.541 (4.140) 10.0
	Modulus, GPa (lbf/in.^{2} x 10^6) Rel. σ, %	10.955 (1.589) 11.7	12.512 (1.815) 22.4	8.859 (1.285) 6.4	9.121 (1.323) 4.4	7.990 (1.159) 3.5
	Strain, μm/m Rel. σ, %	4202 13.0	3593 21.1	3762 12.4	3468 19.0	4198 14.5
727-7A	Stress, MPa (lbf/in.^{2} x 10^3) Rel. σ, %	39.268 (5.696) 18.3	36.524 (5.298) 6.7	31.575 (4.580) 9.7	30.534 (4.429) 11.3	26.121 (3.789) 9.6
	Modulus, GPa (lbf/in.^{2} x 10^6) Rel. σ, %	10.210 (1.481) 3.5	10.113 (1.467) 8.4	8.921 (1.294) 4.6	9.514 (1.380) 15.1	7.783 (1.129) 7.0
	Strain, μm/m Rel. σ, %	3620 19.7	3280 11.0	3638 10.1	3229 14.5	3800 11.0
727-9A	Stress, MPa (lbf/in.^{2} x 10^3) Rel. σ, %	— — —	38.207 (5.542) 17.8	— — —	— — —	— — —
	Modulus, GPa (lbf/in.^{2} x 10^6) Rel. σ, %	— — —	9.576 (1.389) 1.7	— — —	— — —	— — —
	Strain, μm/m Rel. σ, %	— —	4612 19.6	— —	— —	— —

Five specimens tested per condition

[a]Exposed to 49°C (120°F) and 95% relative humidity until moisture equilibrium obtained (500 hr maximum)

Table 63. DMA Test Matrix

Prepreg batch number	Unexposed	Exposed to 49°C (120°F) and 100% relative humidity for 2 weeks	Dried at 49°C (120°F) for 30 min after humidity exposure
Narmco			
1073	X	X	X
1074	X	X	X
1076	X	X	X
Hercules			
707-1A	X	X	X
727-3A	X	X	X
727-4A	X	X	X

Table 64. Analysis of Viscosity Profiles for Narmco Matrix

Batch number	Lowest η, Pa · s (a)	Time span, min $\eta = 10$ (a)	Time span, min $\eta = 100$ (a)	Time span, min $\eta = 1000$ (a)
289	0.18 (0.10)	42.0	60.5	71
290A	0.13 (0.09)	45.1 (44.0)	58.7 (60.0)	65.5 (61.0)
300	0.18 (0.20)	41.0 (41.0)	59.0 (60.0)	67 (68.0)
293	0.12 (0.09)	43.0 (45.0)	61.0 (60.0)	70 (70.0)
294	0.15 (0.15)	39.5 (41.0)	56.5 (59.0)	65 (66.0)

a Numbers in parentheses are data obtained with 50% strain

Table 65. Fracture Toughness of Hercules Laminates

Batch number	Load, kg (lb)	G_{IC}, $J/m^2 \times 10^{-6}$ (in.-lb/in.^{2})
707-1A	8.6 (19) 8.6 (19) 13.2 (29) 14.1 (31)	5.39 (0.074) 5.39 (0.074) 12.54 (0.172) 14.36 (0.197)
727-1A	6.4 (14) a	2.92 (0.040)
727-2A	12.7 (28) 17.2 (38) 6.6 (14.5) 7.7 (17)	11.74 (0.161) 21.58 (0.296) 3.13 (0.043) 4.30 (0.059)
727-3A	6.1 (13.5) 9.5 (21) 6.6 (14.5) 7.5 (16.5)	2.70 (0.037) 6.56 (0.090) 3.13 (0.043) 4.08 (0.056)
727-5A	11.8 (26) 7.9 (17.5) 10.2 (22.5)	10.06 (0.138) 4.59 (0.063) 7.58 (0.104)
727-6A	5.9 (13) 8.6 (19) 13.6 (30) 10.0 (22)	2.55 (0.035) 5.39 (0.074) 13.41 (0.184) 7.22 (0.099)
727-7A	6.4 (14) 9.5 (21)	2.92 (0.040) 6.56 (0.090)
727-8A	10.0 (22) 11.8 (26) 12.9 (28.5)	7.22 (0.099) 10.06 (0.138) 12.10 (0.166)
727-10A	10.0 (22) 13.2 (29) 9.5 (21)	7.22 (0.099) 12.54 (0.172) 6.56 (0.090)

[a]Specimen broke during handling due to embrittlement
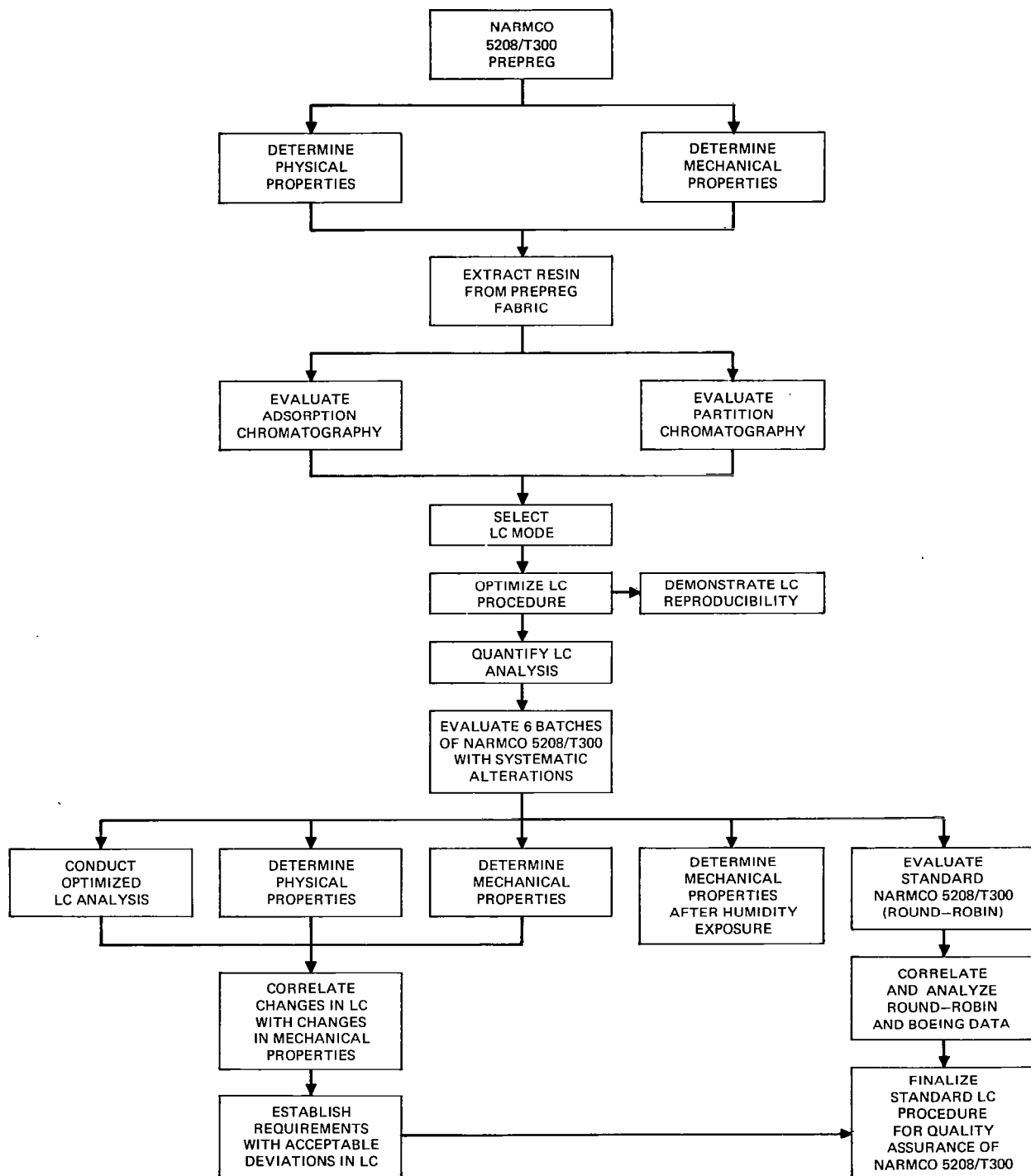
Figure 1. Task A Work Flow
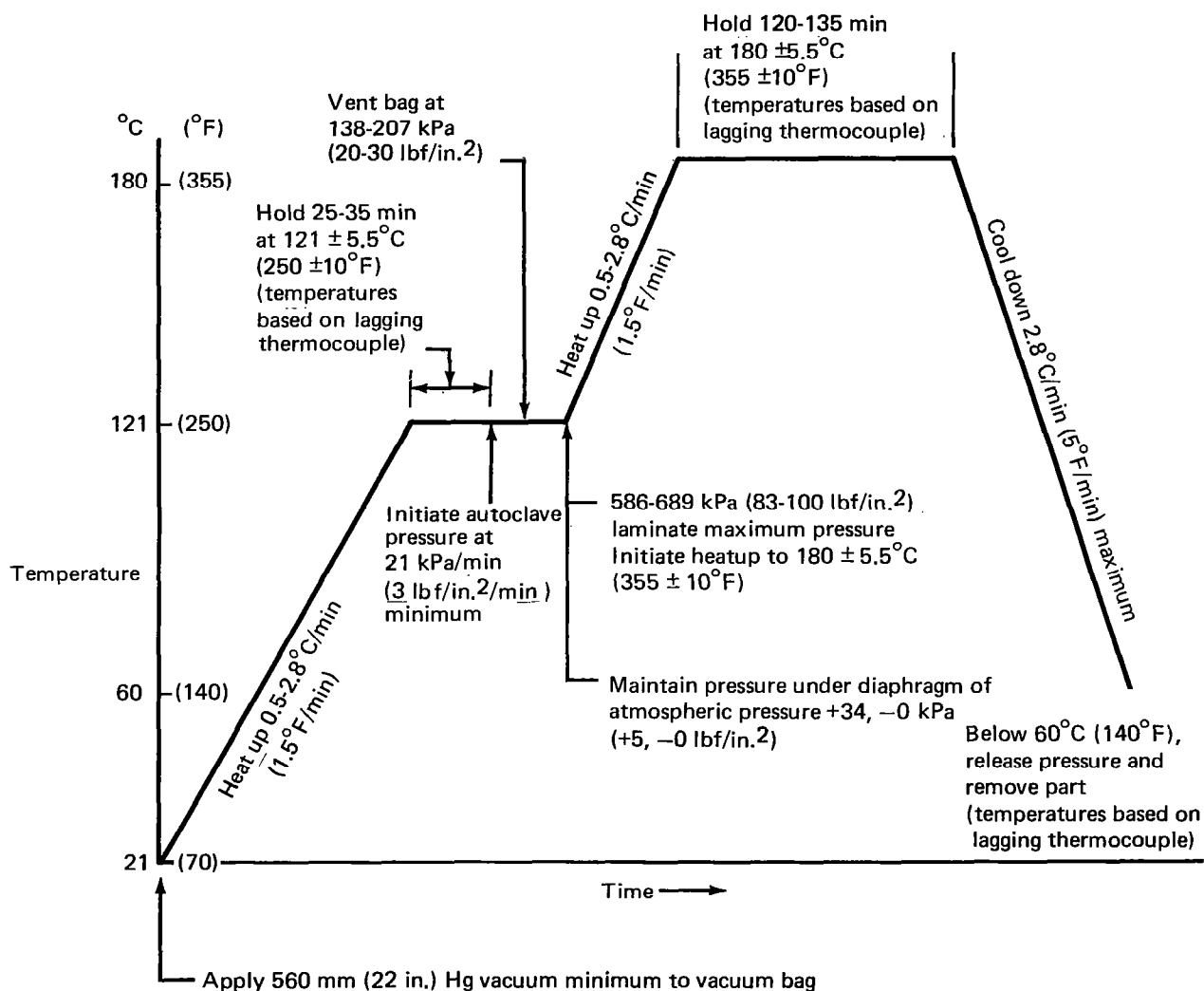
Figure 2. Laminate Cure Cycle

1.27 (0.5) 0° tension
2.54 (1.0) ± 45° tension

0.076 (0.030) 0° specimen
or
0.254 (0.10) cross-plied
specimen

6.35
(2.5)

17.78
(7.0)

Dimensions
in cm (in.)

Load tabs
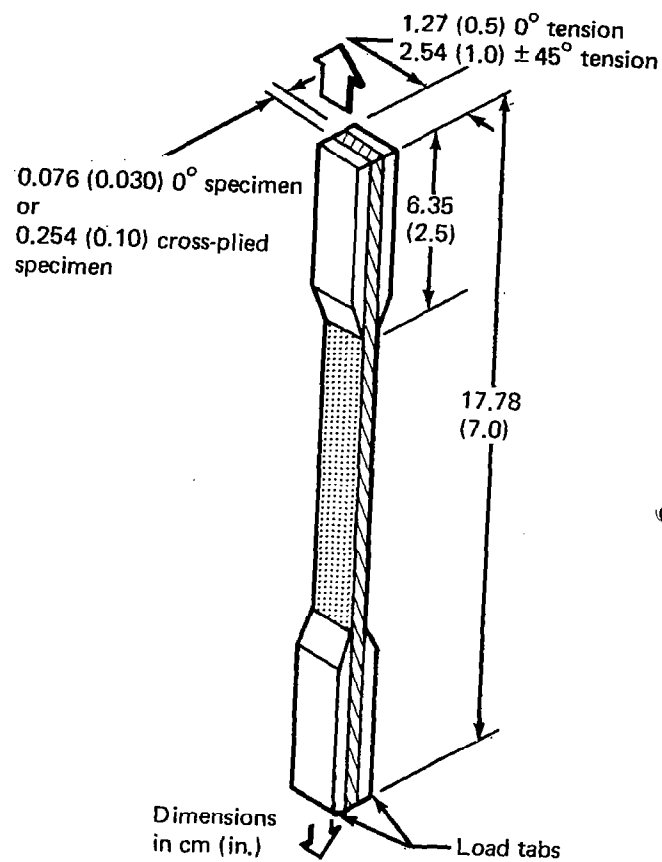
Figure 3. Tension Test Specimen

0.254
(0.10)

0.635
(0.25)

1.524
(0.60)

1.016
(0.40)

Dimensions
in cm (in.)
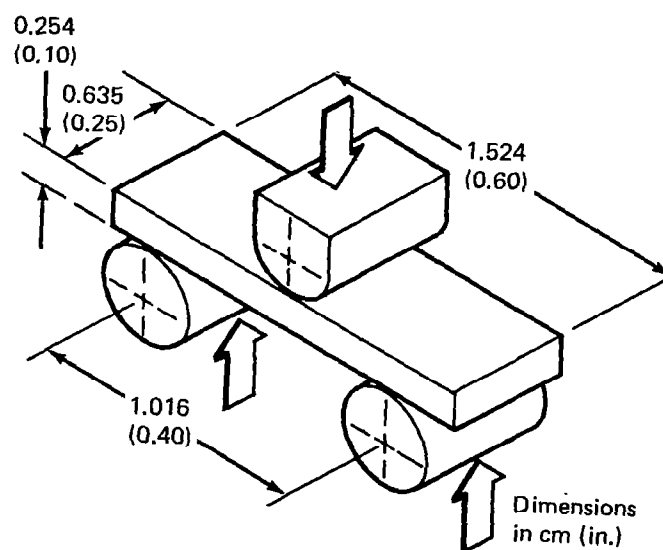
Figure 4. Short-Beam-Shear Test Specimen

Figure 5. SEM Photomicrograph of Prepreg Fiber After THF Wash
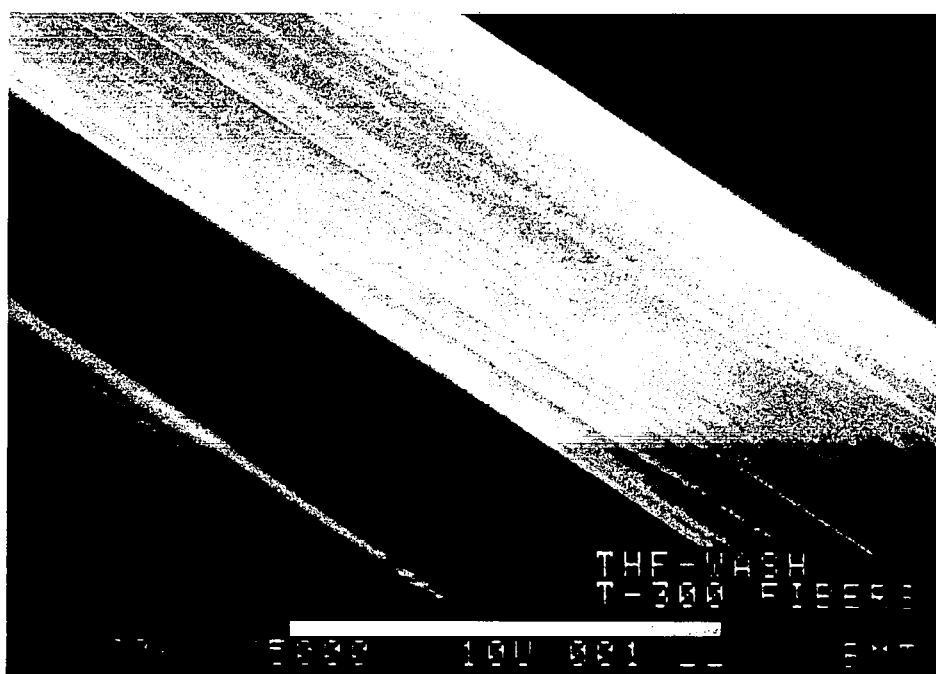
Figure 6. SEM Photomicrograph of Controlled T300 Fiber After THF Wash

Column:	Waters μ-Bondapak/C$_{18}$
Solvent:	30/70% CH$_3$CN/H$_2$O
	in 15 min, linear
Flow rate:	1.8 ml/min
Detector:	UV, 280 cm

Detector
response

Elution time, min
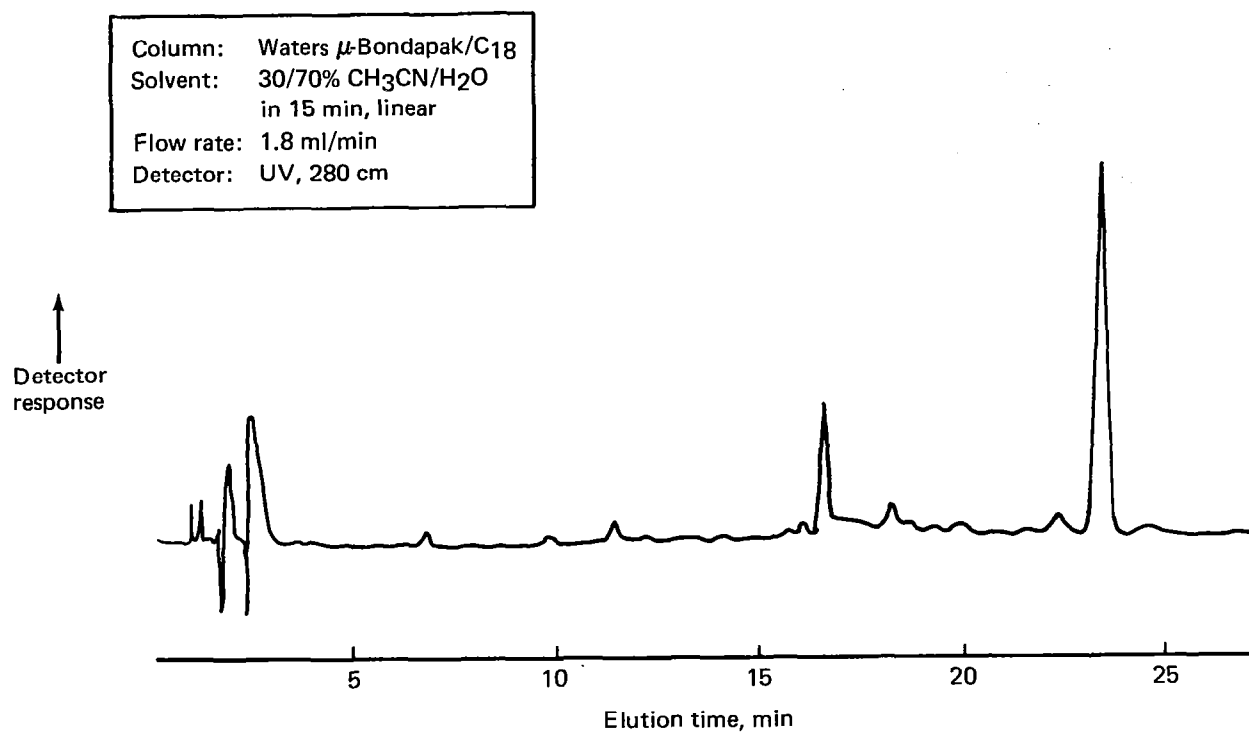
Figure 7. LC Chromatogram of T300 Fiber Finish
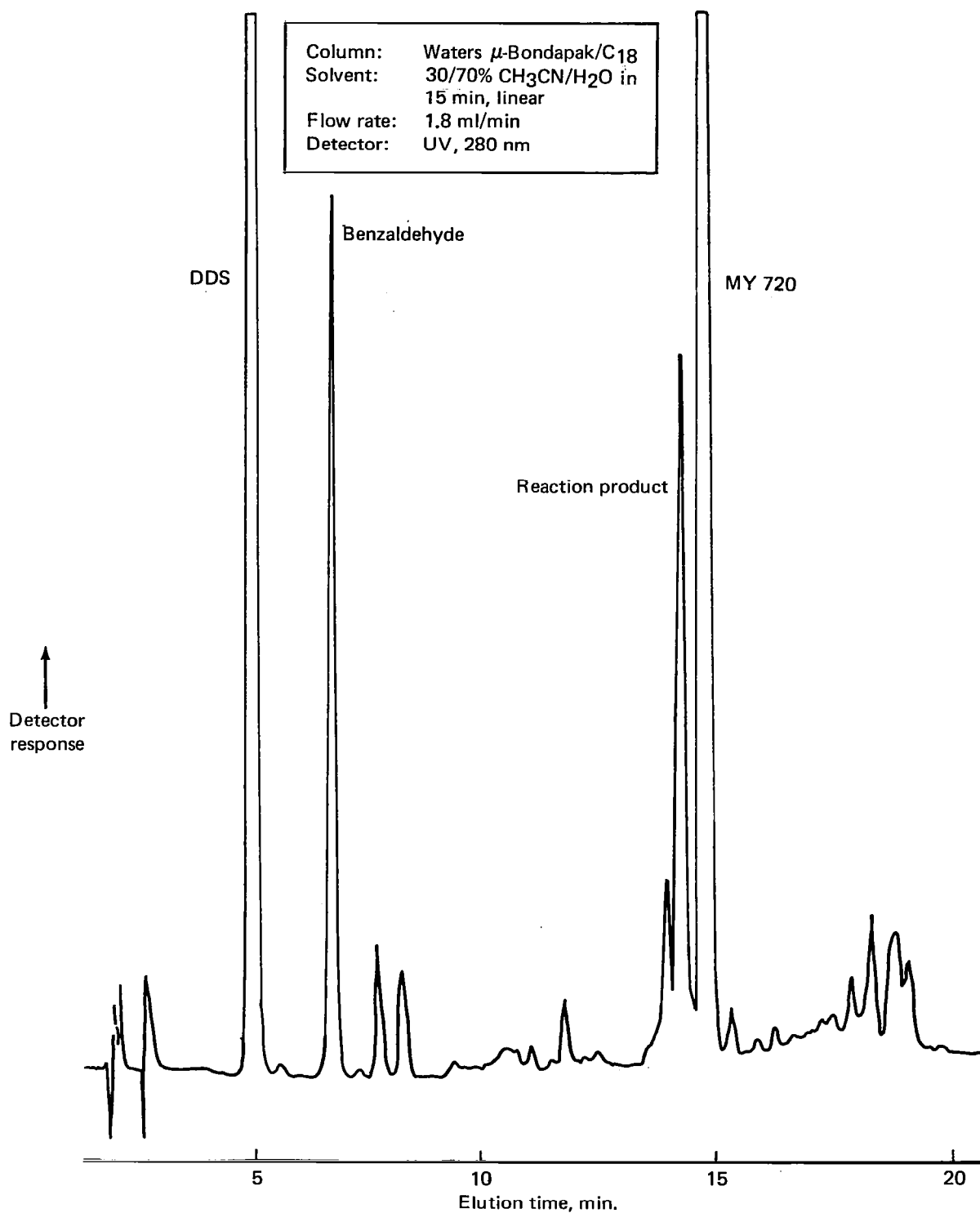
Figure 8. LC Chromatogram of Narmco Resin Matrix

Figure 9. *TLC Evaluation of Narmco Resin Using Different Solvents, RP-2 Plate*
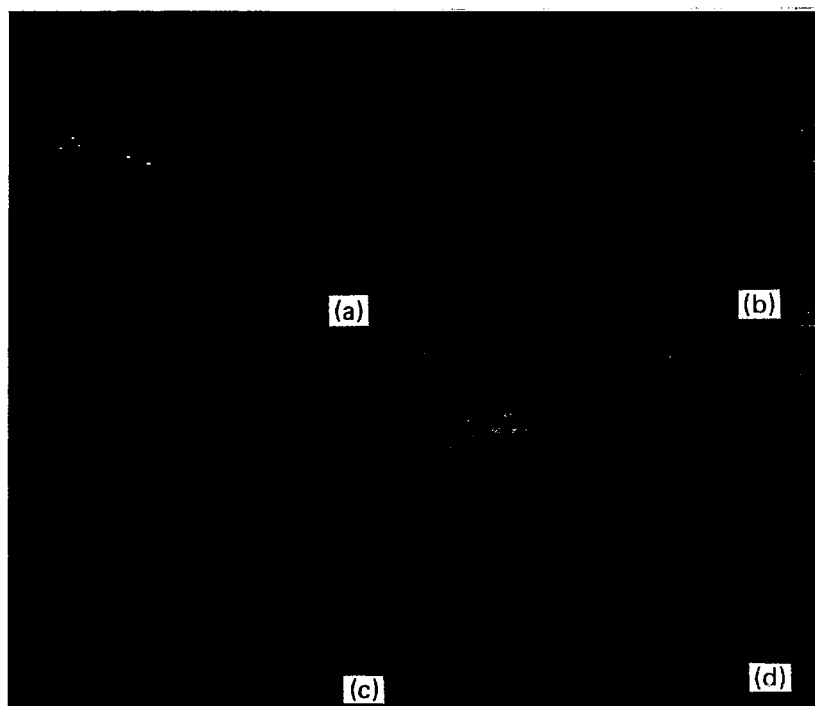
(a) 7.2% acetonitrile in chloroform
(b) 6.2% acetonitrile in toluene
(c) 0.2% methanol in chloroform
(d) 1.8% propanol in chloroform

Figure 10. *TLC Evaluation of Narmco Resin Using Different Solvents, GF Plate*
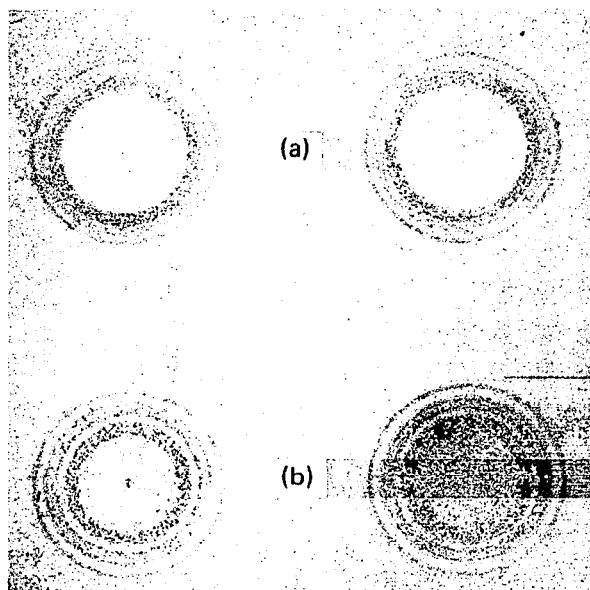
(a) 8.45% methanol in chlorobenzene
(b) 8.15% methanol in toluene
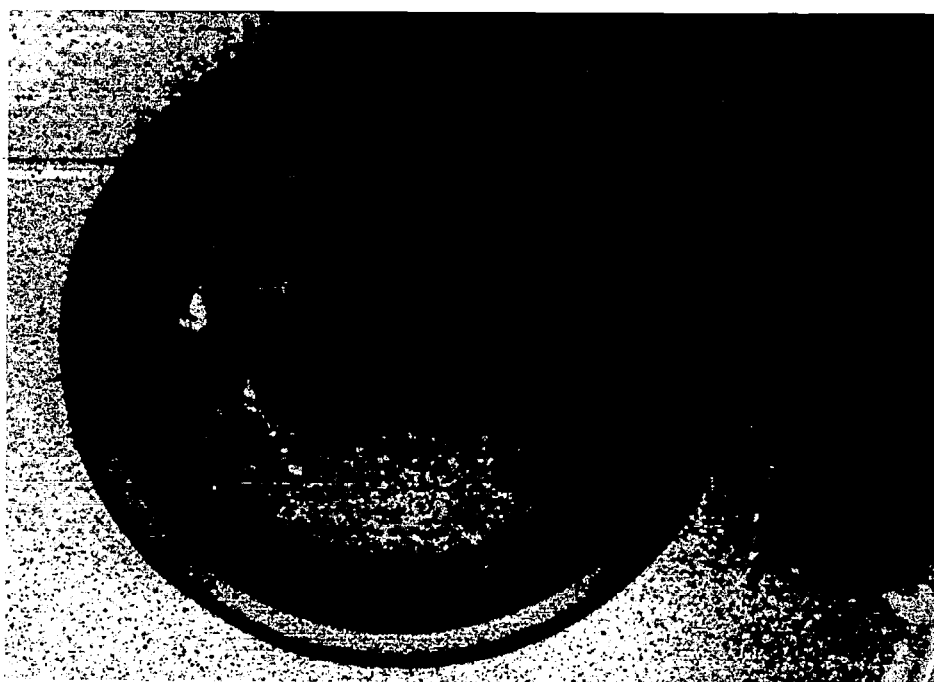
Figure 11. TLC Evaluation of Narmco Resin Using 8.15% Methanol
in Toluene, GF Plate

Column: Merck Lichrosorb RP-2,
           10 μm
Solvent: 0.2% CH₃OH in CHCl₃,
           isocratic
Flow rate: 0.5 ml/min
Detector: UV, 280 nm

Detector response

5   10

Elution time, min
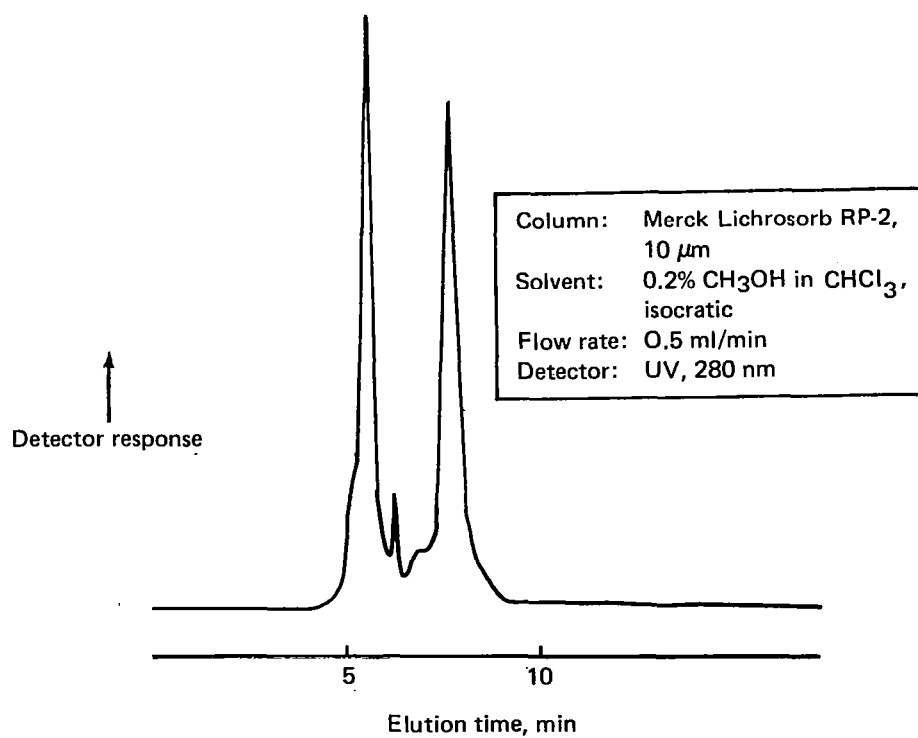
Figure 12. LC Chromatogram of Optimized TLC Mobile Phase
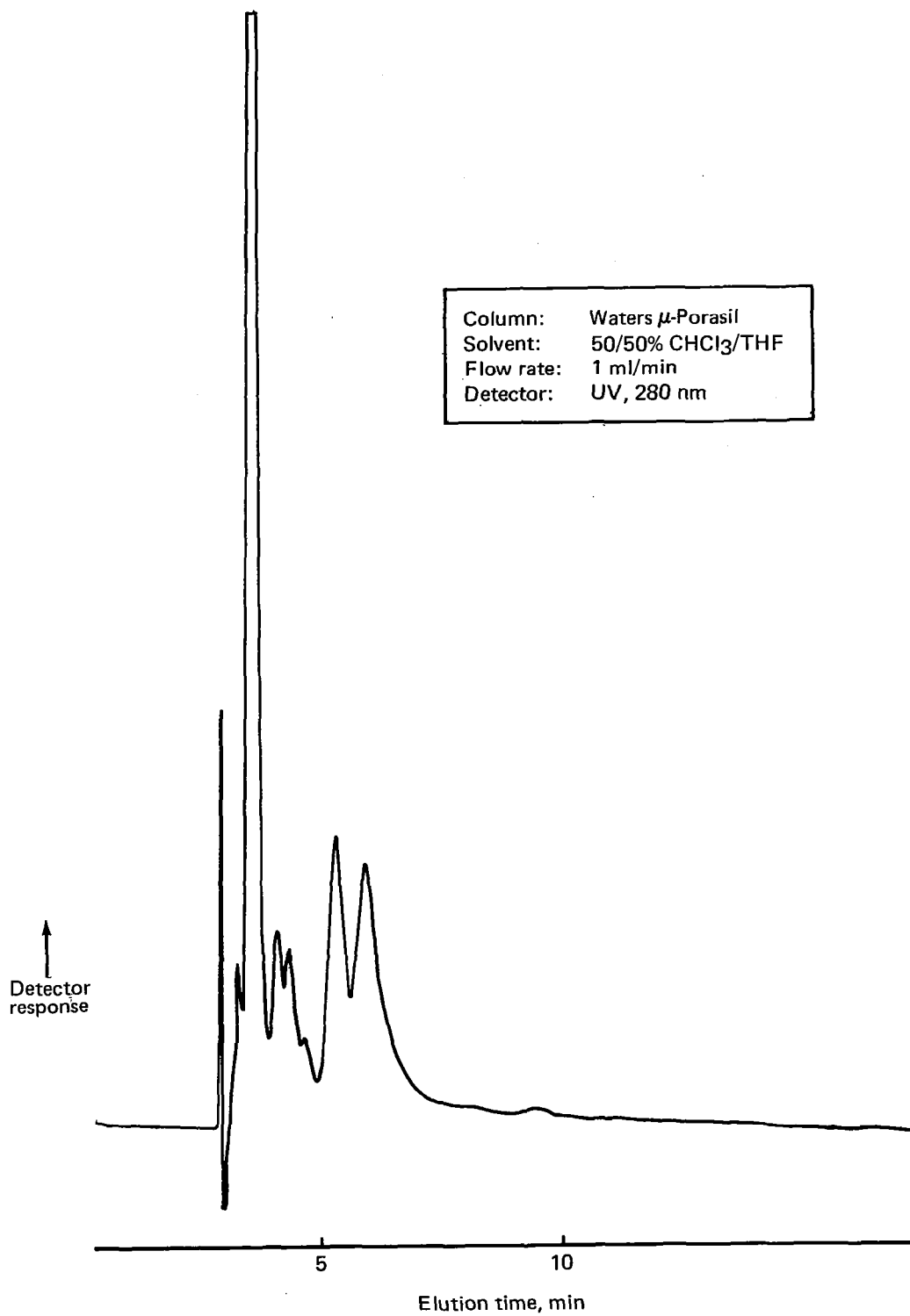
Figure 13. LC Chromatogram of MY 720

MY 720

DDS

Column:	Waters μ-Porasil
Solvent:	50/50% $CHCl_3$/THF
Flow rate:	1 ml/min
Detector:	UV, 280 nm

Possibly reaction
product

Detector
response

5   10   15

Elution time, min
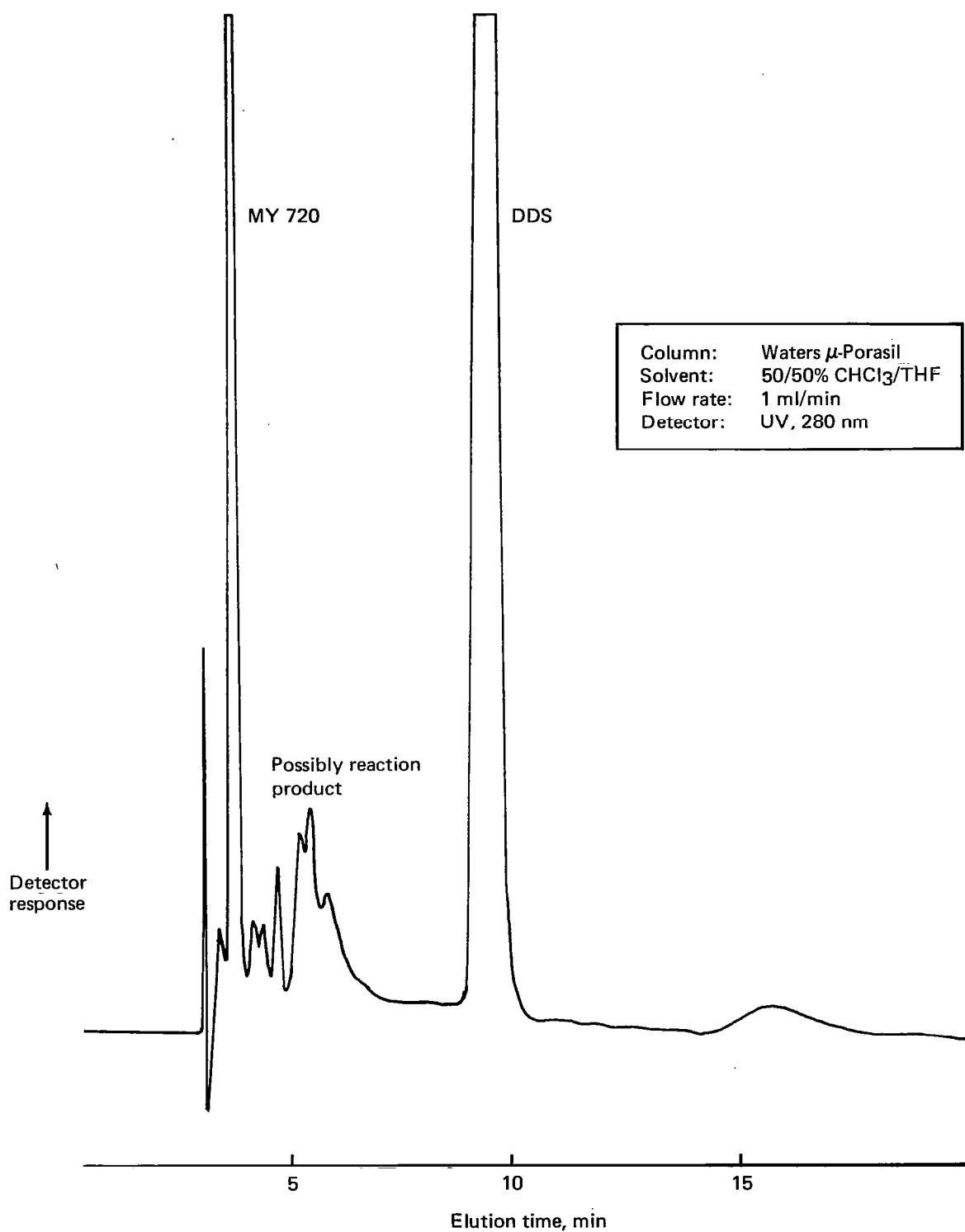
Figure 14. LC Chromatogram of Narmco Batch 286, Flow Rate: 1 ml/min

MY 720   DDS

Column: Waters μ-Porasil
Solvent: 50/50% $CHCl_3$/THF
Flow rate: 2 ml/min
Detector: UV, 280 nm

Detector
response

Elution time, min
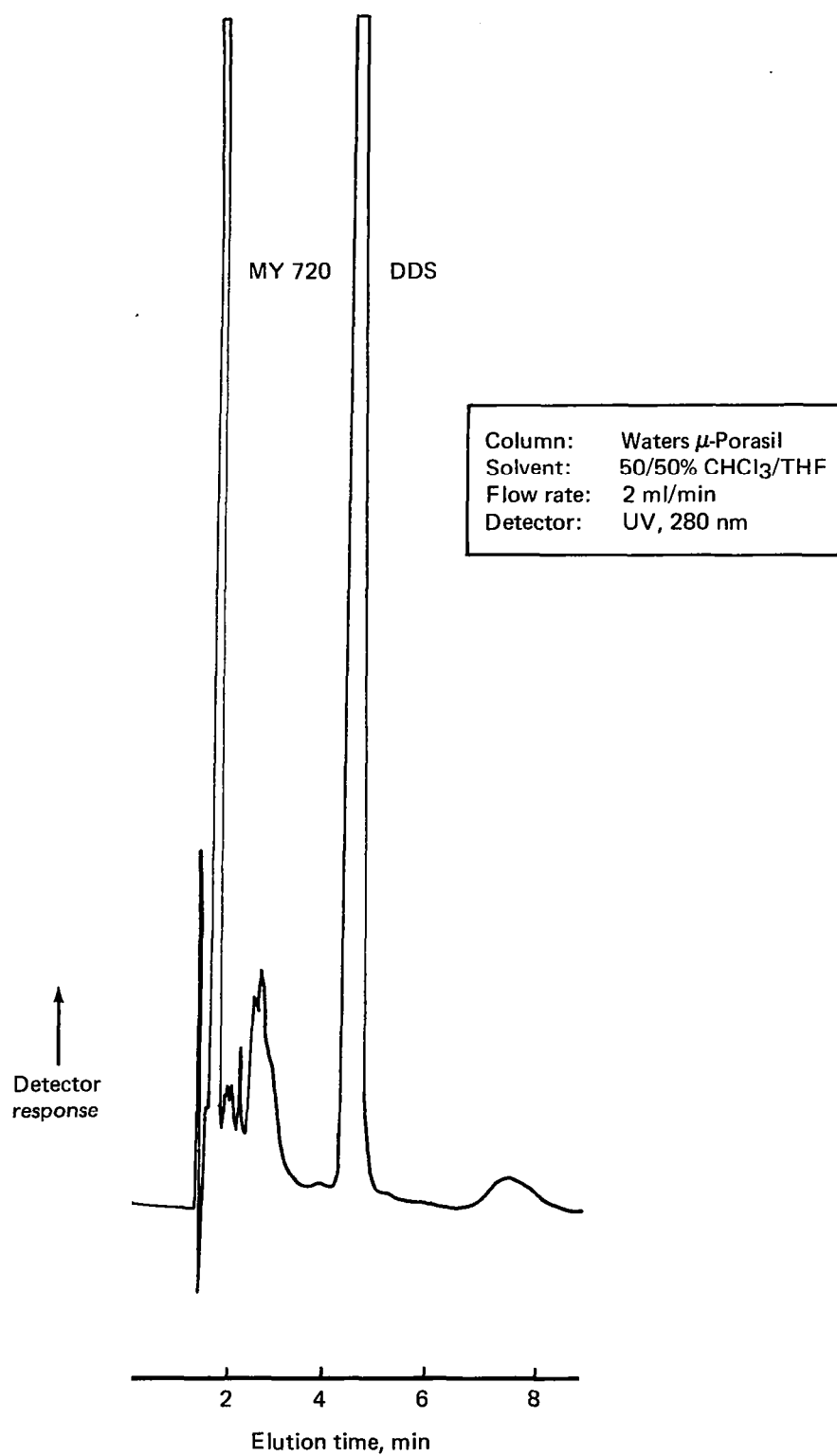
Figure 15. LC Chromatogram of Narmco Batch 286, Flow Rate: 2 ml/min
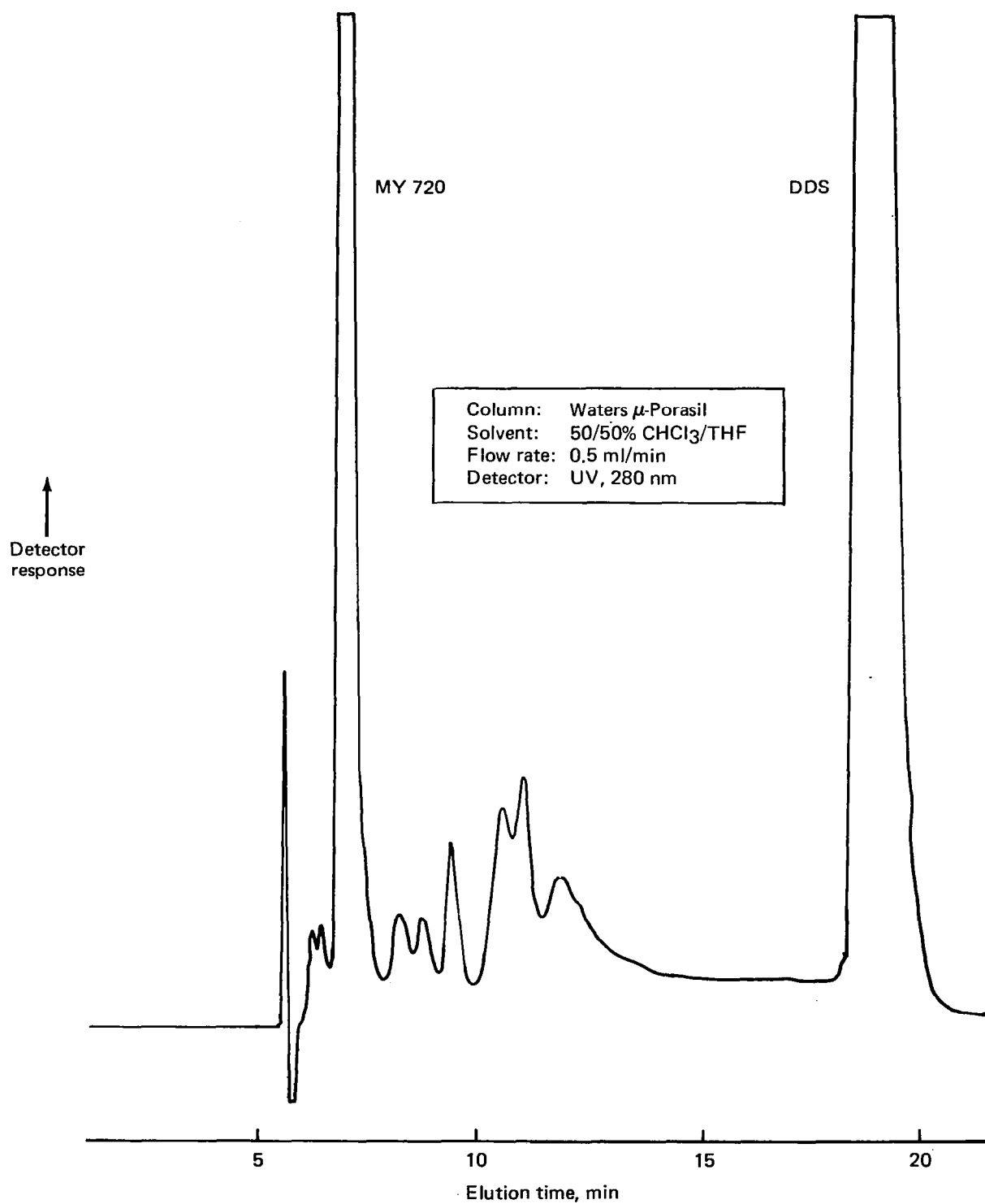
Figure 16. LC Chromatogram of Narmco Batch 286, Flow Rate: 0.5 ml/min

MY 720

DDS

Column:	Waters μ-Porasil
Solvent:	50/50% CHCl₃/THF, isocratic
Flow rate:	1 ml/min
Detector:	UV, 254 nm

Detector
response

5   10   15

Elution time, min
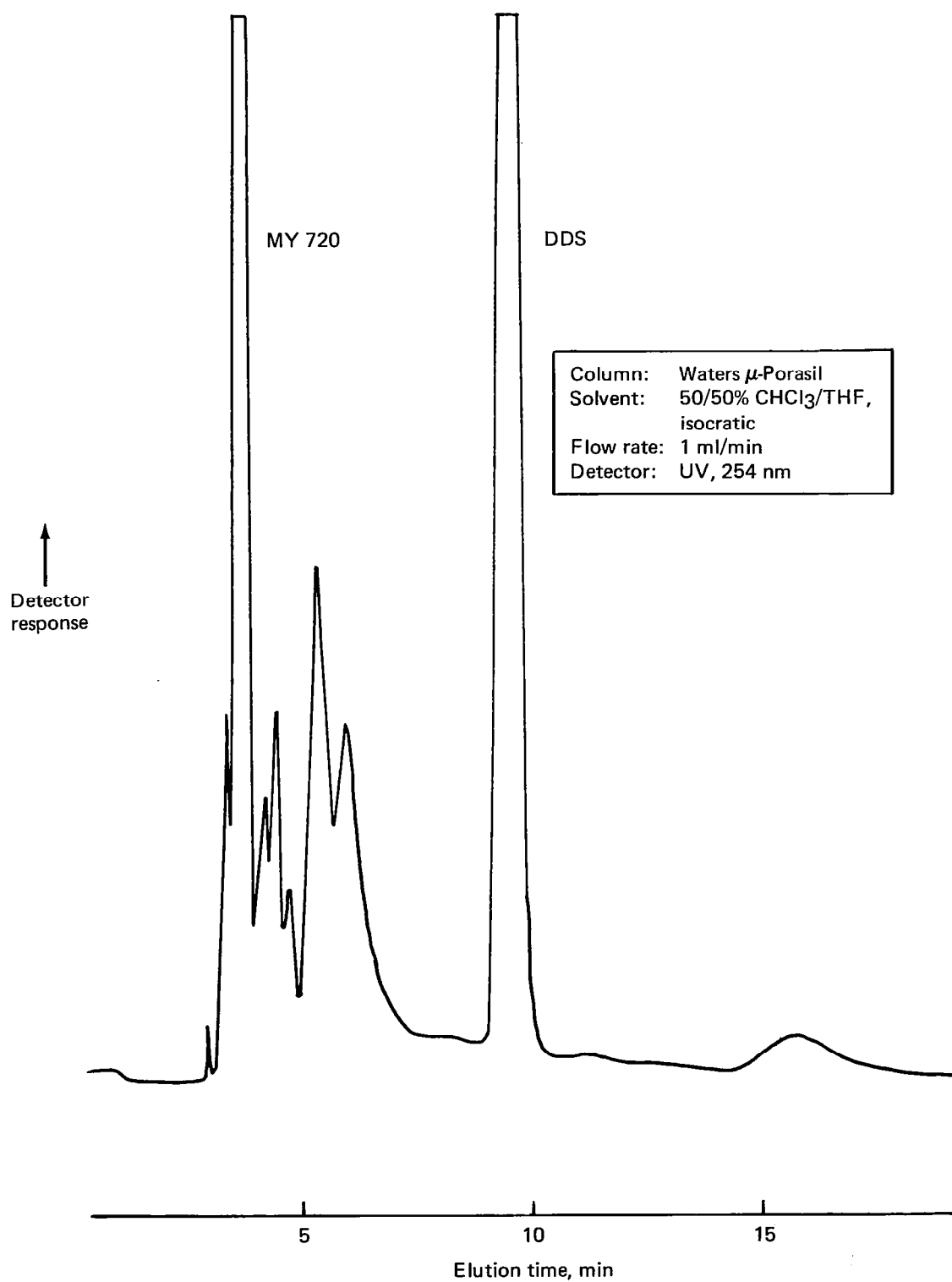
Figure 17. LC Chromatogram of Narmco Batch 286, Detector: UV, 254 nm

DDS

Column:	Waters μ-Porasil
Solvent:	10/50% THF/CHCl$_3$ in 15 min, curve 7
Flow rate:	1 ml/min
Detector:	UV, 280 nm

Detector response

5   10   15   20

Elution time, min
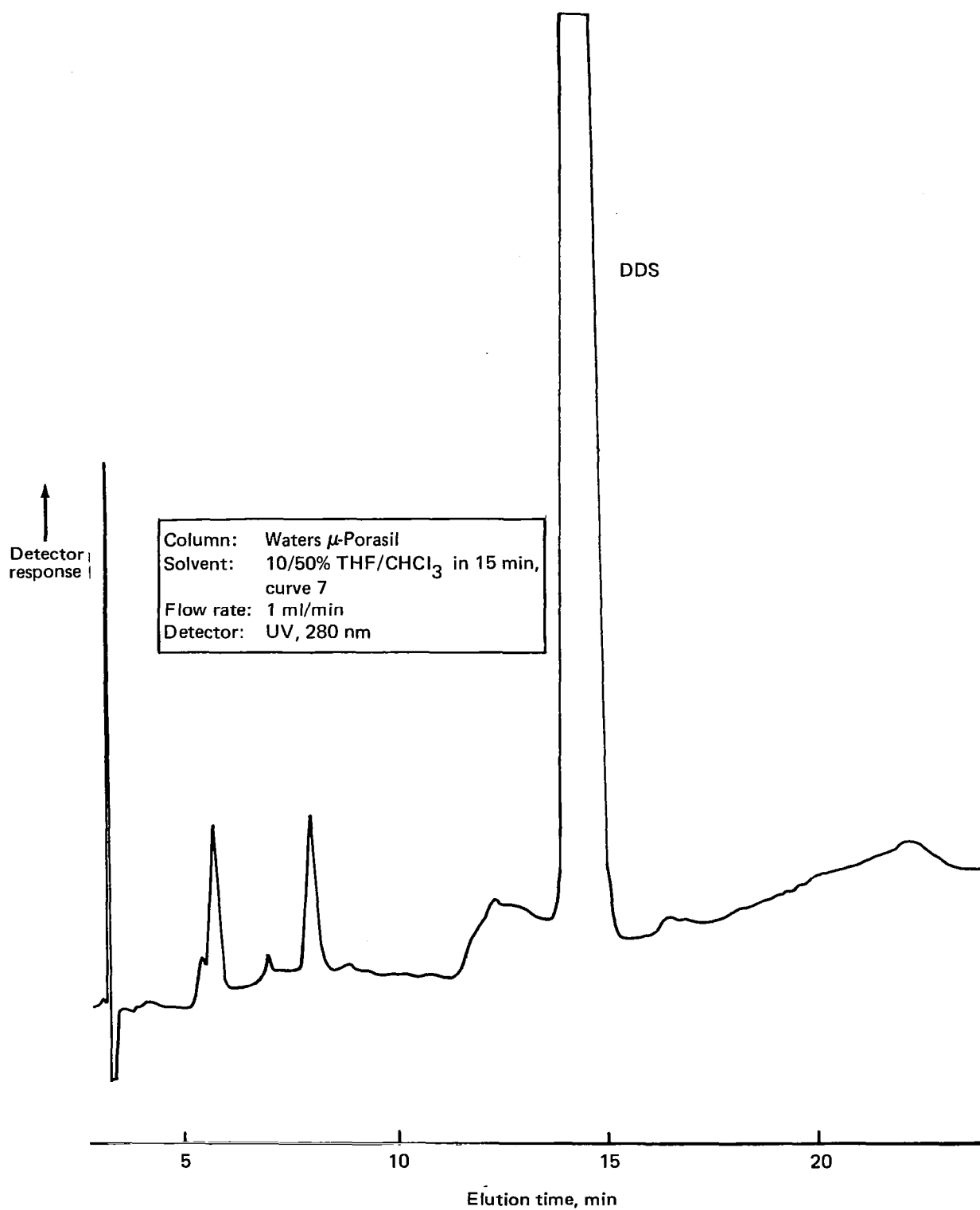
Figure 18. LC Chromatogram of DDS, Solvent: THF/CHCl$_3$

MY 720

Column:	Waters μ-Porasil
Solvent:	10/50% THF/CHCl$_3$ in 15 min, curve 7.
Flow rate:	1 ml/min
Detector:	UV, 280 nm

response

5   10   15   20

Elution time, min
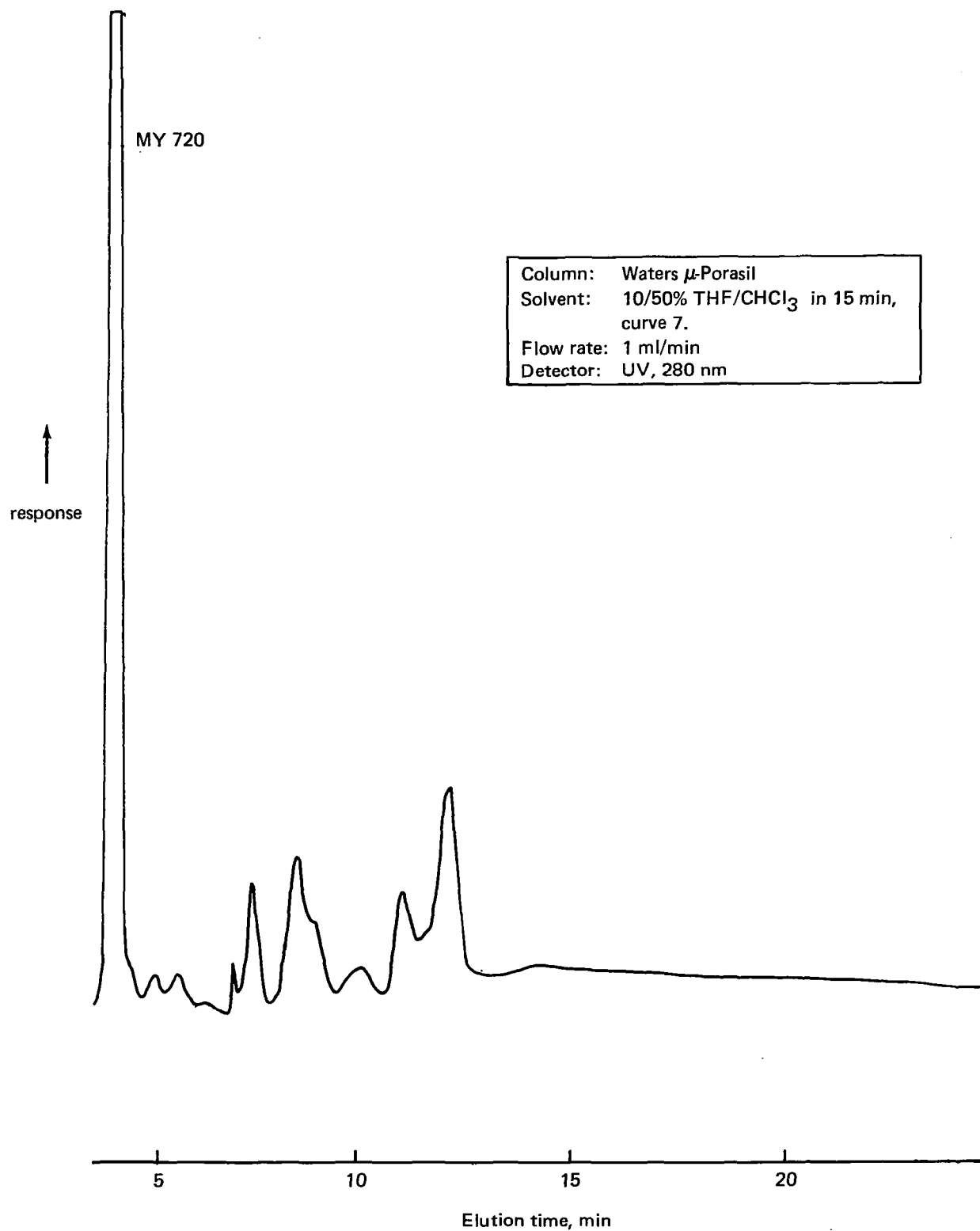
Figure 19. LC Chromatogram of MY 720, Solvent: THF/CHCl$_3$

MY 720

DDS

Detector

Column: Waters μ-Porasil
Solvent: 10/50% THF/CHCl$_3$ in 15 min,
          curve 7
Flow rate: 1 ml/min
Detector: UV, 280 nm

Elution time, min
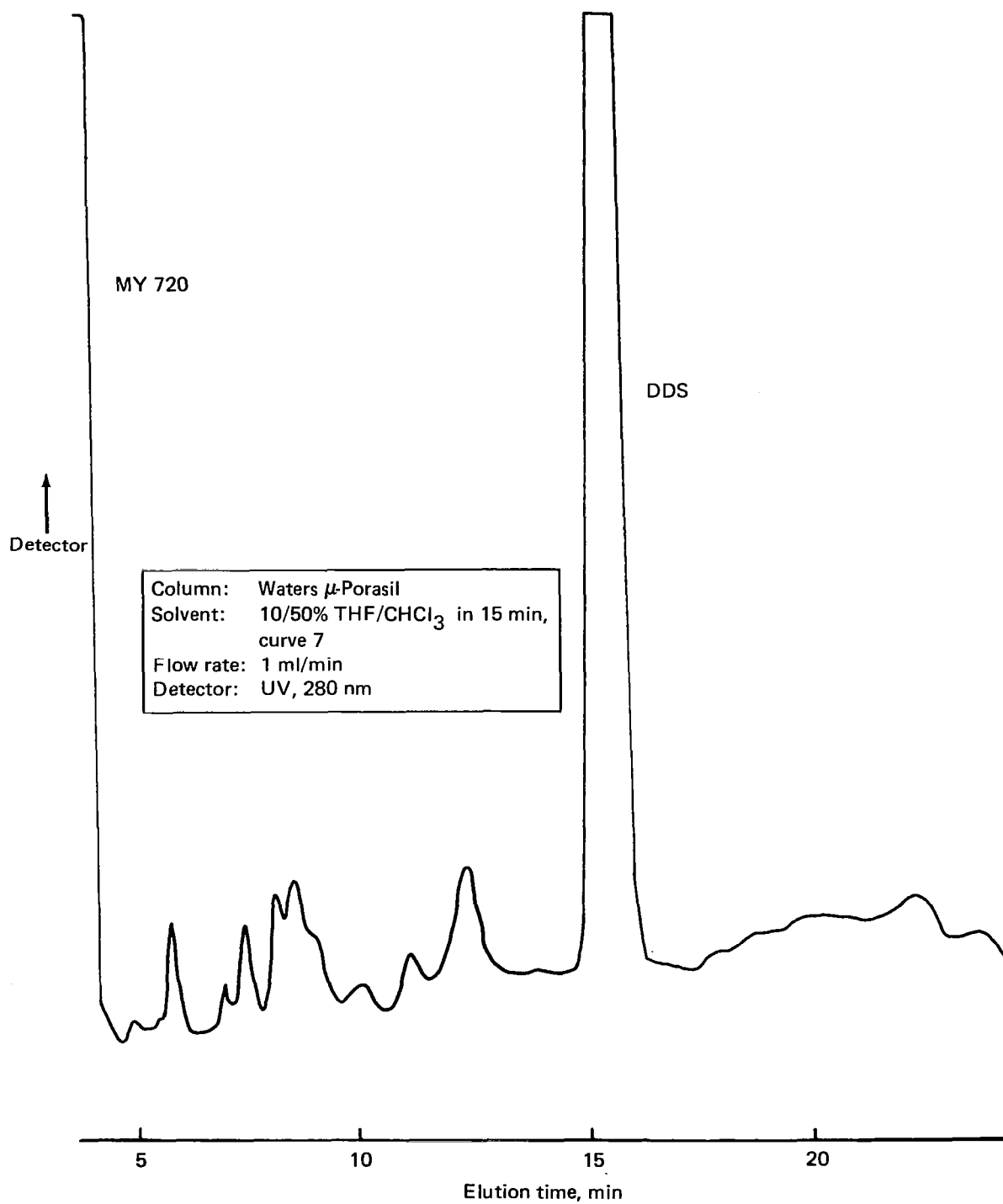
Figure 20. LC Chromatogram of Narmco Batch 286, Solvent: THF/CHCl$_3$

DDS

MY 720

Column: Waters μ-Bondapak/C₁₈
Solvent: 24/82% CH₃CN/H₂O in
20 min
Flow rate: 2 ml/min
Detector: UV, 280 nm

↑
Detector
response

Benzaldehyde

Reaction product

5 10 15 20

Elution time, min
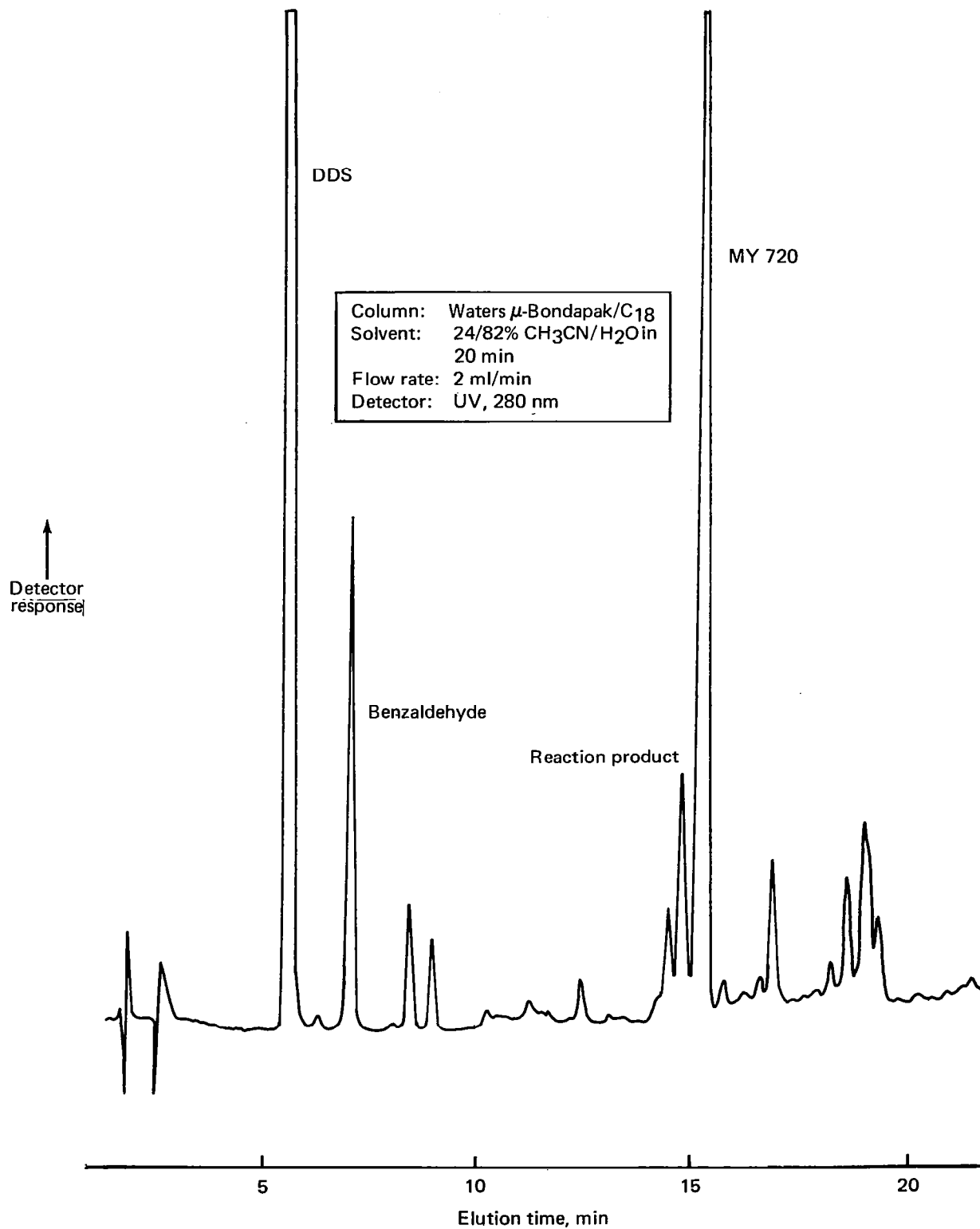
Figure 21. LC Chromatogram of Narmco Batch 286, 24/82% CH₃CN/H₂O

DDS

MY 720

Column:	Waters μ-Bondapak/C_{18}
Solvent:	30/70% CH_3CN/ H_2O in 15 min
Flow rate:	1.8 ml/min
Detector:	UV, 280 nm

Detector response

Benzaldehyde

Reaction product

5   10   15   20

Elution time, min
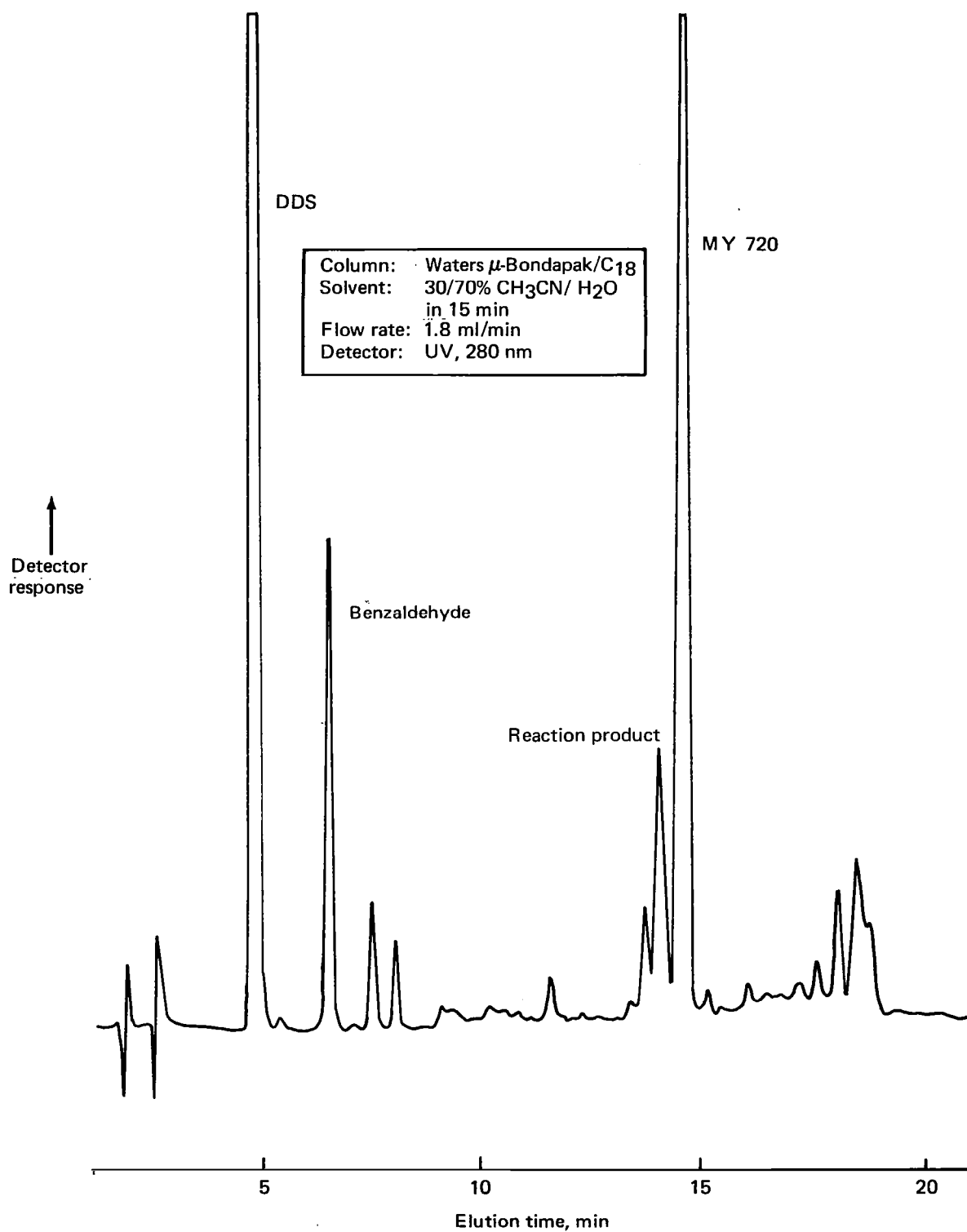
Figure 22. LC Chromatogram of Narmco Batch 286, Solvent: 30/70% CH_3CN/H_2O

DDS

MY 720

Benzal-
dehyde

Column: Waters μ-Bondapak/C$_{18}$
Solvent: 40/80% CH$_3$CN/H$_2$O in 10 min,
          curve 4
Flow rate: 2 ml/min
Detector: UV, 280 nm

Reaction
product

Detector
response

5

10

Elution time, min
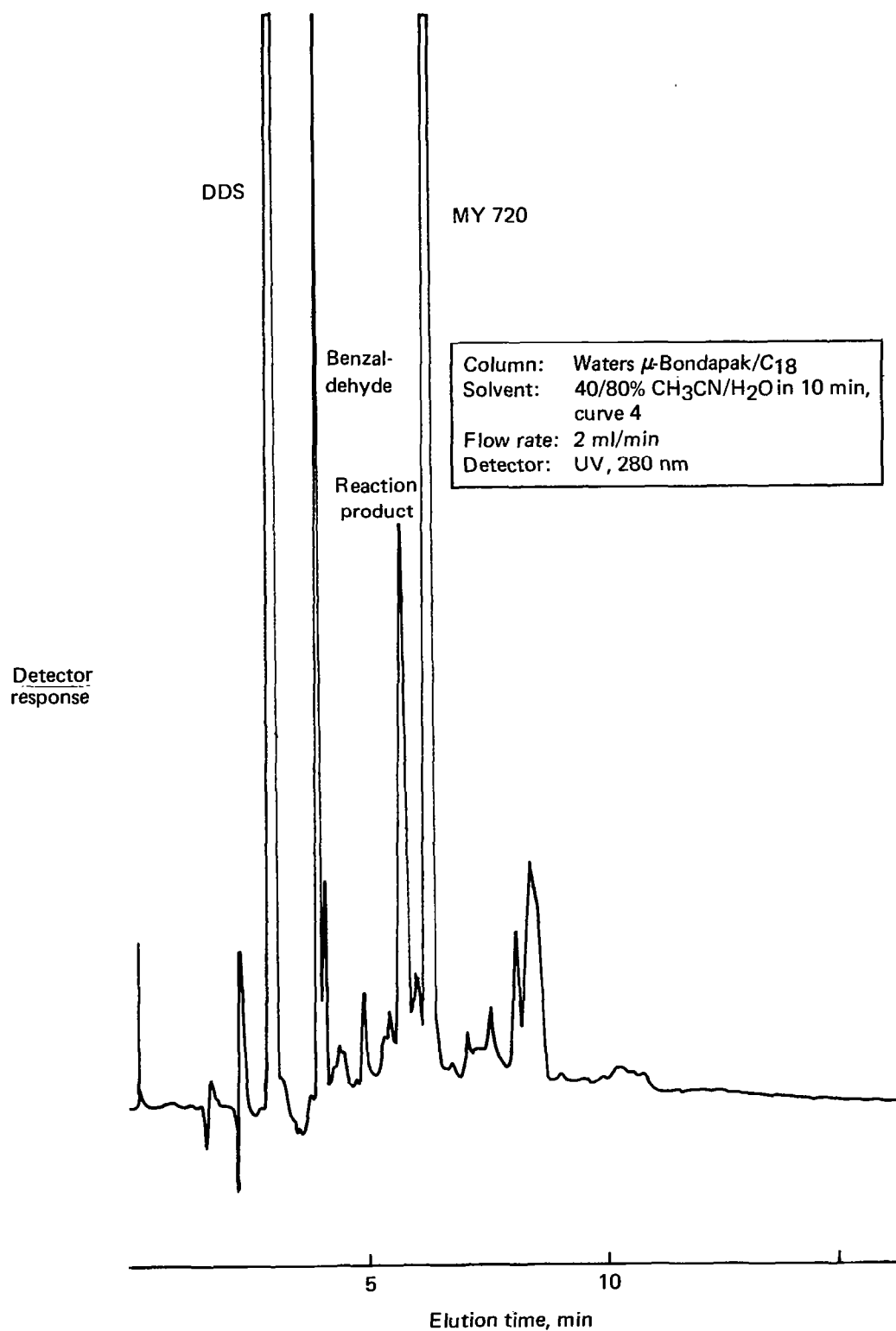
Figure 23. LC Chromatogram of Narmco Batch 286, Solvent: 40/80% CH$_3$CN/H$_2$O
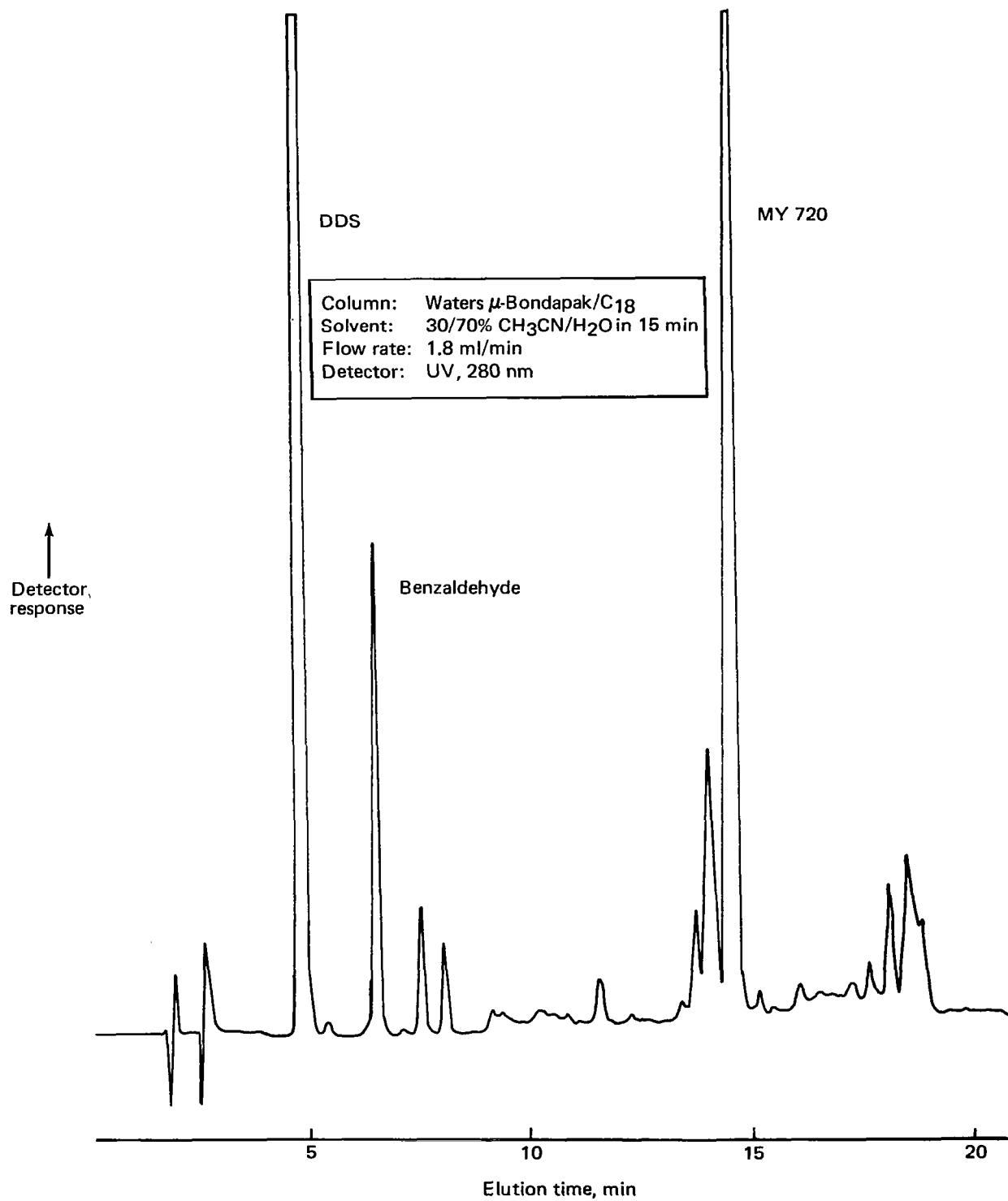
Figure 24. LC Chromatogram of Narmco Batch 286, Column: Waters μ-Bondapak/C₁₈

The figure contains the following labels and annotations:

DDS

MY 720

Column: Waters μ-Bondapak/C$_{18}$
Solvent: 30/70% CH$_3$CN/H$_2$O in 15 min
Flow rate: 1.8 ml/min
Detector: UV, 280 nm

Detector, response

Benzaldehyde

Elution time, min

DDS

MY 720

Column: Merck Lichrosorb RP-8, 5μm
Solvent: 30/70% CH₃CN/H₂O
in 15 min
Flow rate: 1.8 ml/min
Detector: UV, 280 nm

Reaction product

Benzaldehyde

Detector
response

Elution time, min

5   10   15   20

Figure 25. LC Chromatogram of Narmco Batch 286, Column: Merck Lichrosorb RP-8, 5μm
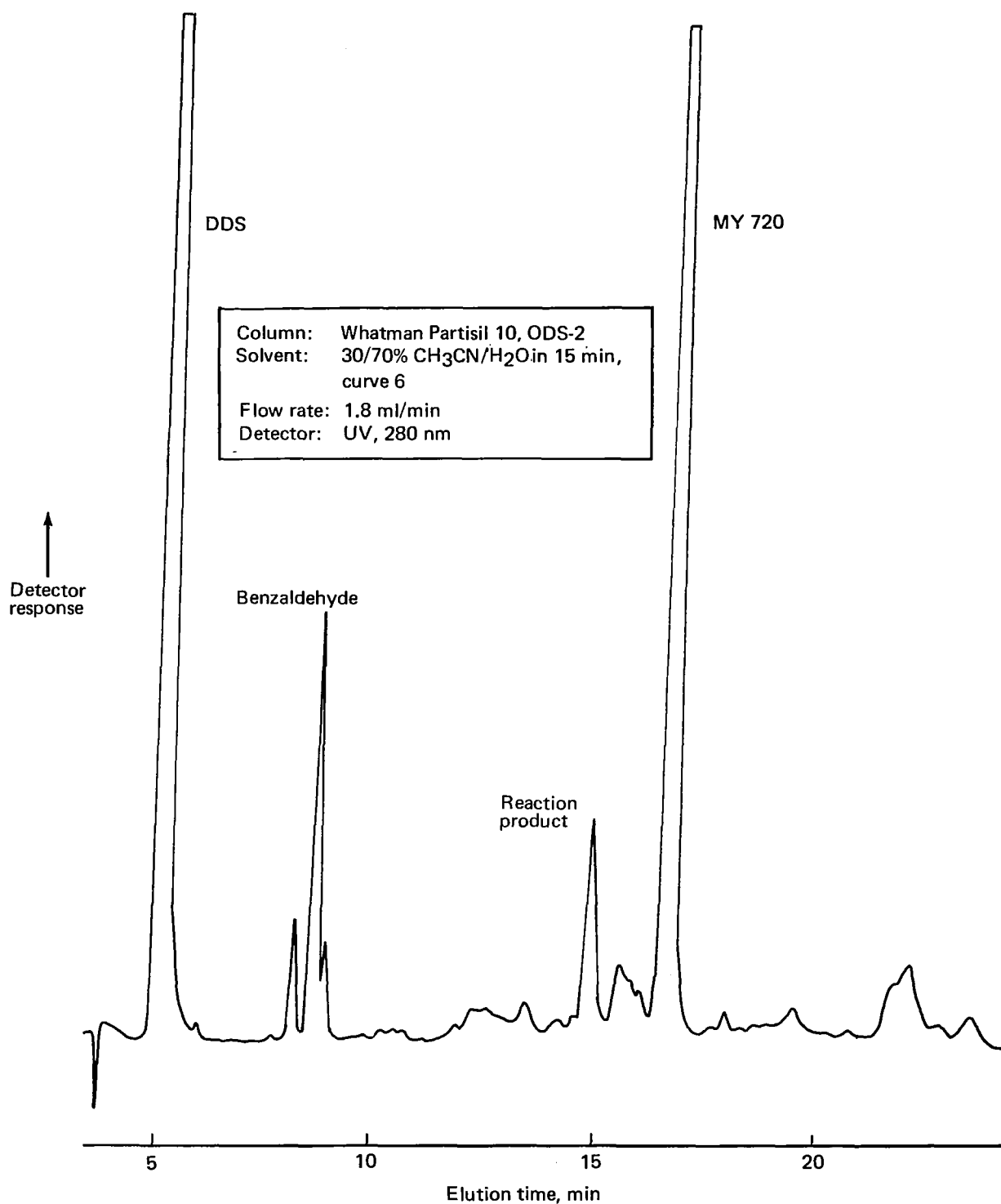
Figure 26. LC Chromatogram of Narmco Batch 286, Column: Whatman Partisil 10; ODS-2

Column: Merck Lichrosorb RP-8, 10μm
Solvent: 30/70% CH_3CN/H_2O in 15 min
Flow rate: 1.8 ml/min
Detector: UV, 280 nm

Detector response

Elution time, min
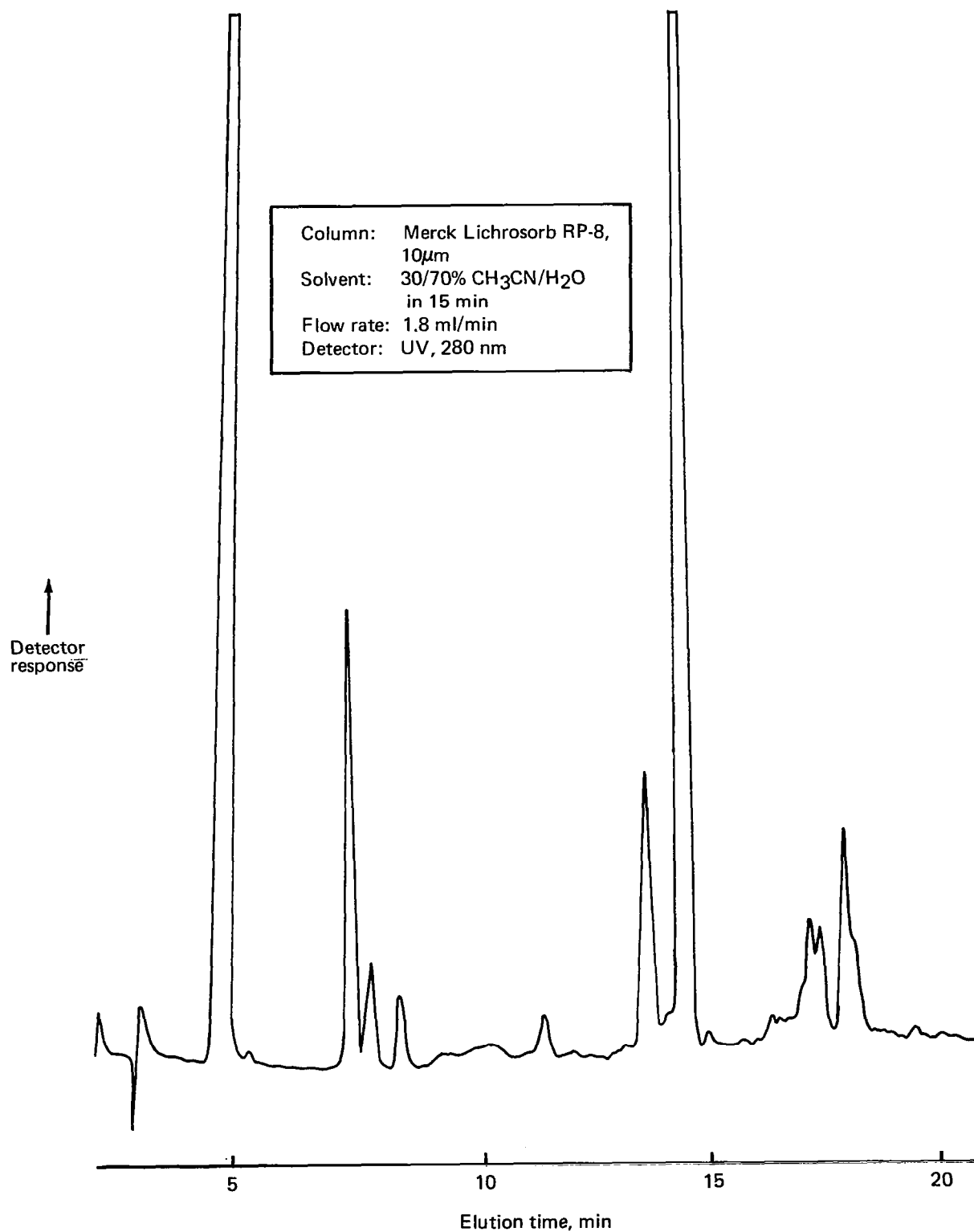
Figure 27. LC Chromatogram of Narmco Batch 286, Column: Merck Lichrosorb RP-8, 10μm

Column: Merck Lichrosorb RP-2,
            10μm
Solvent: 30/70% CH₃CN/H₂O
            in 15 min
Flow rate: 1.8 ml/min
Detector: UV, 280 nm

Detector response

5   10   15   '20
Elution time, min
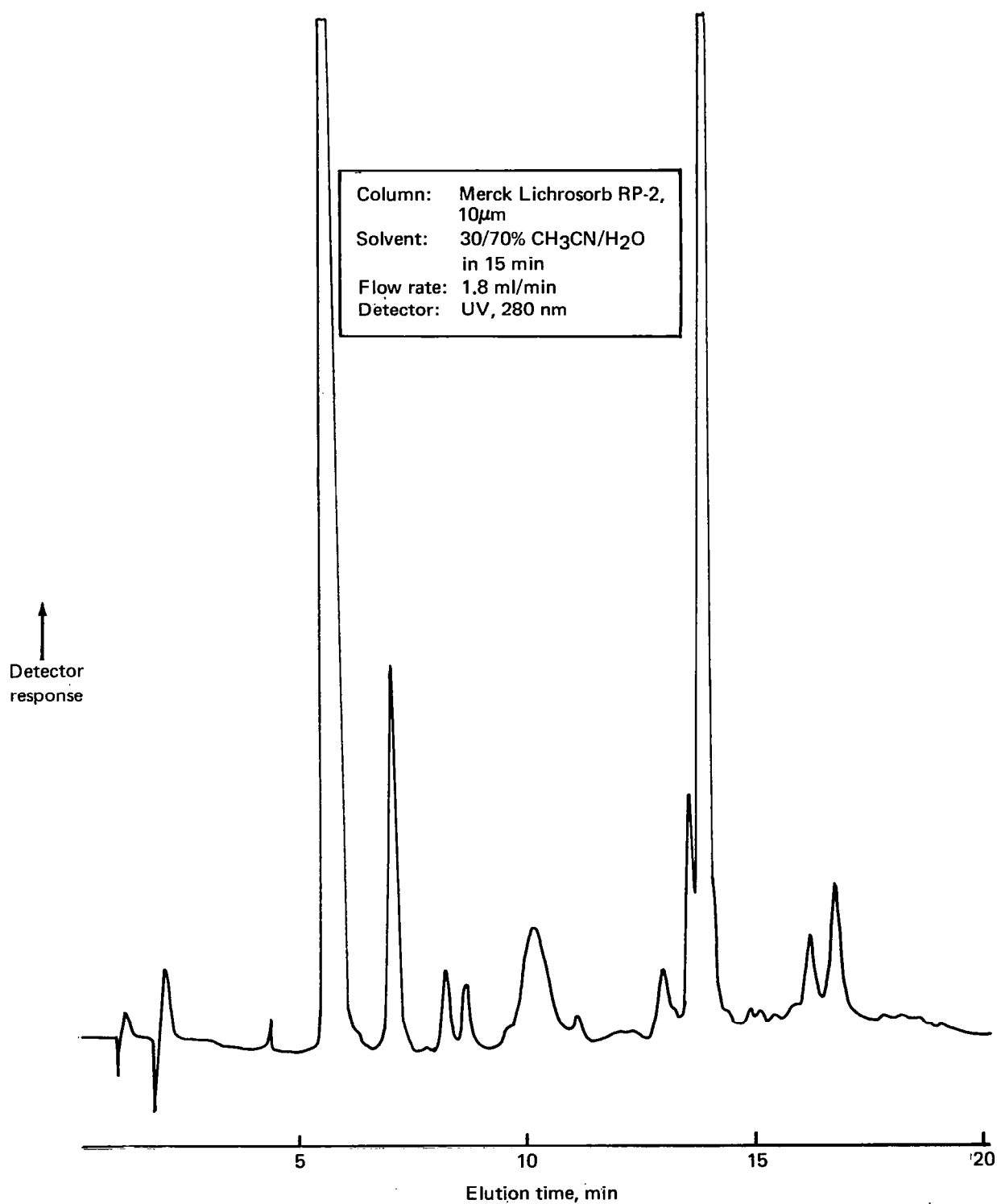
Figure 28. LC Chromatogram of Narmco Batch 286,
Column: Merck Lichrosorb RP-2, 10μm
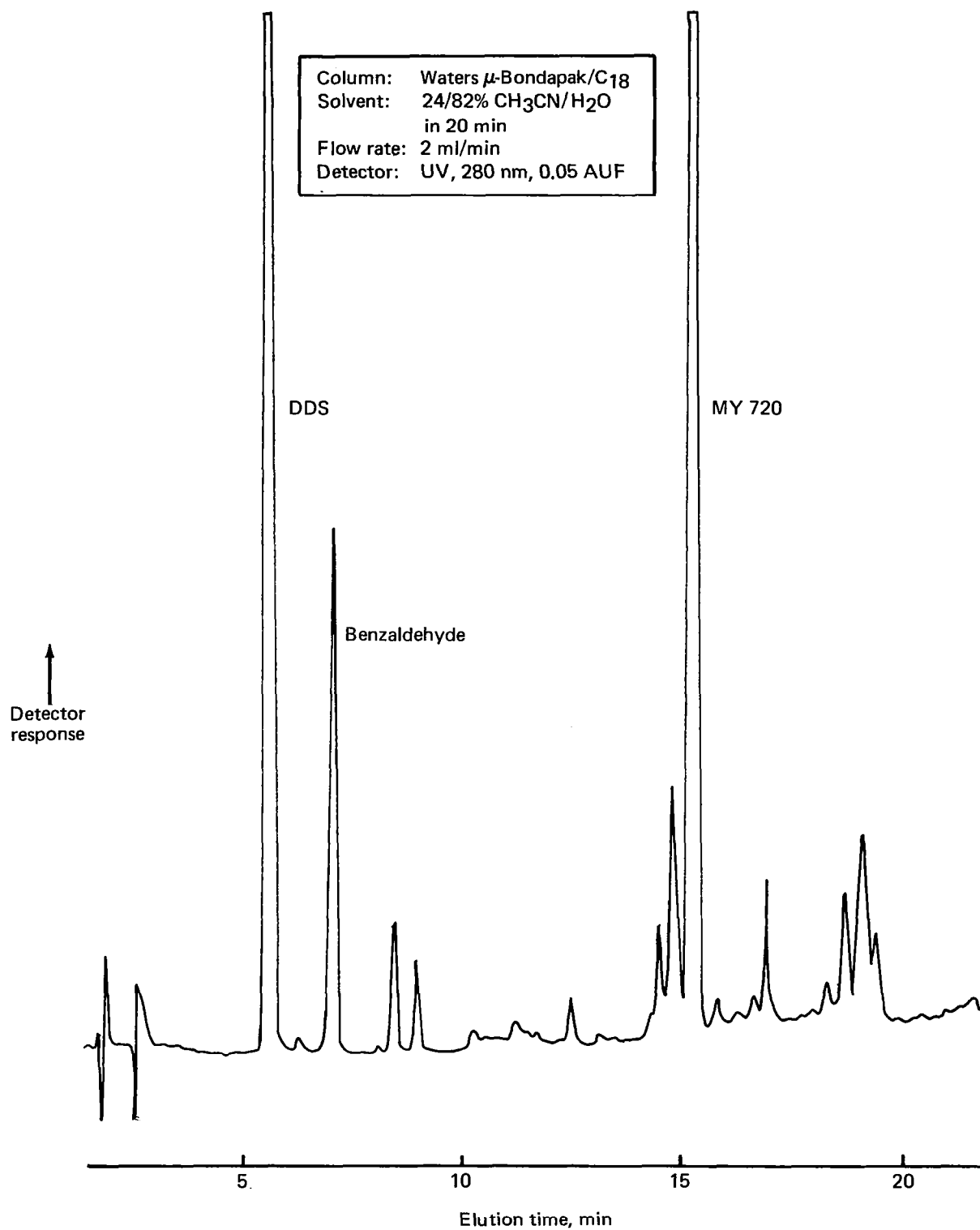
Figure 29. LC Chromatogram of Narmco Batch 286, Mobile Phase 1,
Column: Waters μ-Bondapak/C18
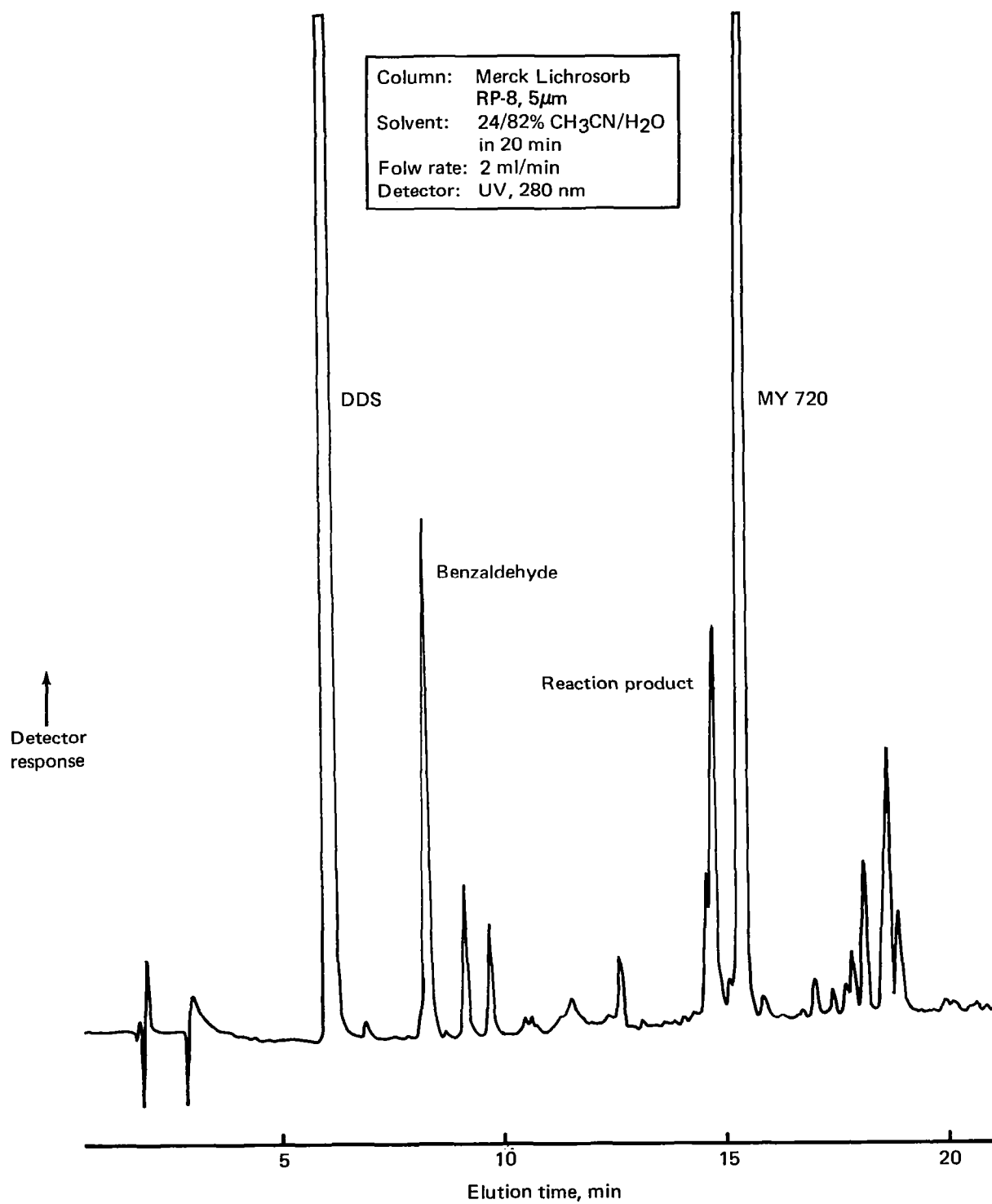
Figure 30. LC Chromatogram of Narmco Batch 286, Mobile Phase 1,
Column: Merck Lichrosorb RP-8, 5μm

DDS

MY 720

Column: Whatman Partisil 10, ODS-2
Solvent: 24/82% CH_3CN/H_2O in 20 min
Flow rate: 2 ml/min
Detector: UV, 280 nm

Detector response

Benzaldehyde

Reaction product

Elution time, min
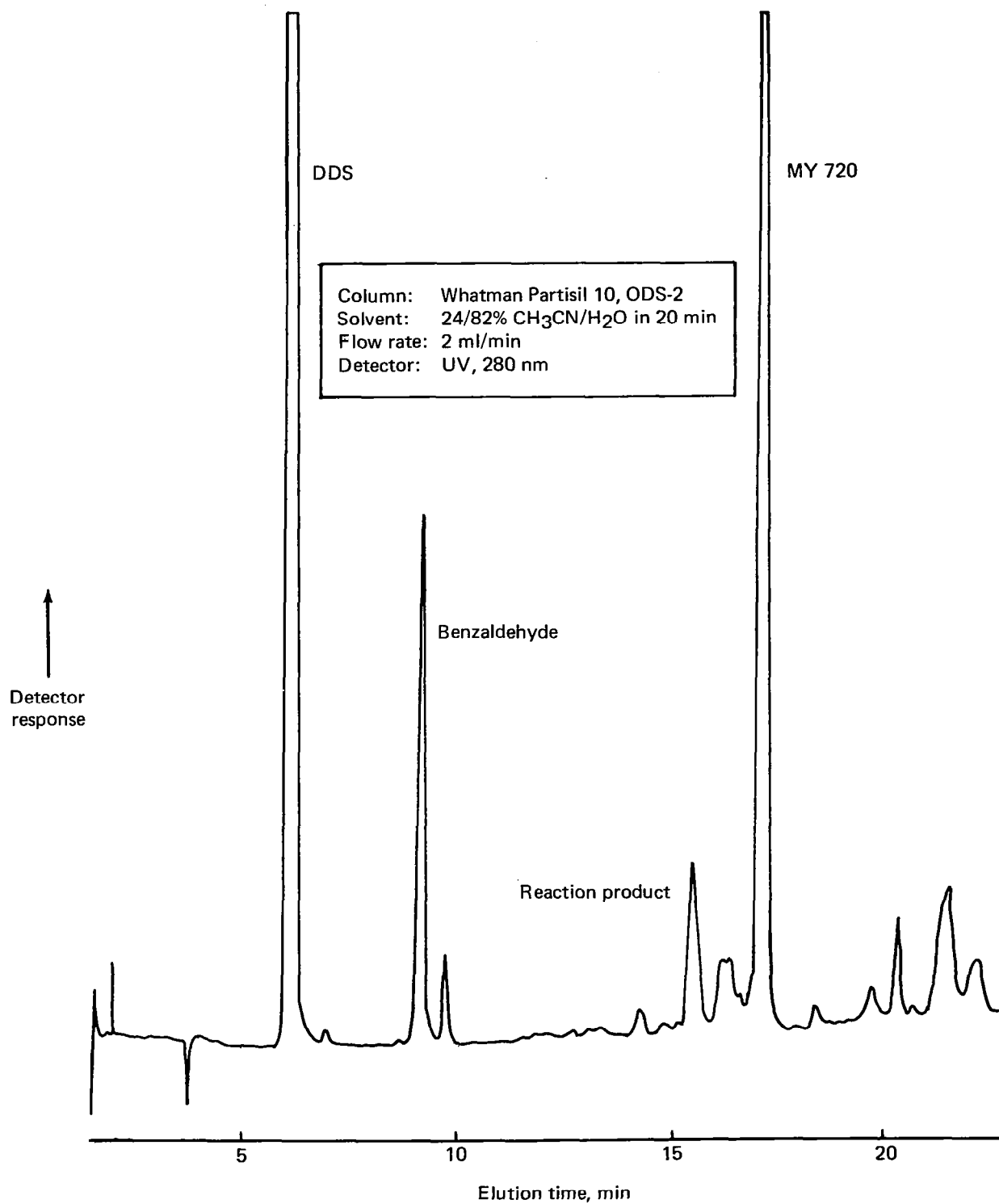
*Figure 31. LC Chromatogram of Narmco Batch 286,
Mobile Phase 1, Column: Whatman Partisil 10, ODS-2*

DDS

MY 720

Column: Waters μ-Bondapak/C$_{18}$
Solvent: 63/37% CH$_3$CN/H$_2$O, isocratic
Flow rate: 1.5 ml/min
Detector: UV, 220 nm, 0.2 AUF

Detector
response

5   10   15

Elution time, min
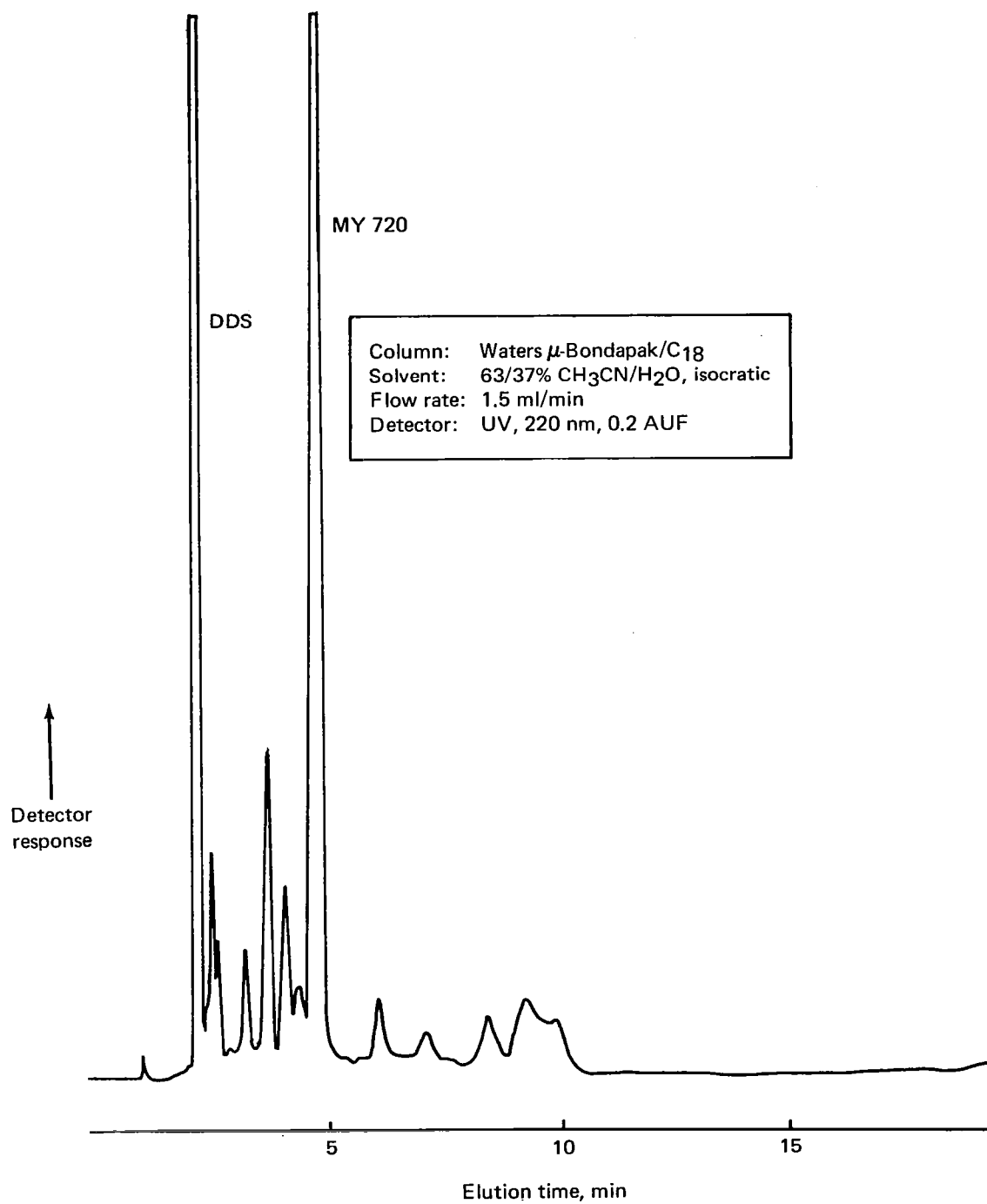
*Figure 32. LC Chromatogram of Narmco Batch 286,
Isocratic Solvent, Column: Waters μ-Bondapak/C$_{18}$*
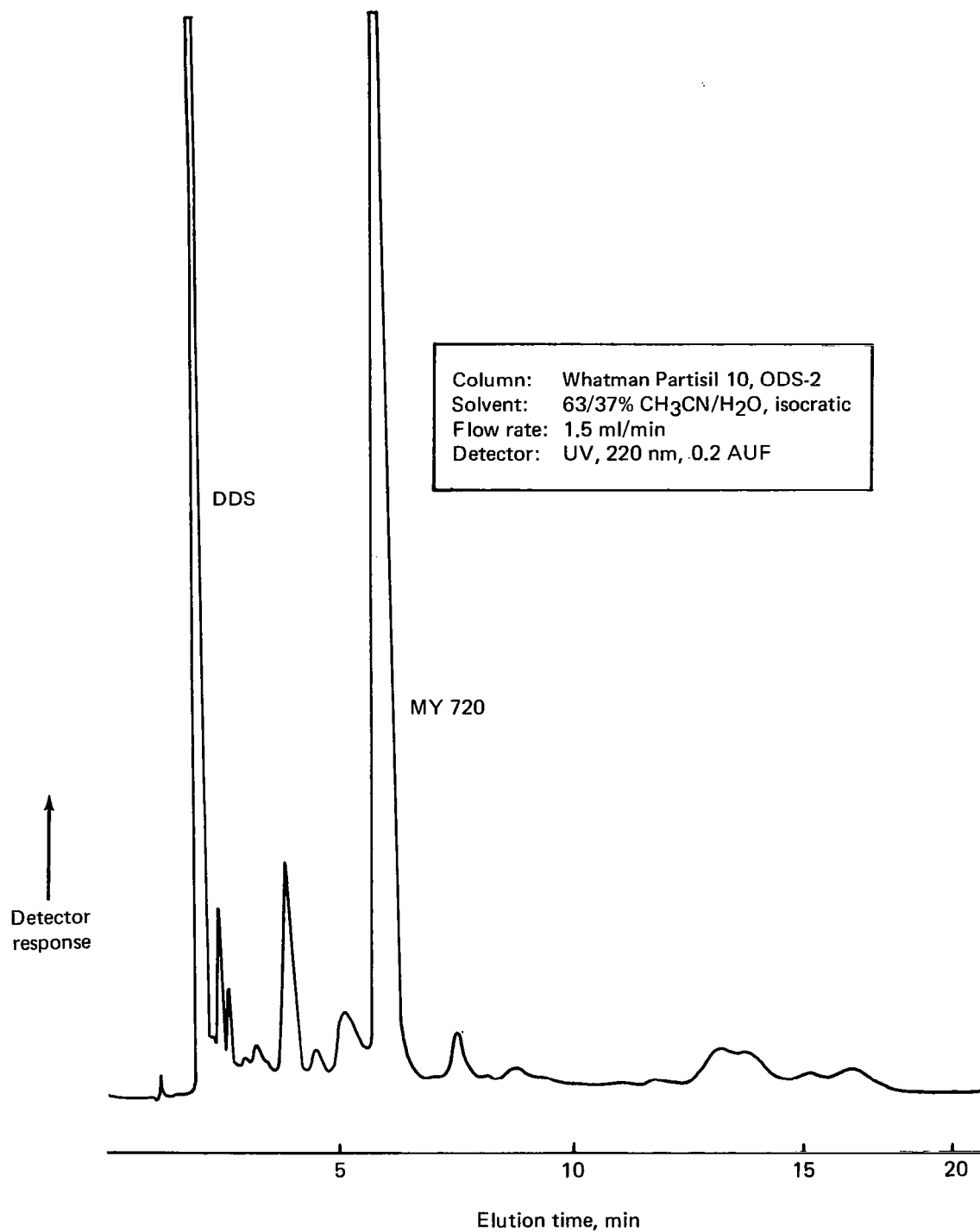
Figure 33. LC Chromatogram of Narmco Batch 286, Isocratic
Solvent, Column: Whatman Partisil 10, ODS-2

Elution time, min

| 5 | 10 | 15 | 20 | 25 |

Detector
response

↓

Detector
response

↑

Detector: UV, 220 nm,
0.2 AUF

Column: Waters μ-Bondapak/C$_{18}$
Solvent: 30/70% CH$_3$CN/H$_2$O in 15 min
Flow rate: 1.8 ml/min

Detector: UV, 280 nm,
0.2 AUF

| 5 | 10 | 15 | 20 | 25 |

Elution time, min
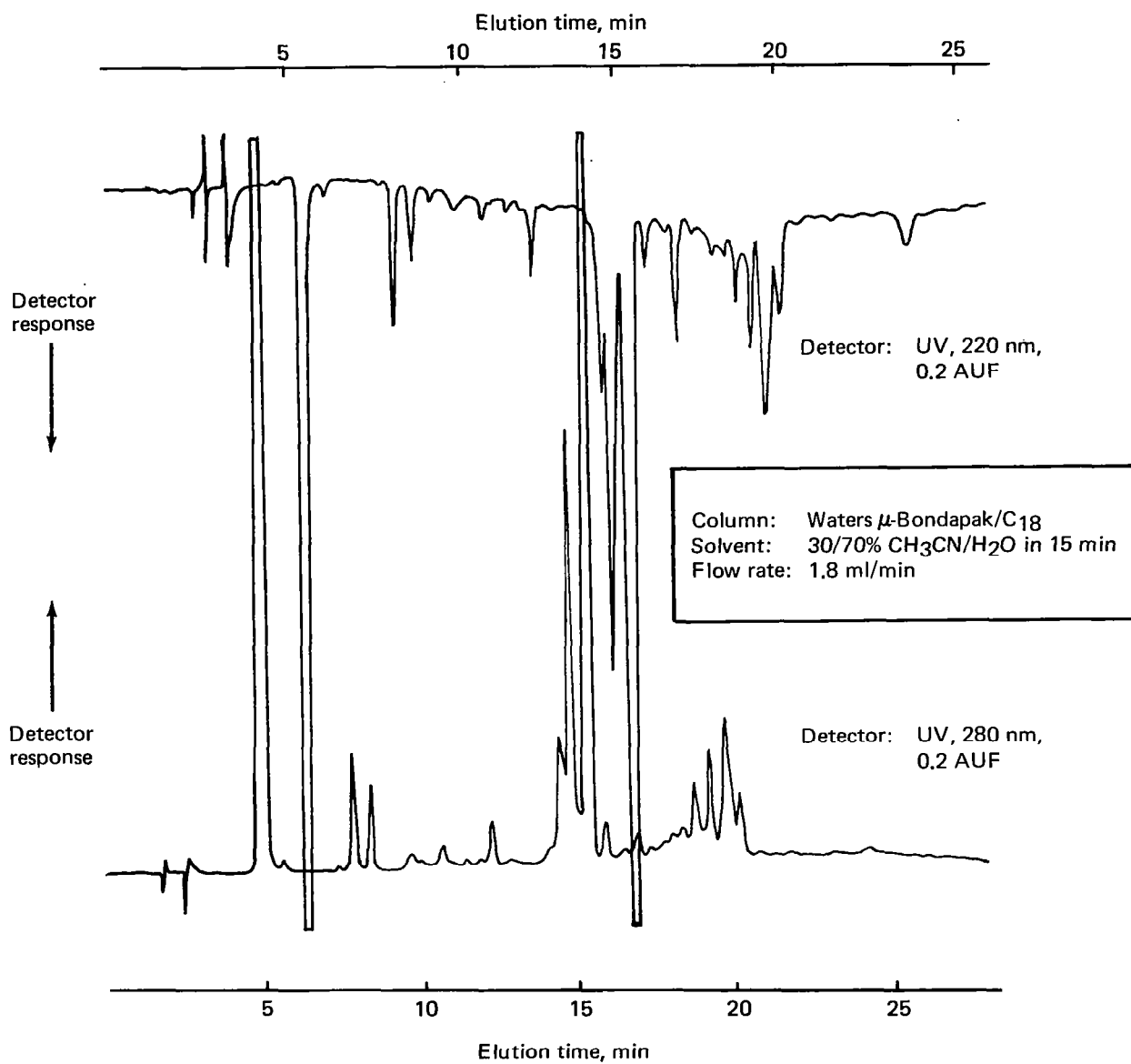
Figure 34. LC Chromatogram of Narmco Batch 286, Detector: UV, 220 nm

125

Elution time, min

5　　　　10　　　　15　　　　20　　　　25

Detector
response

↓

Detector: UV, 230 nm,
0.2 AUF

Column:　　Waters μ-Bondapak/C$_{18}$
Solvent:　　30/70% CH$_3$CN/H$_2$O in 15 min
Flow rate:　1.8 ml/min

Detector
response

↑

Detector: UV, 280 nm,
0.2 AUF

5　　　　10　　　　15　　　　20　　　　25

Elution time, min
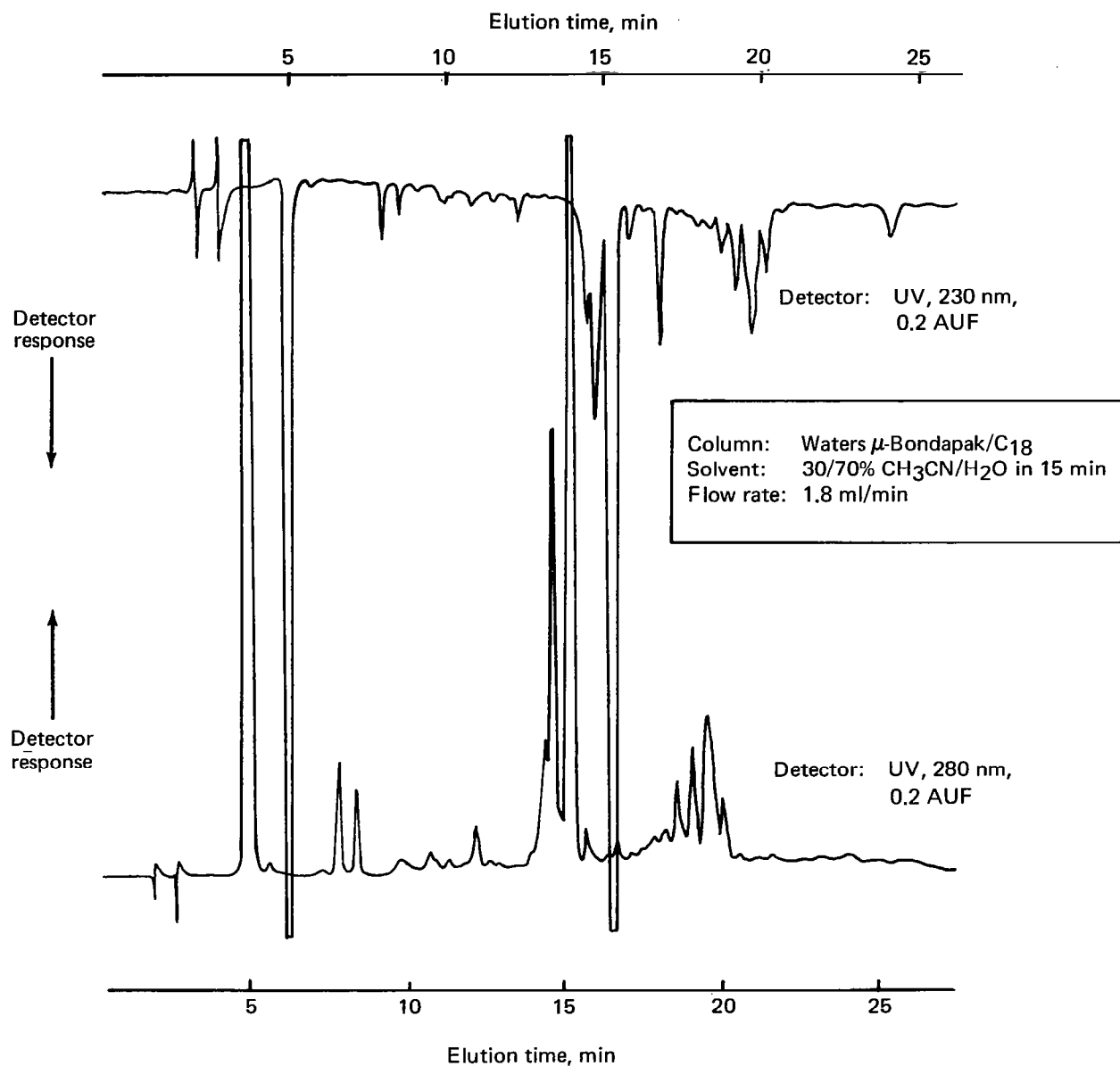
Figure 35. LC Chromatogram of Narmco Batch 286, Detector: UV, 230 nm
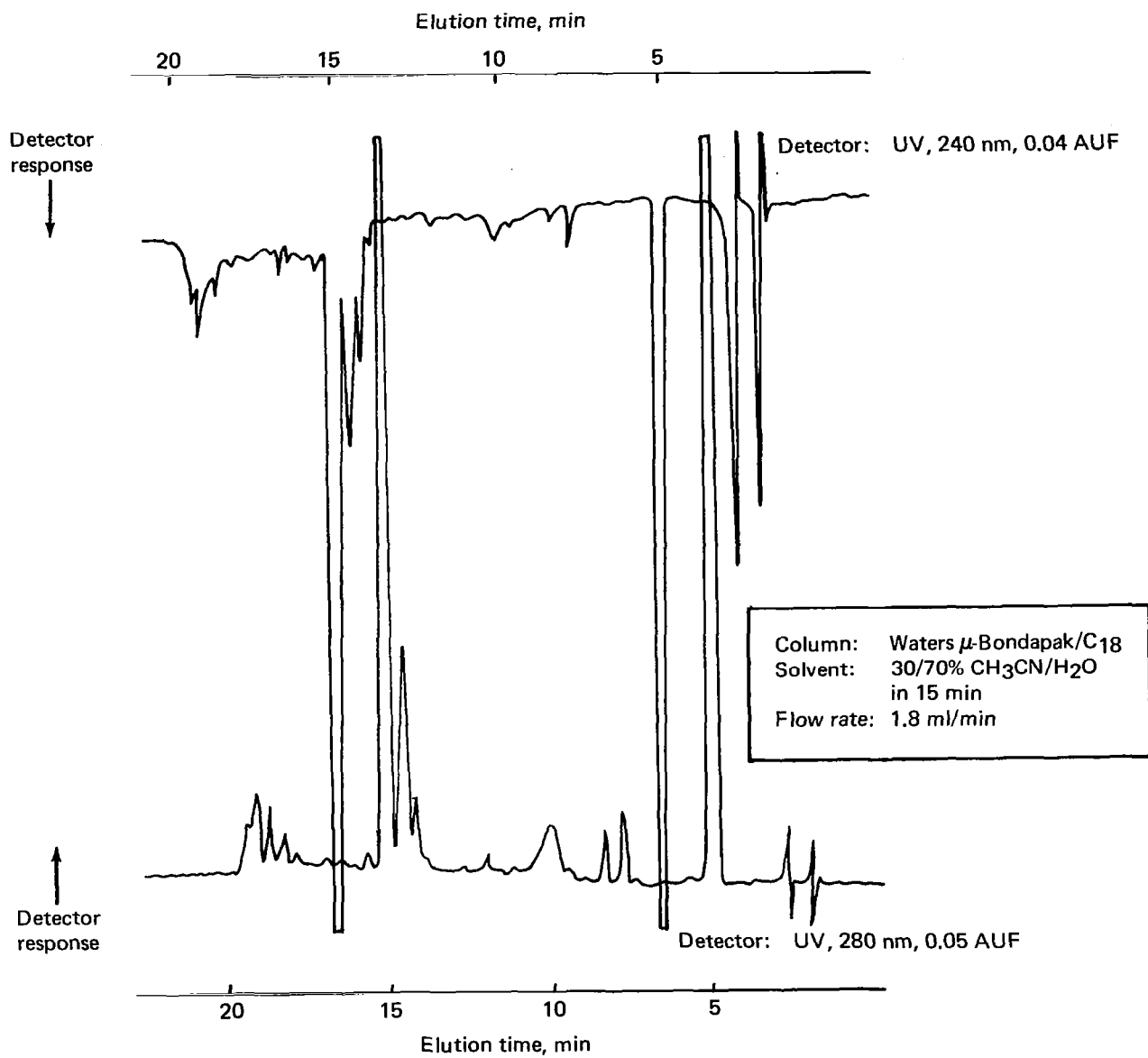
Figure 36. LC Chromatogram of Narmco Batch 286, Detector: UV, 240 nm
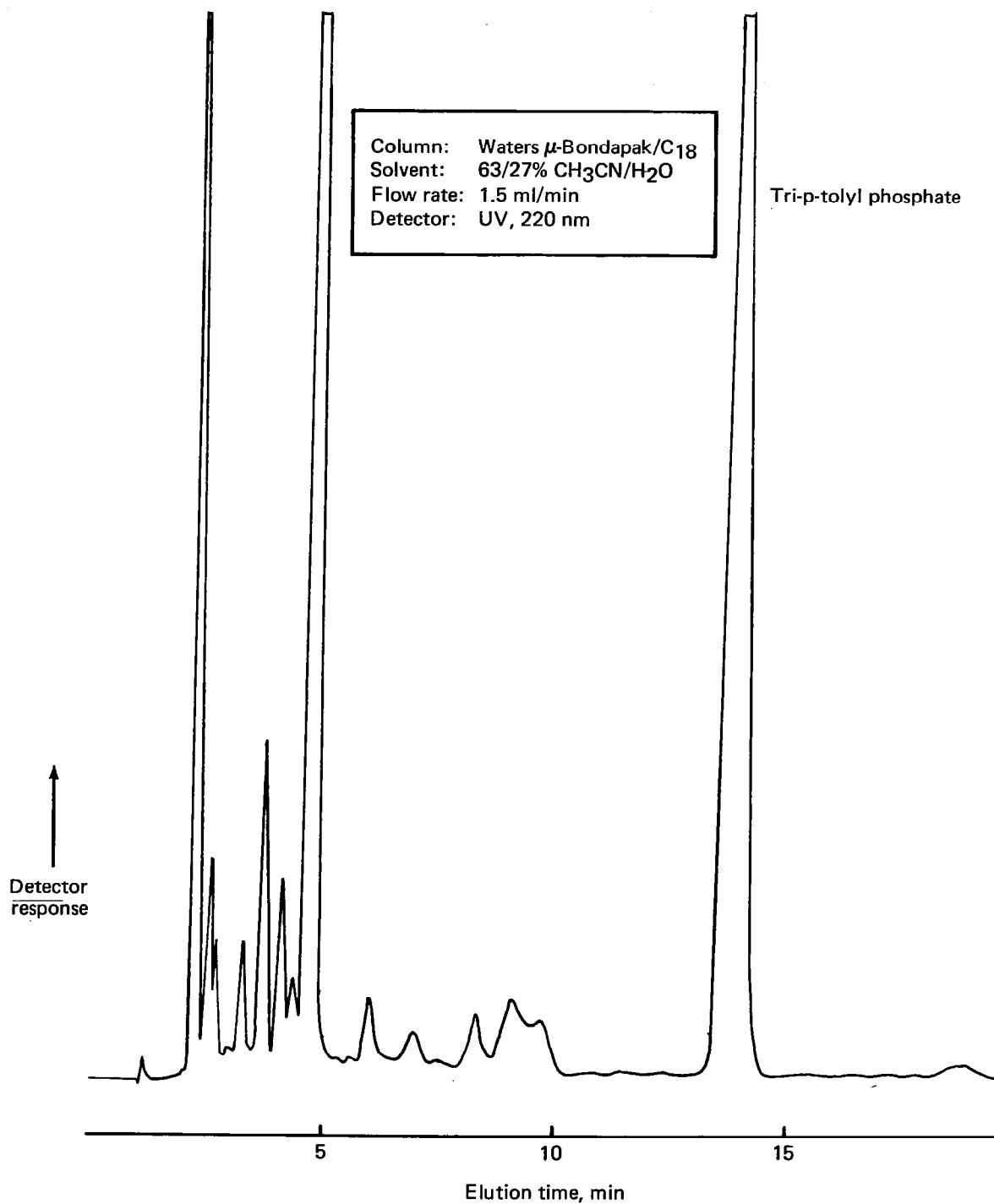
Figure 37. LC Chromatogram of Narmco Batch\286, Internal Standard: Tri-p-tolyl phosphate
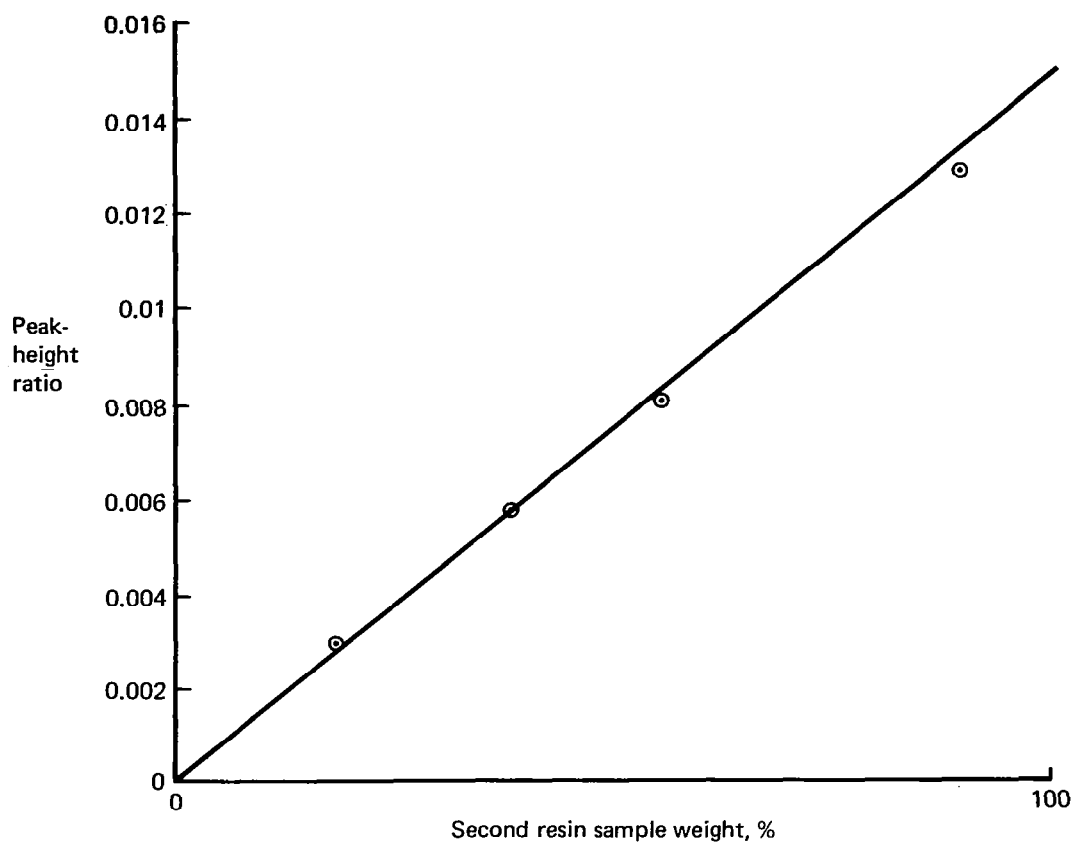
Figure 38. Calibration Curve of Second Resin
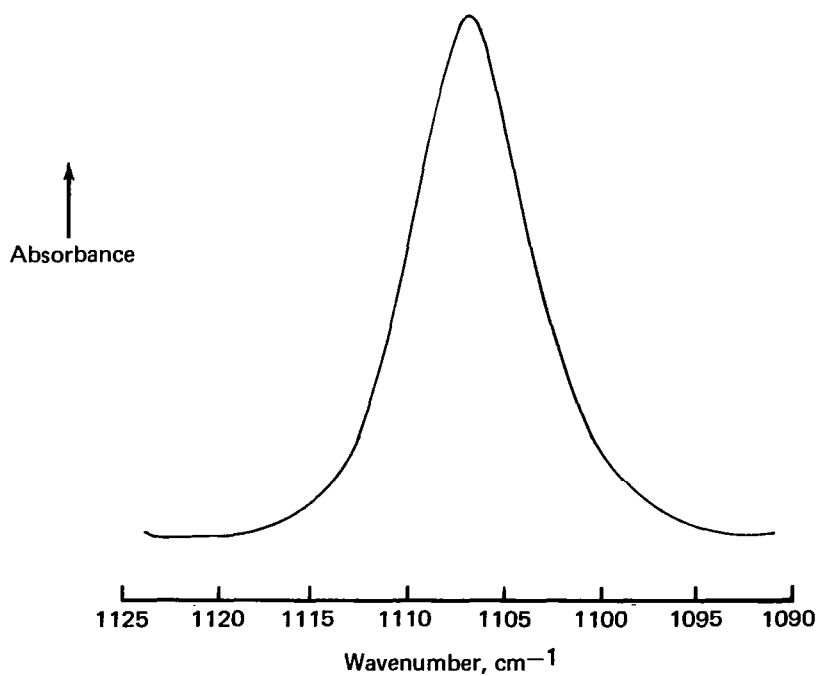
Figure 39. Determination of DDS Concentration by FTIR

Column: Waters μ-Bondapak/C$_{18}$
Solvent: 63/37% CH$_3$CN/H$_2$O, isocratic
Flow rate: 1.5 ml/min
Detector: UV, 220 nm, 0.2 AUF

Detector
response

← Elution time
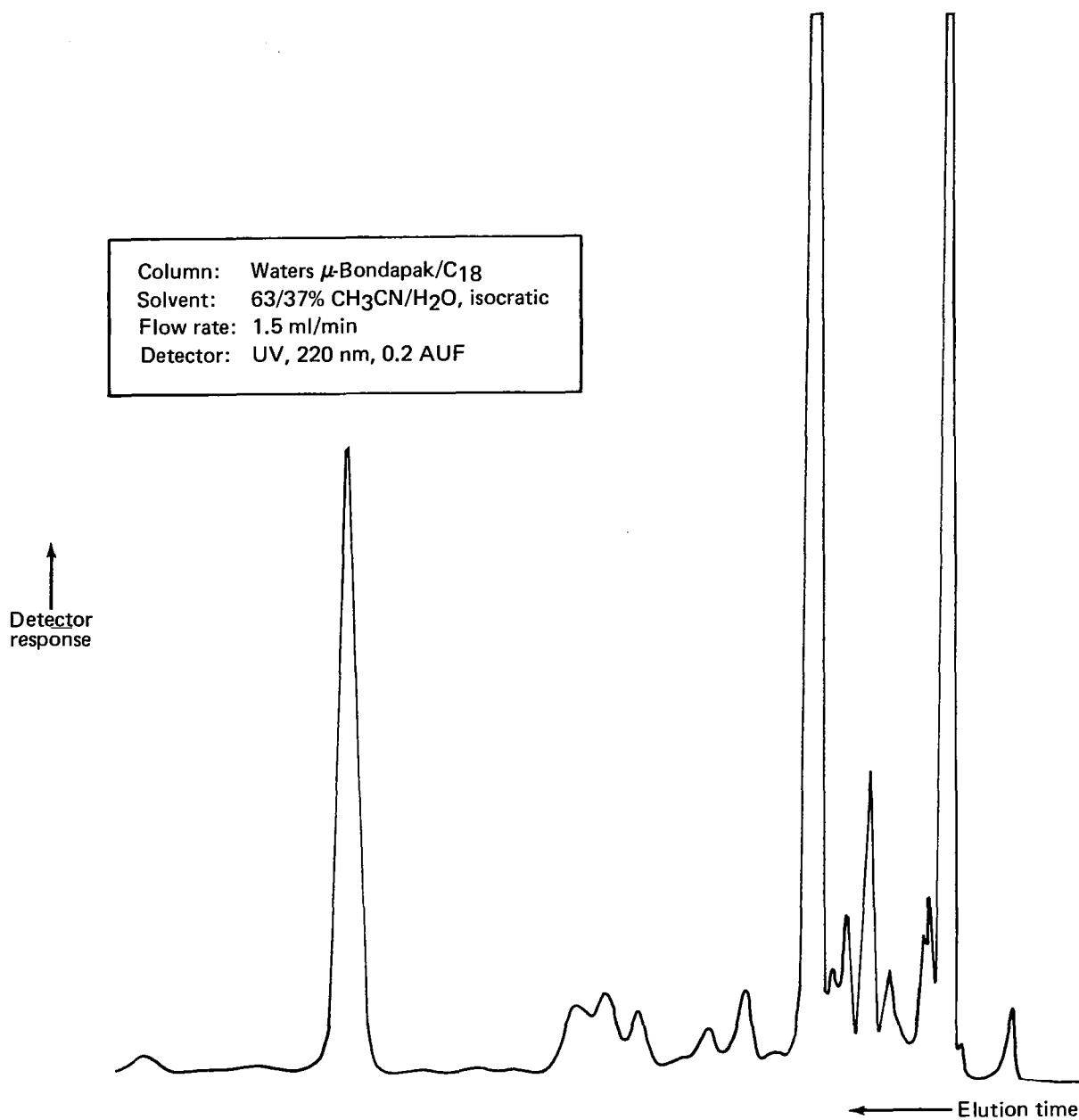
Figure 40. LC Chromatogram of Narmco Prepreg Batch 1072, Round-Robin Participant A
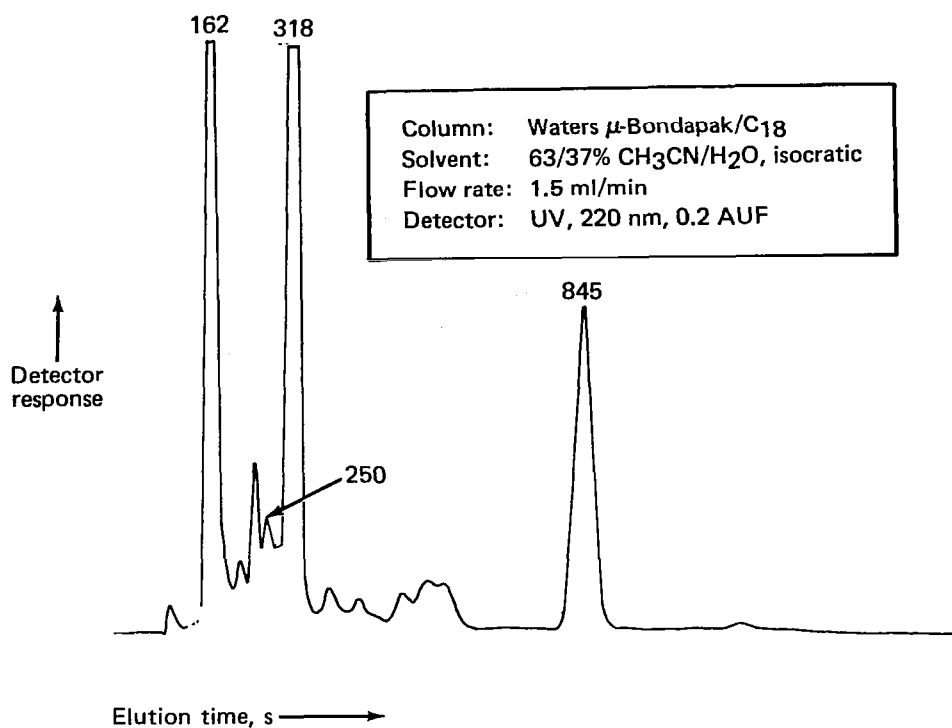
Figure 41. LC Chromatogram of Narmco Prepreg Batch 1072, Round-Robin Participant B
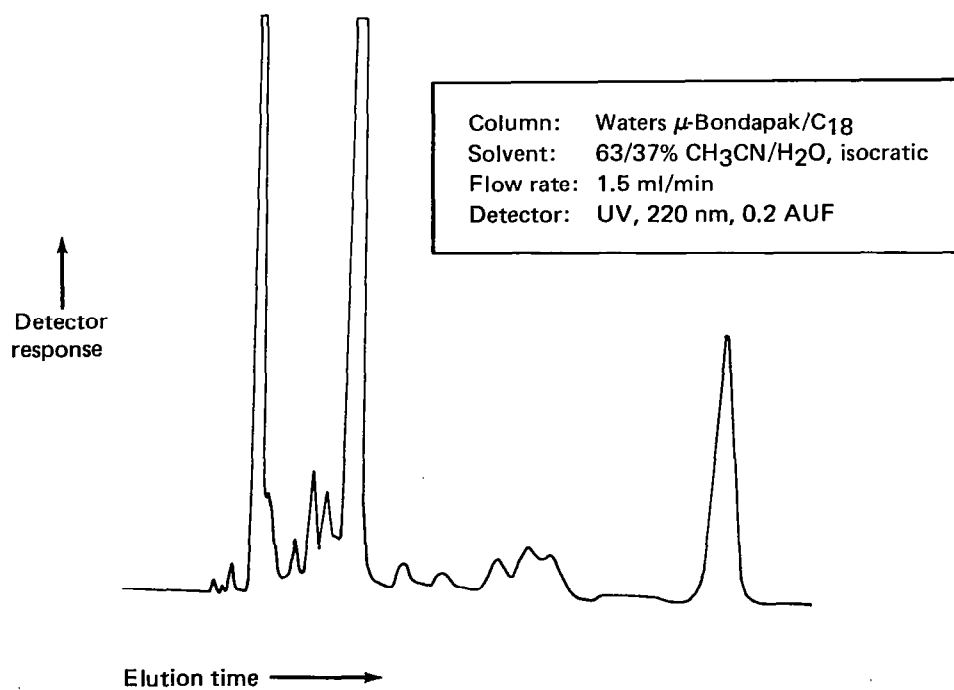
Figure 42. LC Chromatogram of Narmco Prepreg Batch 1072, Round-Robin Participant C

Column: Waters μ-Bondapak/C_{18}
Solvent: 63/37% CH_3CN/H_2O, isocratic
Flow rate: 1.5 ml/min
Detector: UV, 220 nm, 0.2 AUF

Detector response

140   283

762

226

Elution time, s ⟶
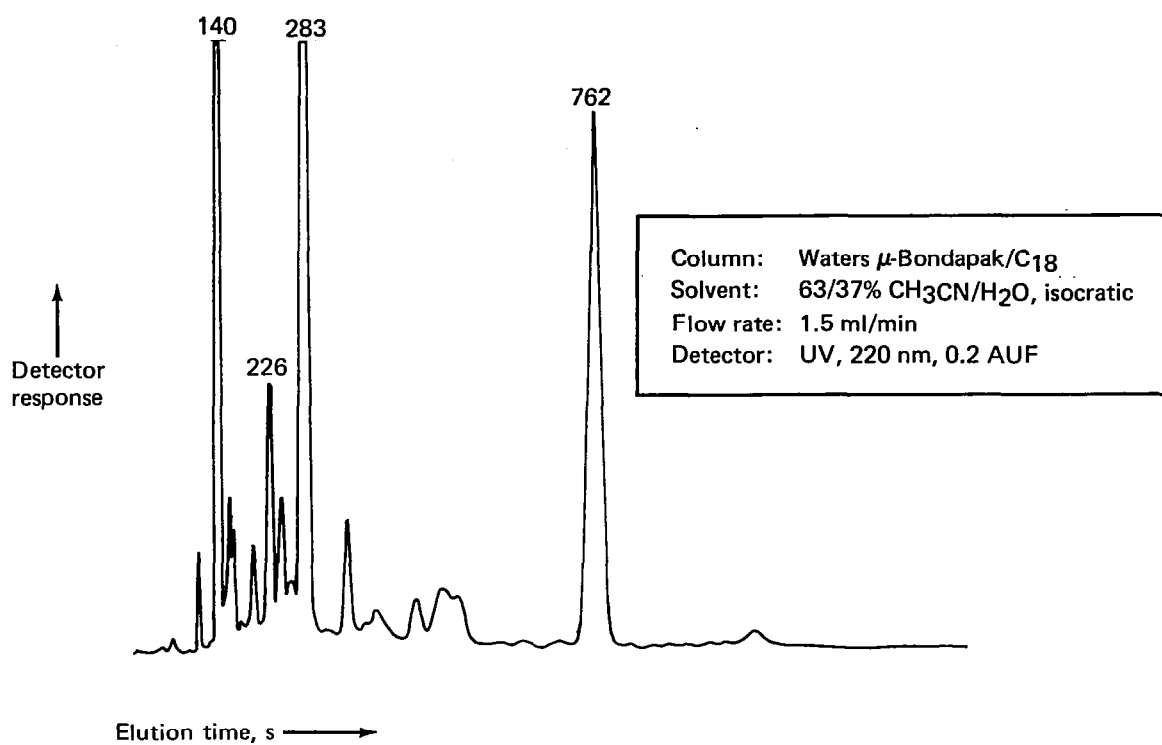
Figure 43. LC Chromatogram of Narmco Prepreg Batch 1072, Round-Robin Participant D

Column: Waters μ-Bondapak/C_{18}
Solvent: 63/37% CH_3CN/H_2O, isocratic
Flow rate: 1.5 ml/min
Detector: UV, 220 nm, 0.2 AUF

Detector response

2.16   4.22

3.40

10.63

Elution time, min ⟶
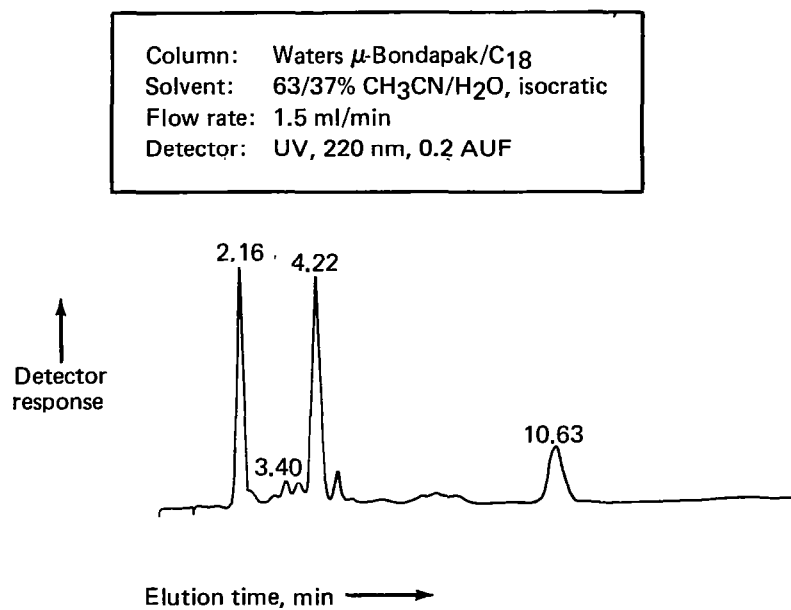
Figure 44. LC Chromatogram of Narmco Propreg Batch 1072, Round-Robin Participant E

132

Column: Waters μ-Bondapak/C_{18}
Solvent: 63/37% CH_3CN/H_2O, isocratic
Flow rate: 1.5 ml/min
Detector: UV, 220nm, 0.2 AUF

Detector response

← Elution time
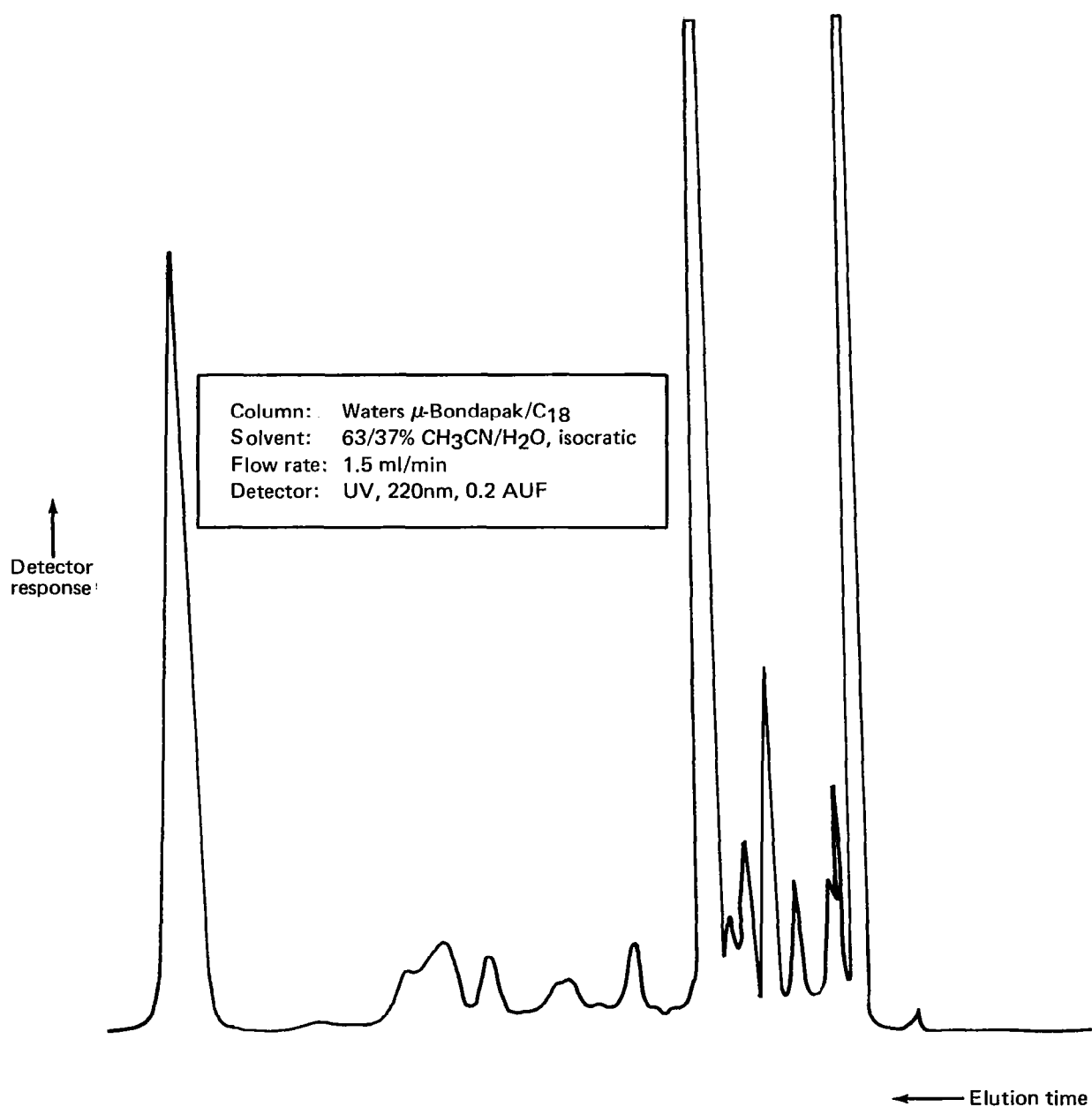
Figure 45. LC Chromatogram of Narmco Prepreg
Batch 1072, Round-Robin Participant F

Column: Waters μ-Bondapak/C$_{18}$
Solvent: 63/37% CH$_3$CN/H$_2$O, isocratic
Flow rate: 1.5 ml/min
Detector: UV, 220 nm, 0.2 AUF
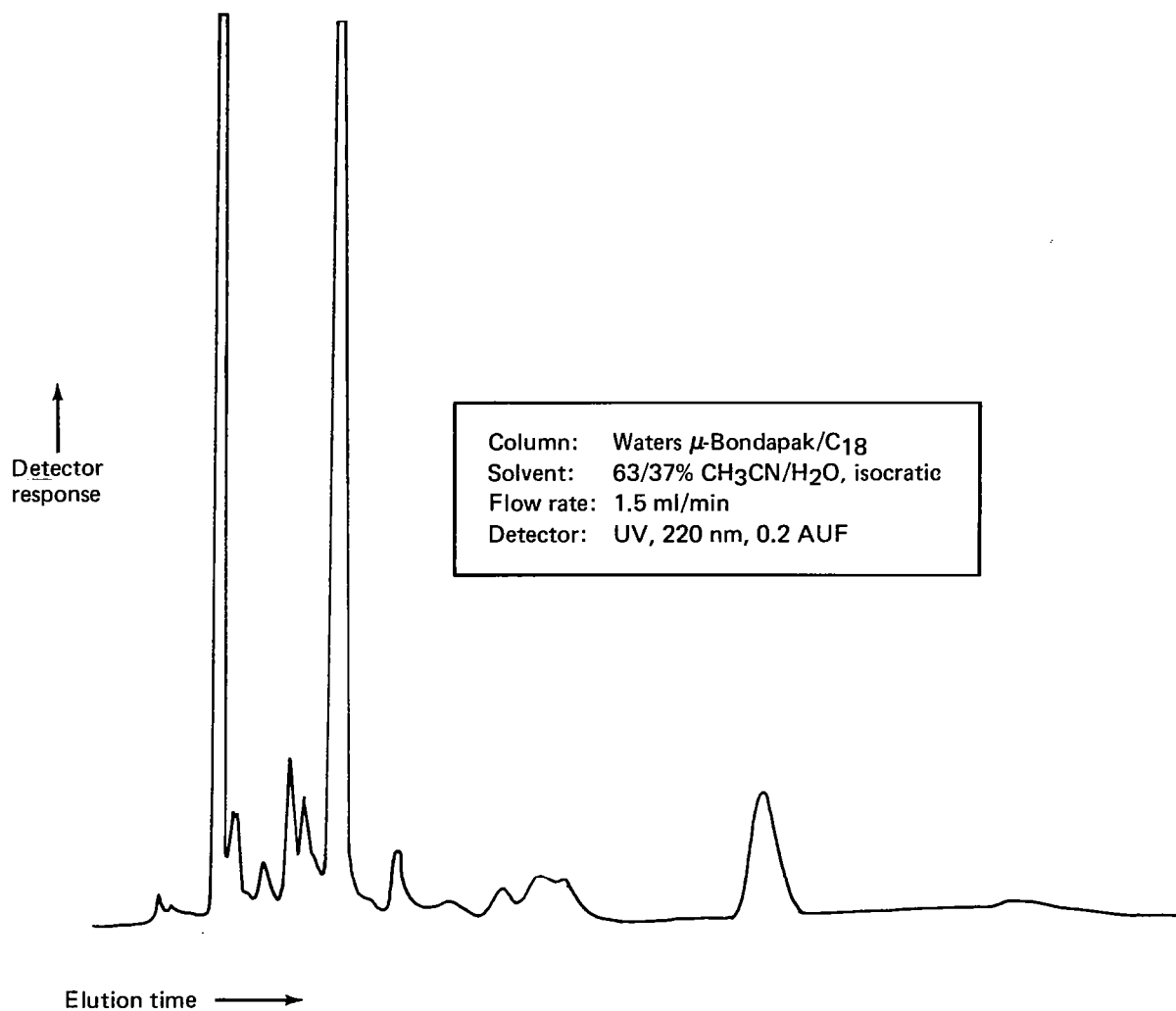
Figure 46. LC Chromatogram of Narmco Prepreg Batch 1072, Round-Robin Participant H

Column: Waters μ-Bondapak/C$_{18}$
Solvent: 63/37% CH$_3$CN/H$_2$O, isocratic
Flow rate: 1.5 ml/min
Detector: UV, 220 nm, 0.2 AUF
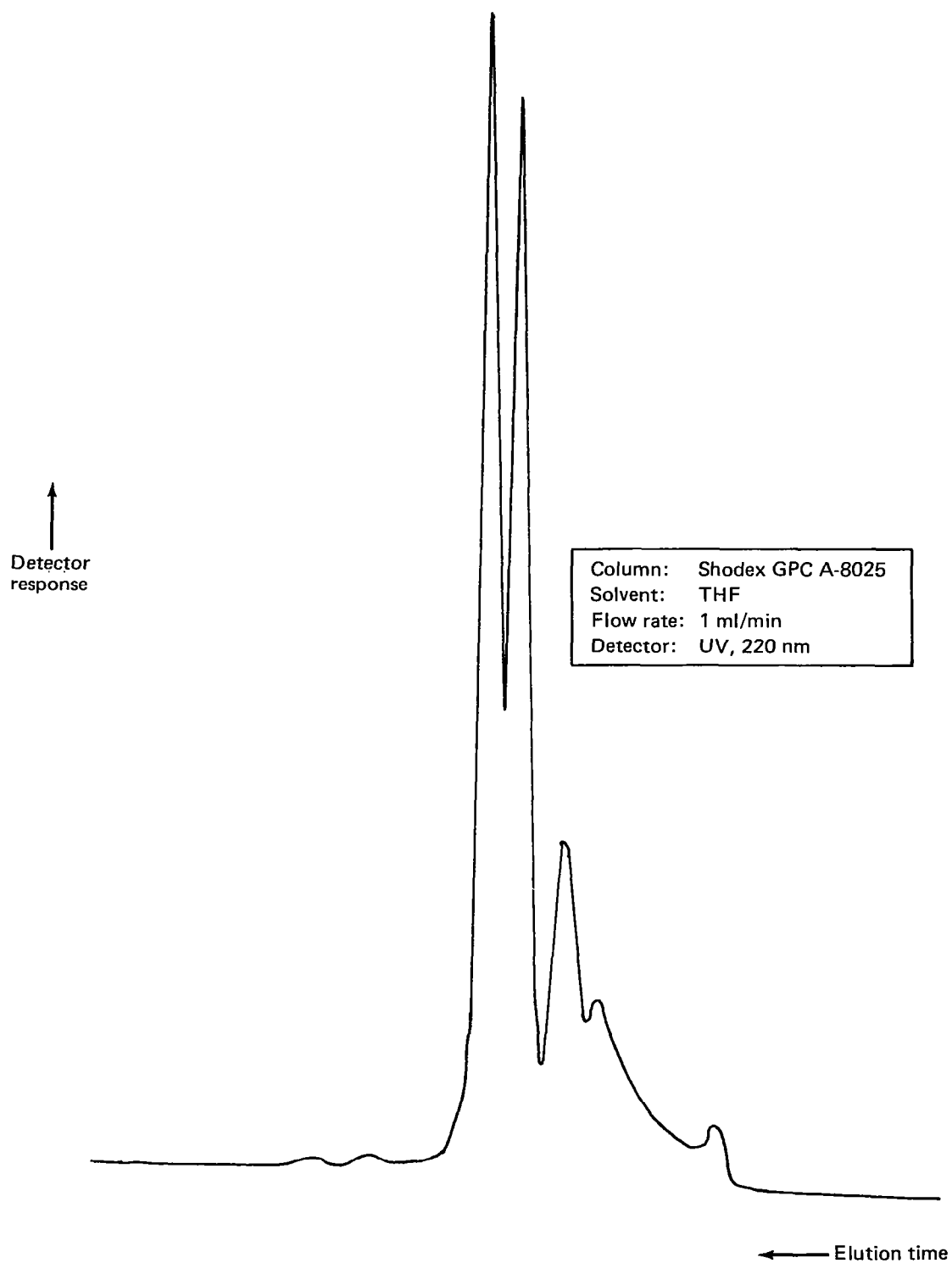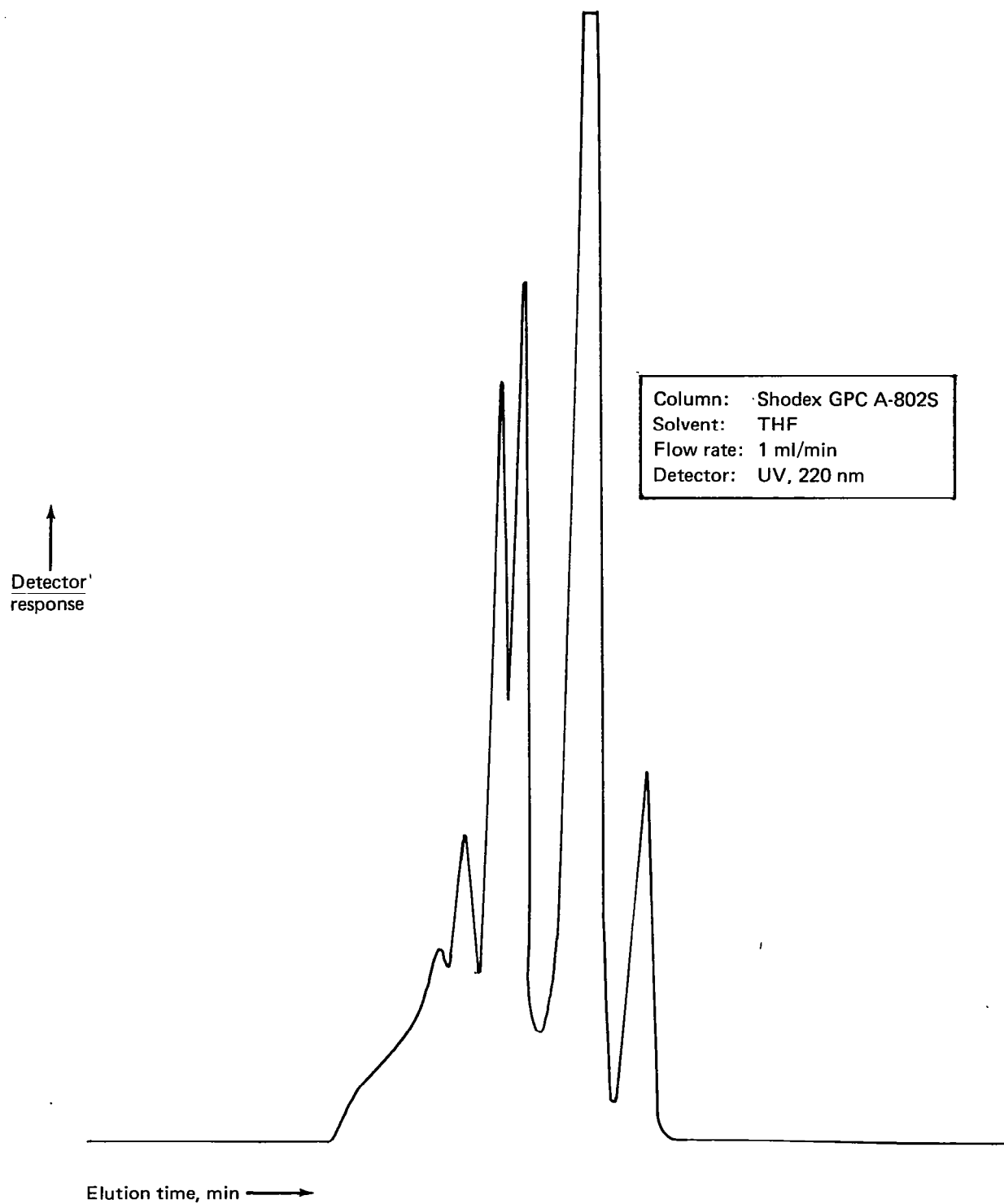
Detector
response

◄——— Elution time
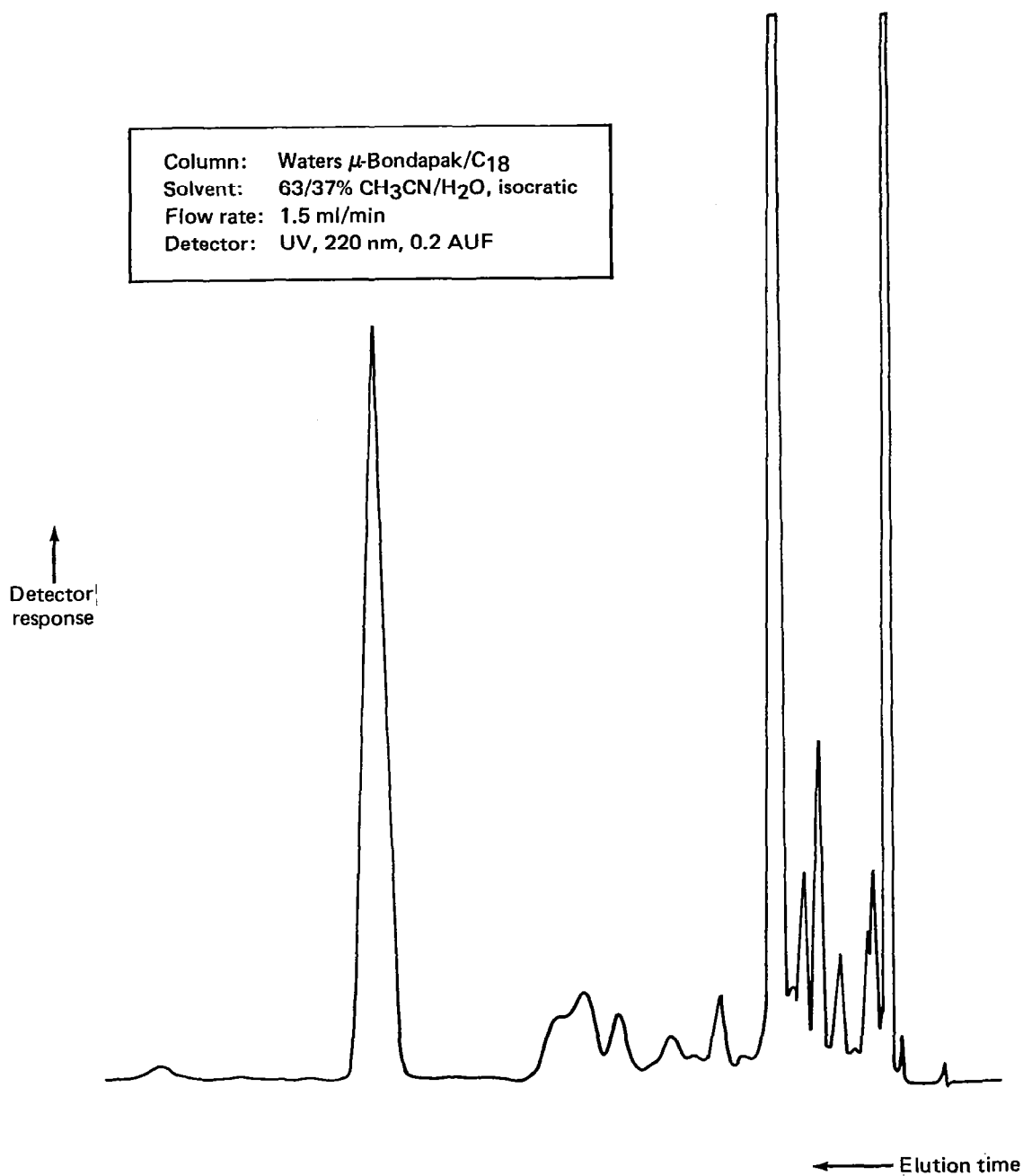
Figure 47. LC Chromatogram of Narmco Prepreg Batch 1072, Round-Robin Participant I
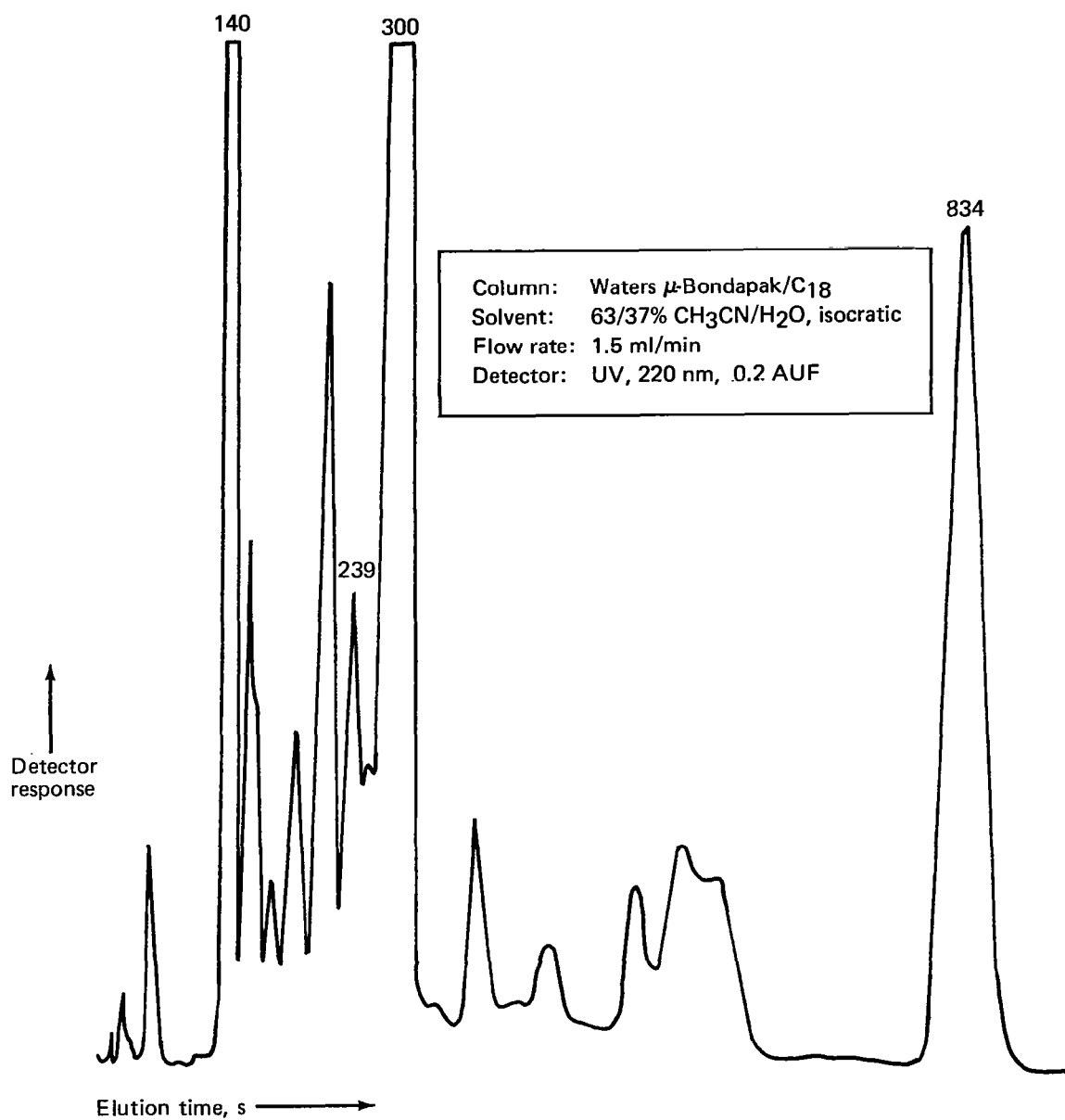
Figure 48. LC Chromatogram of Narmco Prepreg Batch 1072, Round-Robin Participant J
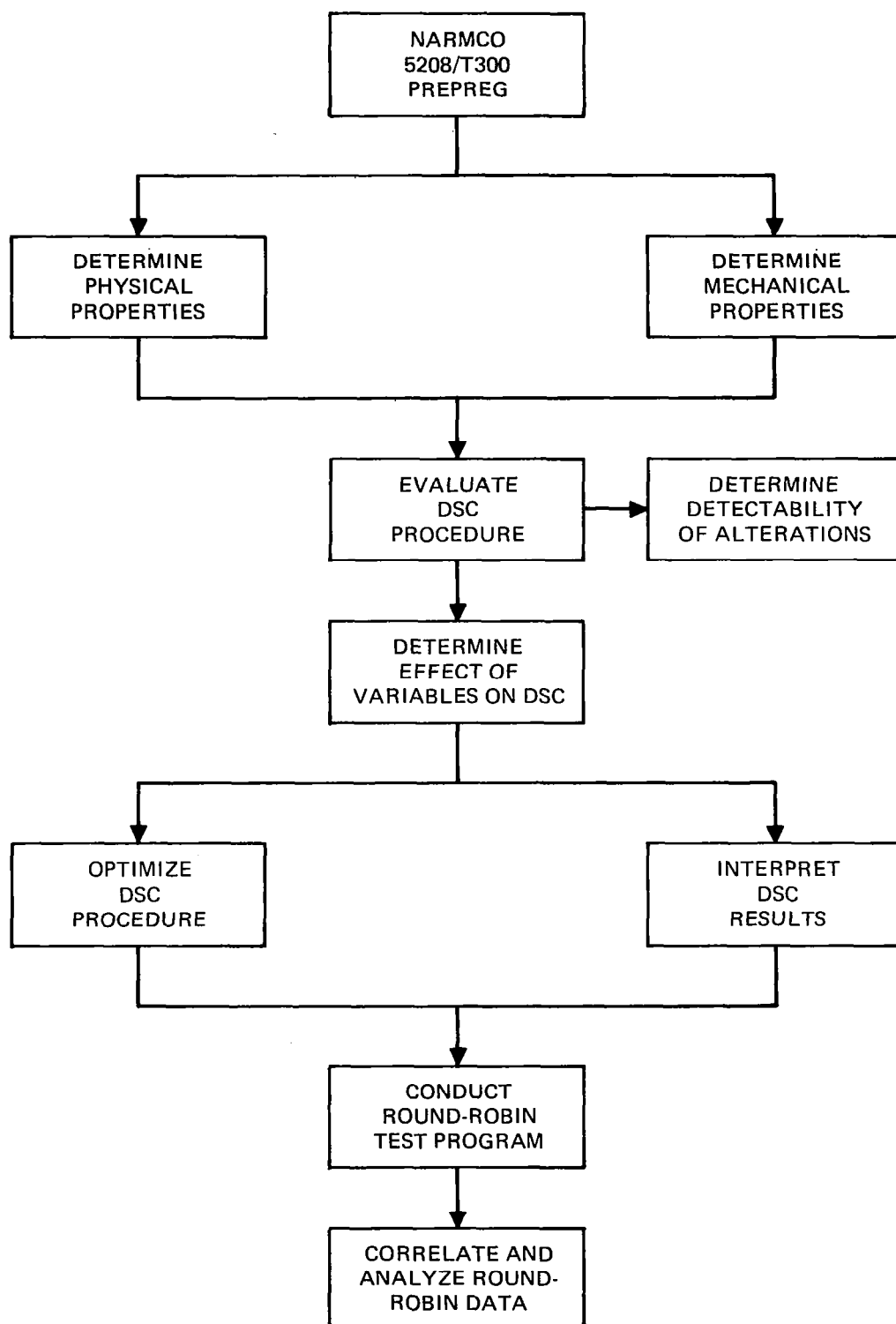
Figure 49. Task B Work Flow

ΔH_p exotherm

| 0 | 100 | 200 | 300|°C |

| 0 | 100 | 200 | 300 | 400 | 500 | (°F) |

Temperature
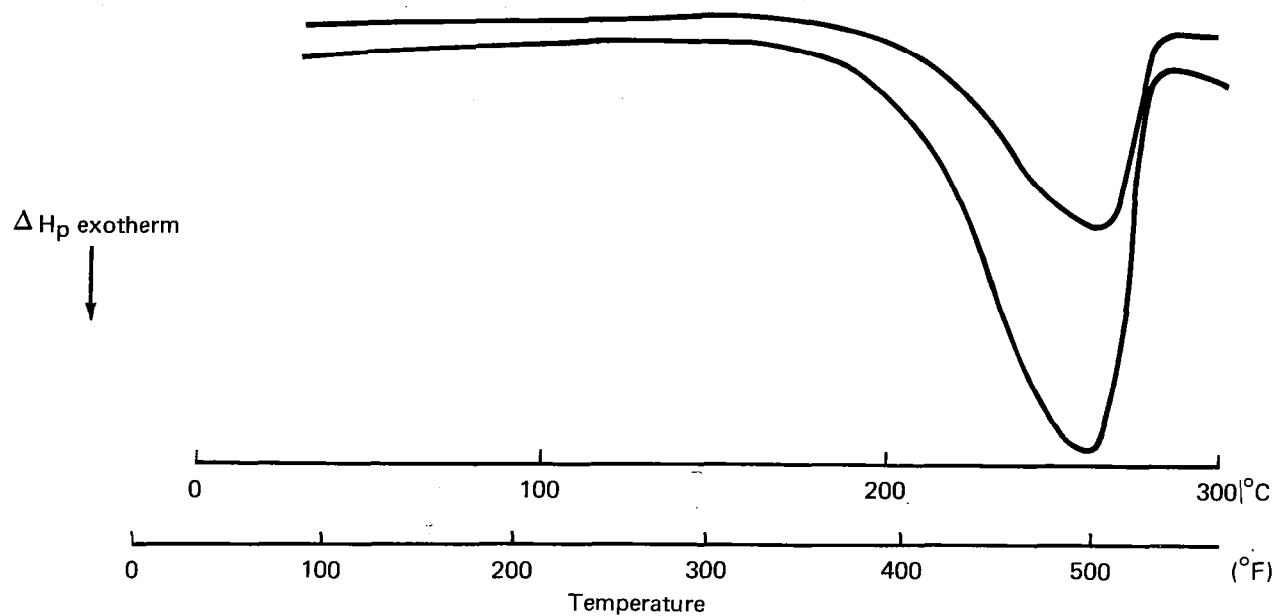
Figure 50. DSC Scan of Narmco Neat Resin Batch 300

ΔH_p exotherm.

DSC

First
derivative

| 0 | 100 | 200 | 300°C |

| 0 | 100 | 200 | 300 | 400 | 500 | (°F) |
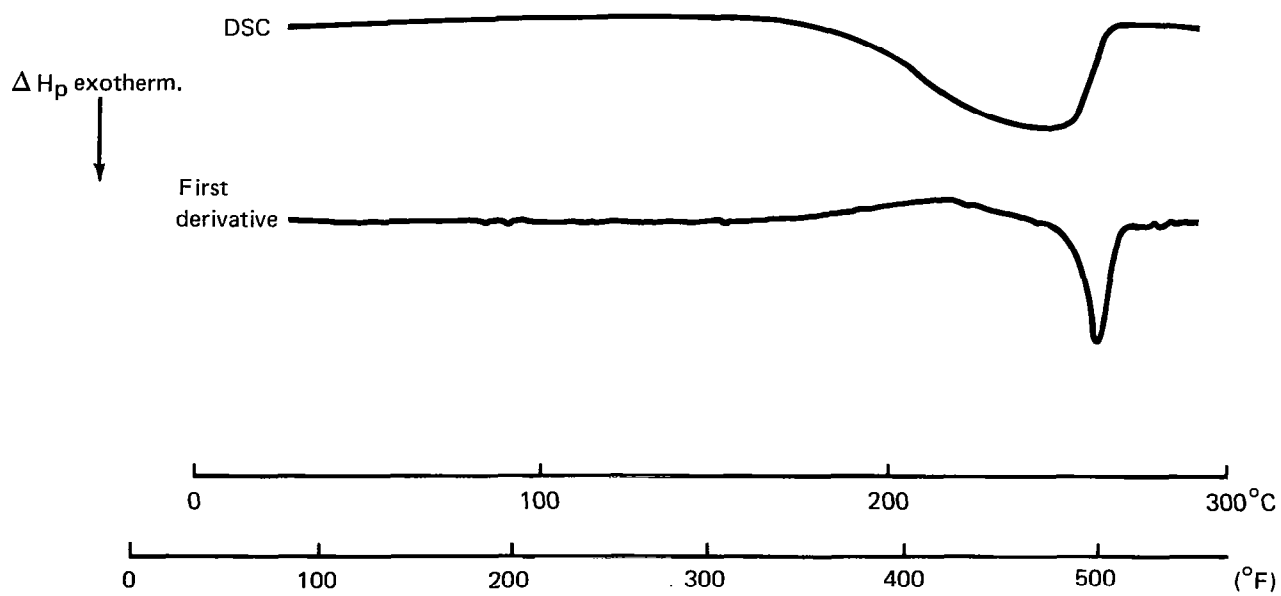
Figure 51. Duplicate DSC Scan of Narmco Neat Resin Batch 300

138
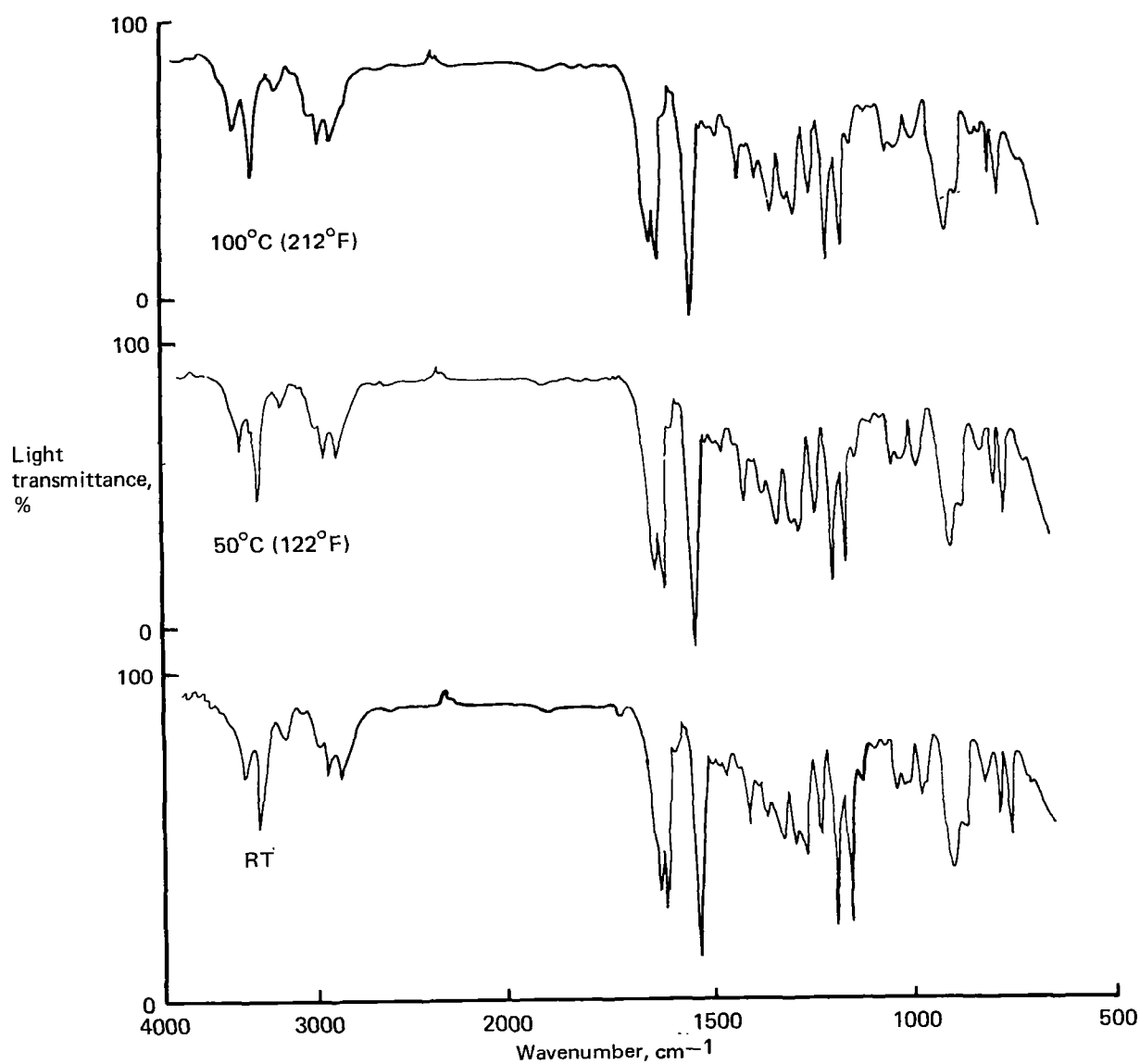
Figure 52. TSIR Spectra of Narmco Neat Resin Batch 300—RT, 50°C, and 100°C (RT, 122°F, and 212°F)
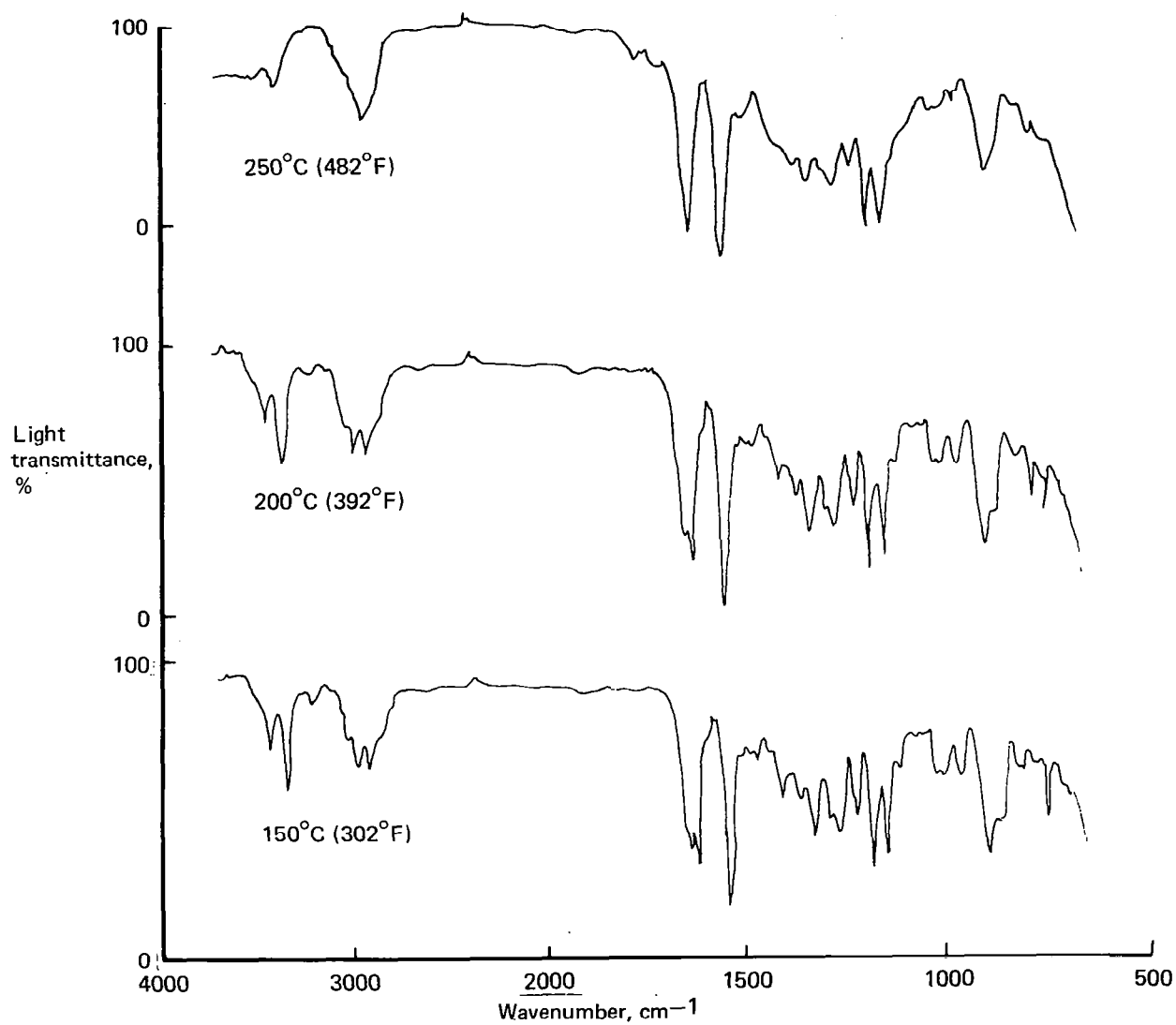
Figure 53. TSIR Spectra of Narmco Neat Resin Batch
300—150, 200, and 250°C | (302, 392, and 482°F)
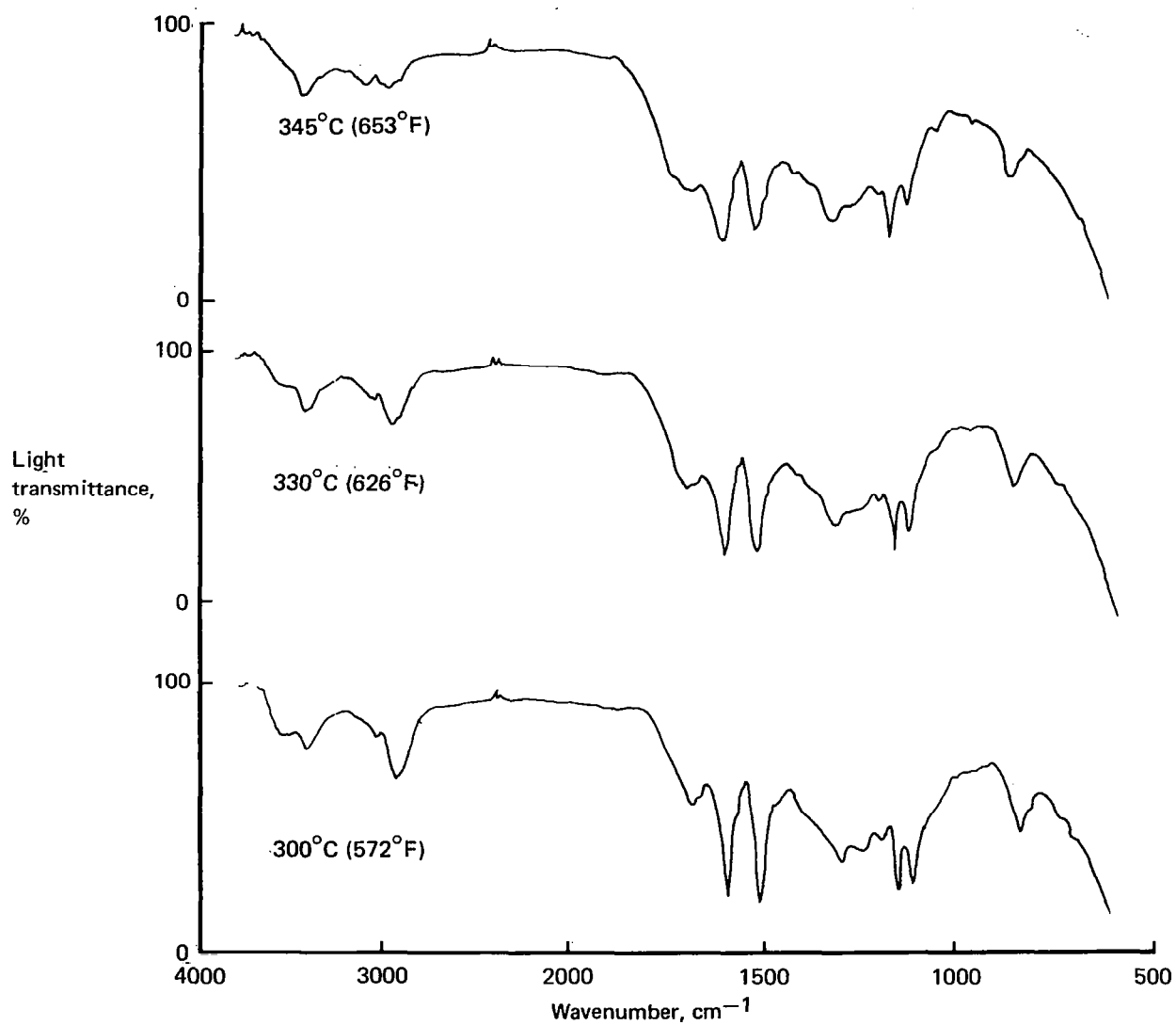
Figure 54. TSIR Spectra of Narmco Neat Resin Batch
300—300, 330, and\345°C (572, 626, and 653°F)

Frequency: 1 kHz
Heating rate: 5°C/min (9°F/min)
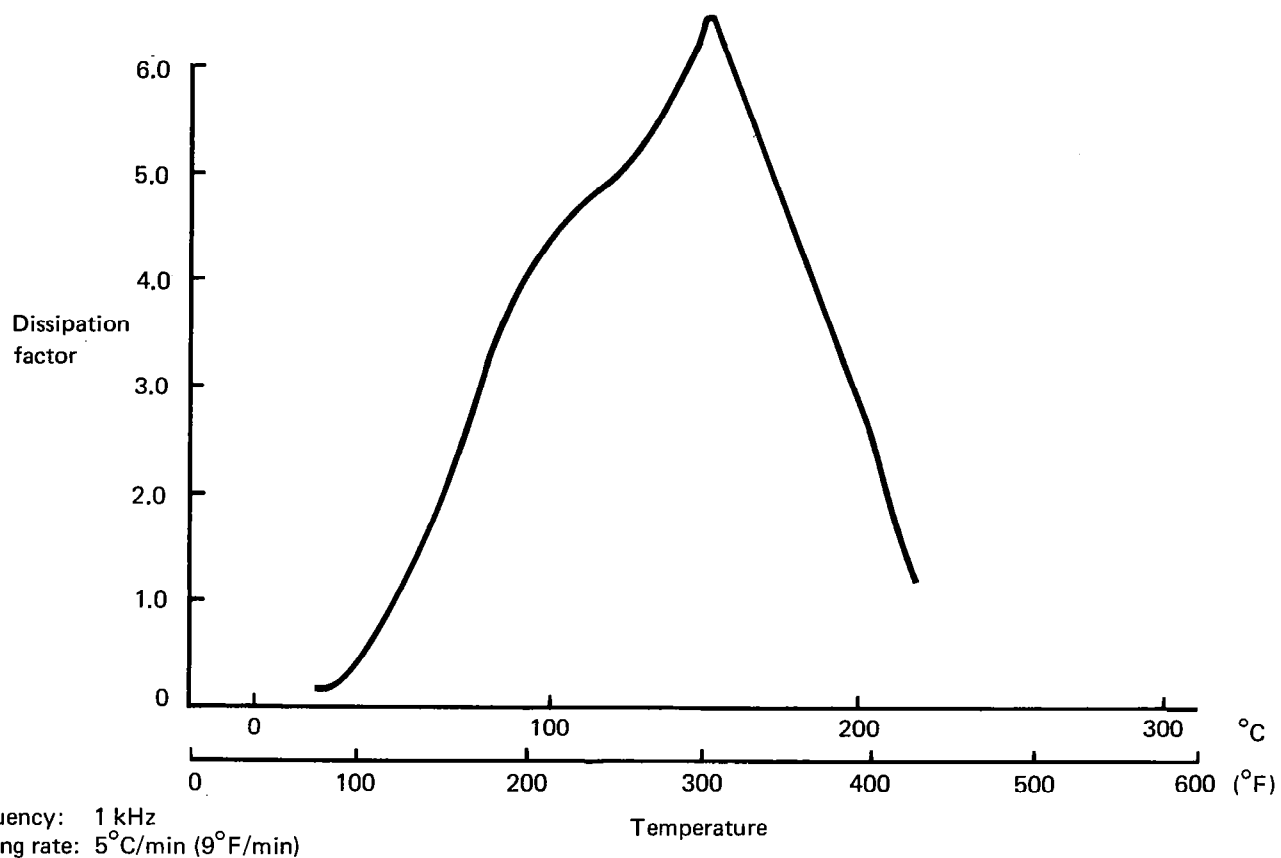
Figure 55. Results of Dielectric Analysis of Narmco Resin Batch 286

Frequency: 1 kHz
Heating rate: 5°C/min (9°F/min)
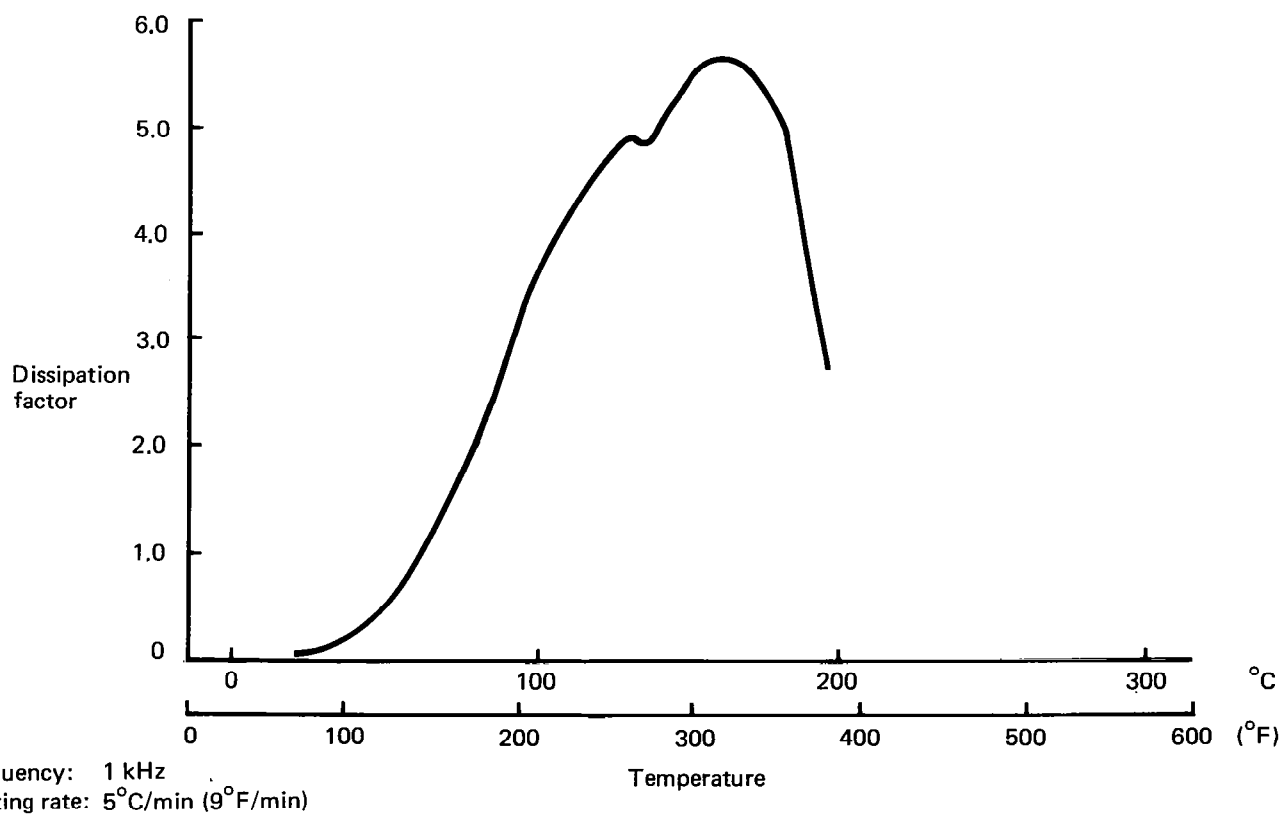
Figure 56. Results of Dielectric Analysis of Narmco Resin Batch 300

142
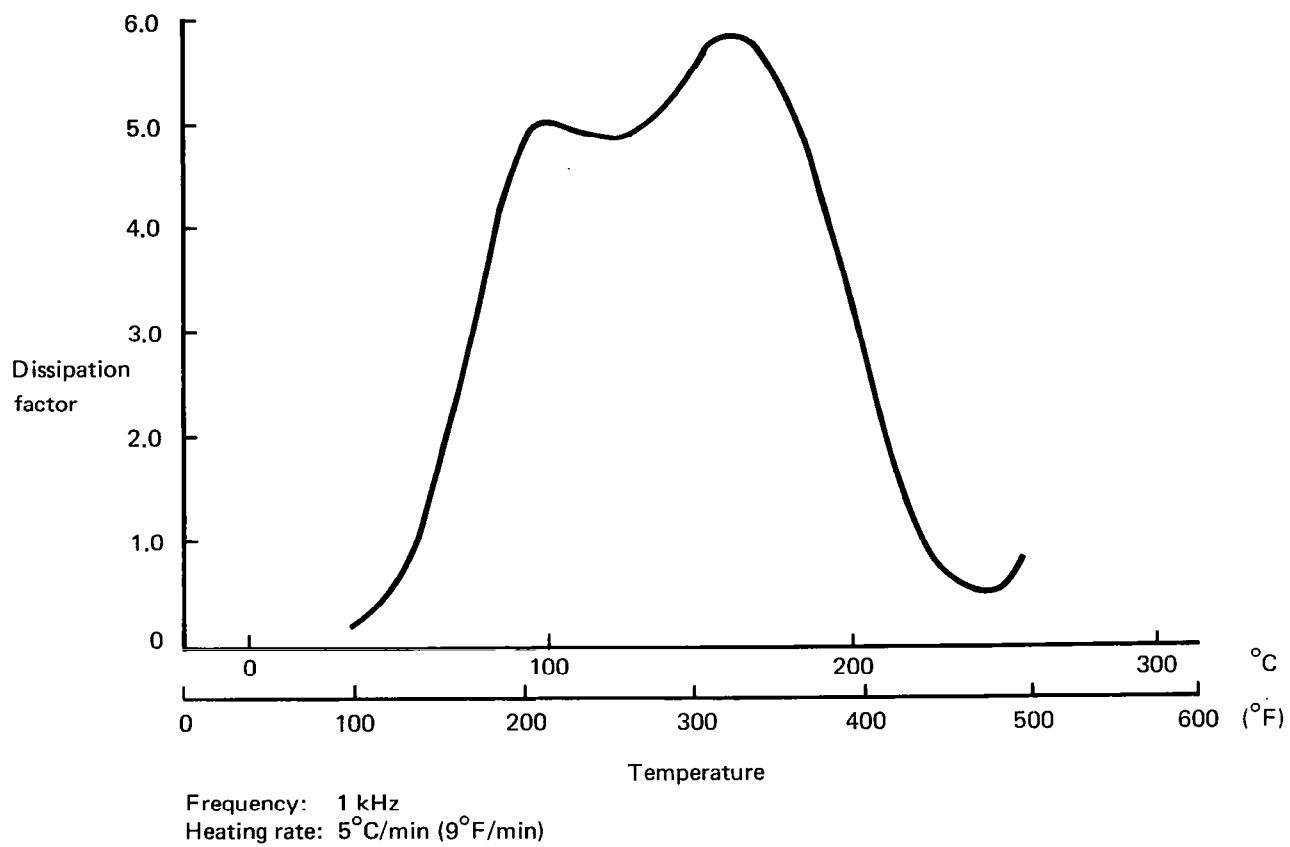
Figure 57. Results of Dielectric Analysis of Narmco Resin Batch 298
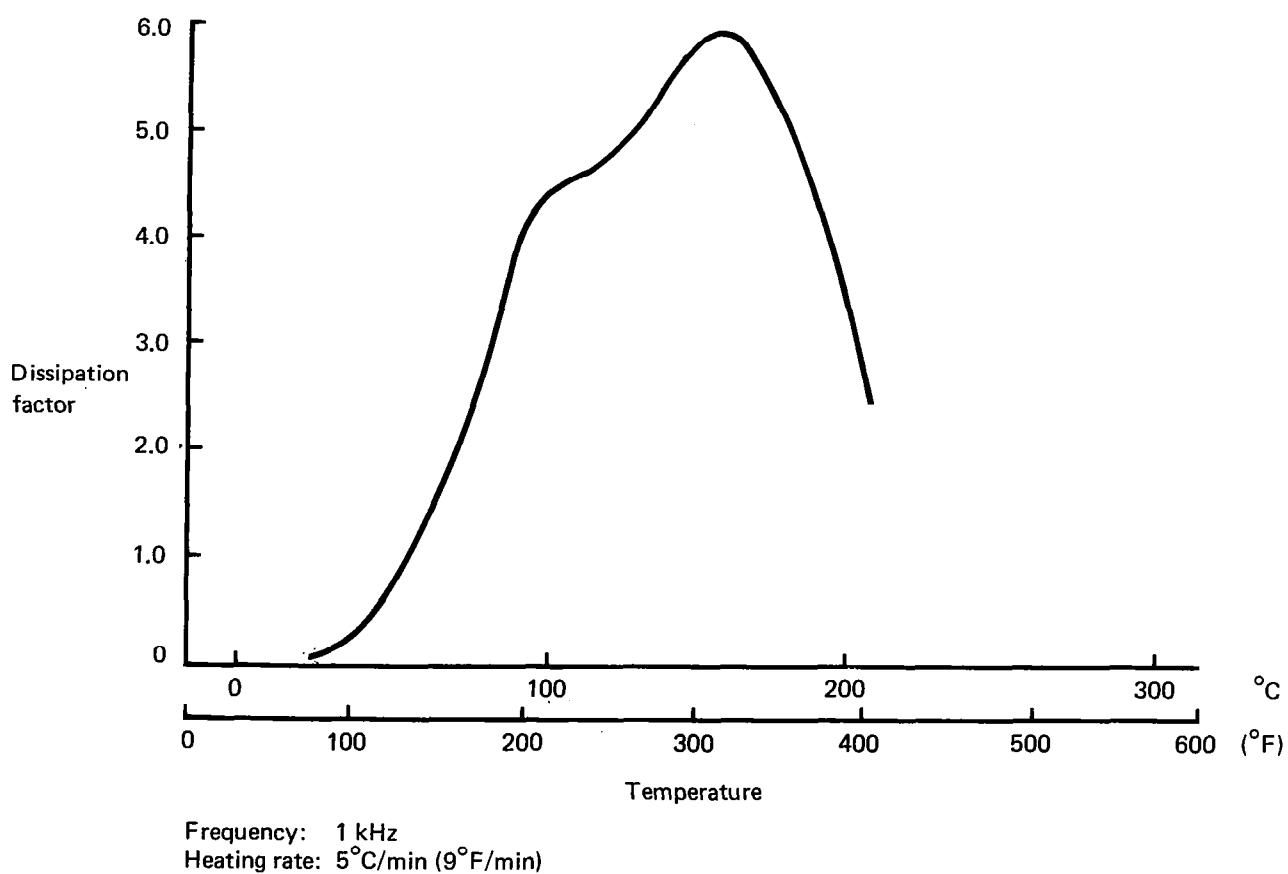
Figure 58. Results of Dielectric Analysis of Narmco Resin Batch 289

Frequency: 1 kHz
Heating rate: 5°C/min (9°F/min)
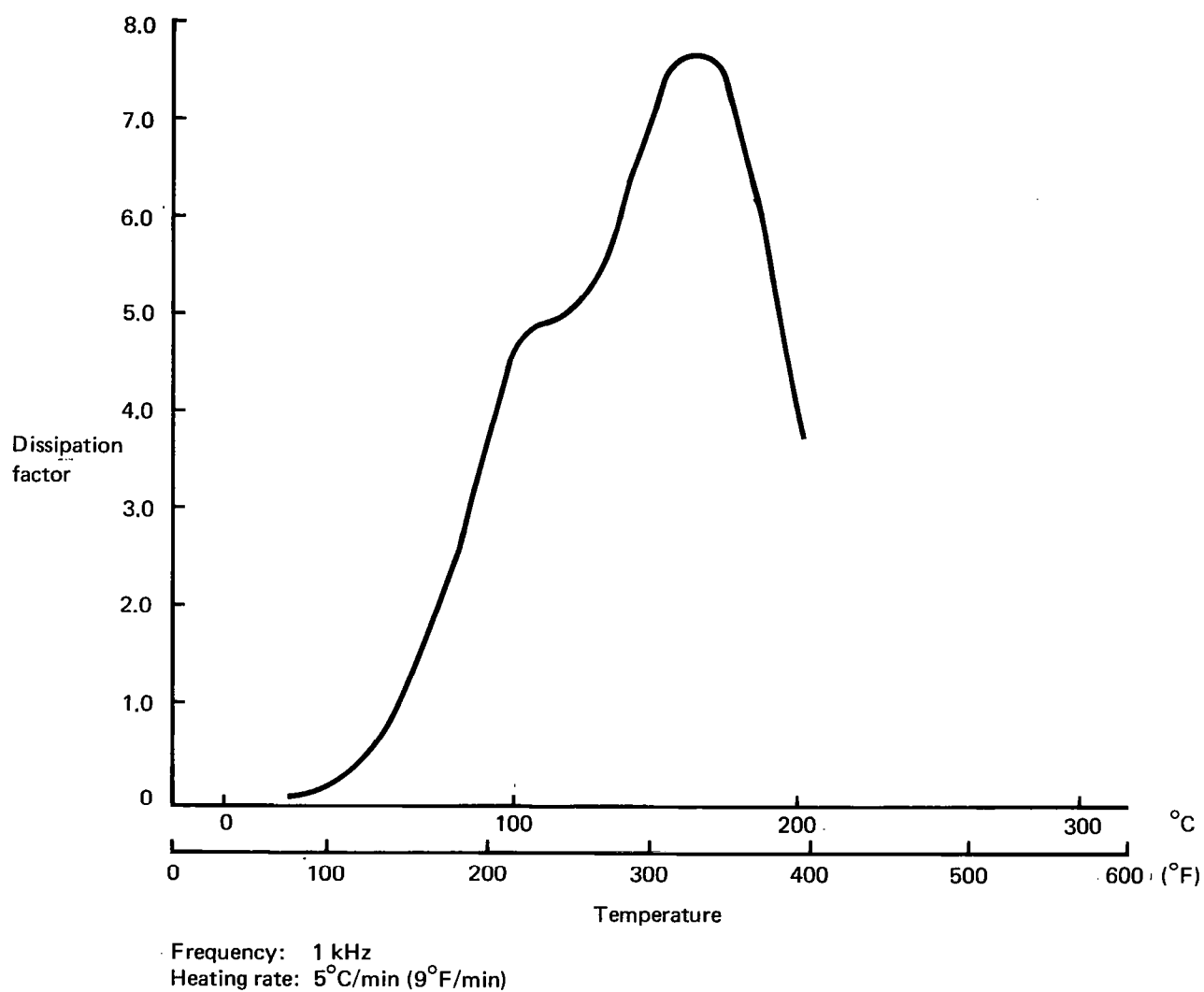
Figure 59. Results of Dielectric Analysis of Narmco Resin Batch 293
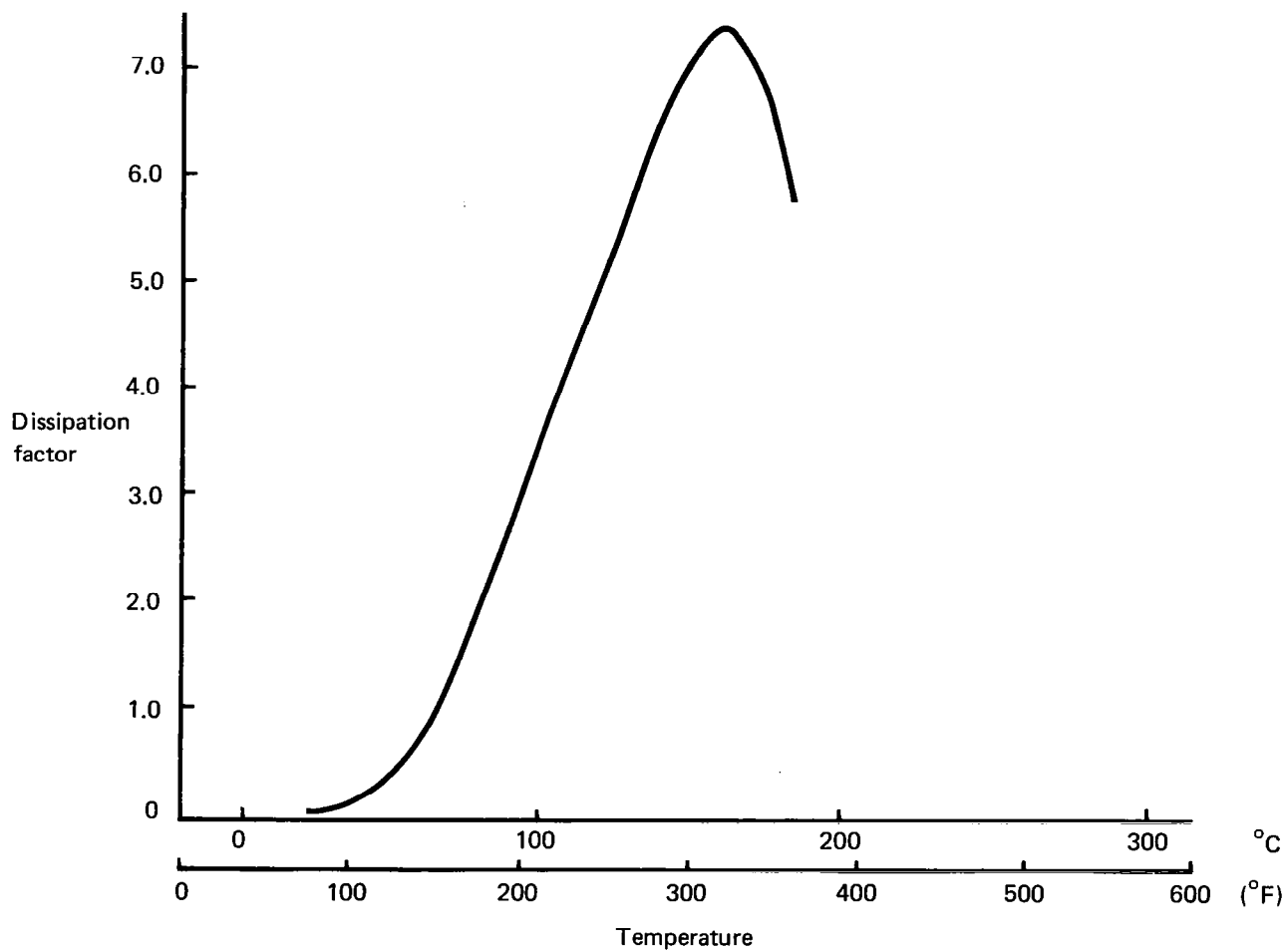
Frequency: 1 kHz
Heating rate: 5°C/min (9°F/min)

Figure 60. Results of Dielectric Analysis of Narmco Resin Batch 294
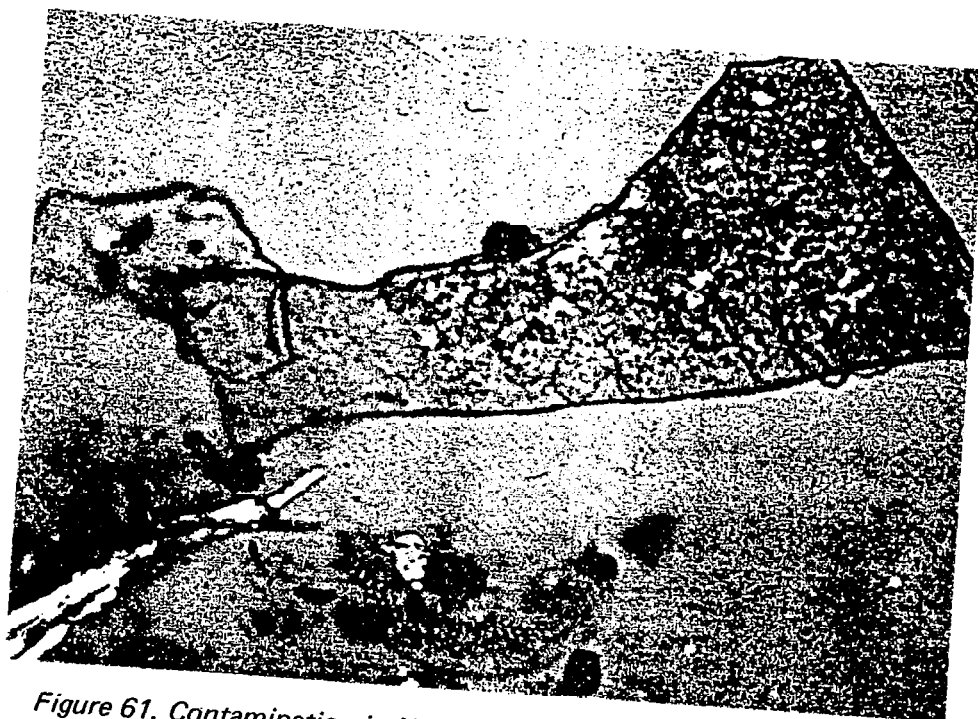
Figure 61. Contamination in Narmco Neat Resin Batch 300—Acetone-Insoluble Resin, Diatom
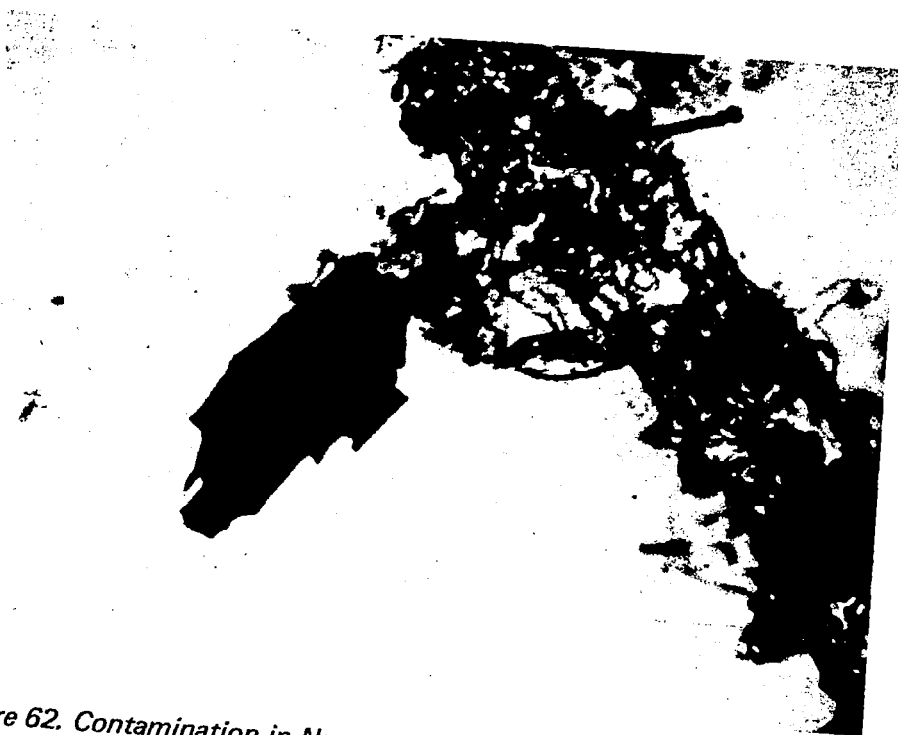
Figure 62. Contamination in Narmco Neat Resin Batch 300—Charred Wood
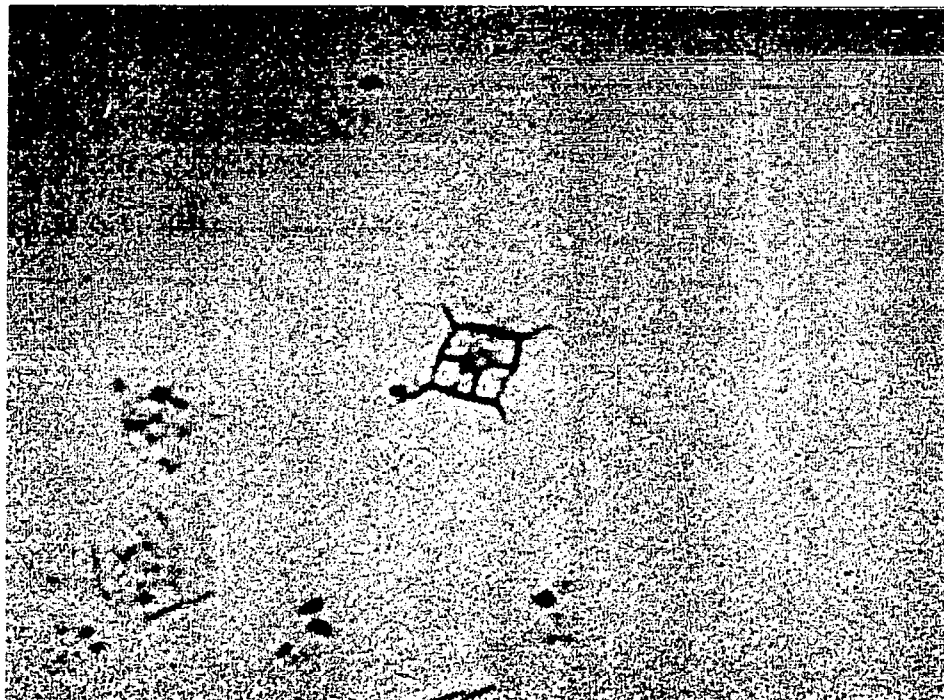
Figure 63. Contamination in Narmco Neat Resin Batch 300—Foraminifera

Figure 64. Contamination in Narmco Neat Resin Batch 300—Hardwood Sawdust
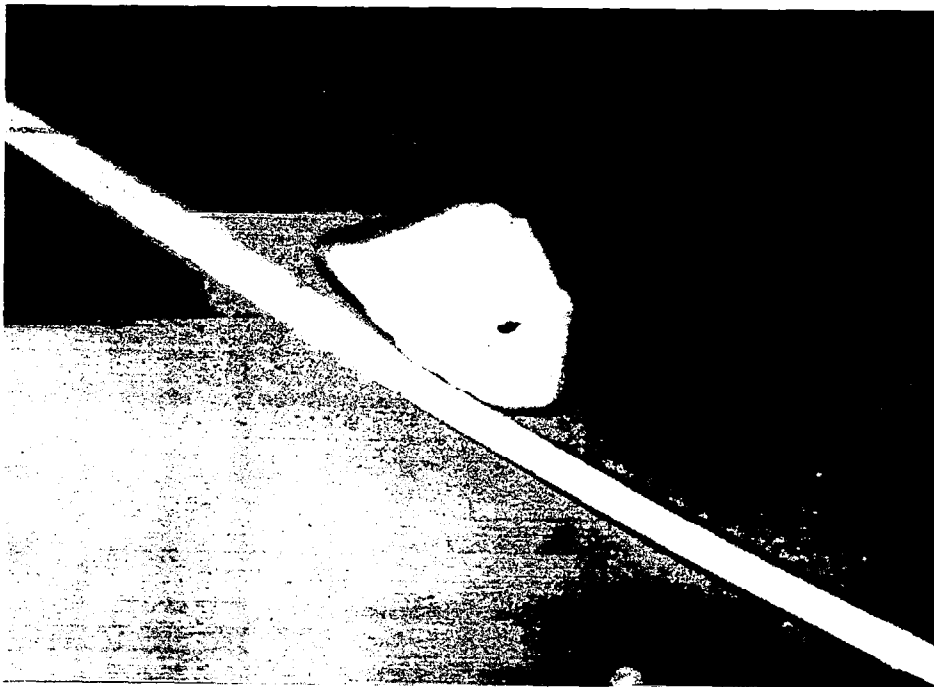
Figure 65. Contamination in Narmco Neat Resin Batch 300—Nylon Fiber, Quartz
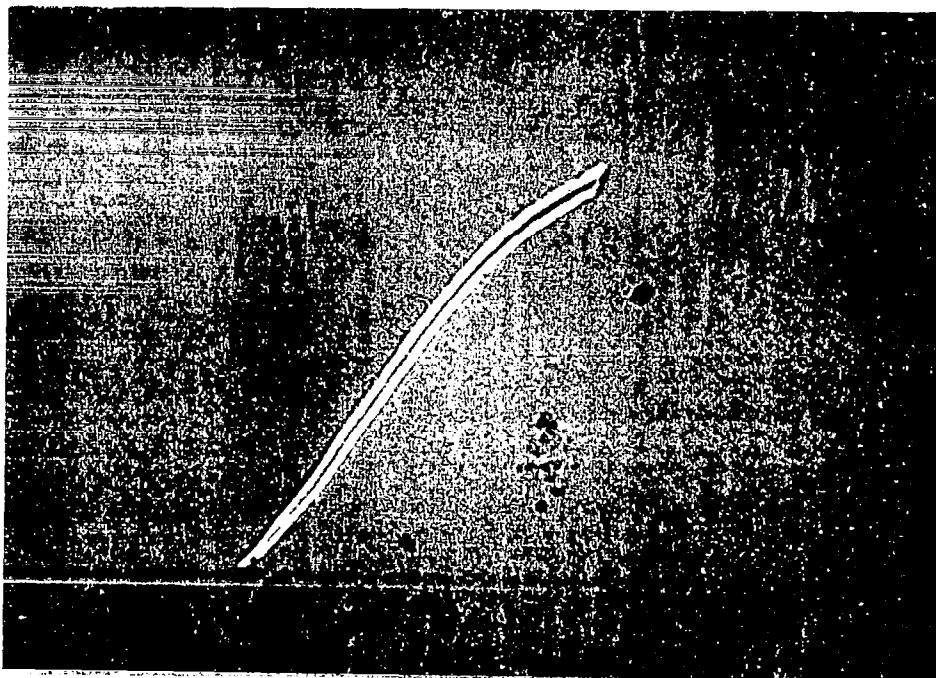
Figure 66. Contamination in Narmco Neat Resin Batch 300—Plant Hair

149
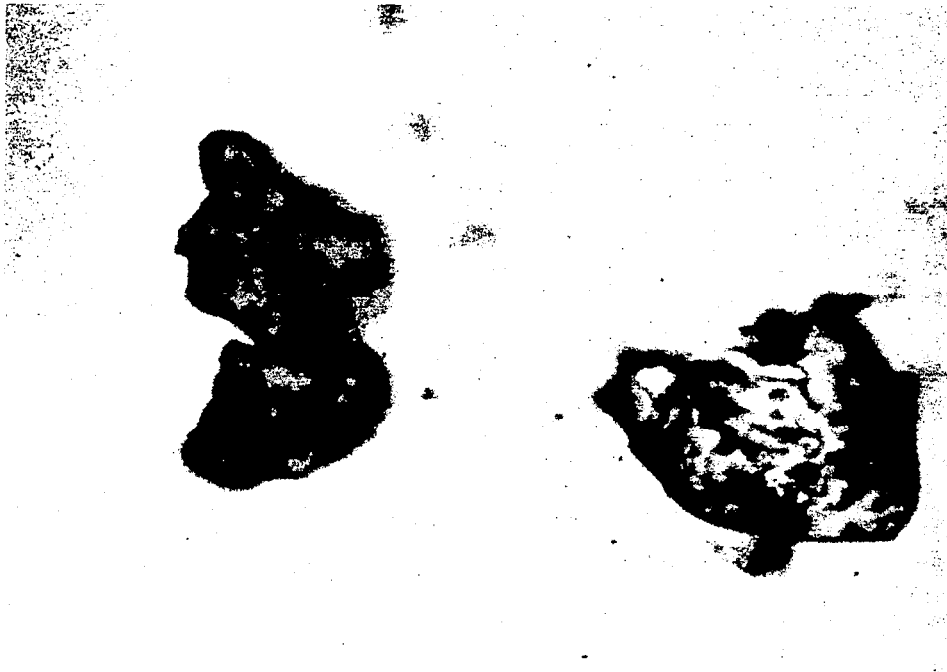
Figure 67. Contamination in Narmco Neat Resin Batch 300—Wear Metal

Figure 68. Contamination in Narmco Neat Resin Batch 300—Wood Fibers

150
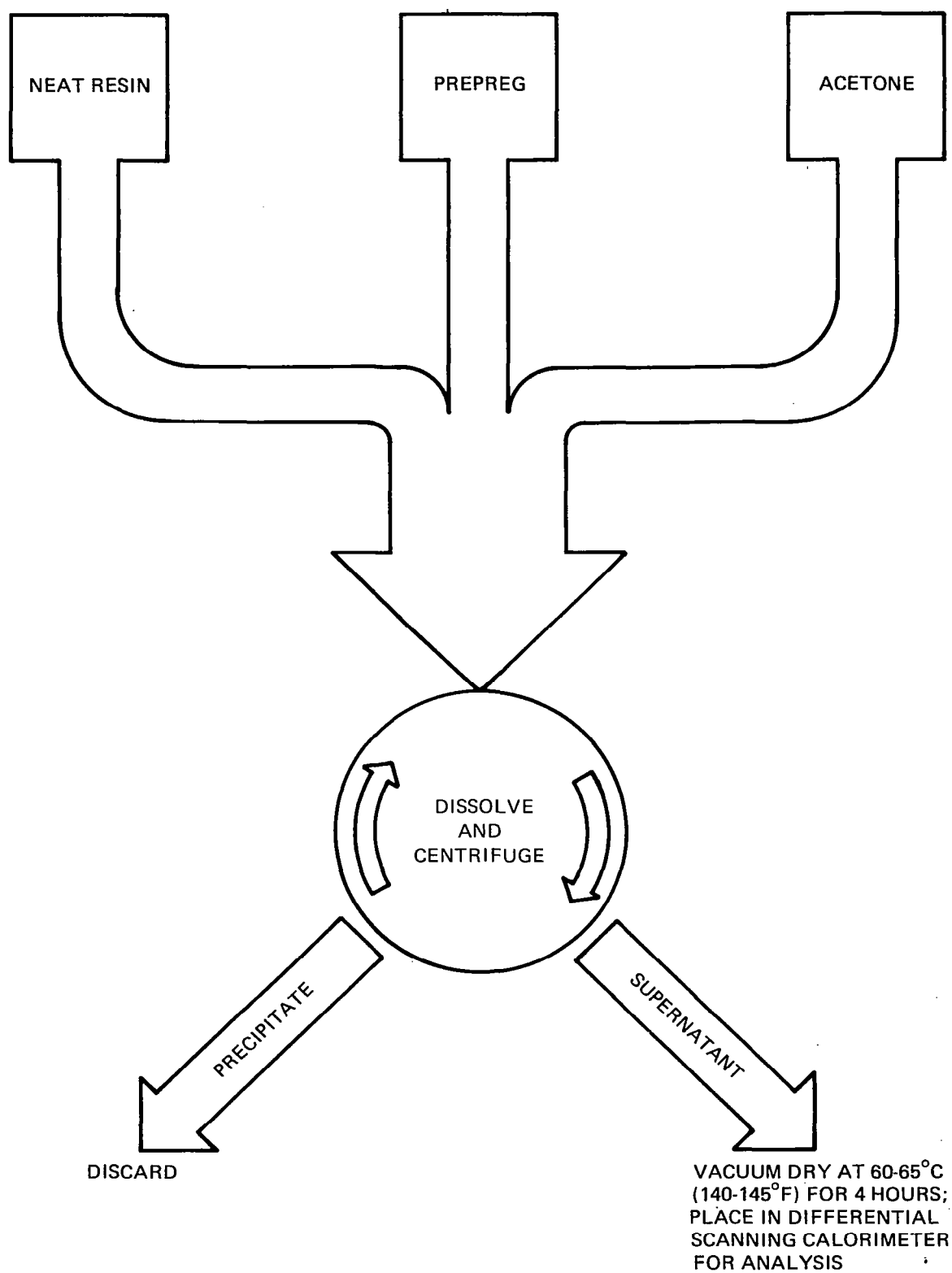
Figure 69. Optimized DSC Method Schematic
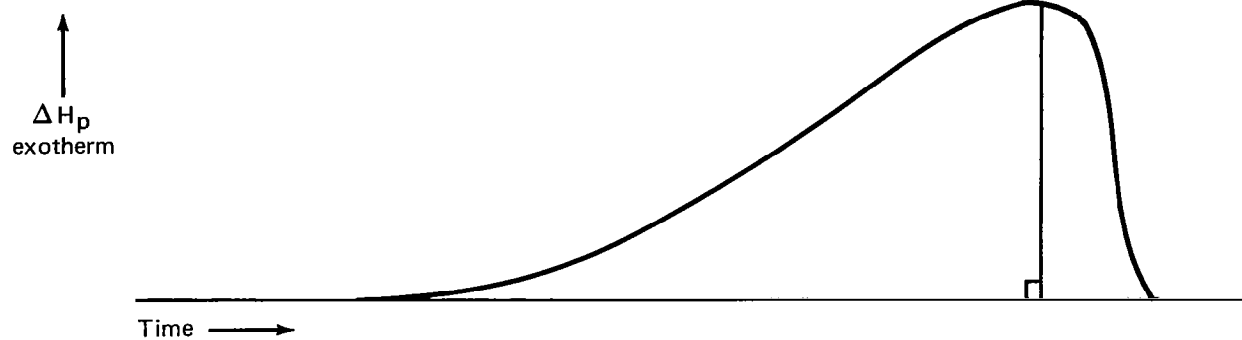
Figure 70. Symmetry Evaluation of DSC Curve for Narmco
Neat Resin Batch 300
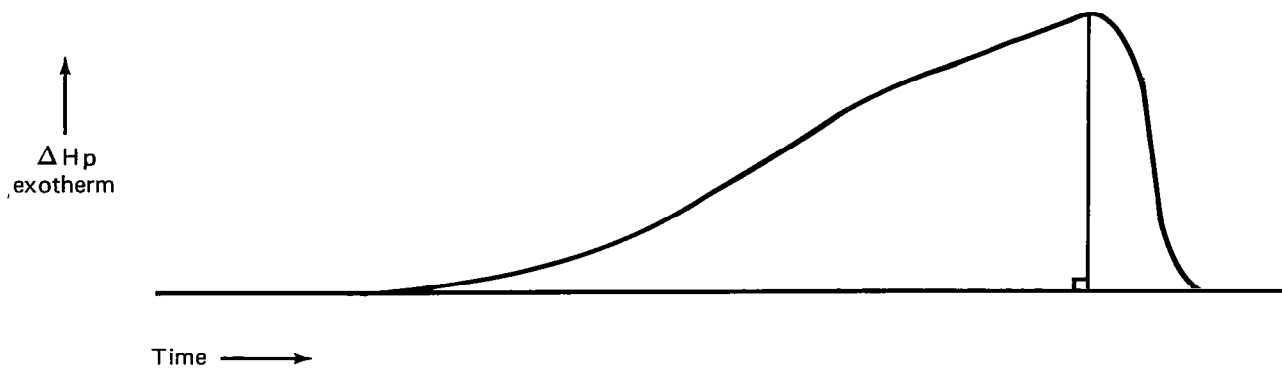
Figure 71. Symmetry Evaluation of DSC Curve for Narmco Resin Batch 286

152

Δ H,p
exotherm

Temperature

Time
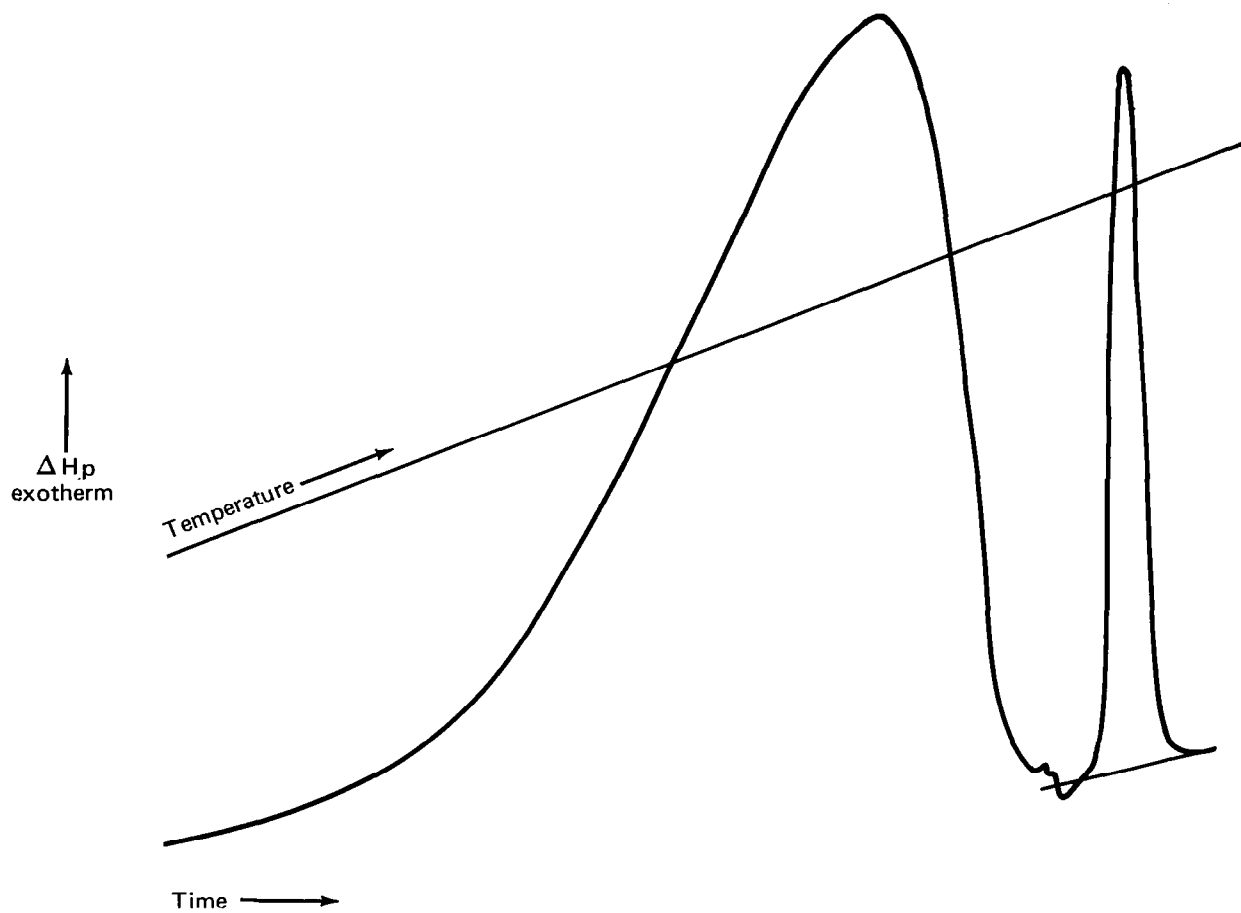
Figure 72. DSC Curve of Narmco Prepreg Batch 1072, Round-Robin Participant A

ΔH_p
exotherm

| 174 | 218 | 282 | 308 | 350 | °C |
| (345) | (424) | (540) | (586) | (662) | (°F) |

Temperature
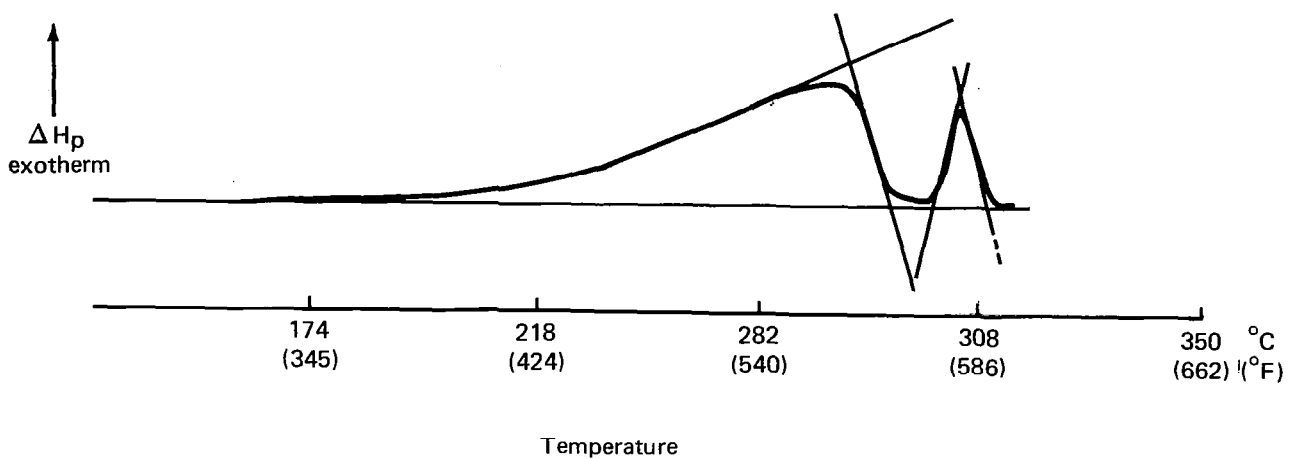
Figure 73. DSC Curve of Narmco Prepreg Batch 1072, Round-Robin Participant B

ΔH_p
exotherm

Time ⟶
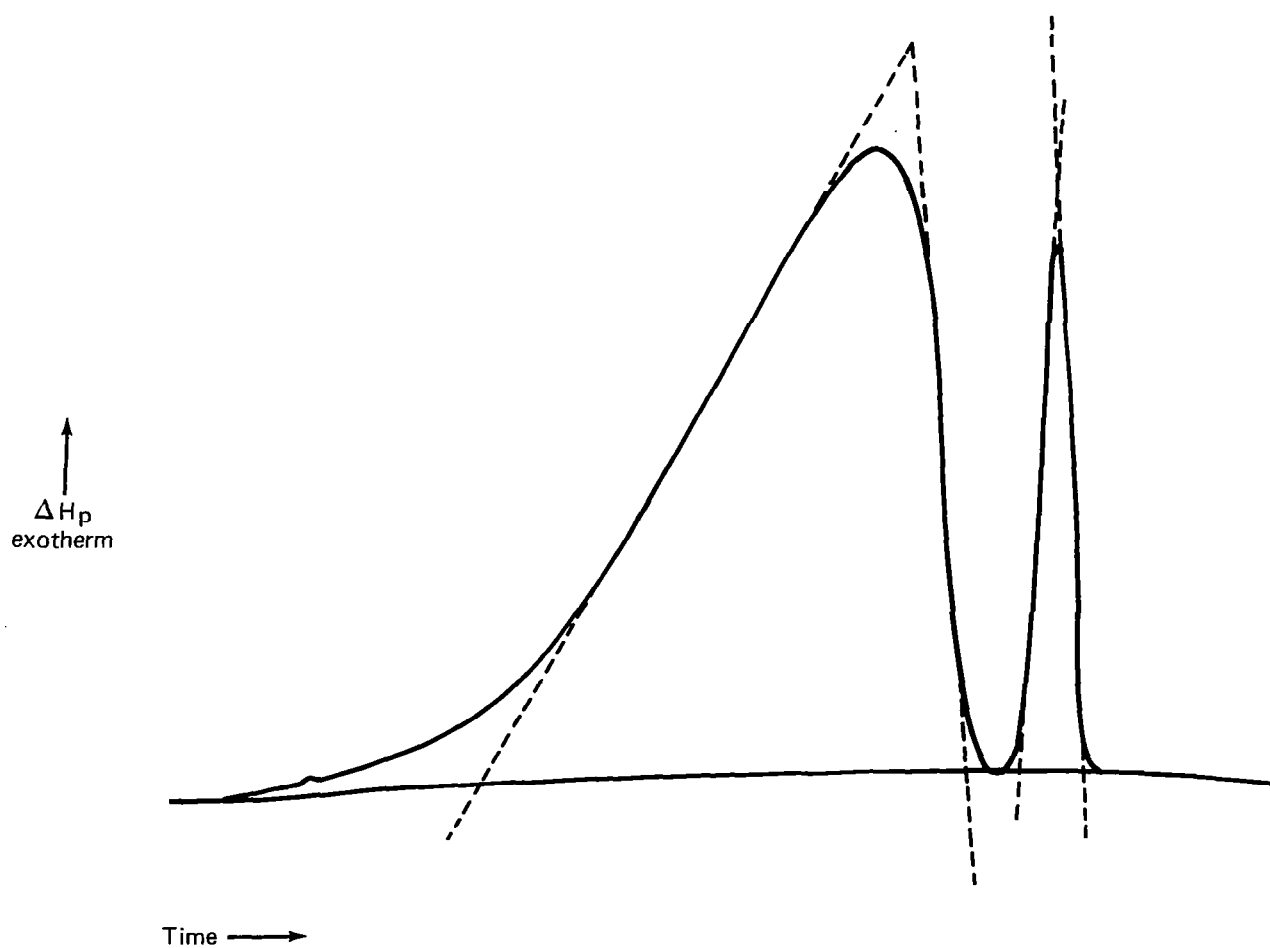
Figure 74. DSC Curve of Narmco Prepreg Batch 1072, Round-Robin Participant C

154
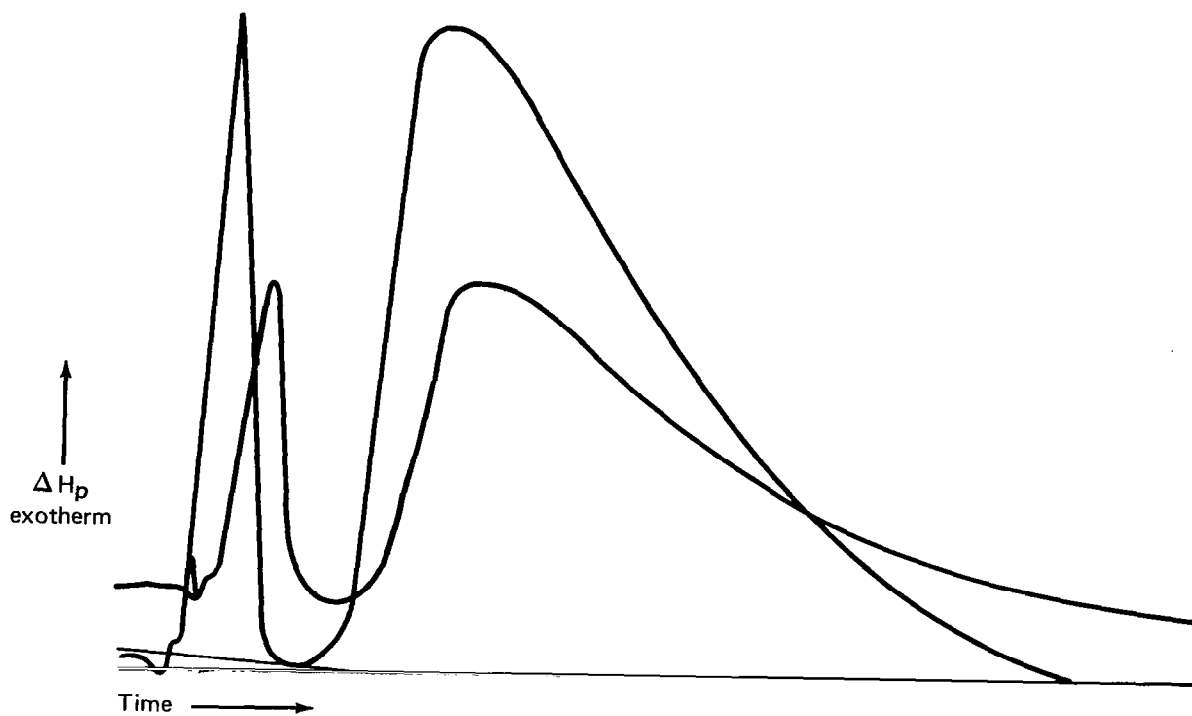
Figure 75. DSC Curve of Narmco Prepreg Batch 1072, Round-Robin Participant D
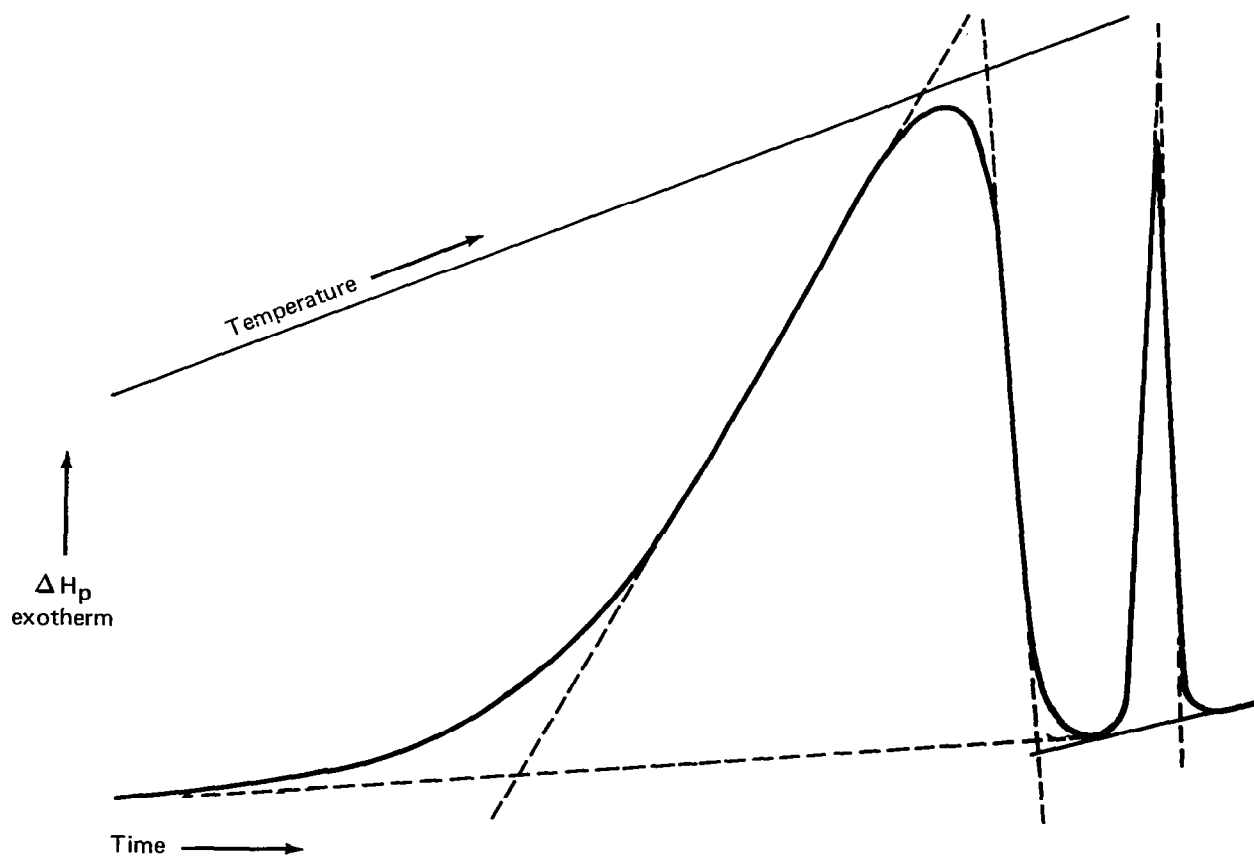
Figure 76. DSC Curve of Narmco Prepreg Batch 1072, Round-Robin Participant E
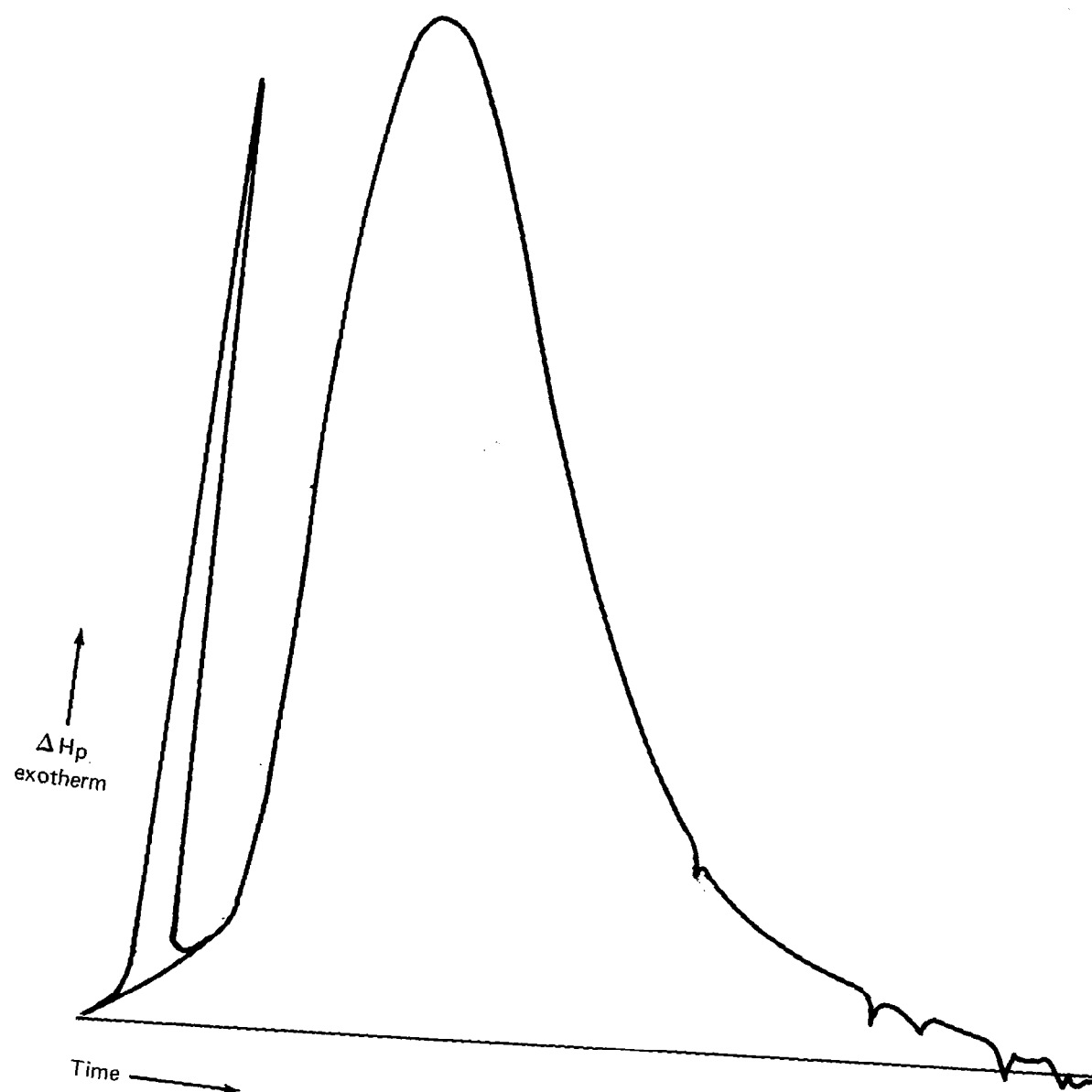
Figure 77. DSC Curve of Narmco Prepreg Batch 1072, Round-Robin Participant F

156
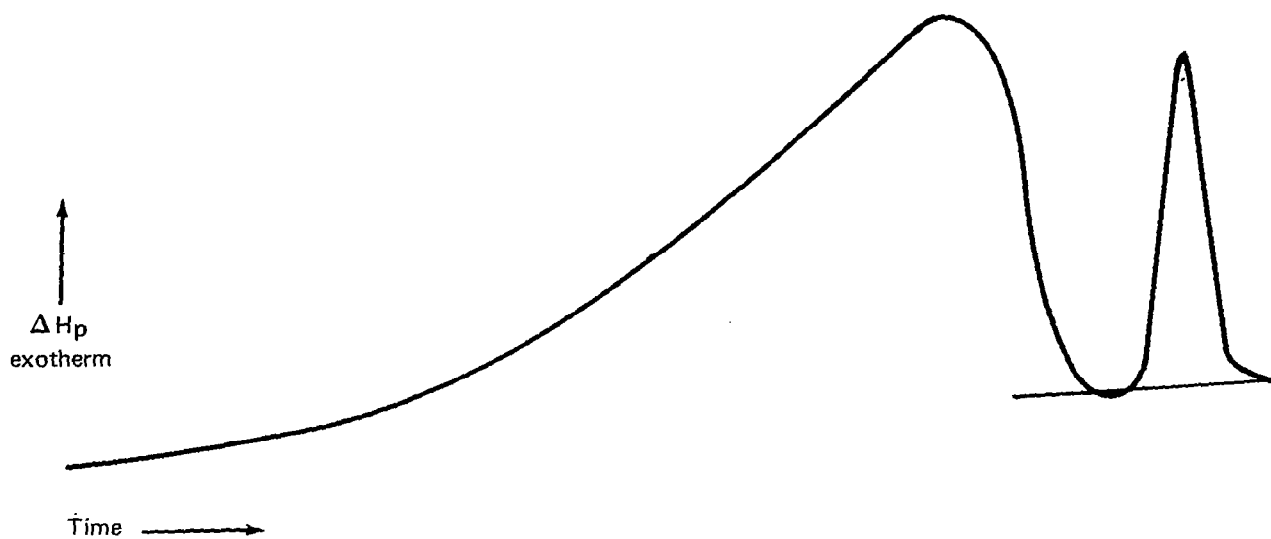
Figure 78. DSC Curve of Narmco Prepreg Batch 1072, Round-Robin Participant G
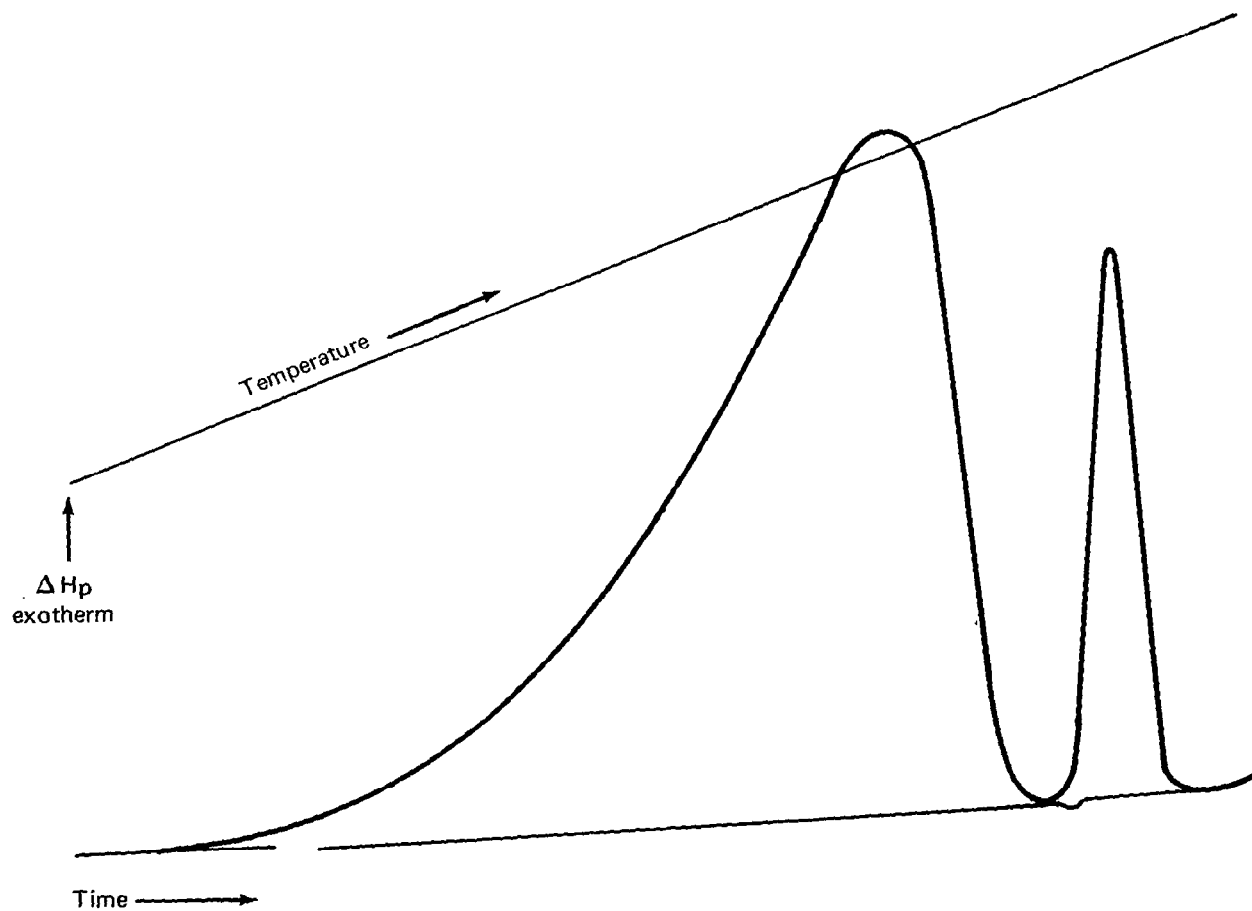
Figure 79. DSC Curve of Narmco Prepreg Batch 1072, Round-Robin Participant H
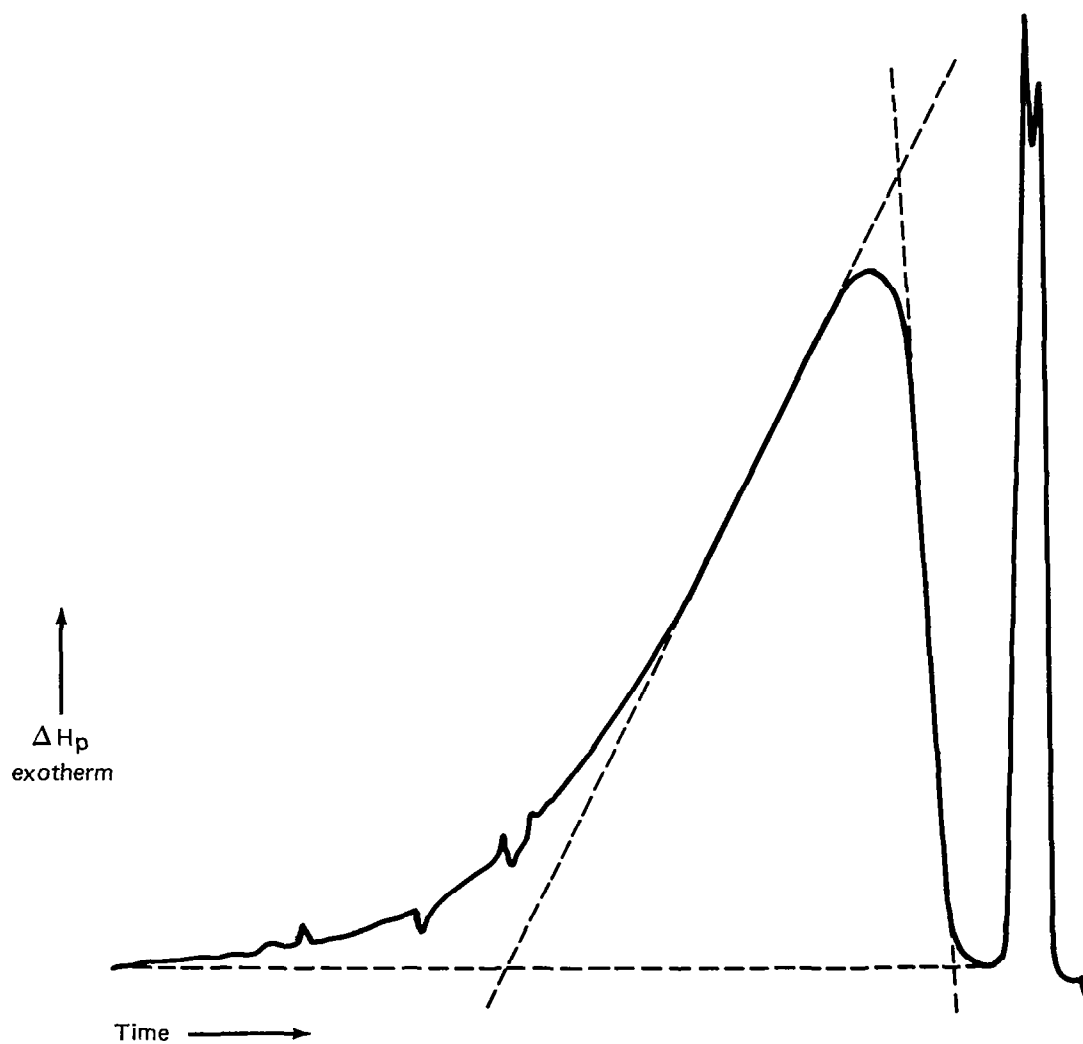
Figure 80. DSC Curve of Narmco Prepreg Batch 1072, Round-Robin Participant I
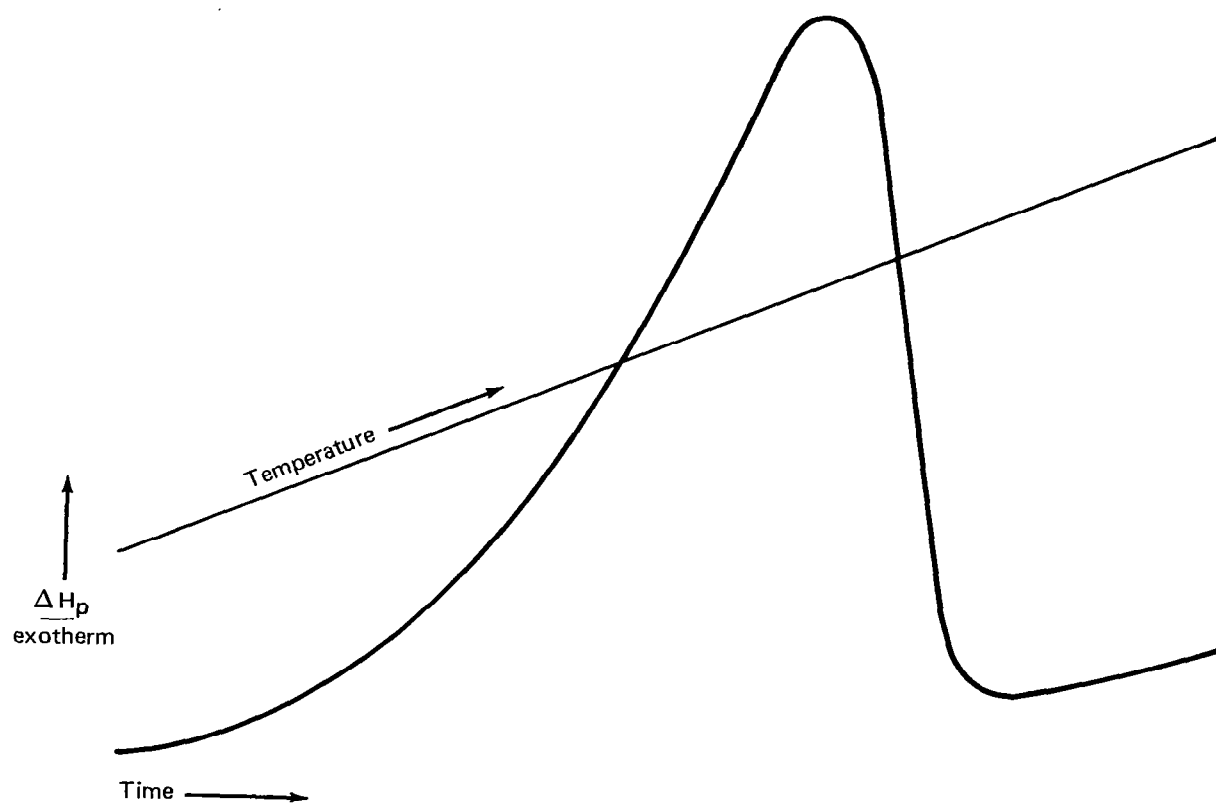
Figure 81. DSC Curve of Narmco Prepreg Batch 1072, Round-Robin Participant J
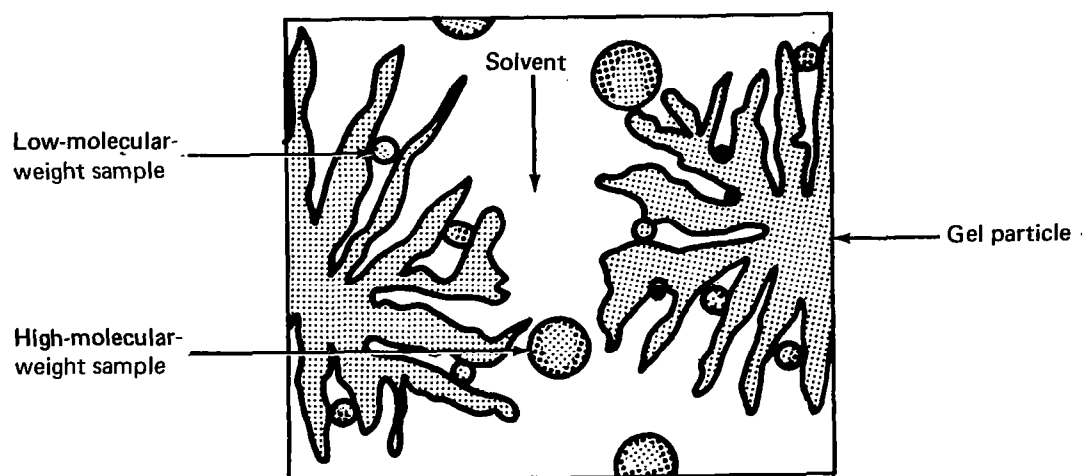
Figure 82. Diagram of GPC Technique
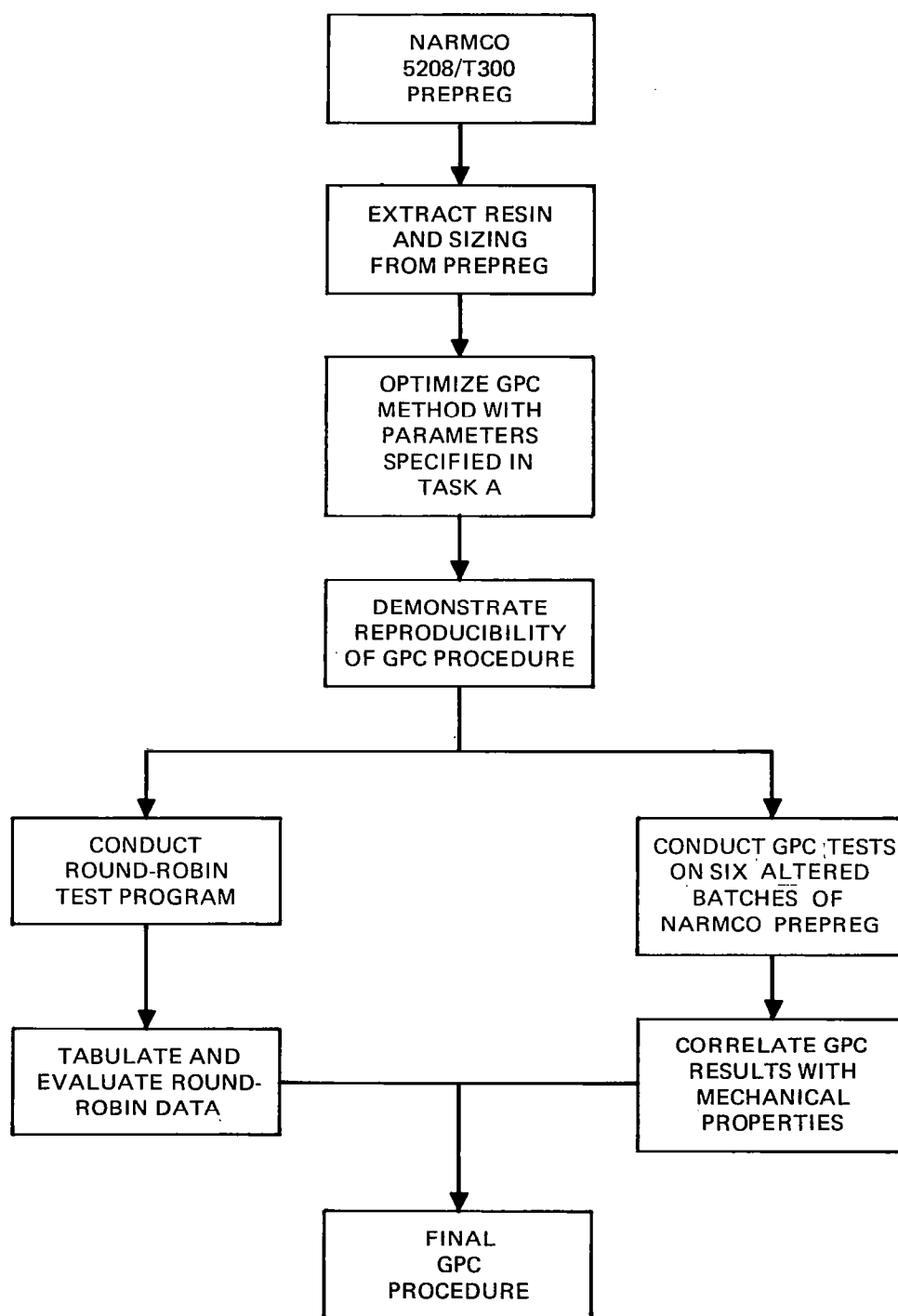
Figure 83. Task C Work Flow

Column: Waters μ-Styragel, 2 x 100Å,
2 x 500Å, 1 x 1000Å
Solvent: THF
Flow rate: 2 ml/min
Detector: UV, 280 nm

DDS

MY 720

Detector
response

0   10   15   20

Elution time, min
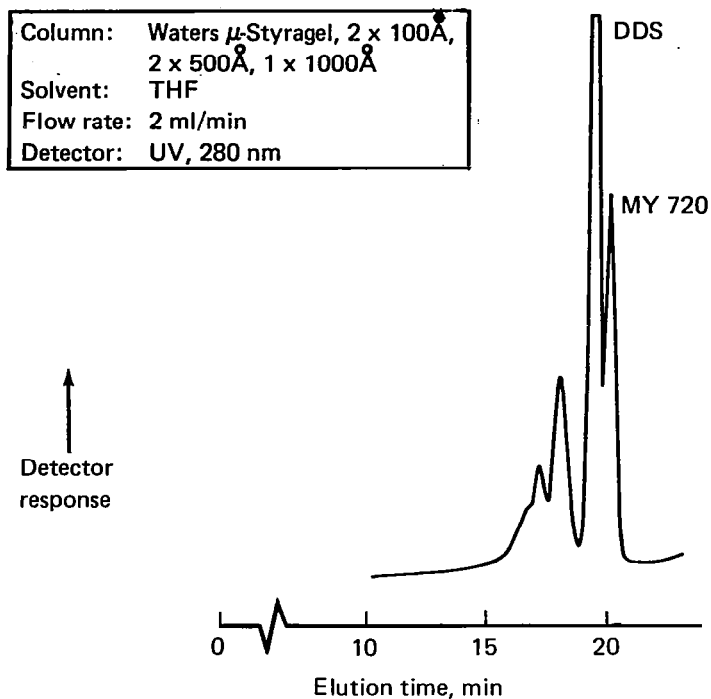
Figure 84. GPC Chromatogram of Narmco Neat Resin Batch 300,
Solvent: THF, Column: Waters μ-Styragel—2 x 100Å, 2 x 500 Å, 1 x 1000Å

Column: Waters μ-Styragel, 2 x 100Å
2 x 500Å,, 1 x 1000Å
Solvent: CHCl$_3$
Flow rate: 2 ml/min
Detector: UV, 280 nm

MY 720

DDS

Detector
response

0   10   15   20   25

Elution time, min
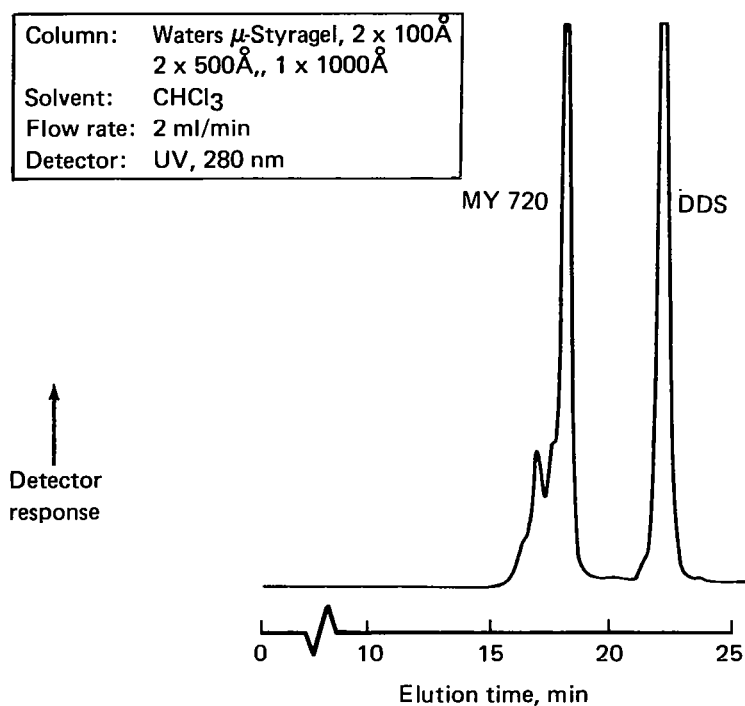
Figure 85. GPC Chromatogram of Narmco Neat Resin Batch 300,
Solvent: CHCl$_3$, Column: Waters μ-Styragel—2 x 100Å, 2 x 500Å, 1 x 1000Å

162
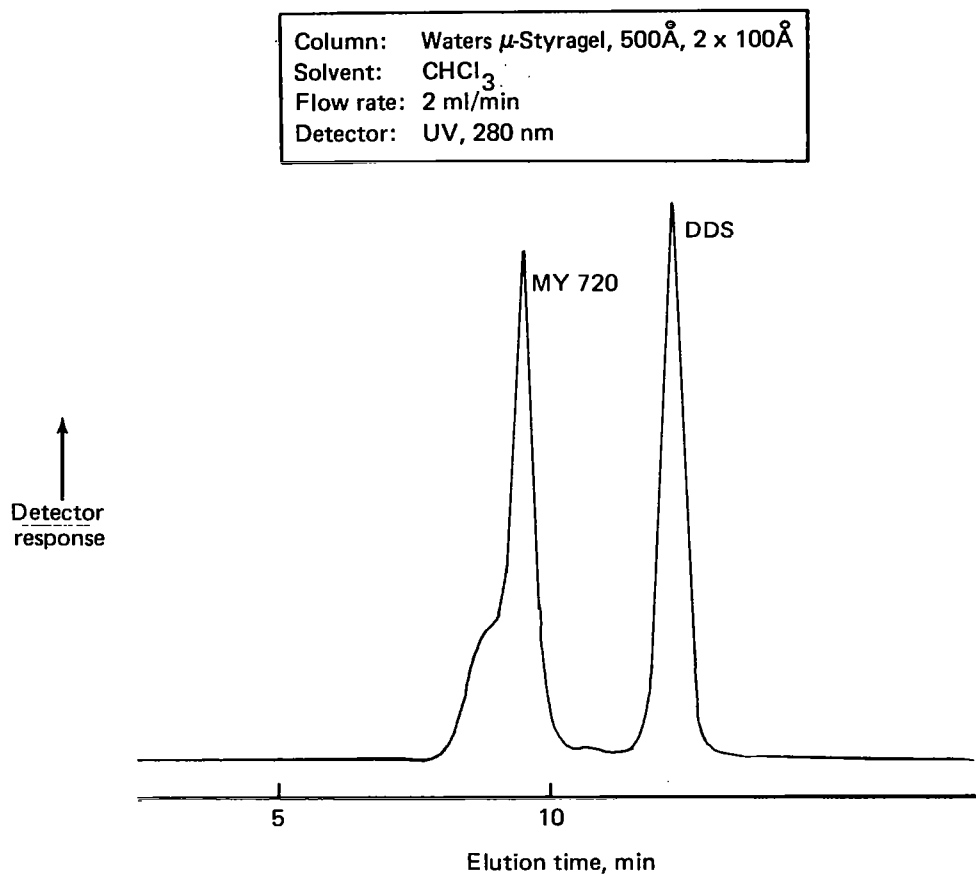
Figure 86. GPC Chromatogram of Narmco Neat Resin Batch 300,
Solvent: CHCl₃, Column: Waters μ-Styragel—500Å, 2 x 100Å
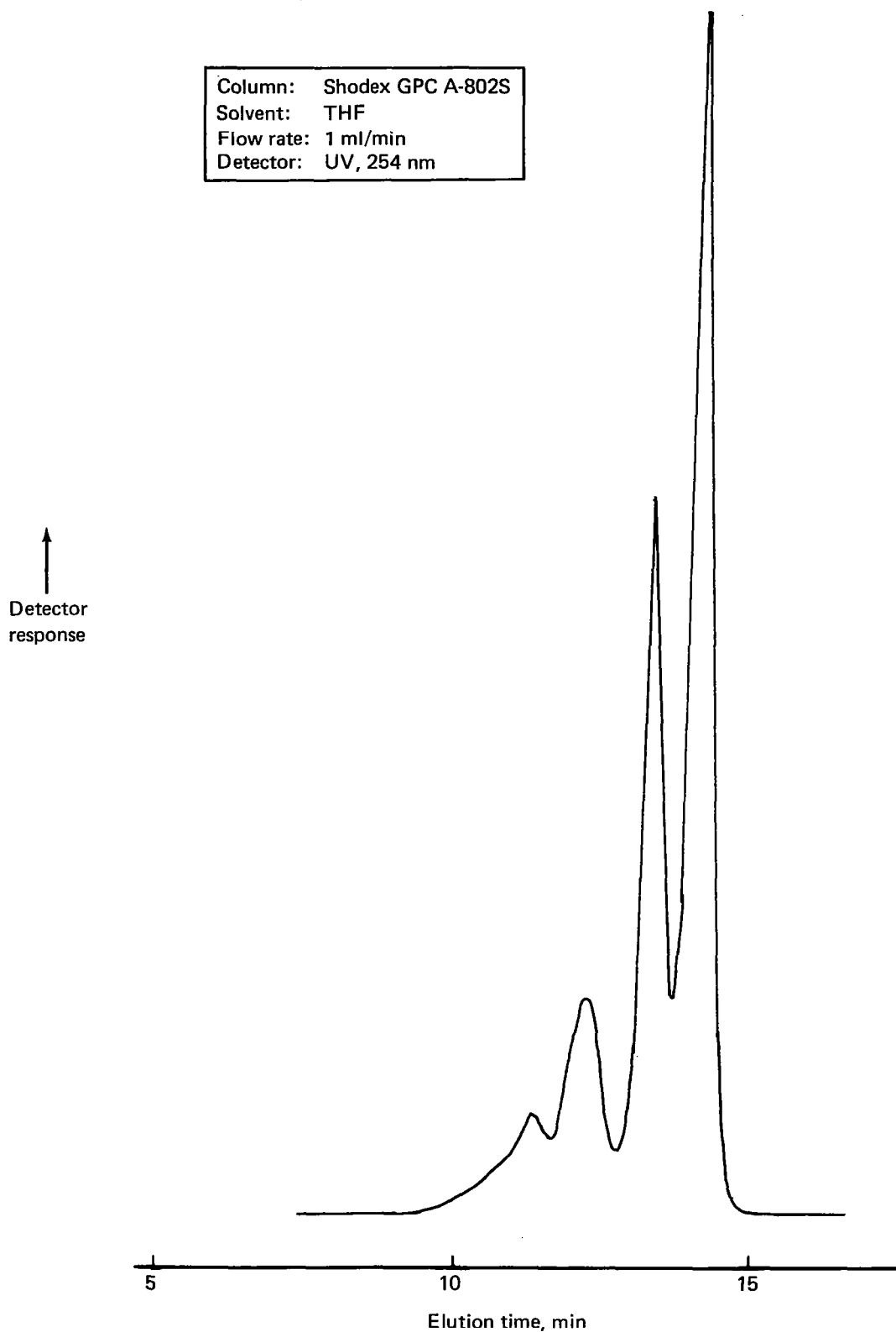
Figure 87. GPC Chromatogram of Narmco Neat Resin Batch 300,
Column: Shodex A-802S, Flow Rate: 0.5 ml/min
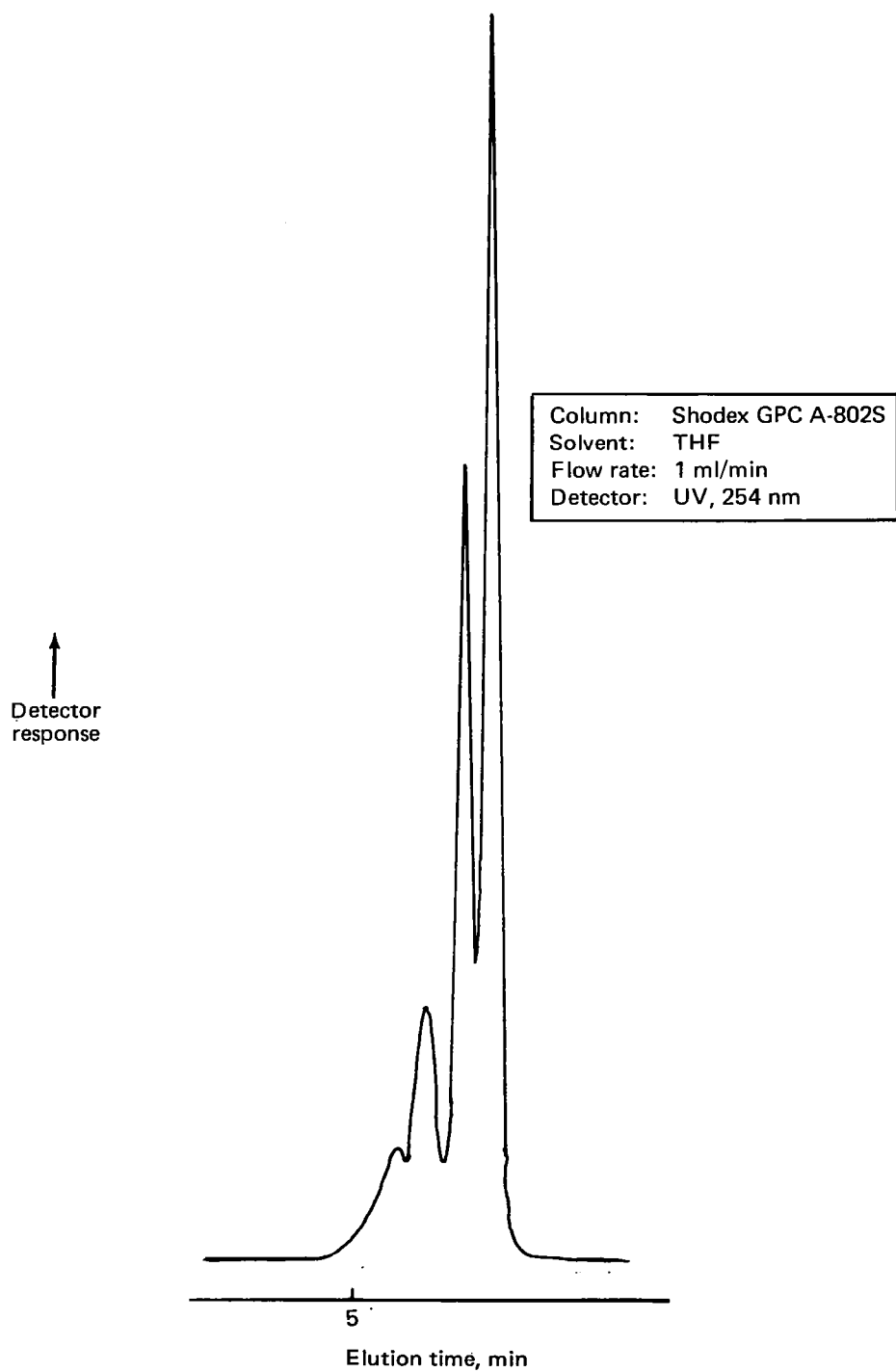
Figure 88. GPC Chromatogram of Narmco Neat Resin Batch 300, Flow Rate: 1 ml/min
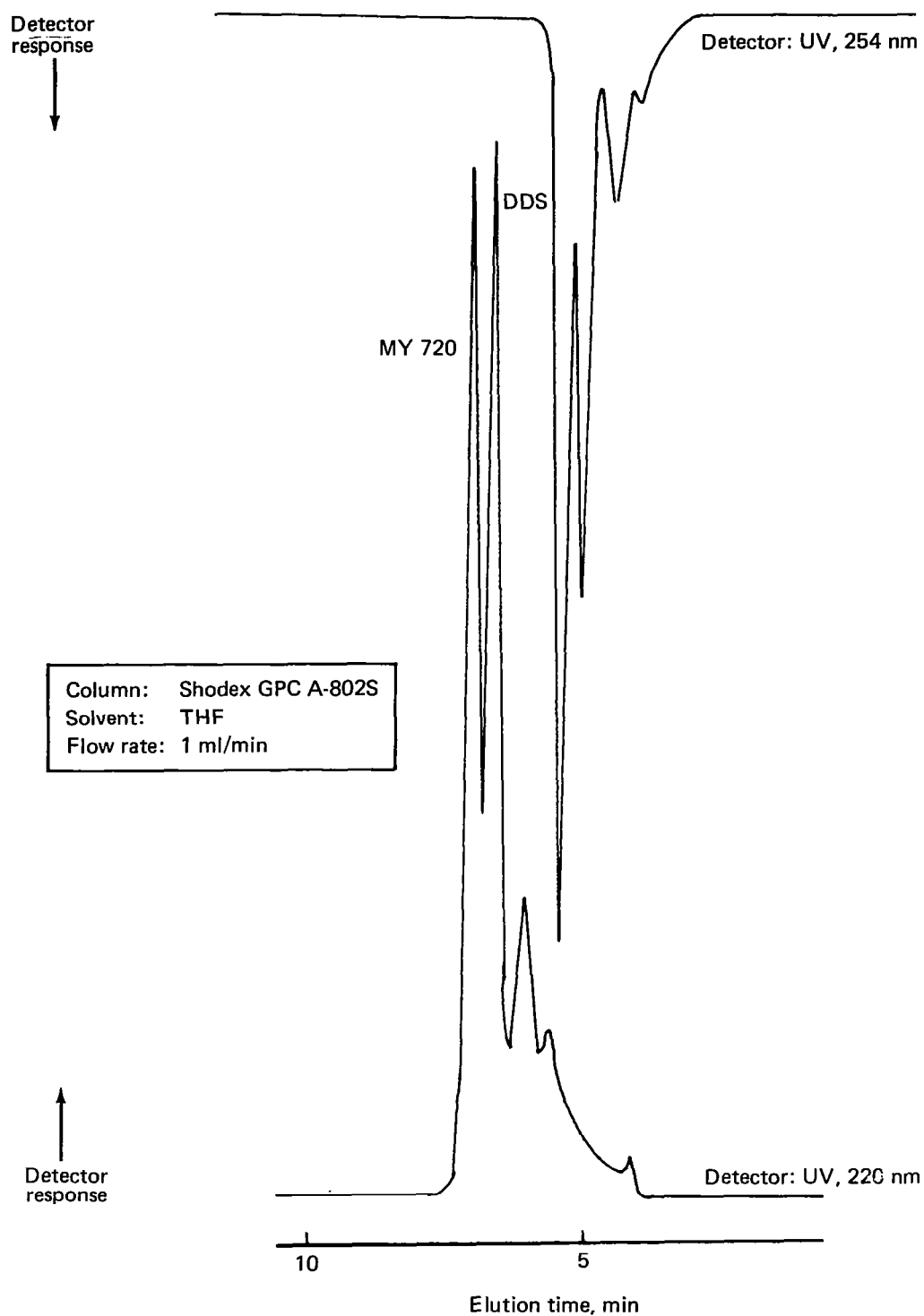
Figure 89. GPC Chromatogram of Narmco Neat Resin Batch 300, Detector: UV, 220 nm
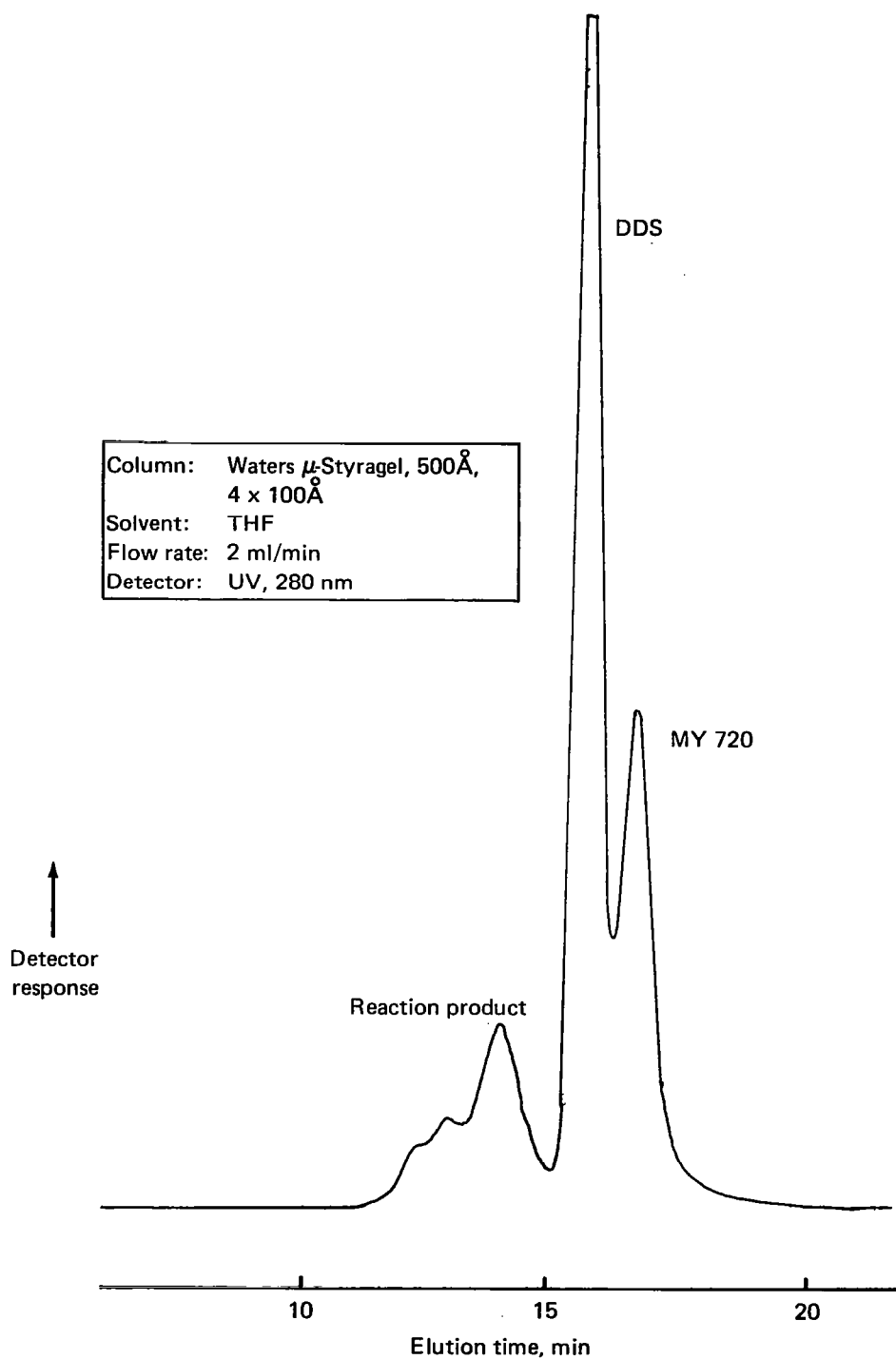
Figure 90. GPC Chromatogram of Narmco Neat Resin Batch 300,
Solvent: THF, Column: Waters μ-Styragel–500Å, 4 x 100Å

Figure 91. GPC Chromatogram of Narmco Neat Resin Batch 300,
Solvent: CHCl₃, Column: Waters μ-Styragel— 500Å, 4 x 100Å

Column: Shodex GPC A-8025
Solvent: THF
Flow rate: 1 ml/min
Detector: UV, 220 nm

Detector response

Elution time

Figure 92. GPC Chromatogram of Narmco Prepreg Batch 1072, Round-Robin Participant A

Column: Shodex GPC A-802S
Solvent: THF
Flow rate: 1 ml/min
Detector: UV, 220 nm

Detector'
response

Elution time, min ⟶

Figure 93. GPC Chromatogram of Narmco Prepreg Batch 1072, Round-Robin Participant C

Detector
response

Column: Shodex GPC A-802S
Solvent: THF
Flow rate: 1 ml/min
Detector: UV, 220 nm

Elution time ⟶
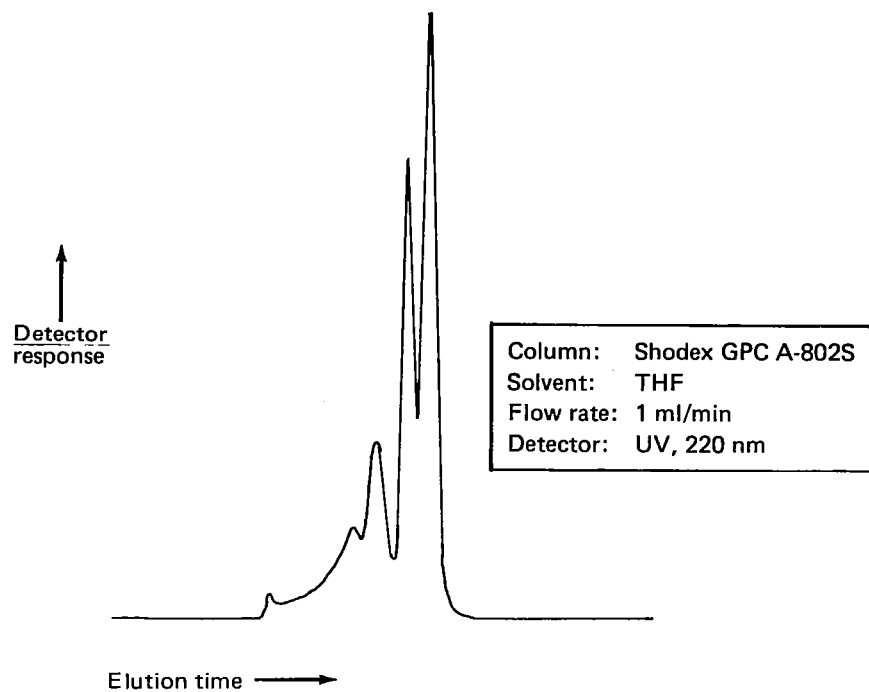
·Figure 94. GPC Chromatogram of Narmco Prepreg Batch 1072, Round-Robin Participant D

9.20

Column: Shodex GPC A-802S
Solvent: THF
Flow rate: 1 ml/min
Detector: UV, 220 nm

7.62

7.21

8.14

Detector
response

Elution time, min⟶
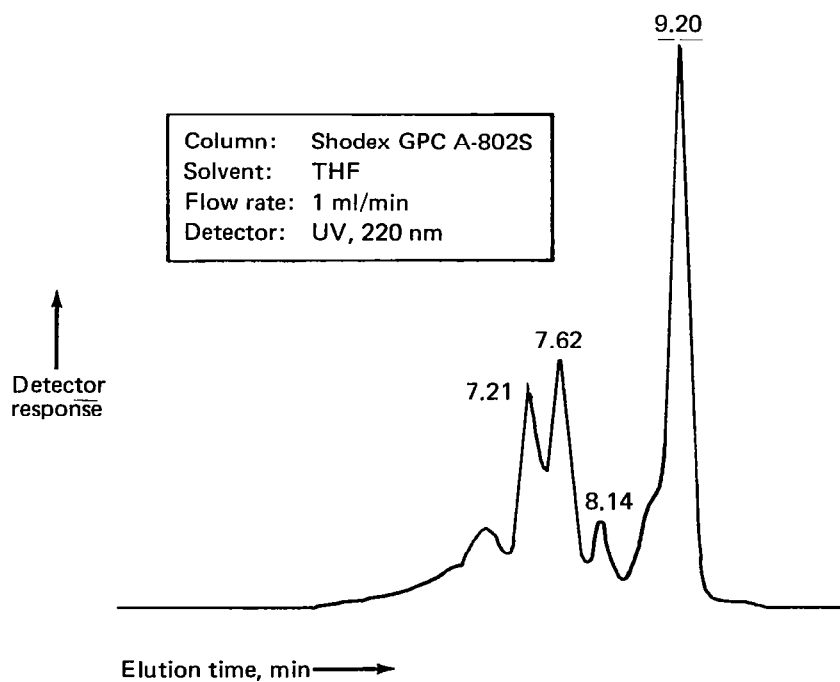
Figure 95. GPC Chromatogram of Narmco Prepreg Batch 1072, Round-Robin ı Participant E

Column: Shodex GPC A-802S
Solvent: THF
Flow rate: 1 ml/min
Detector: UV, 220 nm

Detector
response

Elution time, min
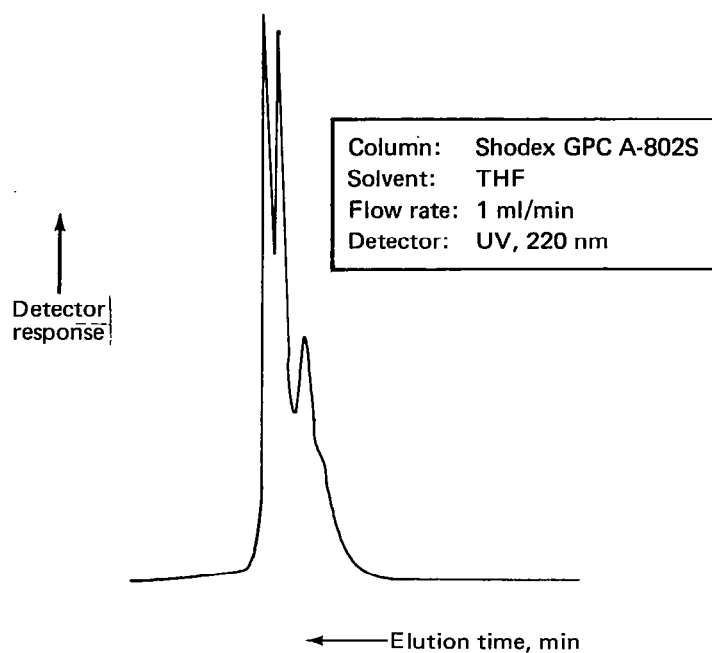
Figure 96. GPC Chromatogram of Narmco Prepreg Batch 1072, Round-Robin Participant F

Column: Shodex GPC A-802S
Solvent: THF
Flow rate: 1 ml/min
Detector: UV, 220 nm

Detector
response

Elution time
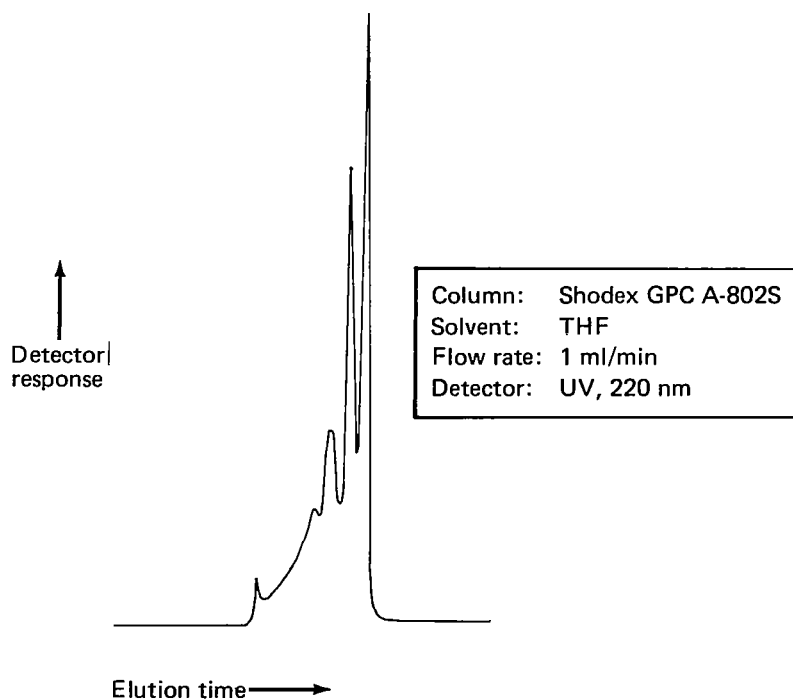
Figure 97. GPC Chromatogram of Narmco Prepreg Batch 1072, Round-Robin Participant H

Column: Shodex GPC A-802S
Solvent: THF
Flow rate: 1 ml/min
Detector: UV, 220 nm

Detector
response

◄───── Elution time
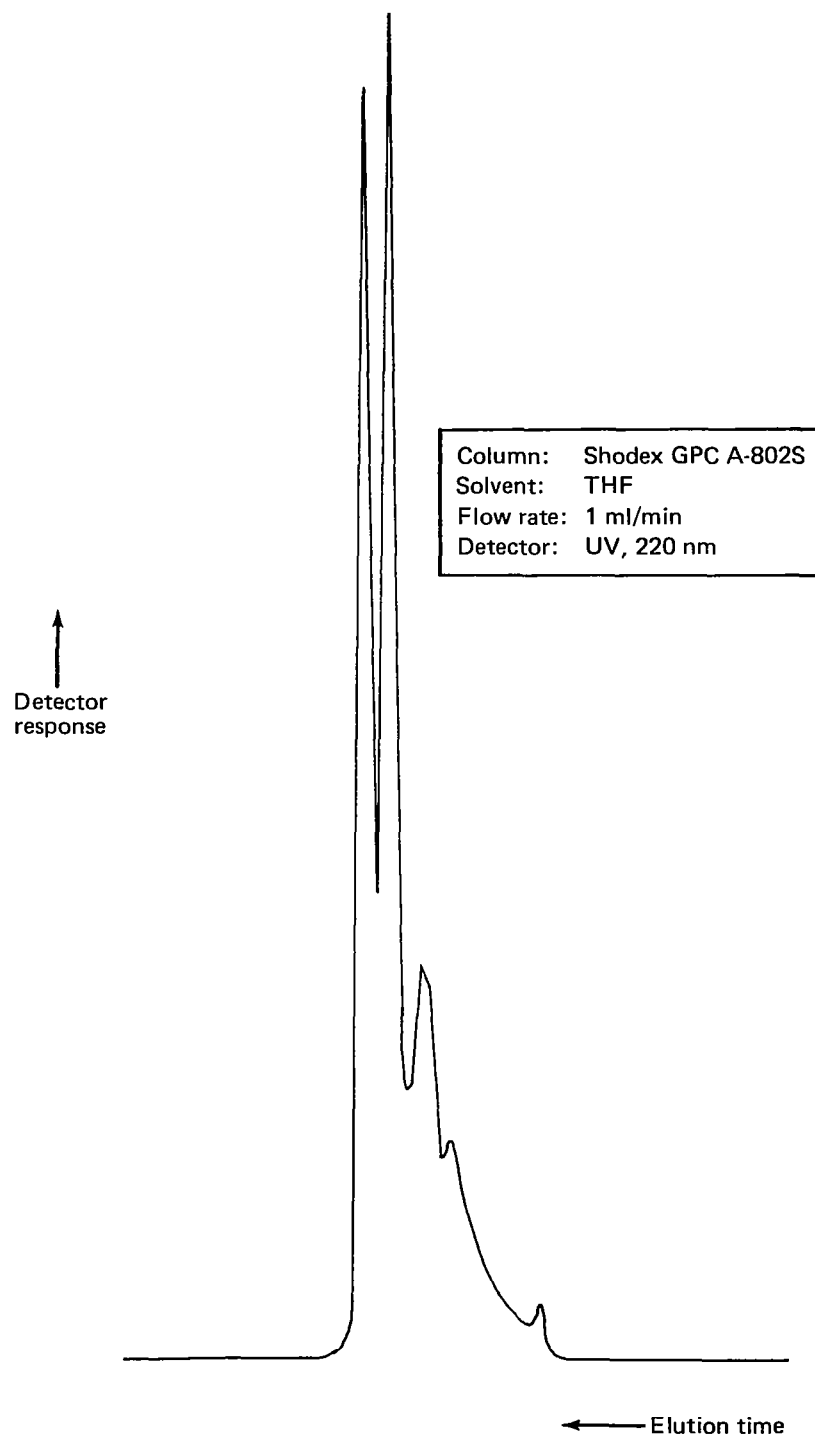
Figure 98. GPC Chromatogram of Narmco Prepreg Batch 1072,
Round-Robin Participant I

2.20   5.06

Detector
response

3.93

Column: Waters μ-Bondapak/C_{18}
Solvent: 63/37% CH_3CN/H_2O, isocratic
Flow rate: 1.5 ml/min
Detector: UV, 220 nm, 0.2 AUF

Elution time, min ⟶

Figure 99. LC Chromatogram of Hercules Batch 707-1A, Using LC Round-Robin Procedure
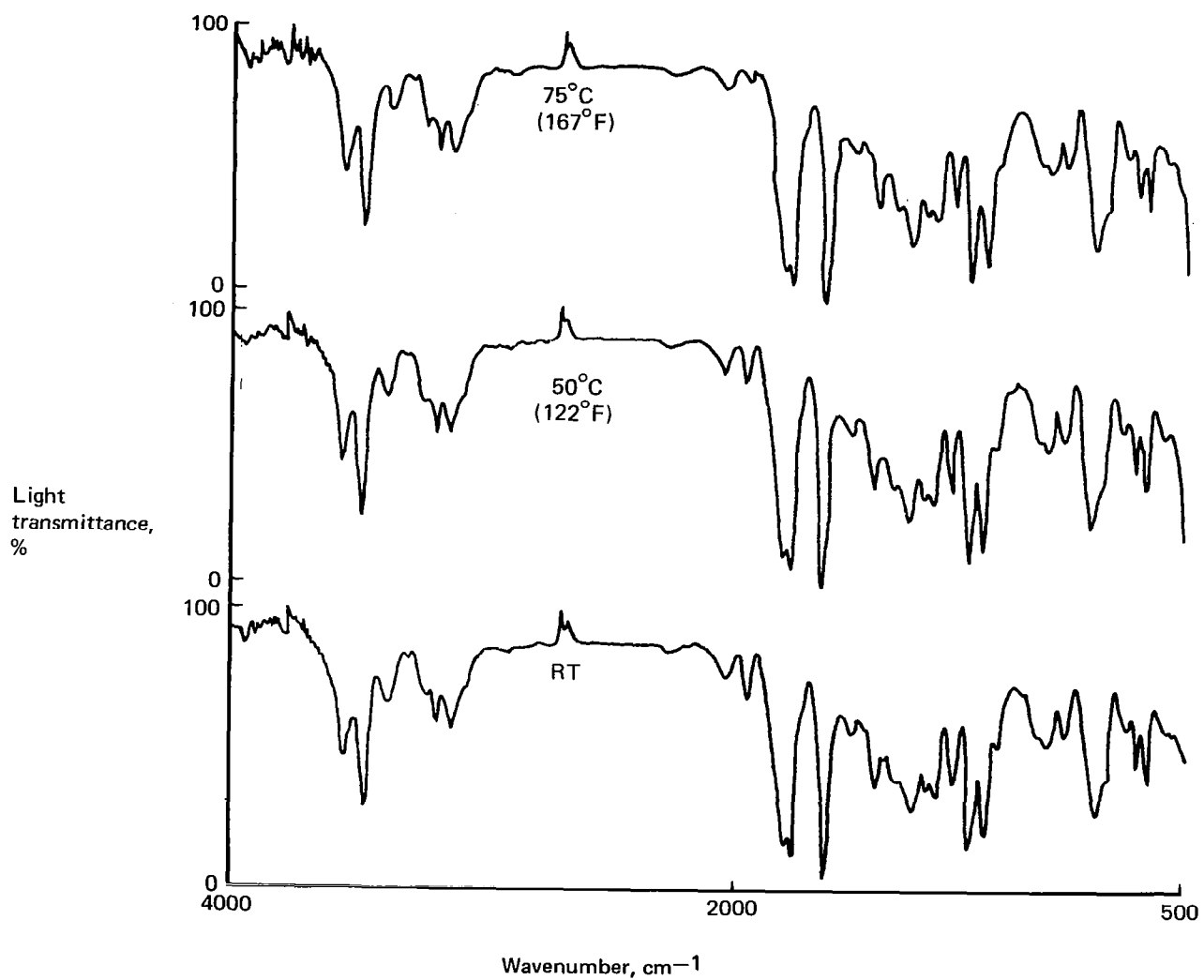
Figure 100. TSIR Spectra of Hercules Resin—RT, 50°C, and 75°C (RT, 122°F, and 167°F)

175
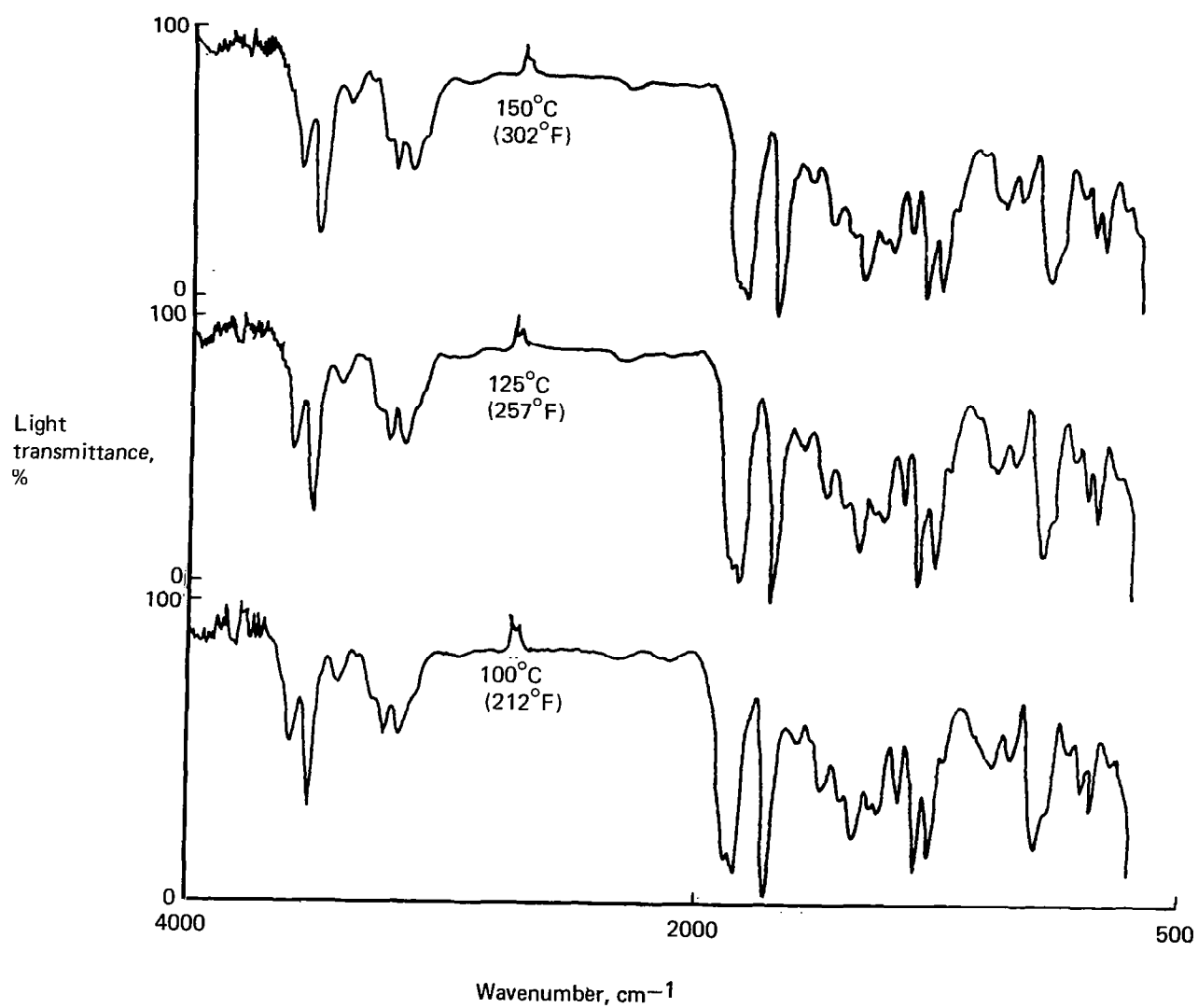
Figure 101. TSIR Spectra of Hercules Resin—100, 125, and 150°C (212, 257, and 302°F)

176
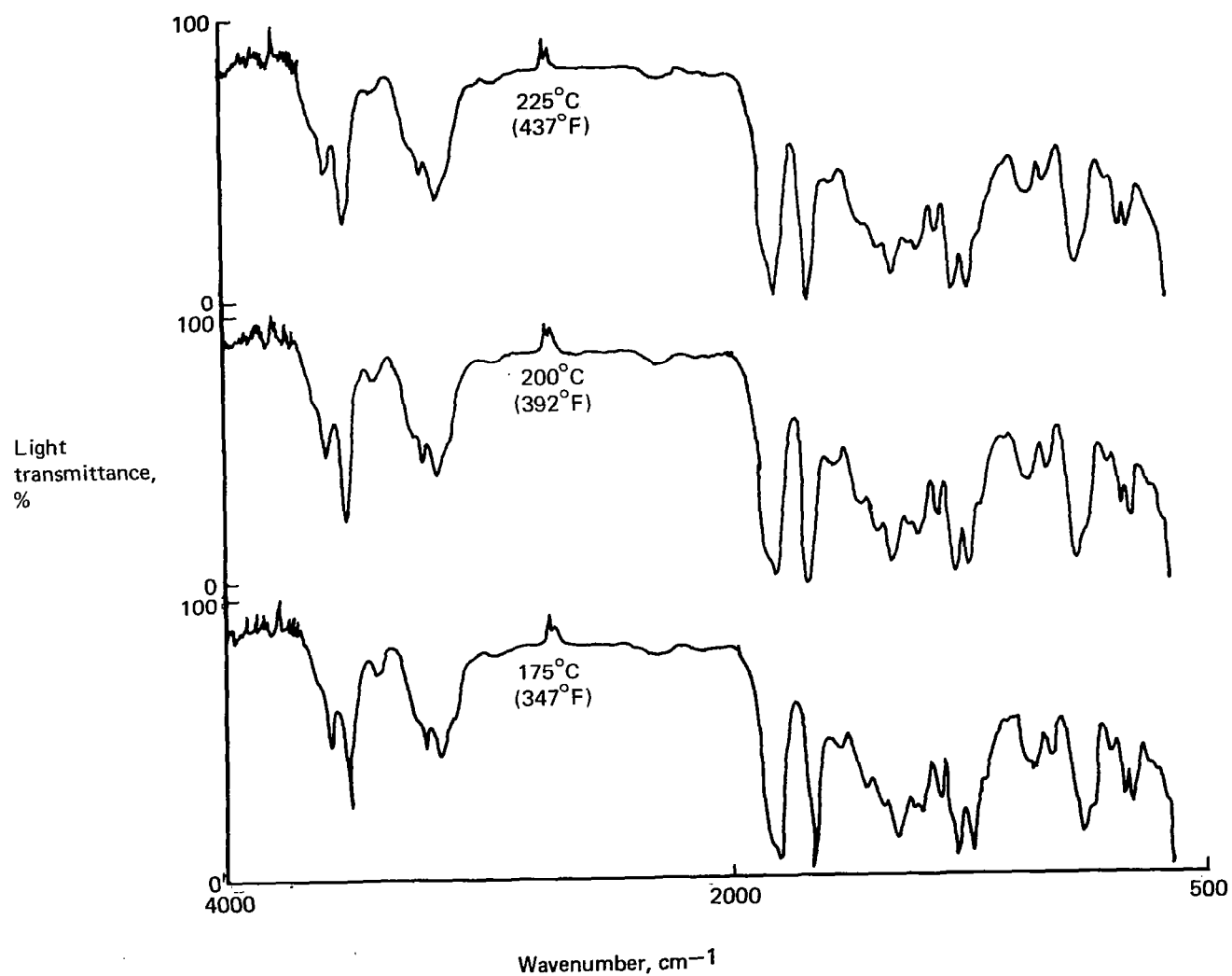
Figure 102. TSIR Spectra of Hercules Resin—175, 200, and 225°C (347, 392, and 437°F)
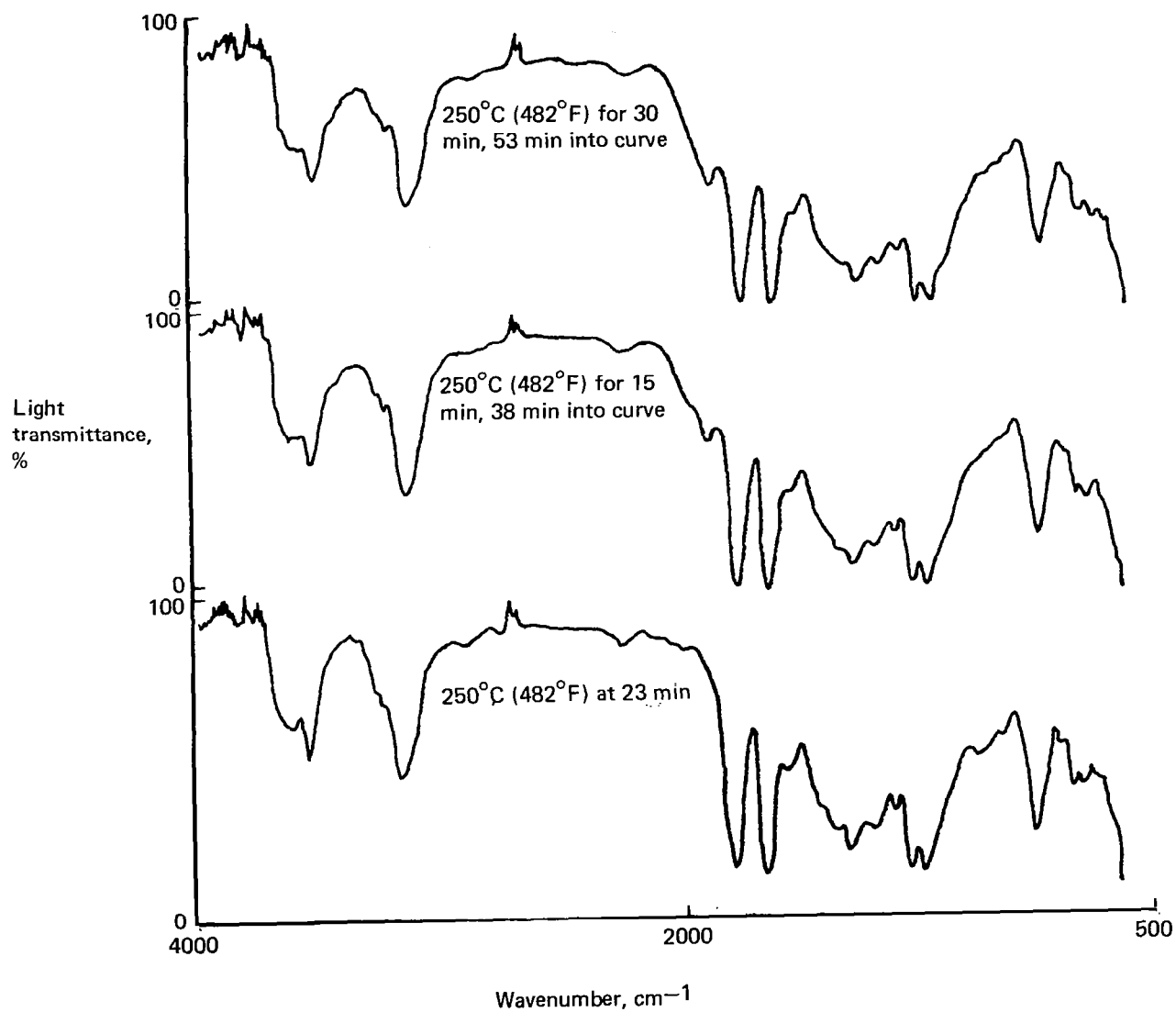
Figure 103. TSIR Spectra of Hercules Resin—250°C (482°F)
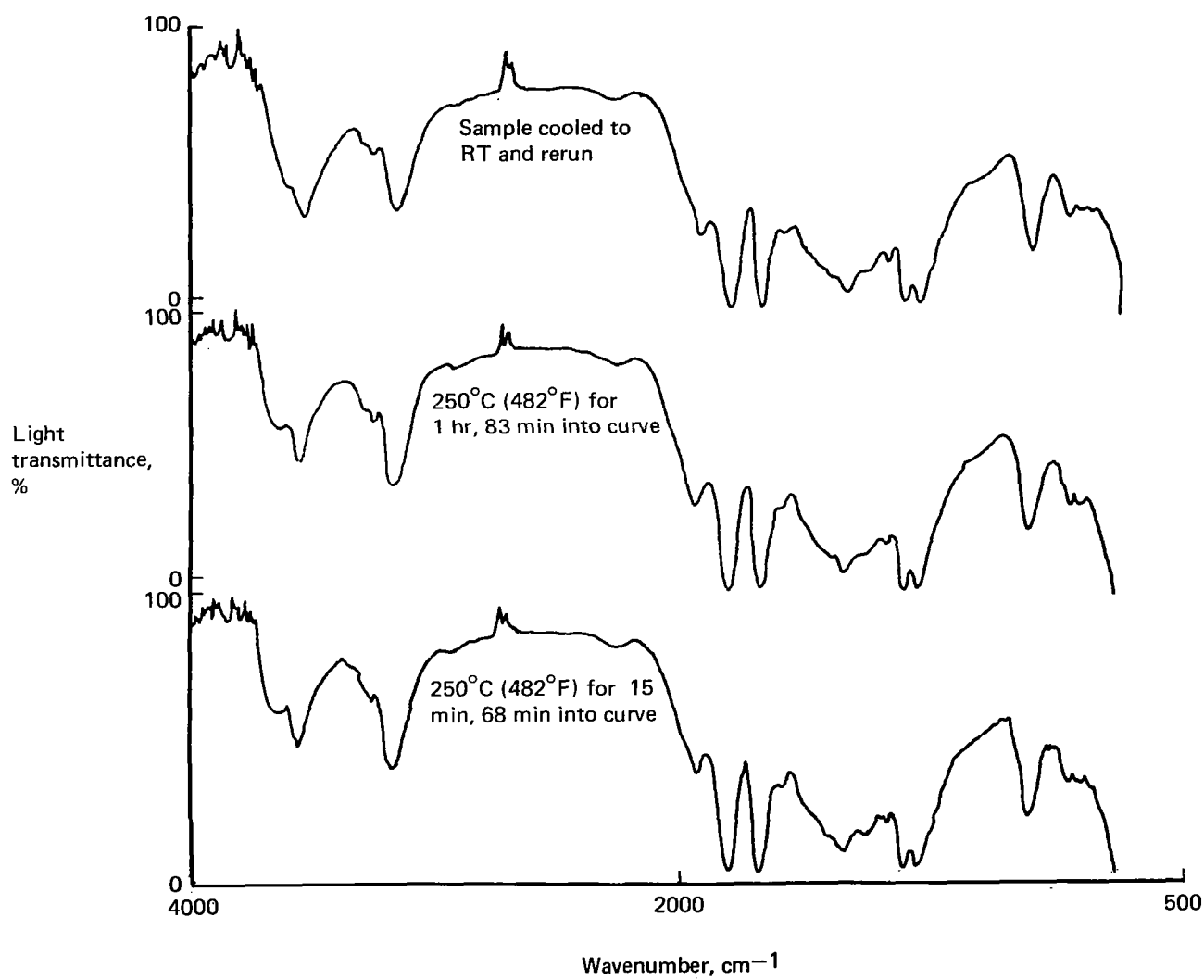
Figure 104. TSIR Spectra of Hercules Resin—RT and 250°C (RT and 482°F)
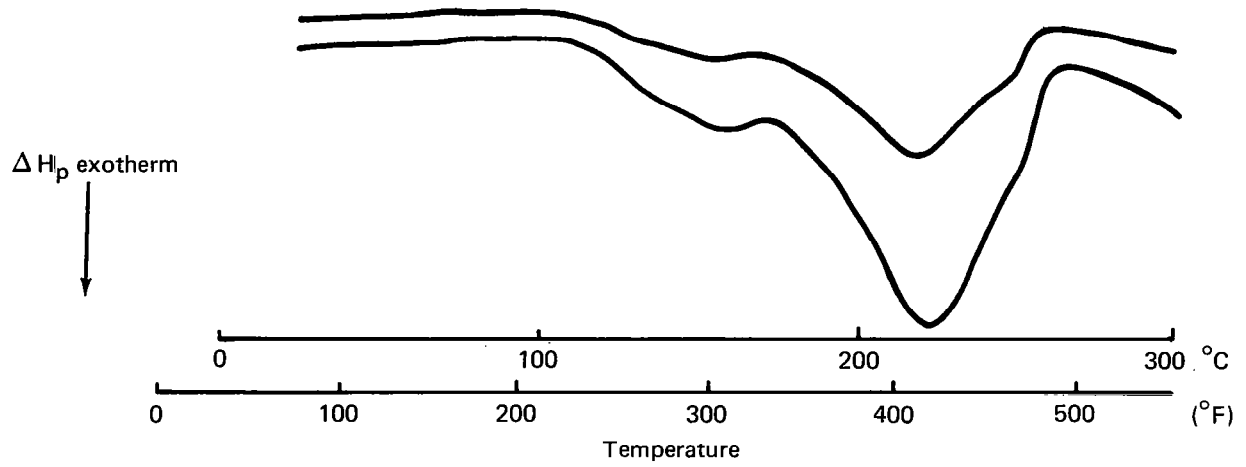
Figure 105. DSC Scan of Hercules Resin
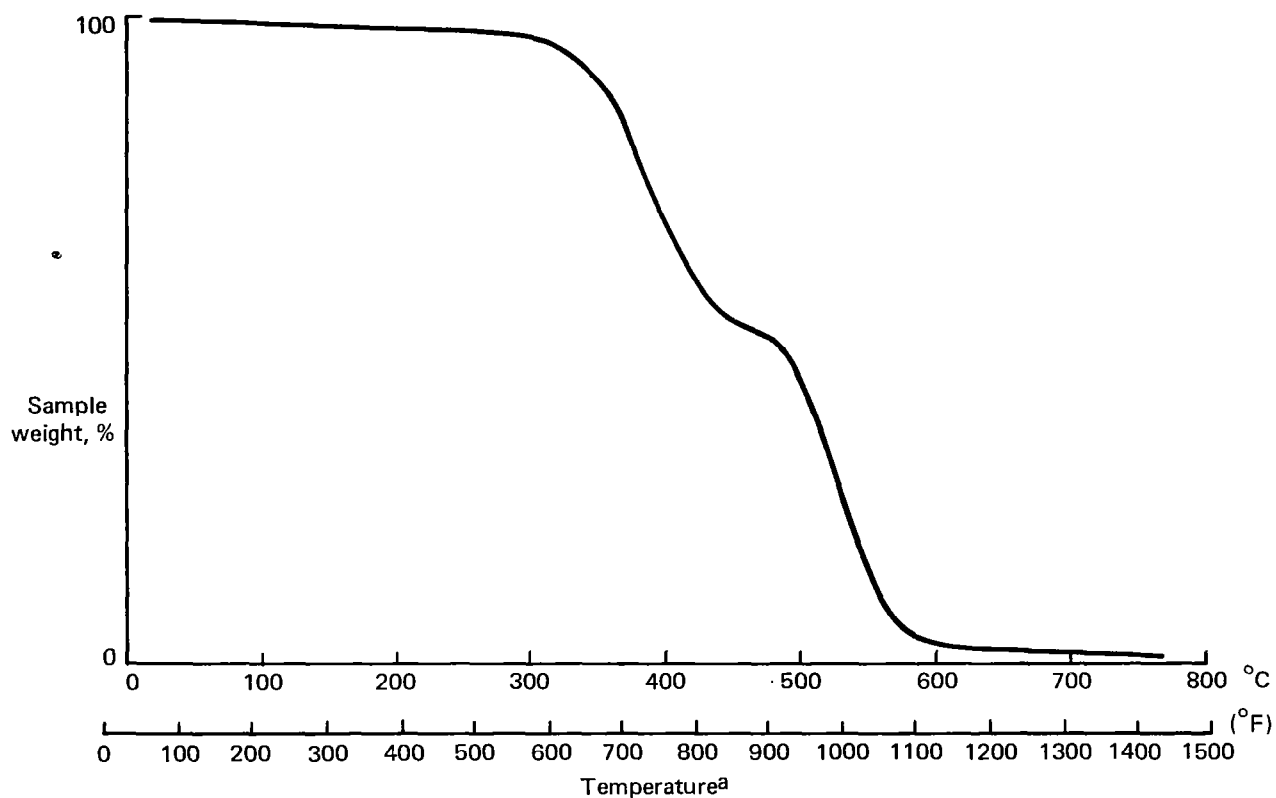
^aCorrected for chromel-alumel thermocouples

Figure 106. TGA Scan of Hercules Resin
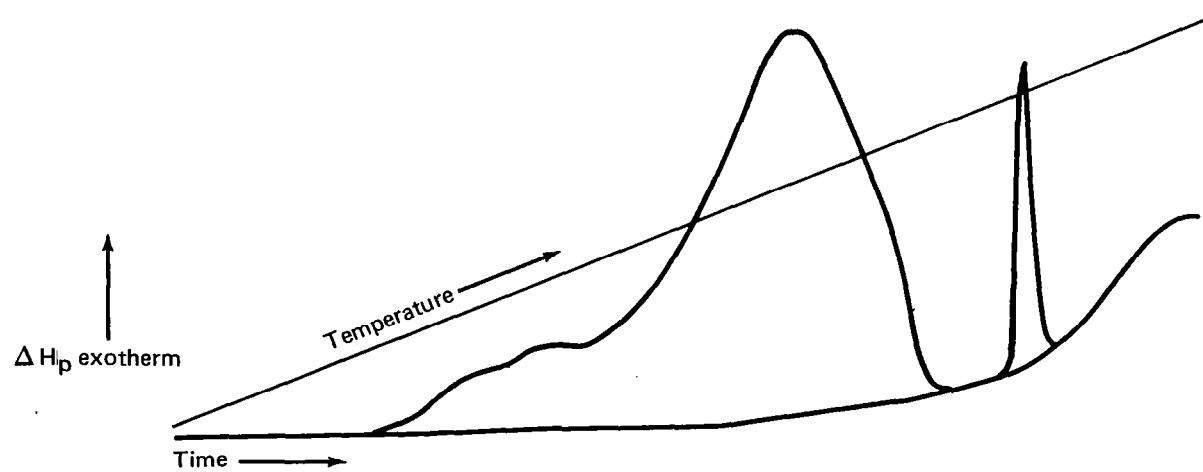
Figure 107. DSC Curve of Hercules Resin Batch 707-1A
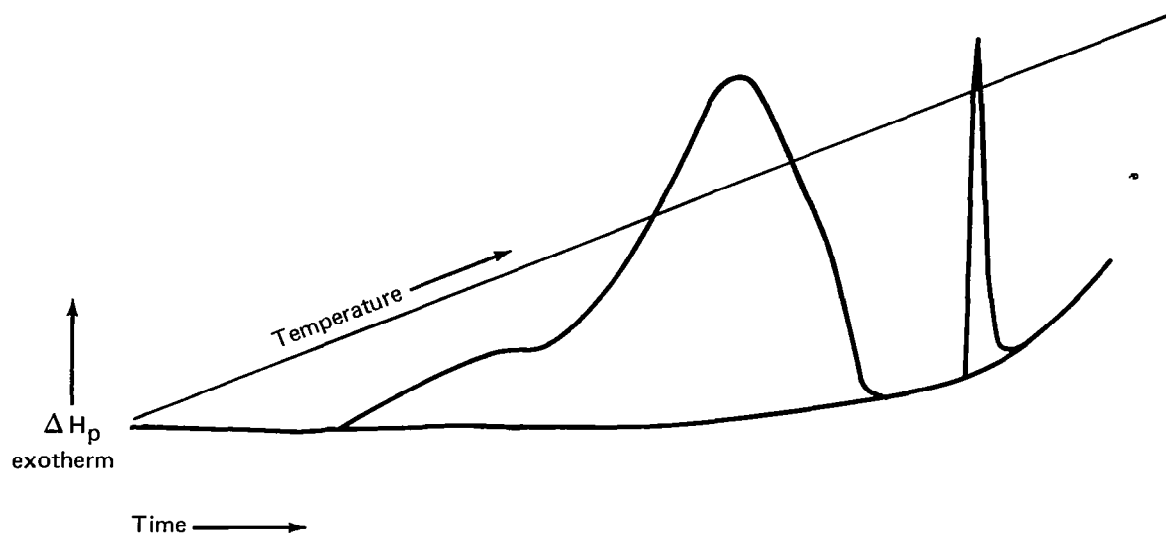
Figure 108. DSC Curve of Hercules Resin Batch 727-3A
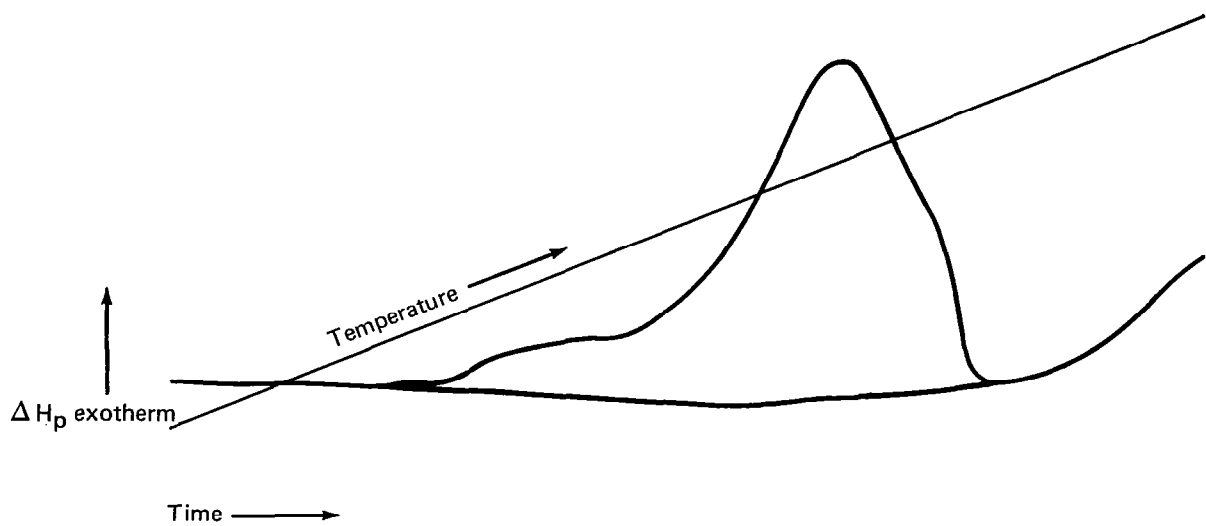
Figure 109. DSC Curve of Hercules Resin Batch 727-7A

Detector
response

```
Column:    Shodex GPC A-802S
Solvent:   THF
Flow rate: 1 ml/min
Detector:  UV, 220 nm
```

◄────── Elution time
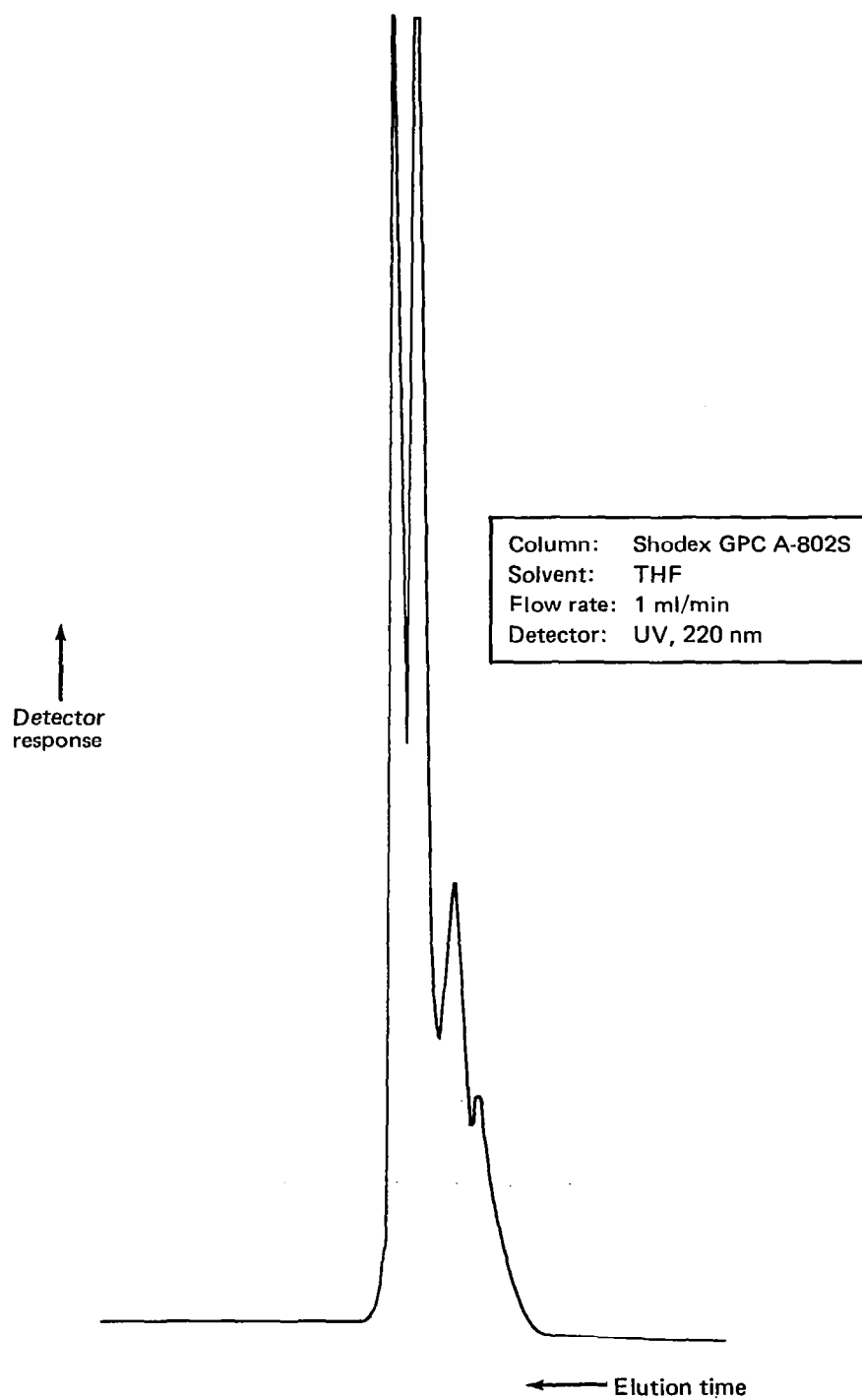
*Figure 110. GPC Chromatogram of Hercules Batch 707-1A,
Using GPC Round-Robin Procedure*
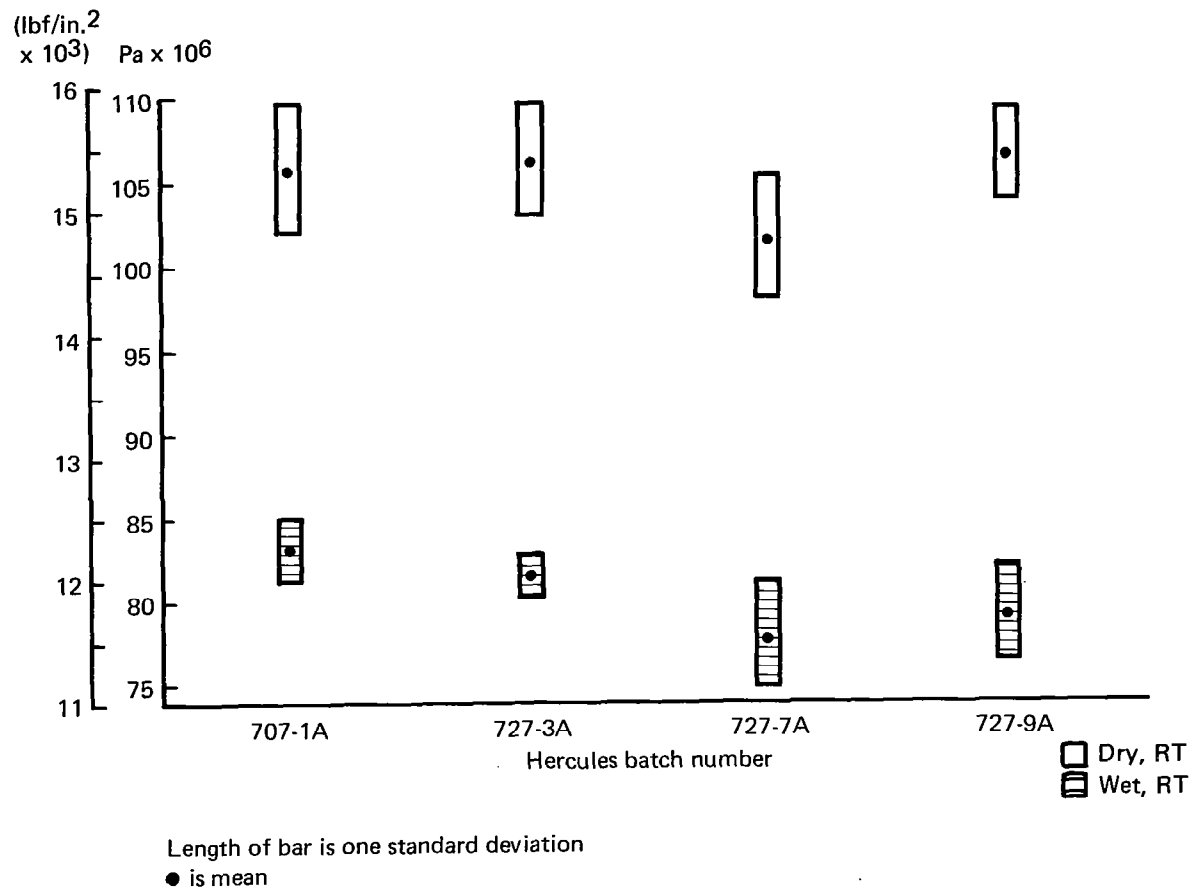
Figure 111. 0-deg Short-Beam-Shear Strength of Hercules Laminates
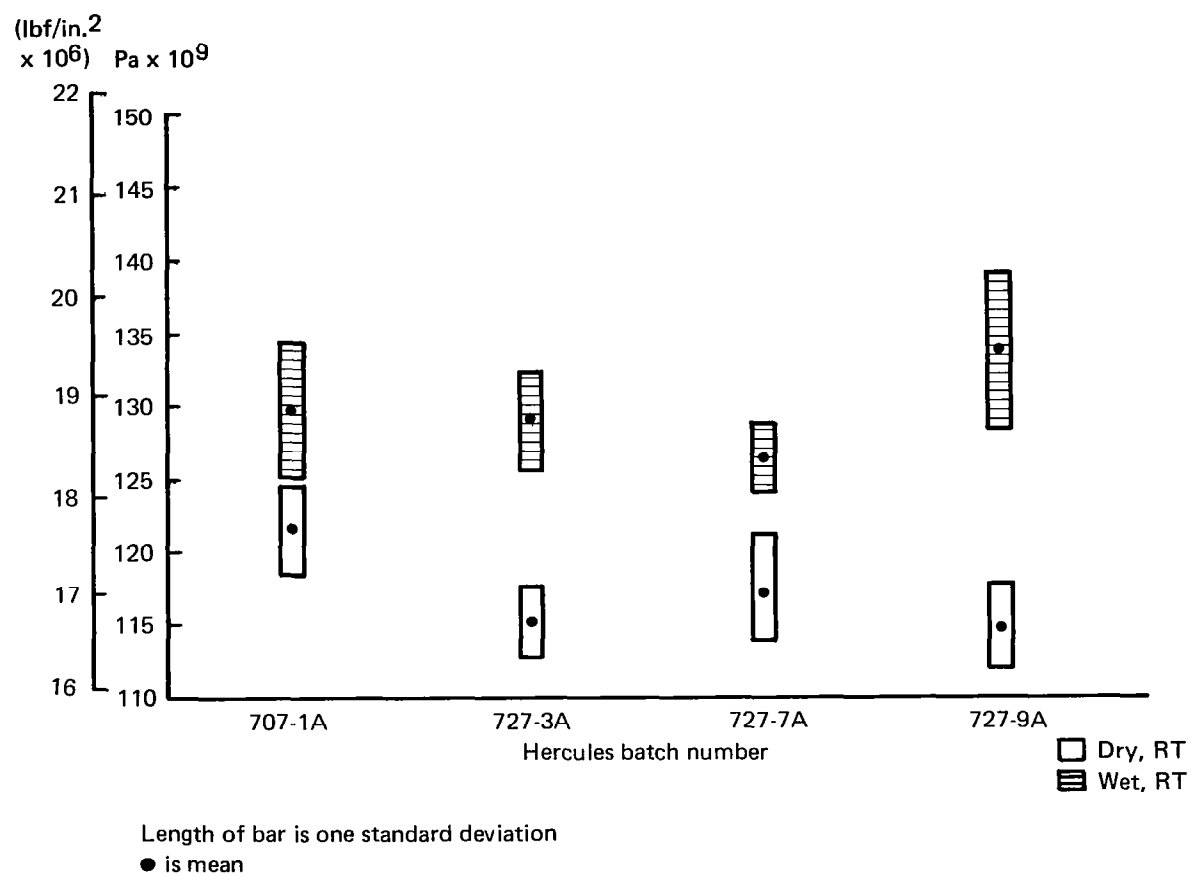
Figure 112. 0-deg Compression Modulus of Hercules Laminates
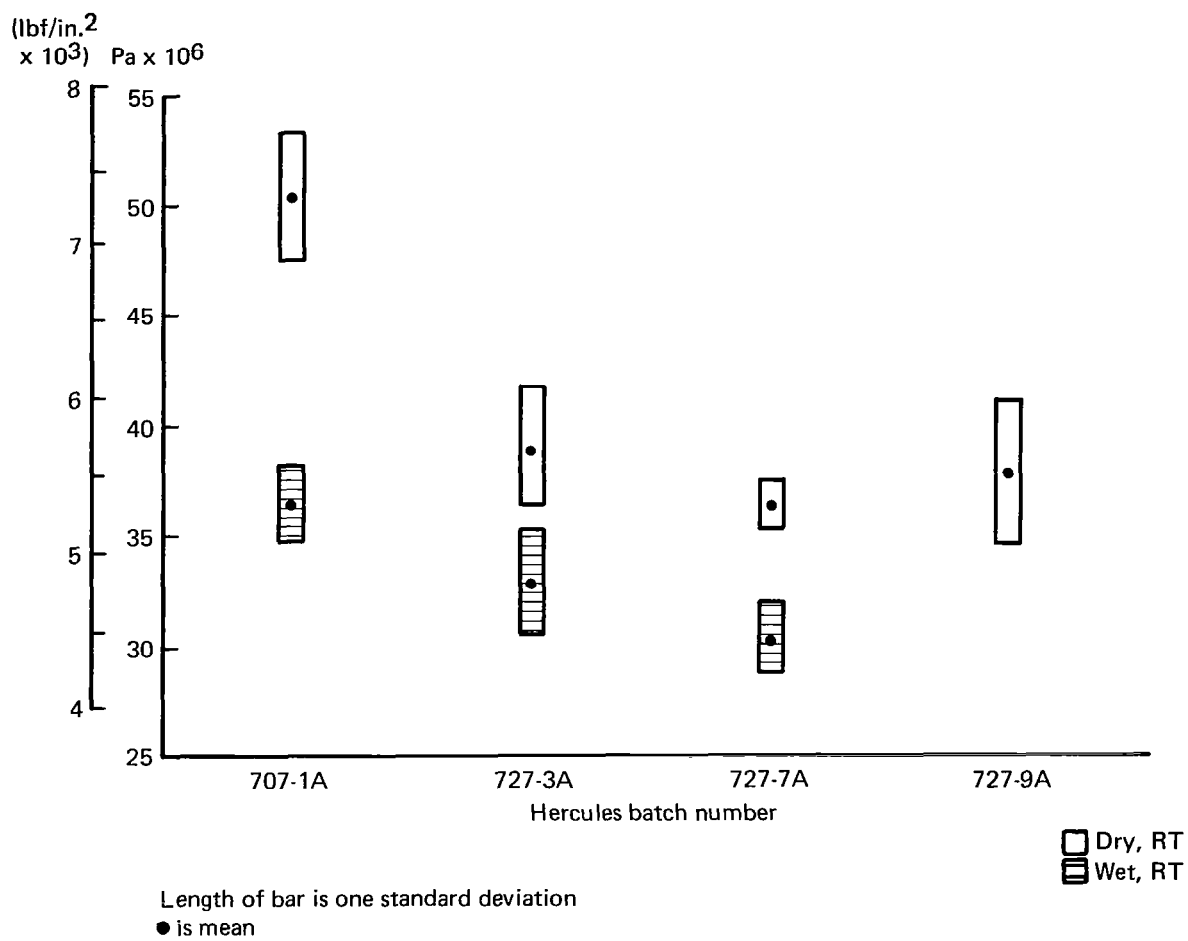
Figure 113. 90-deg Tension Stress of Hercules Laminates

Viscoelastic property

Stress vector

δ

stress
strain

Viscous modulus, G''
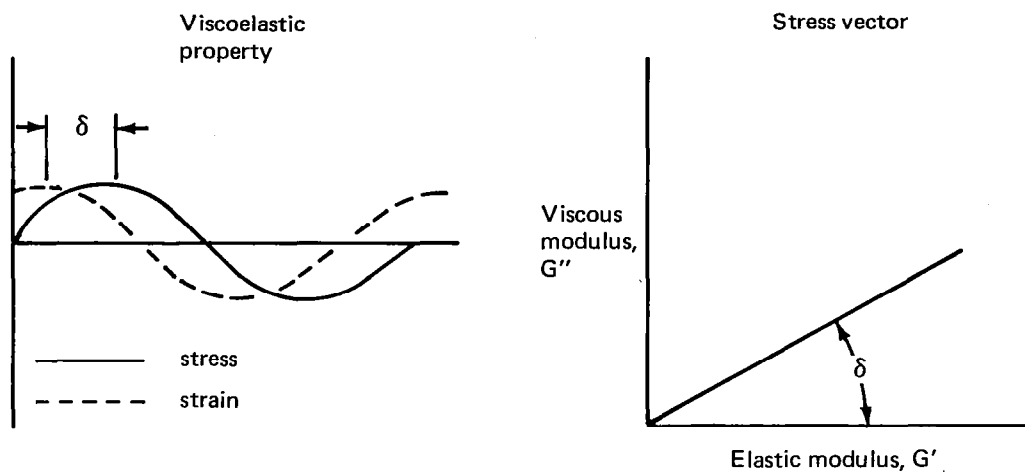
Elastic modulus, G'

$$\text{Elastic modulus, } G' = \frac{\text{in-phase stress}}{\text{applied strain}}$$

$$\text{Viscous modulus, } G'' = \frac{\text{out-of-phase stress}}{\text{applies strain}}$$

$$\tan \delta = G''/G'$$

Figure 114. DMA Measurement Definitions

Glassy   Leathery   Rubbery plateau   Rubbery flow

G'

Liquid flow

tan δ

Temperature ⟶
⟵ log ω.

ω = frequency
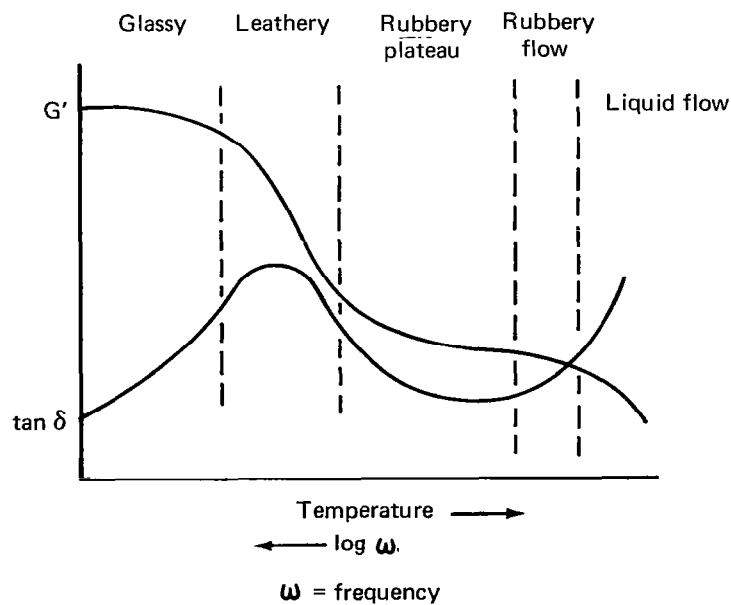
Figure 115. Typical Dynamic Mechanical Response
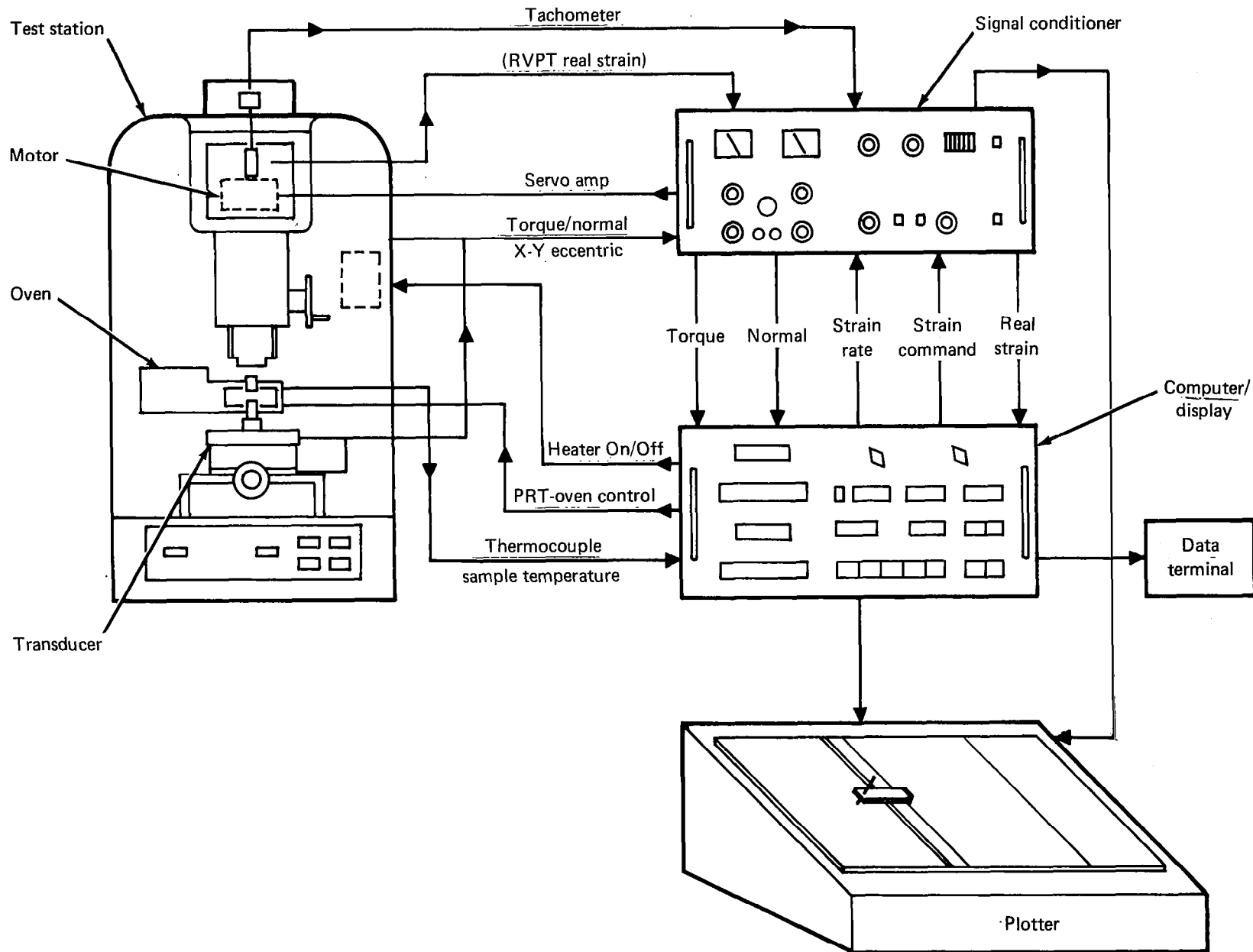
Figure 116. Schematic of RMS System Flow
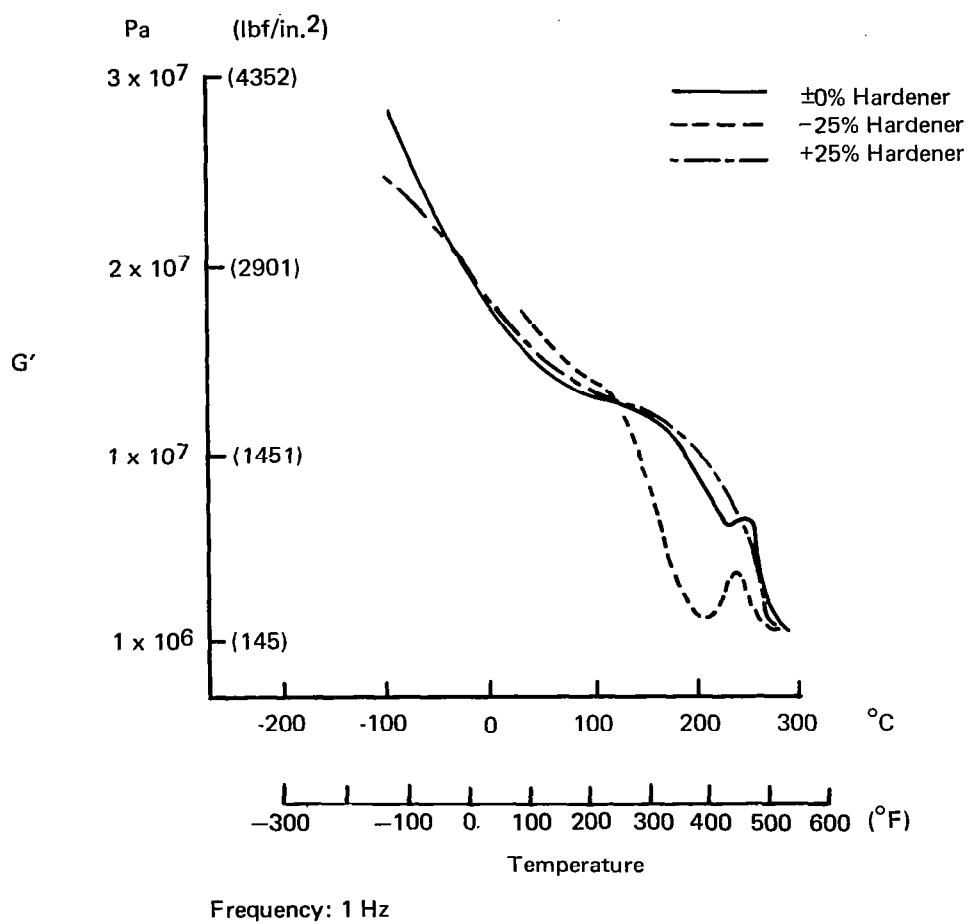
Figure 117. Elastic Modulus Versus Temperature, Narmco Matrix
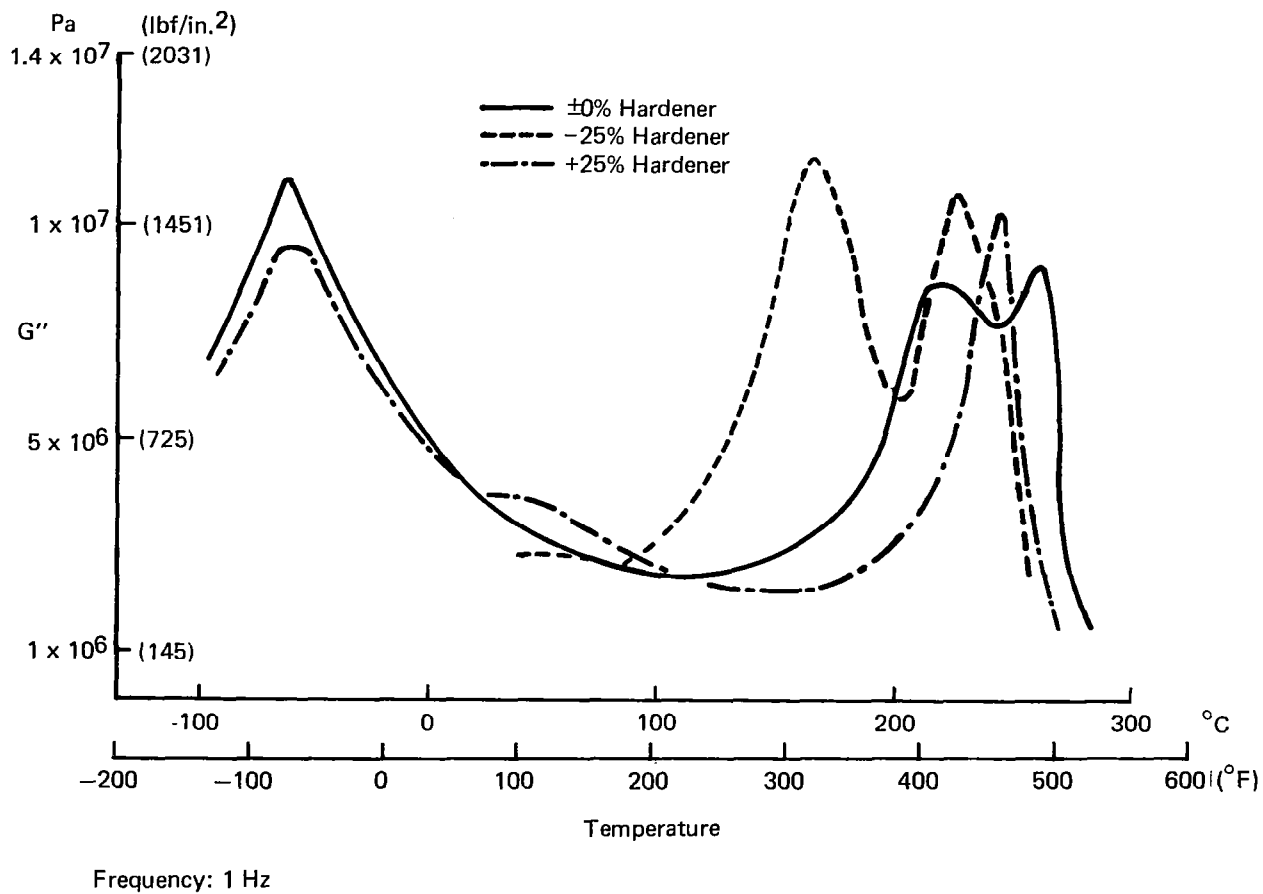
Figure 118. Viscous Modulus Versus Temperature, Narmco Matrix
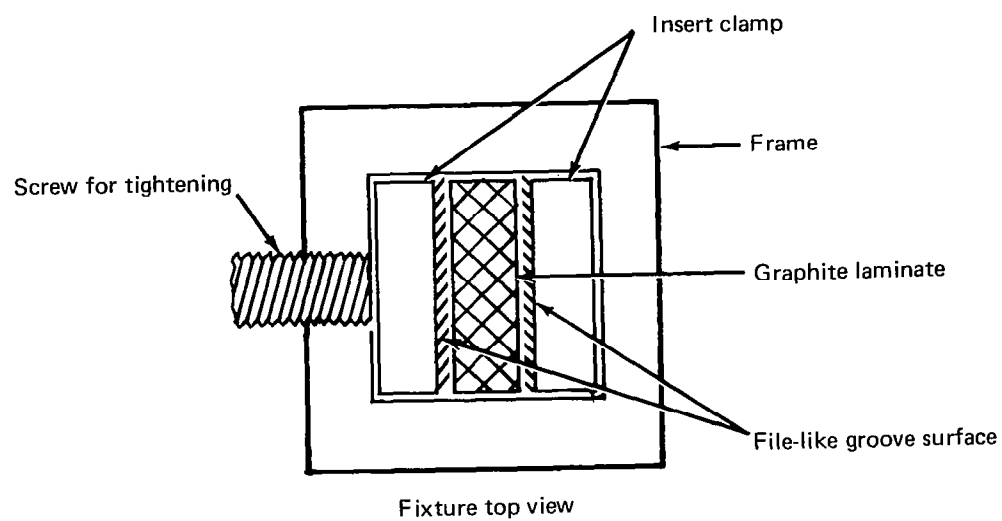
Figure 119. Fixture for DMA Testing of Epoxy Graphite Laminates
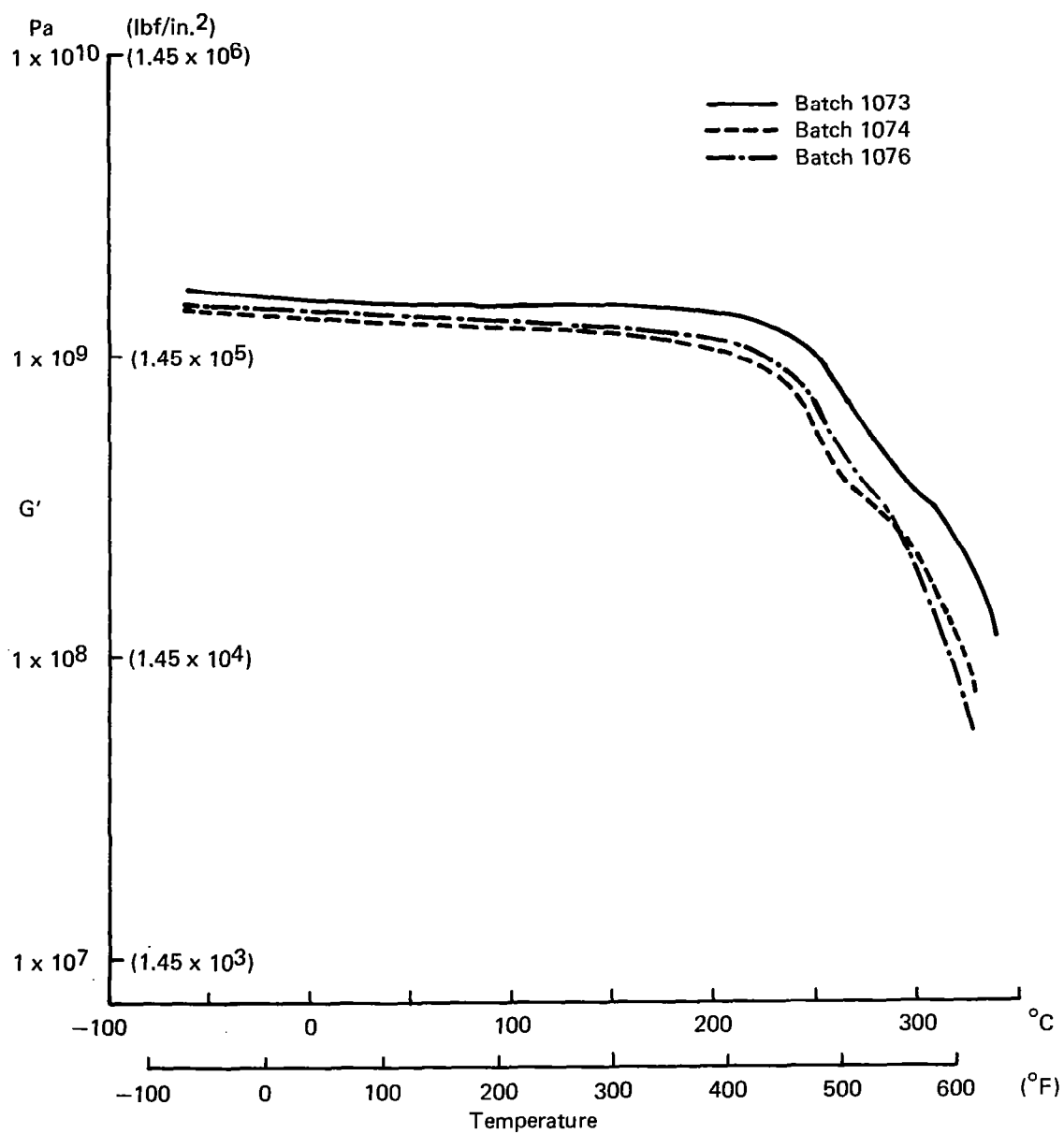
Figure 120. G' Versus Temperature, Narmco Laminates
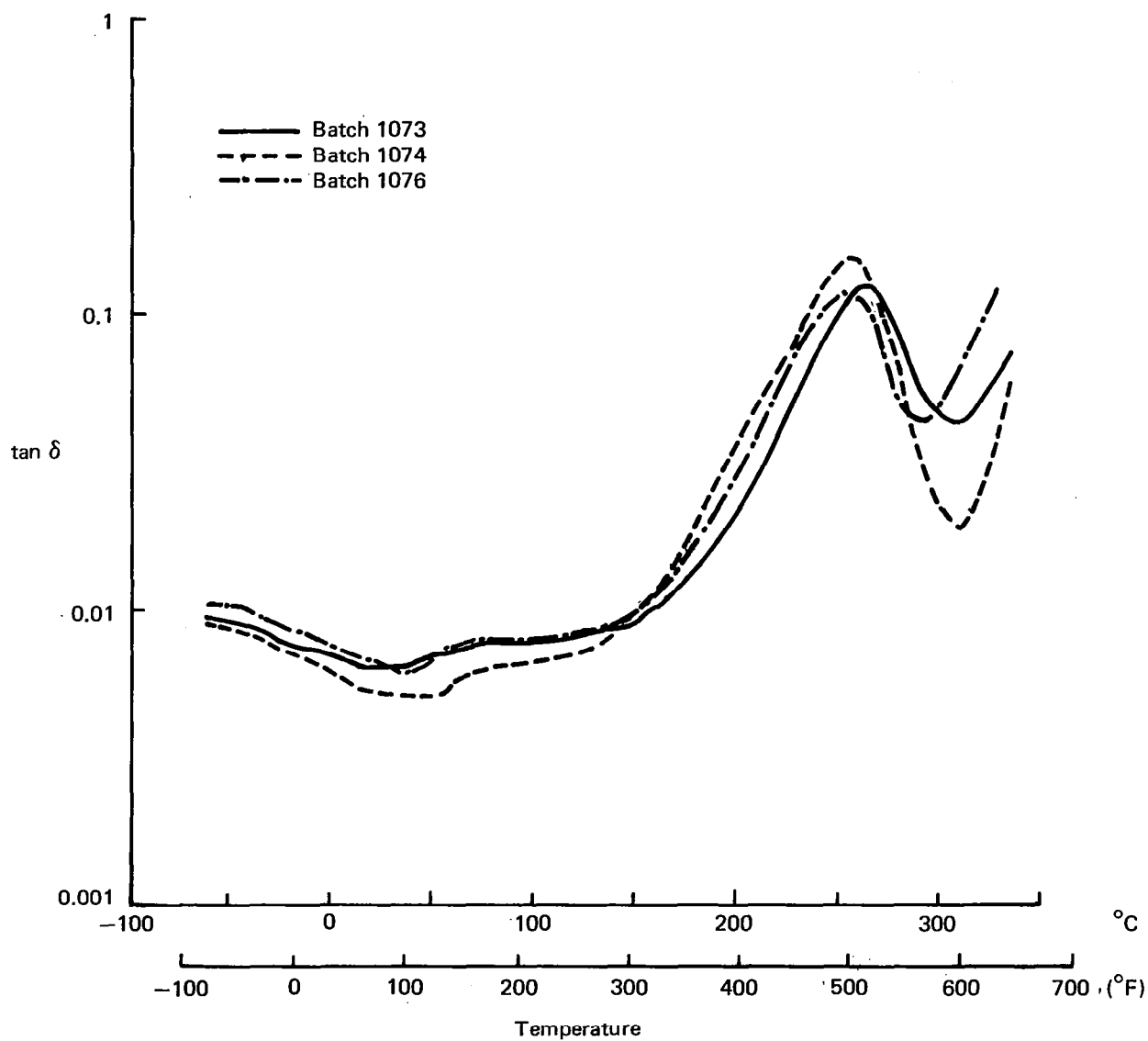
Figure 121. Tan δ Versus Temperature, Narmco Laminates
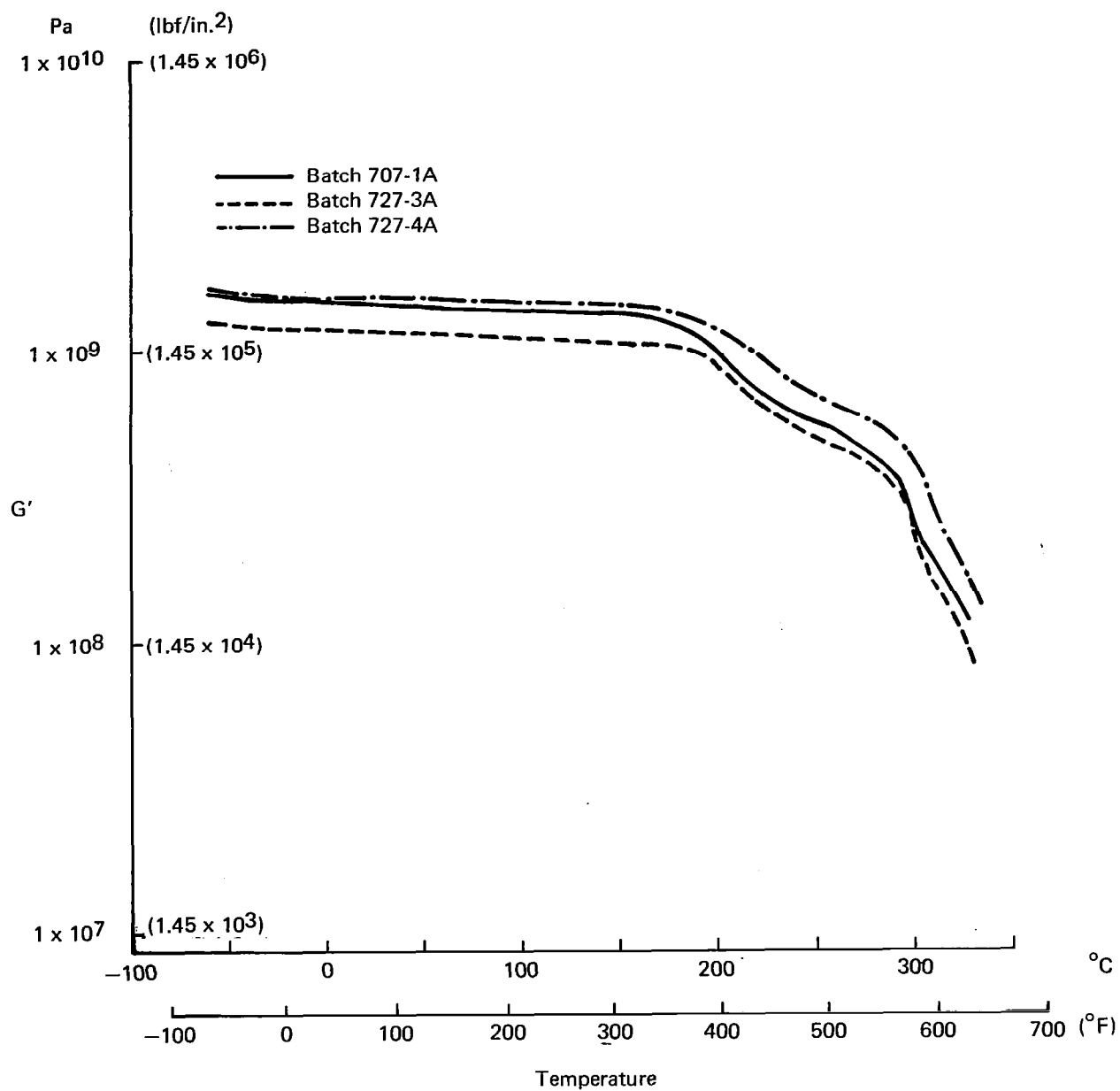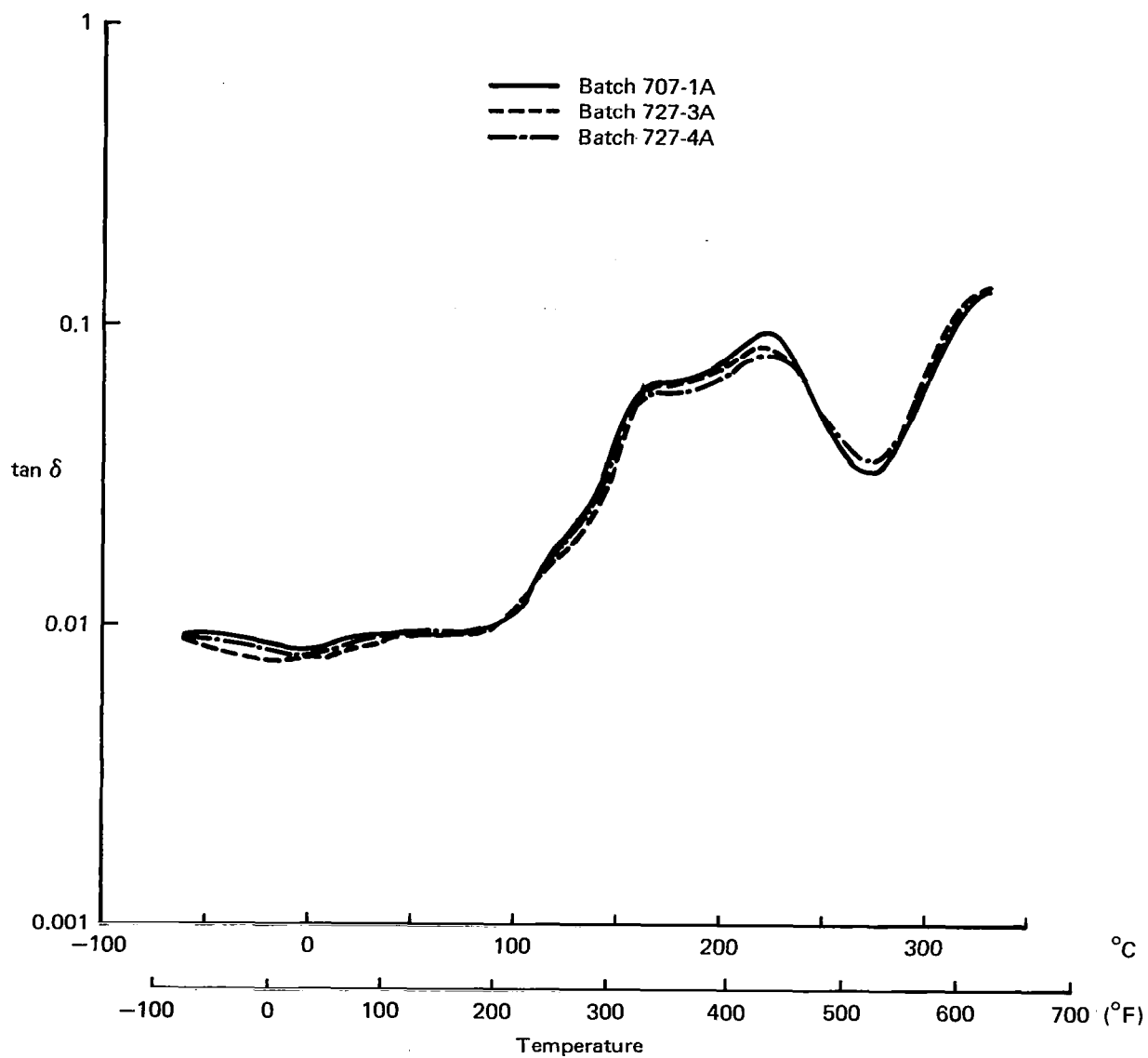
Figure 122. *G' Versus Temperature, Hercules Laminates*
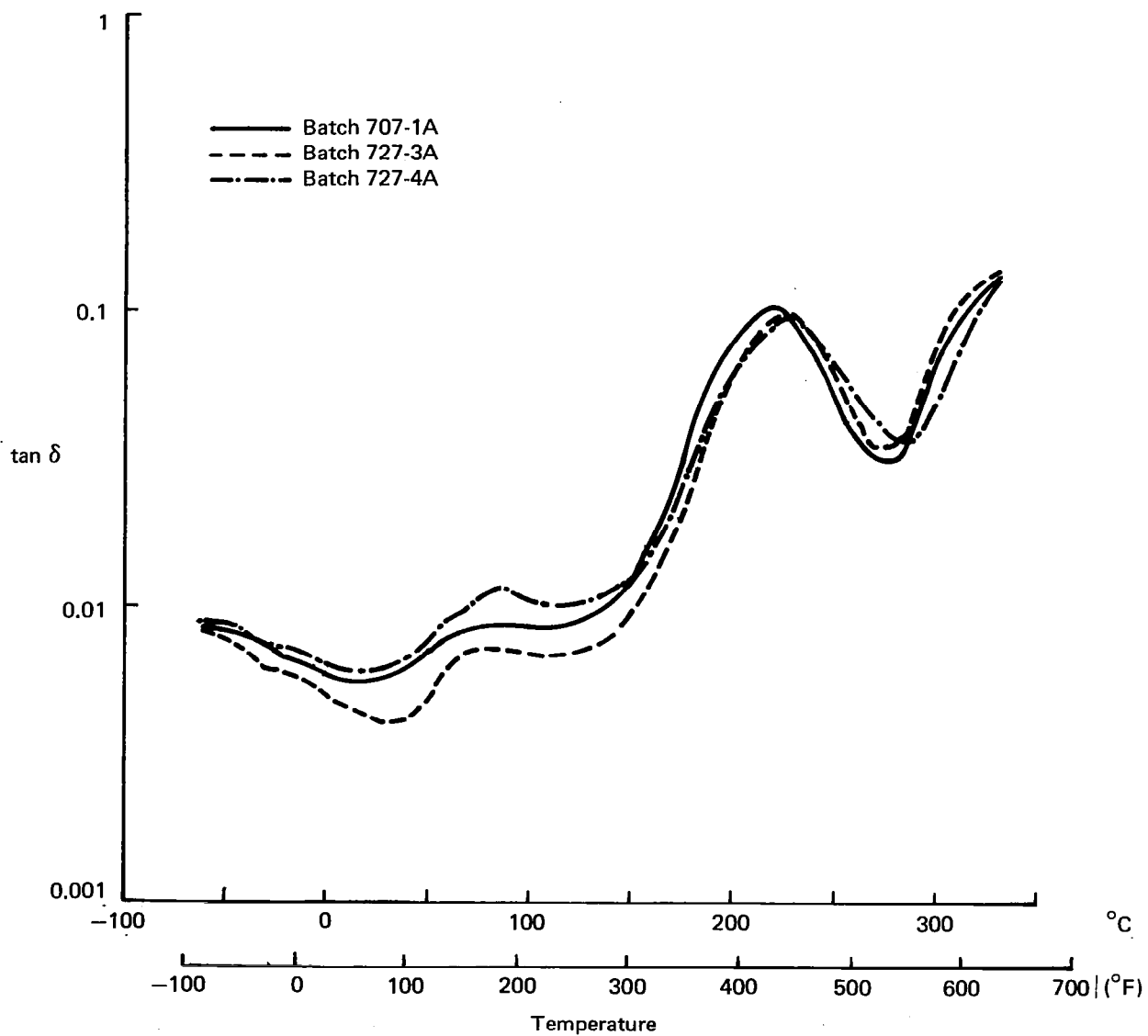
Figure 123. Tan δ Versus Temperature, Hercules Laminates
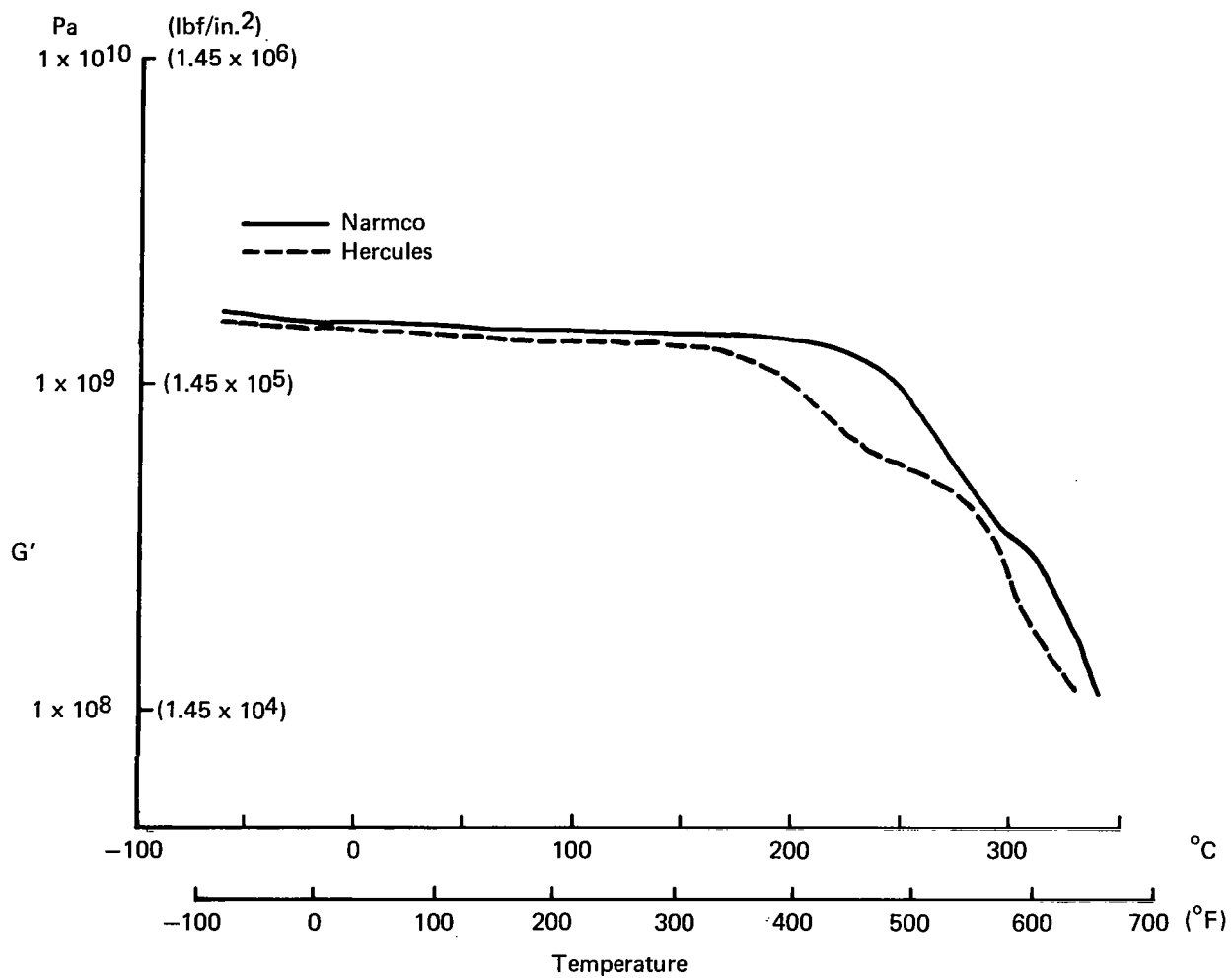
Figure 124. G' Versus Temperature, Narmco and Hercules Standard Batches
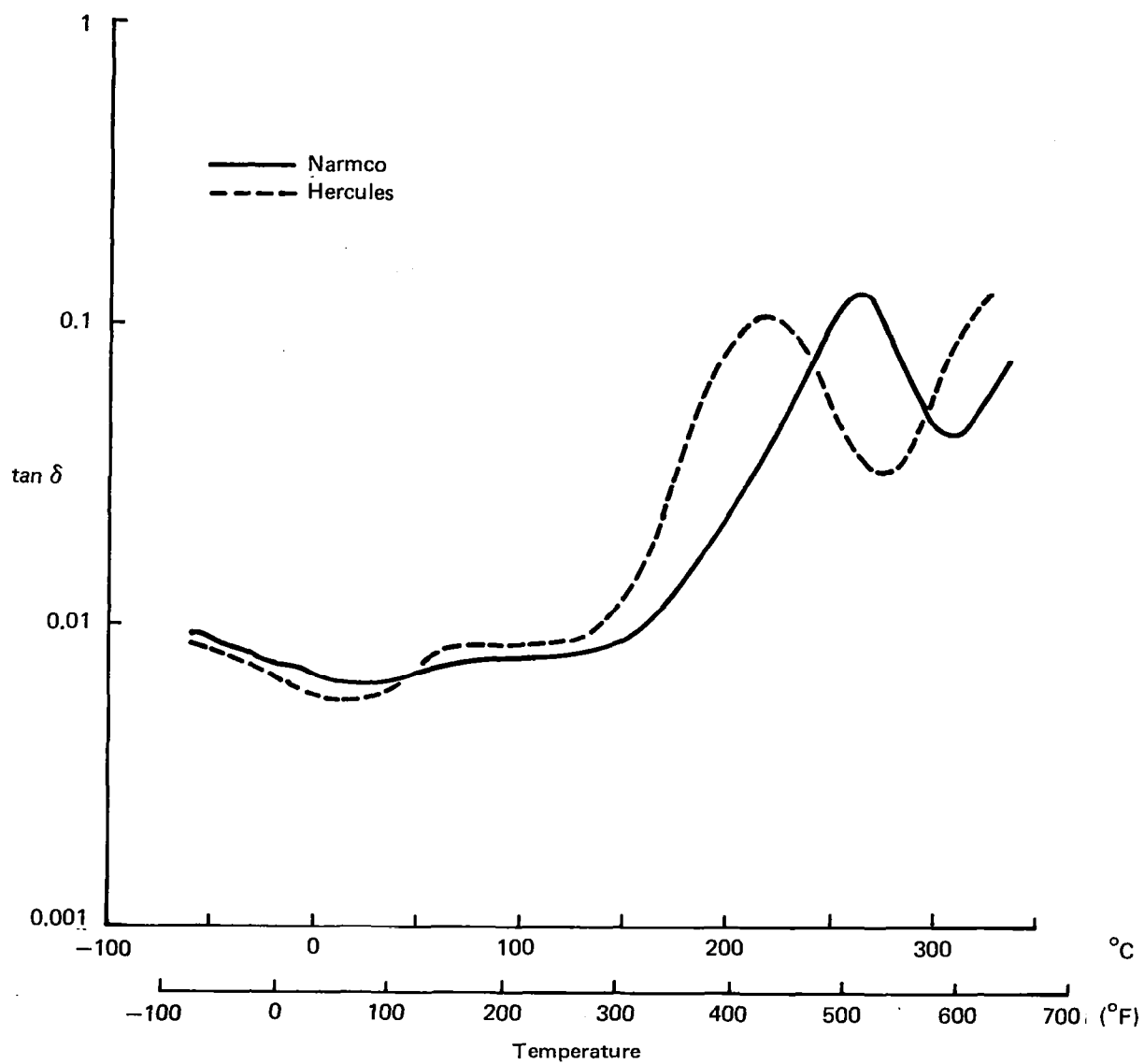
Figure 125. Tan δ Versus Temperature, Narmco and Hercules Standard Batches
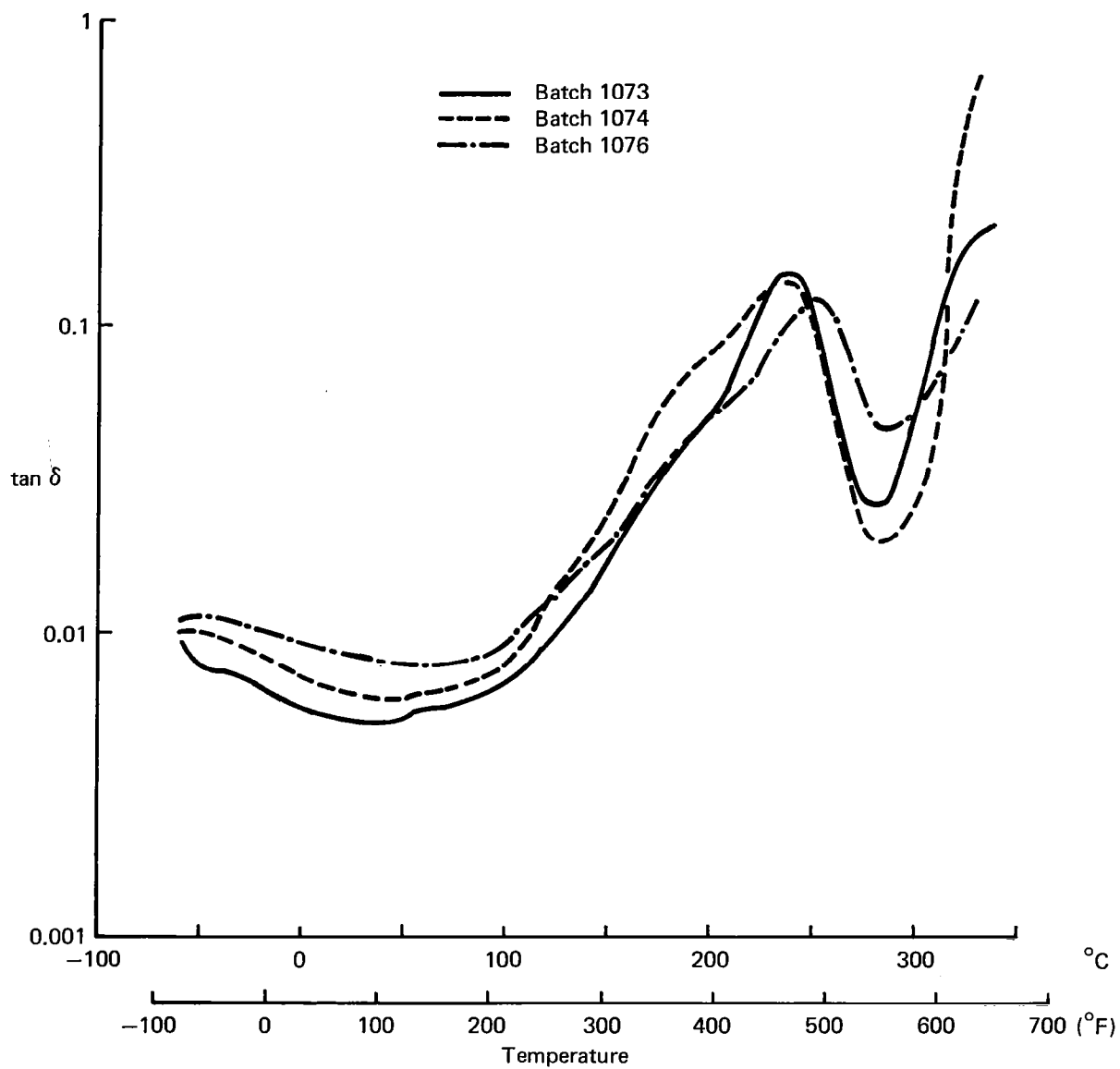
Figure 126. Tan δ Versus Temperature, Narmco Laminates, Humidity Exposed

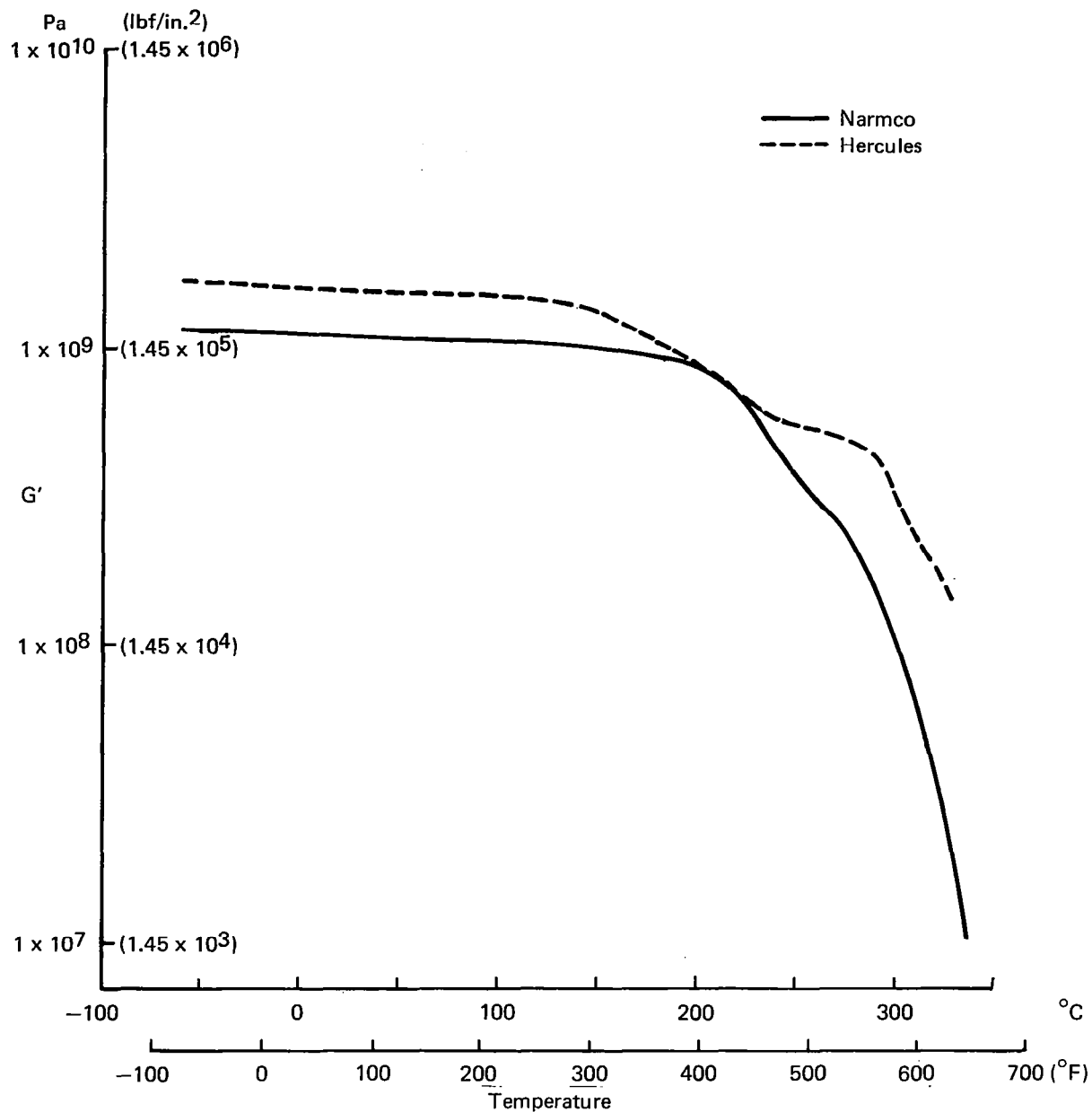Figure 127. Tan δ Versus Temperature, Hercules Laminates, Humidity Exposed

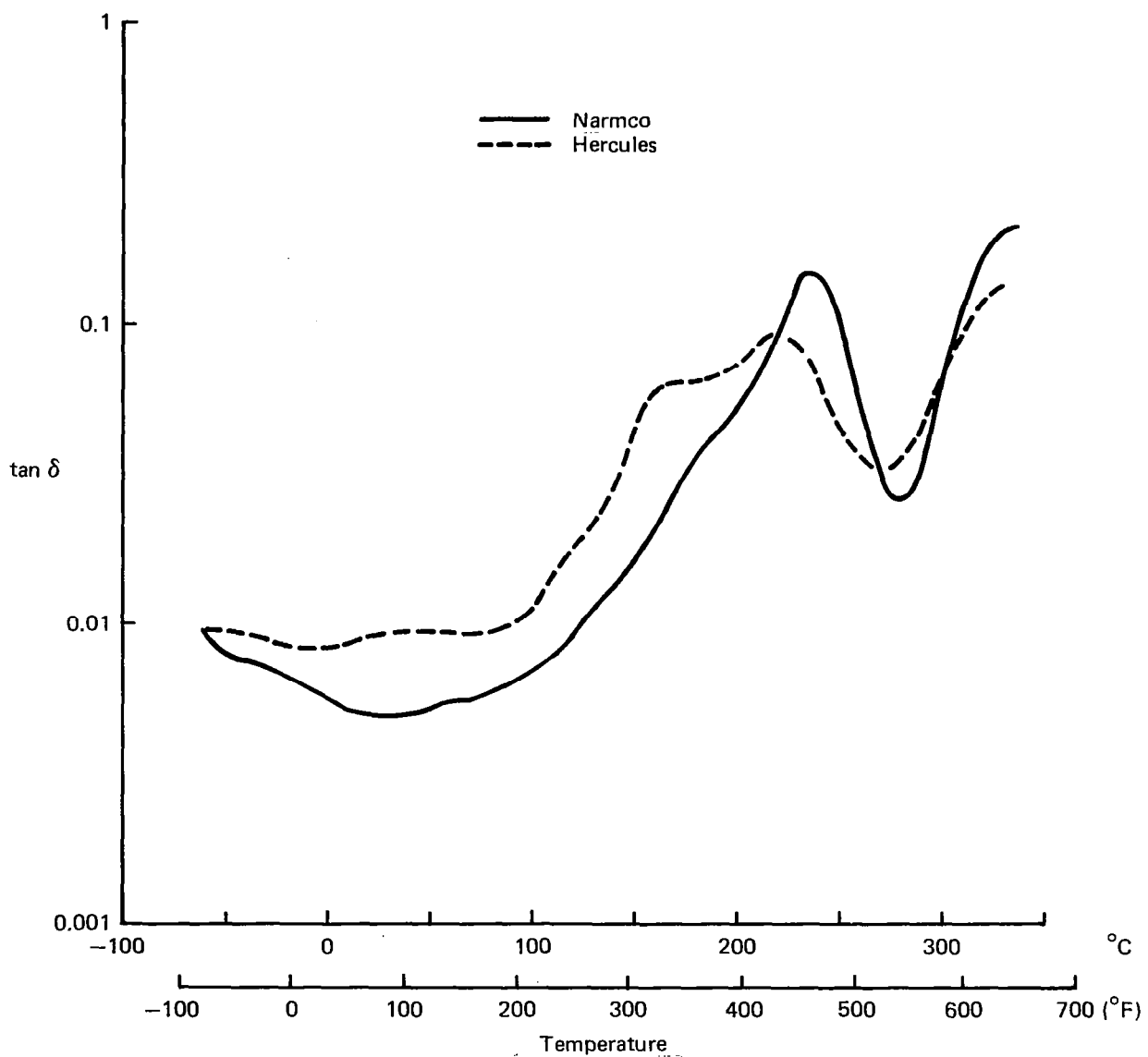*Figure 128. G' Versus Temperature, Narmco and Hercules Standard Batches, Humidity Exposed*

Figure 129. Tan δ Versus Temperature, Narmco and
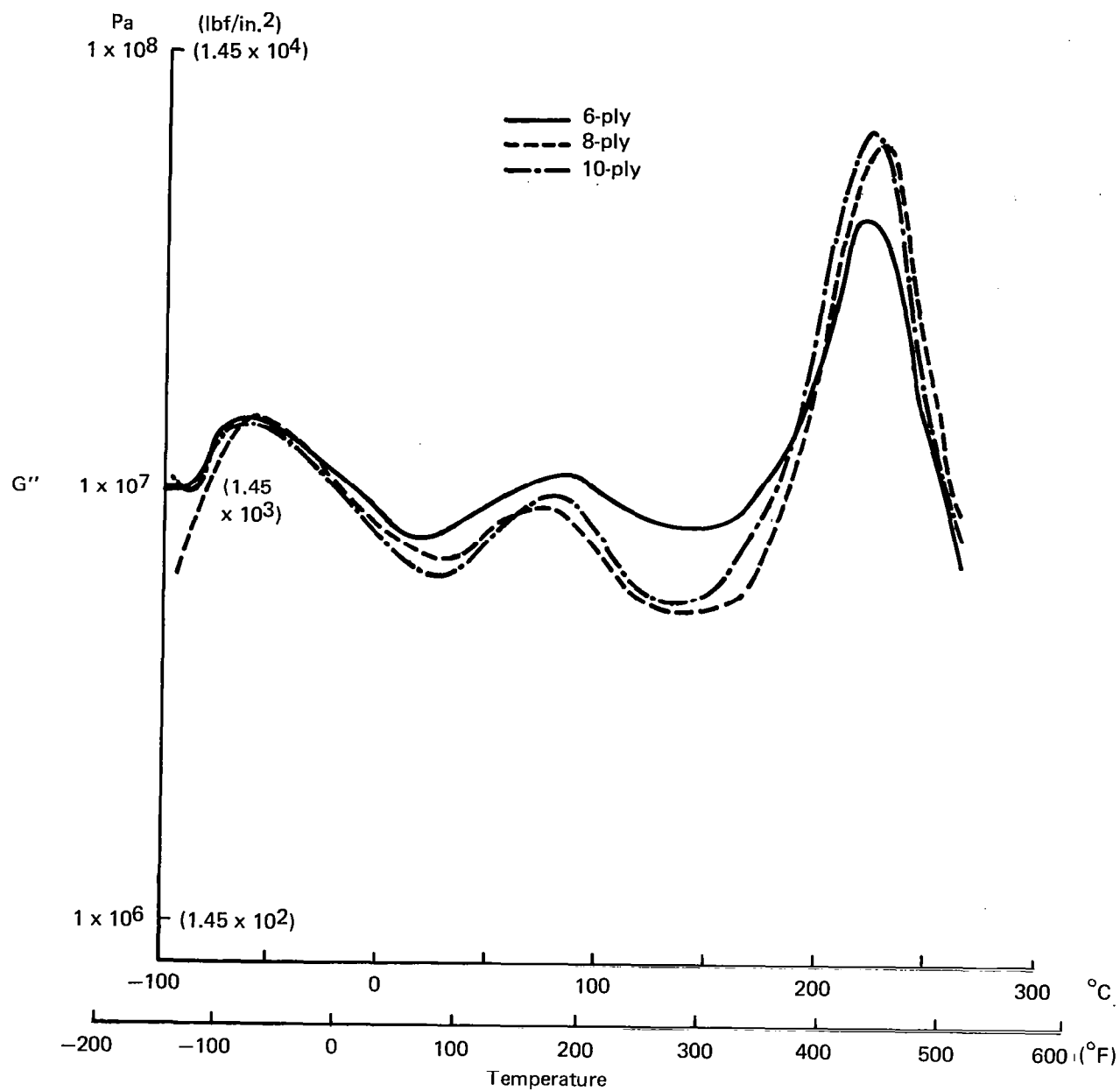Hercules Standard Batches, Humidity Exposed

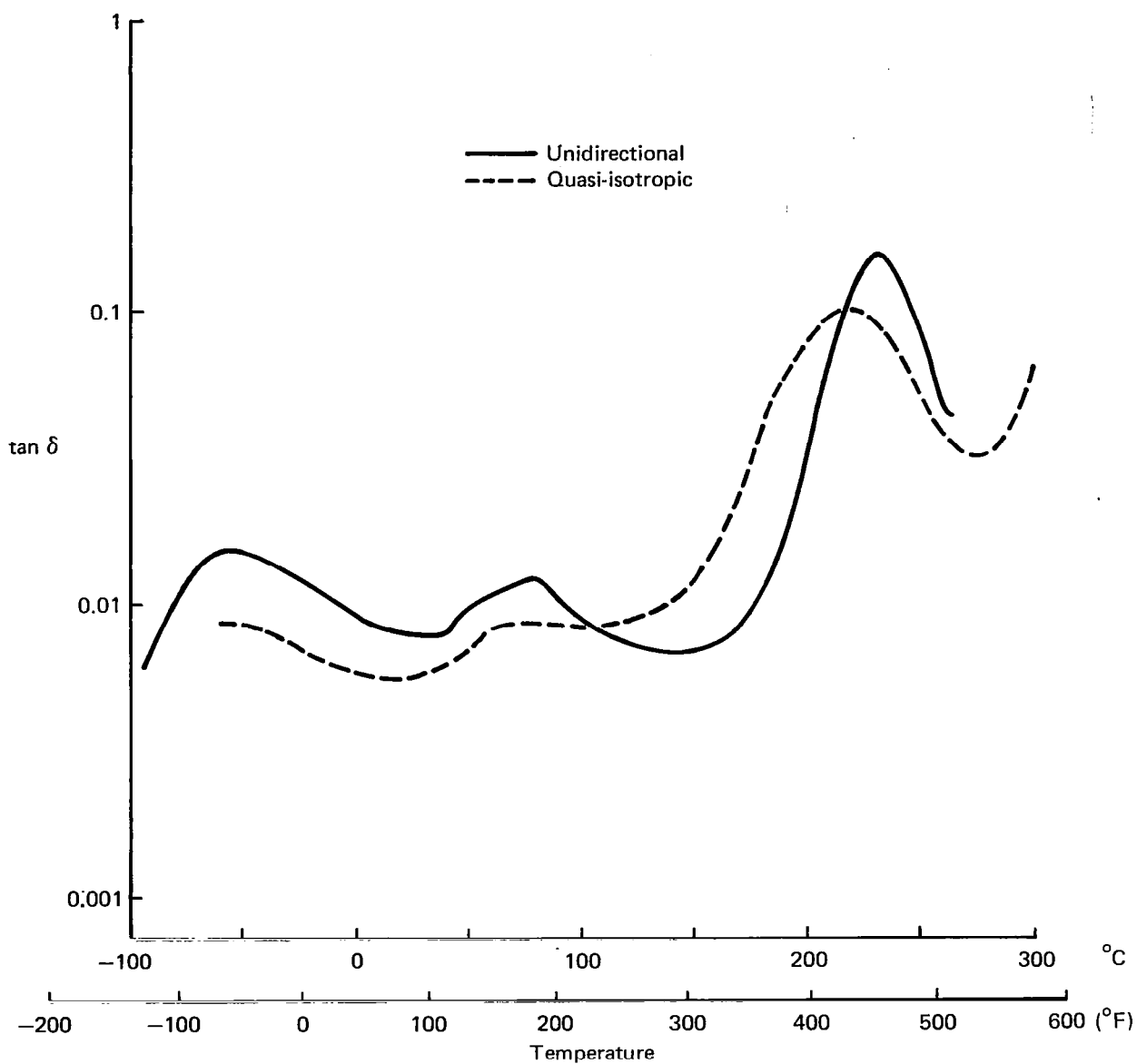Figure 130. G" Versus Temperature, Hercules Laminates—6, 8, and 10 Plies

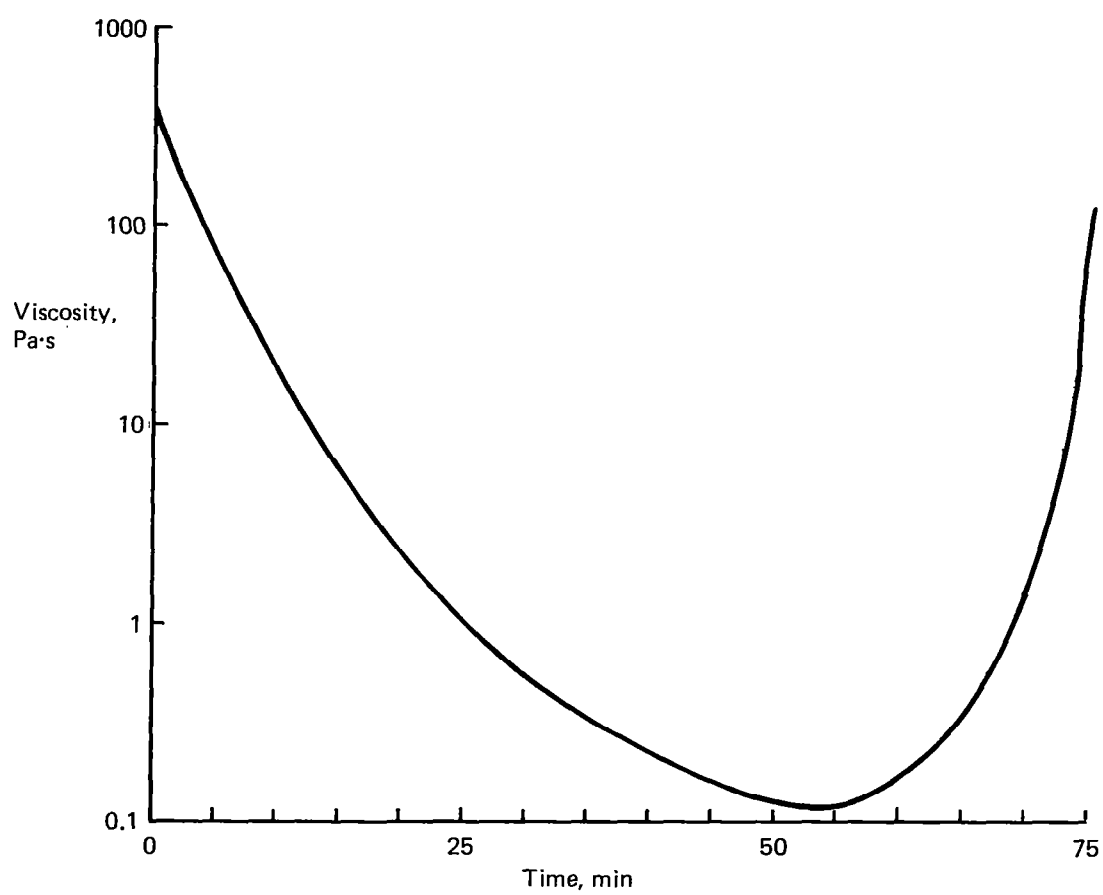*Figure 131. Tan δ Versus Temperature, Hercules Laminates—Unidirectional and Quasi-Isotropic*

Figure 132. Viscosity Versus Time, Narmco Resin Batch 293

1. Report No. NASA CR-3531	2. Government Accession No.	3. Recipient's Catalog No.
4. Title and Subtitle DEVELOPMENT OF QUALITY ASSURANCE METHODS FOR EPOXY GRAPHITE PREPREG		5. Report Date March 1982
		6. Performing Organization Code
7. Author(s) J.S. Chen and A.B. Hunter		8. Performing Organization Report No. D6-51235
9. Performing Organization Name and Address Boeing Commercial Airplane Company P.O. Box 3707 Seattle, Washington 98124		10. Work Unit No.
		11. Contract or Grant No. NAS1-15222
12. Sponsoring Agency Name and Address National Aeronautics and Space Administration Washington, D C 20546		13. Type of Report and Period Covered Contractor Report
		14. Sponsoring Agency Code

15. Supplementary Notes

Langley Technical Monitor: Norman J. Johnston
Final Report

16. Abstract

The objective of this program was to develop quality assurance methods for graphite epoxy prepregs. Liquid chromatography, differential scanning calorimetry, and gel permeation chromatography were investigated. These methods were applied to a second prepreg system. The program also sought to correlate the resin matrix formulation with mechanical properties. Dynamic mechanical analysis and fracture toughness methods were investigated.

Liquid chromatography, differential scanning calorimetry, and gel permeation chromatography were all successfully developed as quality assurance methods for graphite epoxy prepregs. The liquid chromatography method was the most sensitive to changes in resin formulation. All three methods were successfully applied to a second prepreg system. No correlation could be established between mechanical properties and the resin formulation variations defined within this contract.

17. Key Words Quality assurance Graphite epoxy Composites	18. Distribution Statement UNCLASSIFIED — UNLIMITED Subject Category 24	
19. Security Classif. (of this report) UNCLASSIFIED	20. Security Classif. (of this page) UNCLASSIFIED	21. No. of Pages 219	22. Price A10